



HAL
open science

Fault diagnosis & root cause analysis of invertible dynamic system

Mei Zhang

► **To cite this version:**

Mei Zhang. Fault diagnosis & root cause analysis of invertible dynamic system. Automatic Control Engineering. Université Paul Sabatier - Toulouse III, 2017. English. NNT : 2017TOU30260 . tel-01930729

HAL Id: tel-01930729

<https://theses.hal.science/tel-01930729>

Submitted on 22 Nov 2018

HAL is a multi-disciplinary open access archive for the deposit and dissemination of scientific research documents, whether they are published or not. The documents may come from teaching and research institutions in France or abroad, or from public or private research centers.

L'archive ouverte pluridisciplinaire **HAL**, est destinée au dépôt et à la diffusion de documents scientifiques de niveau recherche, publiés ou non, émanant des établissements d'enseignement et de recherche français ou étrangers, des laboratoires publics ou privés.



THÈSE

En vue de l'obtention du

DOCTORAT DE L'UNIVERSITÉ DE TOULOUSE

Délivré par *l'Université Toulouse III - Paul Sabatier*

Discipline ou spécialité : *Automatique*

Cotutelle internationale avec "Guizhou university CHINA"

Présentée et soutenue par *Mei ZHANG*

Le Date de la soutenance *17 July 2017*

Titre : *Diagnostic de panne et analyse des causes profondes du système dynamique inversible*
Fault Diagnosis & Root Cause Analysis of Invertible Dynamic System

JURY

Mohamed MASSD (**Rapporteur**)

Jing NA (**Rapporteur**)

Wei WEI

Bin CAO

Zhenghang HAO

Ecole doctorale : *EDSYS*

Unité de recherche : *LGC-CNRS*

Directeur(s) de Thèse : *M. Boutaib DAHHOU (Professeur)*

M. Michel CABASSUD (Professeur)

M. Ze-tao LI (Professeur)

*Fault Diagnosis & Root Cause
Analysis of Invertible Dynamic System*

Special thanks to my advisors M. Boutaib DAHOU
M. Michel CABASSUD
M. Ze-tao LI

To My Family

Contents

Acknowledgement.....	I
Summary.....	II
Résumé	IV
List of Figures	VI
Chapter 1 Introduction.....	1
1.1 Background and Significance	1
1.2 Motivation of the Thesis	4
1.2.1 Status of Current Main Methodologies	4
1.2.2 Challenges and Trends in FDD	9
1.3 Objectives of the Thesis	10
1.3.1 Form an Invertible Interconnected System Structure	12
1.3.2 Performance Monitoring of the Interconnected System	15
1.3.3 Multi-level Fault Diagnosis and Root Cause Analysis	16
1.4 Contributions and Challenges of the Thesis	18
1.5 Thesis Outlines	19
Chapter 2 Model Based Fault Detection and Diagnosis Techniques.....	22
2.1 Basic Concepts	22
2.1.1 Definitions of the Terminology	23
2.1.2 Classification of Fault Detection and Diagnosis Techniques	27
2.2 Quantitative Model-Based Fault Detection and Diagnosis Techniques.....	31
2.2.1 Introduction of Quantitative Model-based FDD Scheme.....	31
2.2.2 System and Fault Model for FDD	32
2.2.3 Residual Generation Method	34
2.2.4 Residual Evaluation Method	36
2.3 Observer Based Fault Detection and Diagnosis Approach.....	36
2.3.1 A Brief Description of the Observers	36
2.3.2 Different Observer Design Methods for Nonlinear System	37
2.3.2 Observer Schemes.....	45
2.4 Fault Detection and Diagnosis Approach of Interconnected System.....	47
2.4.1 Introduction.....	47
2.4.2 Distributed and Decentralized Fault Detection and Isolation	49
2.5 Summary.....	51
Chapter 3 Introduction to System Inversion.....	52
3.1 Introduction.....	52
3.2 Some Definitions and Notations.....	53
3.3 Left Inversion of Linear system	59
3.3.1 Input Output Description of Linear System	60
3.3.2 State Space Description of Linear System.....	61
3.4 Inversion of Nonlinear System	62
3.5 Some Related Work.....	63
3.5.1 Inversion for Unknown Input Reconstruction	64
3.5.2 Inversion for FDI Purpose.....	66

3.5.3 Inversion for System Identification	68
3.5.4 Inversion for Control Purpose	69
Chapter 4 Invertibility of Interconnected System.....	70
4.1 Introduction of Interconnected System	70
4.2 Basic Notion of Mappings and Differential Algebra	72
4.3 Inversion of Nonlinear Interconnected System	75
4.3.1 Interconnected System Modelling	75
4.3.2 Inversion of Interconnected System	76
4.4 On the Condition of Invertibility of Interconnected System	79
4.5 Invertibility Checking	80
4.6 Computing the Inverse Dynamics	82
4.6.1 Inverse of Interconnected Nonlinear System	82
4.6.2 Structure Algorithm	83
4.7 Numerical Simulations	87
4.8 Summary	95
Chapter 5 Observer Design for Invertible Interconnected System	96
5.1 Introduction	96
5.2 Motivation and Problem Formulation	98
5.3 Observer Design	100
5.3.1 Observer Design for the Interconnected System.....	101
5.3.2 Observer Analysis	107
5.3.3 Particular example: two high gain observers interconnected	108
5.4 Numerical Simulation	109
5.4.1 System Modelling	109
5.4.2 Observer Design	111
5.4.3 Numerical Simulations Results.....	111
5.5 Conclusion	118
A. Appendix 5.1: Proof of Assumption 5.2.....	118
B. Appendix 5.2: Proof of Theorem 5.1.....	119
C. Appendix 5.3: Proof of (5.12)	119
D. Appendix 5.4: Proof of (5.16)	120
E. Appendix 5.5: Proof of Theorem 5.2.....	121
F. Appendix 5.6: Proof of (5.30)	124
Chapter 6 Input Reconstructions by means of system inversion and sliding mode observer ...	125
6.1 Introduction	125
6.2 Problem Formulation	127
6.3 Input Reconstruction by System Inversion	129
6.3.1 Fundamentals	130
6.3.2 The procedure of System Inverse Computation	131
6.4 Observer Based Input Estimation	133
6.5 Numerical Simulations	135
6.5.1 System Modelling and Input re-constructor Design.....	135
6.5.2 Simulation Results and Discussion.....	137
6.6 Summary	141

Chapter 7 Fault Diagnosis and Root Cause Analysis for Interconnected System	143
7.1 Introduction	143
7.2 Problem Formulation	146
7.3 Fault Diagnosis and Root Cause Analysis Architecture	148
7.3.1 Performance Supervision and Fault Detection	148
7.3.2 Fault Detection	149
7.3.3 Root Cause Analysis	149
7.4 On Condition of Fault Distinguishability Locally and Globally	151
7.4.1 Fault analysis and Faulty model	151
7.4.2 On Condition of Fault Distinguishability	152
7.4.3 On Condition of One to One Relationship between Estimated ua and Fault Vector V	153
7.4.4 On Condition of Invertibility of Nonlinear Interconnected System in Faulty Model	154
7.5 Observer Design for Invertible Interconnected system	155
7.5.1 Observer Design for Performance Supervision	155
7.5.2 Observer Design for Inverse System and Fault Detection	157
7.6 Local Fault Filter for Root Cause Analysis	158
7.6.1 Input Estimation	158
7.6.2 Local Fault Filter Design for RCA	159
7.7 Summary	161
Chapter 8 Application of FD and RCA Scheme to HEX/Reactor System	162
8.1 System Description	162
8.1.1 Introduction of Multifunctional Heat-Exchanger Reactor	162
8.1.2 Characterization of Pilot HEX/reactor	163
8.1.3 Instrumentation Requirements	163
8.2 Problem Formulation	164
8.2.1 Preliminary	164
8.2.2 Main Contribution	166
8.3 Process Subsystem Modelling	167
8.3.1 Background	167
8.3.2 Cell-based Intensified HEX/Reactor model	168
8.3.3 Mathematical model	168
8.3.3 Cell based diagnostic dynamic model	169
8.4 Actuator Subsystem Modelling	169
8.4.1 Background	169
8.4.2 Mathematical Model	170
8.4.3 Fault Analysis and Modelling	171
8.5 Fault Diagnosis & Root Cause Analysis Architecture	172
8.5.1 Structure of the FD&RCA Method	172
8.5.2 Observer Design for Performance Supervision	174
8.5 Local Filter Design for Root Cause Analysis of Control Valve Fault	176
8.5.1 Input Estimator	176
8.5.2 RCA filter design	177

8.6 Numerical Simulation Results	178
8.5 Summary	182
Appendix 8.1A	183
Chapter 9 Summary, Conclusion and Suggestion or Future Work	186
9.1 Conclusions	186
9.2 Future Work	187
Bibliography	189

ACKNOWLEDGEMENT

It is a pleasure to thank those people who have helped me to finish this thesis. First and the most, I would like to show my deepest gratitude to my academic supervisors, Professor B. DAHHOU, Prof. M.CABASSUD and Prof. Z. LI. They are respectable, responsible and resourceful scholars who have guided and helped me in every matter during my study. Professor B. DAHHOU has always supported me to understand how to find the direction of my research with his broad knowledge, creative thinking and deep insight in the subject of automation. I am especially grateful to Prof. M.CABASSUD for giving me the opportunity of graduate study at LGC and for encouraging me technically and spiritually all through the thesis research. I am also deeply grateful to Prof. LI for his patronage, suggestions, constant encouragement and enthusiasm during the research. It is really a wonderful feeling to do research under their supervision and I would treasure this period of time as my most valuable memory.

I would like to thank all colleagues at the School of Electrical Engineering, Guizhou University, and Lab. of LGC, France, especially people in the STPI Group, LGC, and the department of automation Guizhou University. I want to express my gratitude to my colleagues Fatine BERDOUZI, Omar YALA, Lixia YANG, Pei San KONG, Na RONG, Xiaoliu YANG, Menling HE, Xue HAN and Peng TIAN for their useful advices, research assistantship and for their friendship during all through my graduate study.

Of course, I would like to express a special acknowledgement to my parents, my husband and my cute son for their understood and encouragement during all these years.

SUMMARY

Many of the vital services of everyday life depend on highly complex and interconnected engineering systems; these systems consist of large number of interconnected sensors, actuators and system components. The study of interconnected systems plays a significant role in the study of reliability theory of dynamic systems, as it allows one to investigate the properties of an interconnected system by analyzing its less complicated subcomponents. Fault diagnosis is crucial in achieving safe and reliable operations of interconnected control systems. In all situations, the global system and/or each subsystem can be analyzed at different levels in investigating the reliability of the overall system; where different levels mean from system level down to the subcomponent level. In some cases, it is important to determine the abnormal information of the internal variables of local subsystem, in order to isolate the causes that contribute to the anomalous operation of the overall process. For example, if a certain fault appears in an actuator, the origin of that malfunction can have different causes: zero deviation, leakage, clogging etc. These origins can be represented as root cause of an actuator fault.

This thesis concerns with the challenges of applying system inverse theory and model based FDD techniques to handle the joint problem of fault diagnosis & root cause analysis (FD & RCA) locally and performance monitoring globally. By considering actuator as individual dynamic subsystem connected with process dynamic subsystem in cascade, we propose an interconnected nonlinear system structure. We then investigate the problem of left invertibility, fault observability and fault diagnosability of the interconnected system, forming a novel model based multilevel FD & RCA algorithm. This diagnostic algorithm enables individual component to monitor internal dynamics locally to improve plant efficiency and diagnose potential fault resources to locate malfunction when operation performance of global system degrades. Hence, a means of a combination of local intelligence with a more advanced diagnostic capability (combining fault monitoring and diagnosis at both local and global levels) to perform FDD functions on different levels of the plant is provided. As a result, improved fault localization and better predictive maintenance aids can be expected. The new system structure, together with the fault diagnosis algorithm, is the first to emphasize the importance of fault RCA of field devices, as well as the influences of local internal dynamics on the global dynamics. The developed model based multi-level FD & RCA algorithm is then a first effort to combine the strength of the system level model based fault diagnosis with the component level model based fault diagnosis.

The contributions of this thesis include the following:

Firstly, we propose a left invertible interconnected nonlinear system structure which guarantees that fault occurred in field device subsystem will affect the measured output of the global system uniquely and distinguishably. A necessary and sufficient condition is developed to ensure invertibility of the interconnected system which requires invertibility of individual subsystems.

Second, a two level interconnected observer is developed which consists of two state estimators, aims at providing accurately estimates of states of each subsystem, as well as the unknown interconnection. In addition, it will also provide initial condition for the input reconstructor and local fault filter once FD & RCA procedure is triggered by any fault. Two underlying issues are worth to be highlighted: for one hand, the measurement used in the estimator of the former subsystem is assumed not accessible; the solution is to replace it by the estimate provided by the estimator of the latter subsystem. In fact, this unknown output is the unknown interconnection of the interconnected system, and also the input of the latter subsystem. For the other, in the latter subsystem, the unknown interconnection is treated as an additional state, forming a new extended subsystem; and expression of the new state is obtained by computing derivatives of output equation of the previous subsystem.

Moreover, by combining the left inversion and sliding mode observer, we propose a kind of algebraic unknown input estimation method by which successive output derivatives are avoided. We employ a second order sliding mode observer to estimate the time derivatives of the output, thus avoiding the potential serious errors arise by the derivatives computation. The estimation is then used to substitute the derivatives of outputs in the differential algebraic polynomial obtained via system inversion.

In addition, a novel FD & RCA scheme is investigated where a local fault filter is designed for the actuator subsystem, thus achieving root cause analysis of the detected actuator fault. Each local fault filter consists of two modules: a fault detection and isolation module is developed to identify an occurrence of any fault variable in the actuator subsystem; and banks of fault isolation estimators are employed to determine the particular faulty variables that have occurred in the subsystem. An input reconstructor is used to determine the unknown interconnection of the interconnected system or determine the output of the actuator subsystem. The fault detectability, isolability and distinguishability are rigorously investigated; characterizing the class of faults in each subsystem that are detectable and isolable by the proposed method.

Finally, the effectiveness of the above FD & RCA schemes is illustrated by using simulations of the nonlinear model of an intensified Hex reactor system. Different fault scenarios are considered to verify the diagnosis performances, and the satisfactory performances of the proposed method are validated by the good simulation results.

Key Words: invertibility; interconnected system; fault distinguishability; interconnected observer; root cause analysis; input reconstruction; local fault filter; distributed FDD algorithm; unknown interconnection; local internal dynamic; subcomponent; field device.

RESUME

Beaucoup de services vitaux de la vie quotidienne dépendent de systèmes d'ingénierie hautement complexes et interconnectés; Ces systèmes sont constitués d'un grand nombre de capteurs interconnectés, d'actionneurs et de composants du système. L'étude des systèmes interconnectés joue un rôle important dans l'étude de la fiabilité des systèmes dynamiques; car elle permet d'étudier les propriétés d'un système interconnecté en analysant ses sous-composants moins complexes. Le diagnostic des pannes est essentiel pour assurer des opérations sûres et fiables des systèmes de contrôle interconnectés. Dans toutes les situations, le système global et / ou chaque sous-système peuvent être analysés à différents niveaux pour déterminer la fiabilité du système global. Dans certains cas, il est important de déterminer les informations anormales des variables internes du sous-système local, car ce sont les causes qui contribuent au fonctionnement anormal du processus global.

Cette thèse porte sur les défis de l'application de la théorie inverse du système et des techniques FDD basées sur des modèles pour traiter le problème articulaire du diagnostic des fautes et de l'analyse des causes racines (FD et RCA). Nous étudions ensuite le problème de l'inversibilité de la gauche, de l'observabilité et de la diagnosticabilité des fautes du système interconnecté formant un algorithme FD et RCA multi-niveaux basé sur un modèle. Ce système de diagnostic permet aux composants individuels de surveiller la dynamique interne localement afin d'améliorer l'efficacité du système et de diagnostiquer des ressources de fautes potentielles pour localiser un dysfonctionnement lorsque les performances du système global se dégradent. Par conséquent, un moyen d'une combinaison d'intelligence locale avec une capacité de diagnostic plus avancée pour effectuer des fonctions FDD à différents niveaux du système est fourni. En conséquence, on peut s'attendre à une amélioration de la localisation des fautes et à de meilleurs moyens de maintenance prédictive. La nouvelle structure du système, ainsi que l'algorithme de diagnostic des fautes, met l'accent sur l'importance de la RCA de défaut des dispositifs de terrain, ainsi que sur l'influence de la dynamique interne locale sur la dynamique globale.

Les contributions de cette thèse sont les suivantes:

Tout d'abord, nous proposons une structure de système non linéaire interconnecté inversible qui garantit le fautes dans le sous-système de périphérique de terrain affecte la sortie mesurée du système global de manière unique et distincte. Une condition nécessaire et suffisante est développé pour assurer l'inversibilité du système interconnecté qui nécessite l'inversibilité de sous-systèmes individuels.

Deuxièmement, un observateur interconnecté à deux niveaux est développé. Il se compose de deux estimateurs d'état, vise à fournir des estimations précises des états de chaque sous-système, ainsi que l'interconnexion inconnue. En outre, il fournira également une

condition initiale pour le reconstituer de données et le filtre de fautes local une fois que la procédure FD et RCA est déclenchée par tout fautes. D'une part, la mesure utilisée dans l'estimateur de l'ancien sous-système est supposée non accessible; La solution est de la remplacer par l'estimation fournie par l'estimateur de ce dernier sous-système. En fait, cette sortie inconnue est l'interconnexion inconnue du système interconnecté, ainsi que l'entrée de ce dernier sous-système. Pour l'autre, dans ce dernier sous-système, l'interconnexion inconnue est traitée comme un état supplémentaire, formant un nouveau sous-système étendu; Et l'expression du nouvel état est obtenue en calculant les dérivées de l'équation de sortie du sous-système précédent.

De plus, en combinant l'inverseur gauche et l'observateur en mode coulissant, nous proposons une sorte de méthode d'estimation d'entrée algébrique inconnue par laquelle des dérivés de sortie successifs sont évités. Nous employons un observateur en mode coulissant de deuxième ordre pour estimer les dérivées temporelles de la sortie, évitant ainsi les erreurs sérieuses éventuelles résultant du calcul des dérivées. L'estimation est ensuite utilisée pour substituer les dérivées des sorties au polynôme algébrique différentiel obtenu par inversion du système.

En outre, un nouveau système FD & RCA est étudié filtre de fautes local est conçu pour le sous-système de l'actionneur, ce qui permet d'obtenir une analyse de la cause racine du fautes détecté de l'actionneur. Chaque filtre de fautes local se compose de deux modules: un module de détection et d'isolation de fautes est développé pour identifier une occurrence de toute variable de fautes dans le sous-système de l'actionneur. Un reconstituer d'entrée est utilisé pour déterminer l'interconnexion inconnue du système interconnecté ou déterminer la sortie du sous-système de l'actionneur. La détection, l'isolabilité et la distinction des fautes sont rigoureusement étudiés; Caractérisant la classe de fautes dans chaque sous-système qui sont détectables et isolables par la méthode proposée.

Enfin, l'efficacité des schémas FD et RCA ci-dessus est illustrée en utilisant la simulation sur le système de réacteur Hex intensifié Différents scénarios de fautes sont considérés pour vérifier les performances du diagnostic et les performances satisfaisantes de la méthode proposée sont validées par les bons résultats de simulation.

Mots clés: invertibilité système interconnecté fautes de distinction; observateur interconnecté analyse de la cause originelle; reconstruction des intrants; filtre de défaut local; algorithme distribué FDD; interconnexion inconnue; dynamique interne locale; sous-composant; appareil de terrain.

LIST OF FIGURES

- Fig. 1.1 Fault types and effects in system
- Fig. 1.2 Typical usages of different categories of FDD methods
- Fig. 1.3 System decomposition and interconnections
- Fig. 1.4 An interconnected system structure
- Fig. 1.5 Observer structure for interconnected system
- Fig. 1.6 FDD algorithm for component FDD and RCA
- Fig. 2.1 Common types of actuator faults
- Fig. 2.2 Common types of sensor faults
- Fig. 2.3 Types of fault based on behavior
- Fig. 2.4 Schematic description of the hardware redundancy scheme
- Fig. 2.5 Schematic description of the analytical redundancy scheme
- Fig. 2.6 Schematic description of the signal processing based scheme
- Fig. 2.7 Schematic description of the model based scheme
- Fig. 2.8 Schematic of Generalized Observer Scheme
- Fig. 2.9 Schematic of Generalized Observer Scheme
- Fig. 2.10 Schematic of different structures
- Fig. 3.1 Left inverse
- Fig. 3.2 Right inverse
- Fig. 4.1 Composition of mappings
- Fig. 4.2 Interconnected system structure
- Fig. 4.3 Inversion of interconnected system
- Fig. 4.4 Interconnected inverse system scheme
- Fig. 4.5 Computed and reconstructed fluid flow rate in case 1
- Fig. 4.6 Measured and recovered pneumatic pressured of fluid flow rate in case 1
- Fig. 4.7 Computed and reconstructed flow rate in case 2
- Fig. 4.8 Measured and recovered pneumatic pressured of fluid flow rate in case 2
- Fig. 5.1 Interconnected system structure
- Fig. 5.2 Structure of the proposed interconnected observer
- Fig. 5.3 Output of process fluid temperature
- Fig. 5.4 Output of utility fluid temperature
- Fig. 5.5 Computation and estimation of process fluid flow rate
- Fig. 5.6 Computation and estimation of utility fluid flow rate
- Fig. 5.7 Outlet temperature of process fluid,
- Fig. 5.8 Outlet temperature of utility fluid
- Fig. 5.9 Computation and estimation of process fluid flow rate
- Fig. 5.10 Computation and estimation of utility fluid flow rate
- Fig. 5.11 Outlet temperature of process fluid
- Fig. 5.12 Outlet temperature of utility fluid
- Fig. 5.13 Computation and estimation of process fluid flow rate
- Fig. 5.14 Computation and estimation of utility fluid flow rate
- Fig. 6.1 Reconstructed fluid flow rate in case 1
- Fig. 6.2 Reconstructed fluid flow rate in case 2 where measurement noise power is 0.01

- Fig. 6.3 Reconstructed process fluid flow rate in case 2 where measurement noise power is 0.028
- Fig. 6.4 Reconstructed process fluid flow rate in case 2 where measurement noise power is 0.1
- Fig. 7.1 Interconnected system structure
- Fig. 7.2 Interconnected observer performance supervision
- Fig. 7.3 Observer design for inverse system
- Fig. 7.4 Main idea of the proposed RCA algorithm
- Fig. 7.5 Detector for fault reconstruction
- Fig. 8.1 Heat exchanger/reactor after assembly
- Fig. 8.2 Cascade Hex reactor system structure
- Fig. 8.3 N cell models
- Fig. 8.4 Architecture of the proposed FD&RCA approaches
- Fig. 8.5 Reconstructed input \tilde{F}_u, \tilde{F}_p from output T_p, T_u in CASE (a)
- Fig. 8.6 Detection residual in case (a)
- Fig. 8.7 Residuals for identifying fault cause in process fluid in case (a)
- Fig. 8.8 Residuals for identifying fault cause in utility fluid in case (a)
- Fig. 8.9 Reconstructed input \tilde{F}_u, \tilde{F}_p from output T_p, T_u in CASE (b)
- Fig. 8.10 Detection residual in case (b)
- Fig. 8.11 Residuals for identifying fault cause in process fluid in case (b)
- Fig. 8.12 Residuals for identifying fault cause in utility fluid in case (b)

CHAPTER 1 INTRODUCTION

Fault detection and diagnosis (FDD) is a key enabling technique for increasing safety and reliability of control systems. On the basis of an analysis of advantages and disadvantages of existing methods, this chapter gives a brief description of the motivations and objectives of this study. Additionally, the contribution and challenges of the thesis are also presented. Finally, this chapter outlines the structure of the thesis and the relations between the subsequent chapters.

1.1 Background and Significance

With the fast developments of modern technologies, resulting in ever increasingly interconnection of modern control system, thus a modern system often consists of large number of sensors, actuators and system components which are interconnected. As a consequence, the complexity of the system keeps increasing. The complexity and technological advances mean that these units are increasingly integrated, intelligent and complex. Each unit may consist of more than one component connected in any configuration; therefore each unit itself is a dynamic system and exhibits complicated dynamics of system. For example, a valve actuator is an assembly of positioner, pneumatic servo-motor and control valve, as given in [1] and mathematical models presented in, for example [2][3], have shown that control valve can be seen as a nonlinear dynamic system. Therefore modern control system can be viewed as composed of dynamic subsystems connected in series. In all situations, the global plant and/or each subsystem can be analyzed at different levels down to the component level in estimating the reliability of the whole plant. A typical control system, for example, has at least three cascade subsystems: sensor, process and actuator subsystems. The three parts must function properly so that the whole system can operate properly.

As a result of the increasingly complexities, the probability of occurrence of faults is also increased. The fault may occur at any level of the system, as shown Fig.1.1. Actuators are driven by the input signals $u(t)$ while observation signals $y(t)$ are provided by the array of sensors. The different faults normally are classified by the location (where a fault acts in the system). According to this classification, the fault can be recognized as i) Actuator faults, ii) Sensor faults and iii) Component faults. In a real industrial system, the faults may be related to, for example, pressure drop out in hydraulic components, short circuiting or overheating of electrical components, breakage in bearings due to mechanical stresses, leakages in pipes, sticking of valves, cracks in tanks, drifting of sensors etc. Faults at any level may cause a malfunction of the installation; resulting in a serious impact in equipment, such as production quality, safety, economy, levels of contamination, in the worst of cases a fault may even cause sever accidents.

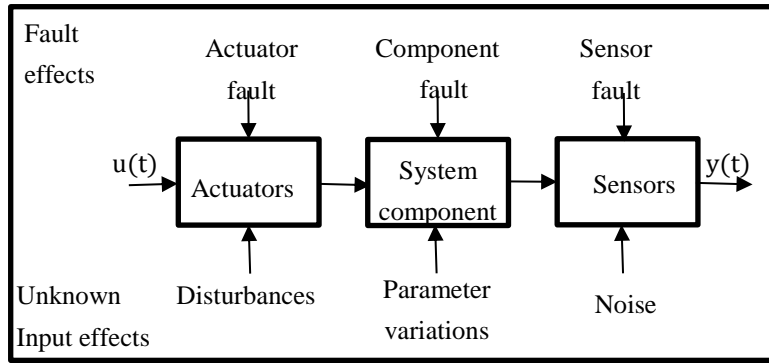


Fig. 1.1 Fault types and effects in system

For one hand, faults connected to manufacturing often decrease the efficiency of the process and lead to a considerable reduction of production and quality of the product. In this context, we can cite some examples: for instance, the estimated cost of one stop production of a specific flotation process in Sweden is 30,000 euros / hour as shown in [4]. For another example in [5], it is claimed that the U.S. petrochemical industry suffers from 20 billion dollar losses annually due to poor abnormal situation management. One more lesson is the sensors drift of feed water flow in steam generator which can result in reactor power output reduction by as much as 3%-in the U.S. [6]. What's more, it reported in [7] that because of fouling, the decline of steam generator thermal efficiency may cause a lower electric output per unit reactor thermal power. While according to [8], about 42% of the potential waste in annual energy consumption is estimated due to leaks of compressed air in a pneumatic system, leaks can degrade machine performance since actuators produce less force, run slower and are less responsive. For the other, some consequences of a fault can be extremely serious in terms of human mortality and environmental impact, especially for safety critical systems such as aircrafts, nuclear reactors etc. Faults may lead to catastrophic incidents. For this point, a lesson is from the well-known TMI-II accident in 1979, it has been proved that this accident was initiated by the valve position failure of feed water pump of the main reactor [9]. Another related incident is an explosion happened in a huge nuclear power plant in the town of Chernobyl in 1986. The main cause for this tragedy was the faulty outdated technology and the lack of a fault handling mechanism [10]. What's more, a stuck open relief valve created a loss of coolant scenario in the Three Mile Island accident, which was a major reason for the disastrous outcome [11]. Single engine fighter is another example of this point, there are reports related to the aircraft area where a fault in an engine can cause the aircraft to crash, which will have catastrophic consequences for the pilot [12]. For example The American Airline DC10 crashed at Chigao-O'Hare International Airport, the pilot had the indication of fault only 15 seconds prior to the accident [13].

Consequently, the demand for safety, reliability, higher performance and cost efficiency are of major importance in the design of a control system, for economic, sociologic and human reasons. To meet these specific characteristics, condition maintenance as part of predictive maintenance is one of the tools used to increase productivity and reliability in industrial process. It can be utilized to detect and identify different type of faults and the root causes occurring at any level of the system so that to

guarantee the stability and performance of the system. In particular, this is true for the modern systems consisting of a number of small parts (dynamic units) which interact to aggregate individual dynamics into collective behavior. Eventually, the diagnostic tool is expected to offer a mean of increasing productivity by identifying potential component or system wide faults. This ranges from the most common issues of operational safety such as condition monitoring, fault detection and isolation, fault diagnosis, fault management and fault tolerance to some more general questions of the operation such as the effect of human factor. Among them, timely detection and diagnosis of faults can avoid, or at least, minimize the severity of economic losses and fatalities by reconfiguration of controllers or safely switching off the process for maintenance. This is done by minimizing unscheduled shutdowns and loss of product quality.

Advanced FDD can help accurate monitoring of process variables and interpreting their behaviors. Therefore the main benefits of FDD are more stable production, improved product quality, the reduction of operation costs, as well as more efficient and appropriate maintenance. In order to welcome the challenges arising from deregulation, the plant economic parameters are monitored on line and optimized with the constraints that the related safety regulations are rigorously satisfied. Since the functional status of sensors, actuators, and process devices are monitored on line, this makes it possible to support real time operation and perform maintenance tasks only when it is necessary. Therefore, significant reduction in plant downtime, considerable maintenance cost savings, and reduction in maintenance errors can be expected. FDD can also provide crucial information for taking corrective actions to adjust the process operation to the fault effects utilizing fault tolerant control or maintenance. For instance, Detroit Edison Company developed a valve monitoring system for the power plant. It is estimated that this system could reduce annual maintenance costs approximately 15% to 20% [14]. Moreover, the diagnostic information can be further utilized to make predictions on the future operation of the process and/or to take corrective actions in terms of predictive maintenance or fault tolerant control [15].

Besides, by developing a FDD system, sever abnormal situations caused by faults can be discovered earlier, which provides a possibility to tackle their effects more effectively, thus preventing the system from getting into undesirable state which may lead to catastrophe. If a fault can be detected and rectified at its incipient stage before abrupt failures occur, the possibility of some accidents can actually be eliminated. Surprisingly, it has been reported that, these above mentioned incidents could have been avoided if there was a suitable fault monitoring and tolerant system. For example, TMI-II accident in 1979 could have been avoided by employing performance monitoring system for the devices, i.e. valve monitoring and diagnosing system [9].

As evidenced by the above technical requirements, process performance monitoring and fault diagnosis plays a central role in modern control system design. The development of FDD is receiving more and more attentions both in academia and industry. Considerable research efforts have been and still are being made to develop FDD methods that can readily be applied to complex real life systems.

1.2 Motivation of the Thesis

1.2.1 Status of Current Main Methodologies

Following the occurrence of a number of technical disasters and industrial catastrophes, the demands on FDD algorithms have increased over the years, dealing with different applications ranging from aeronautic, navigation to civil applications that associated with huge programs, like nuclear power plants, chemical and petrochemical processes.

The last few decades have witnessed significant improvements in fault detection and diagnosis (FDD) techniques. Many advanced FDD methods are presented in the literature for linear or nonlinear process systems subject to fault. Considering the overall dynamical system as illustrated in Fig.1.1, malfunctions may occur either in the actuator and sensor dynamics, as well as in the components of the system. In order to welcome the challenges arising from complexity of dynamics in the overall system, as well as in individual component, based on their mathematical representation, faults appear in any part of the system can be analyzed at different levels. Typical usages of different categories of FDD methods are illustrated in Fig. 1.2. One main approach is system level based diagnosis approach, that aims at detecting and identifying fault existence and location from the view point of global system. Another common kind of methodologies focus on the field device level, that aims at analyzing internal dynamics of a specific component.

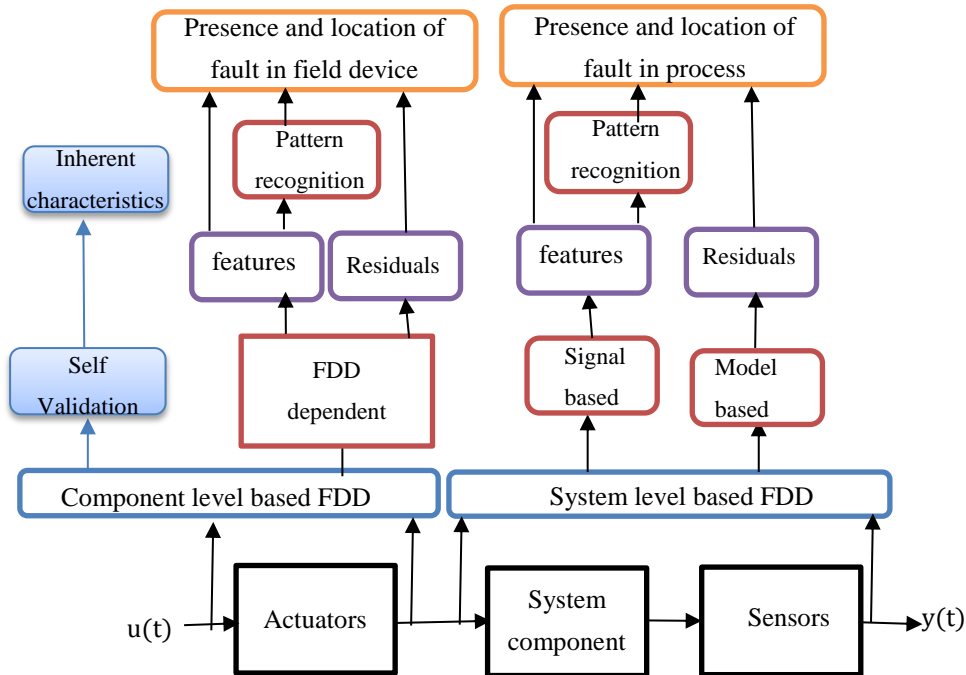


Fig. 1.2 Typical usages of different categories of FDD methods

1-) System level-based diagnosis

Current monitoring systems are typically centralized monitoring systems where intelligence is at the system level of the process plant, rather than at the field device level. In these methods, dynamics of field devices (i.e. actuator) is ignored, instead, they are treated as a component which is viewed as constants in the input or output coefficient matrix (function) of the process system model. The

malfunctions can be treated separately and they enter the process model as actuator or sensor where faults are considered as changes of the input or output coefficient matrix elements; And an actuator and (or) a sensor fault is normally considered as additive effects whilst the component fault shows up through structural and (or) parameter variations of the system, i.e. as multiplicative or parameter varying effects. This assumption is not very restrictive, as various type of faults, such as parameter changes or sensor failures, can be converted into additive type of faults (with some non-negligible implications), therefore internal dynamics of the field device may be lost. As a result, the overall system cannot be precisely described by a centralized mathematical model due to incomplete identification of the field device and some unknown disturbances or control signals. Moreover, model aggregation or simplification which is deliberately designed to make the system manageable may also lead to uncertainties. A main reason leading to this is due to a consequence of complexity of the modern units. Mathematical models of their dynamics may be hard to define precisely and hence modelling uncertainty is a significant challenge if model based methods of control or estimation are to be used. If considered dynamics of the entire component in a single system model may increase the order of the system. The dimension (dynamical order) of the system can be very large; in this case, there may be a large number of states and inputs that need to be handled for a modern control system.

Many different approaches to system level model based fault detection and diagnosis have been introduced. Works in [16][17][18] reviewed process fault detection and diagnosis based on the principle of analytical redundancy. A key approach is based on residuals generation. In [19], a nonlinear FDI filter is designed to solve a fundamental problem of residual generation using a geometric approach. The objective of the filter design is to build a dynamic system for the generation of residuals that are affected by a particular fault and not affected by disturbances and the rest of faults. The problem of component fault isolation is also studied by exploiting the system structure to generate dedicated residuals (see, e.g. [20][21][22]). In this approach, each residual, defined as the discrepancy between state measurements and their expected trajectories, is uniquely sensitive to one fault. Thus, a fault is isolated when the corresponding residual breaches its threshold. In addition, adaptive estimation techniques are used to explicitly account for unstructured modeling uncertainties for a class of Lipschitz nonlinear systems (see, e.g. [23][24][25]). In these results, residuals, defined as output estimation errors, and time varying thresholds are generated using a bank of estimators, and a fault is isolated when the corresponding residuals breach their thresholds. Another approach different to residual generation is fault estimation or fault reconstruction which can determine the size, location and dynamics behavior of the fault. The relevant literature on this topic has its roots in system inversion theory developed for either input observers (left inversion) or preview control (right inversion) like in [26][27][28]. There are several methods typically used for fault reconstruction: sliding mode observers [29][30][26], unknown input observers [31][32][33], input reconstruction [34][35][36]. For instance, a sliding mode observer is designed to reconstruct or estimate faults by decoupling the input in [37]. Reference [38] develops a high gain observer with multiple sliding modes for simultaneous state and

fault estimations for MIMO nonlinear systems. The novelty lies on the observer design that employs the combination of high gain and sliding mode observers.

As result of incomplete identification of internal variables of the components, the application of system level based FDD methodologies are mainly limited to the existence and isolation of a fault from the view point of global level, while root causes of this fault cannot be obtained. For example, reference [39] has shown that decrease of output temperature may be due to decrease of fluid flowrate, and the causes of this decrease of fluid flowrate may be caused by valve clogging, stop of utility fluid pump or leakage. Nevertheless, with respect to the above mentioned system level based FDD methodologies, fault symptoms can be detected and isolated without having the capability to pinpoint the real root cause of the fault. However, root causes of a fault in a component can cause significant process disturbances and influence the quality of the final product. For one hand, in each component system there can be fault types specific for that system, therefore it is not capable of analyzing all the faults at the process level. This is due to the consequence of increased complexity, resulting in an ever increasing complexity of actuators and sensors, potentially a significant number of variables can be involved with nonlinear interrelationships. The connectivity of a continuous process means disturbances that are often propagated which make it impossible to supervise them without extending into another technical system. A fault or disturbance in a field device may occur and manifests as a deviation in measurements of the overall system, typically in flow, pressure, level or temperature. Therefore a system level based approach to fault detection and diagnosis is seldom sufficient for the investigation of a modern process due to the complexity and diversity of features, such as process dynamics, non-linearity, in different parts of the process. However, recognizing root cause of a fault correctly is essential in order to be able to allocate resources effectively to repair the problem and perform maintenance actions of a component, an abnormal deviation of an internal variable inside the field device may not be observable until some internal variable saturates and field device performance is affected. After field device performance is affected by the internal faults, these faults can then be detected through process variables. But the detection may happen too late to keep process performance at an optimal level and to have time to prepare repair work. The above two weaknesses may be the key reasons result in that the research on FDD methods has been very active already for several decades, but still the literature on applications in process industry is in the minority.

2-) Component level-based diagnosis

Field devices are fundamental components in the process industry and they are the most common final control elements in the control loop. For example, there can be thousands of manually operated valves and control valves in a process plant. Many important process variables, such as forces, flows and pressures, are controlled through the field devices. Therefore faults of the field devices can cause significant disturbances to the global process and influence the quality of the final product; in addition, the field devices have considerable potential to support predictive maintenance. Hence, the determination of internal malfunctions of the subcomponents of modern control system, especially

those small and incipient faults before they become seriously has an important influence on safety and productivity. The monitoring of the development of these incipient faults is therefore an issue not only for predicting maintenance schedules but also monitoring the performance of the overall process.

For the purpose of better understanding potential relationship from cause to effect of a subcomponent fault, component level diagnosis can be a solution whereby capability of locating subcomponent faults for root cause analysis is available. In order to achieve this purpose, components of the modern control system have to possess FDD capabilities. Each process plant is then decomposed into individual equipment component subsystems for fault analysis purposes; this allows precise analysis of fault from causes to effects. That is to further divide the control system into certain subsystems with required structure and robustness analysis at hierarchical and/or local levels. In each subsystem, there can be fault types specific for that subsystem; in this case, analysis of root cause of a component fault is achieved. There are already efforts that have been made to locate subcomponent faults for root cause analysis. The development of FDD for field devices can be recognized from publications, normally categorized as intelligent self-validation approaches and FDD dependent methods.

Intelligent self-validation approaches make use of I&C (Instrumentation and Control) technologies, called intelligent devices [49], or smart sensing [41]. It is an instrument that is designed to compensate for its own undesirable inherent characteristics to correct from fault conditions. They are normally FDD method independent. The initiative problem for this research is concerned with developing self-validating reconfigurable control systems. Manufacturers of intelligent devices have the best knowledge about these devices and they know the problems the devices can meet during operation. Therefore it is reasonable for device manufacturers to implement fault detecting and diagnosis features in intelligent devices, as opposed to the traditional system level-based condition monitoring systems. A clear byproduct of this may be an enhancement to the development of intelligent actuation system, e.g. smart positioner in self-validating actuator. Furthermore, digital sensors can be programmed to perform self-diagnostics. Ideally, intelligent autonomous devices can be part of a centralized condition monitoring system and can identify locally all the factors or the problems limiting the efficiency of the local process. While existing intelligent instrument is restricted to self-diagnosis from a low level, they lack capability of supervising performance of the overall plant.

The most active research area in component diagnostics are FDD involved methods. Just like system level scheme, the FDD methods of component level can be categorized into two basic types based on the information they utilize: signal based methods and model based methods. Signal processing is a promising approach for FDD in component. The signal based methods consider input and output of the device measurement signals and their key characteristics. For example, reference [42] propose an algorithm to detect valve stiction for diagnosis oscillation of control valve by signal processing. Wavelet analysis is a major aspect of signal processing method for fault detection. As in [43], it developed automatic feature extraction of waveform signals for process diagnostic performance improvement. And in [44], wavelet transform is applied to detect abrupt changes in the vibration

signals obtained from operating bearings being monitored. More applications of signal processing techniques in FDD can be found in various publications in the literatures therein. Whereas the model based methods use first-principle models or system identification techniques to diagnose fault resource. They rely mainly on system identification procedures to estimate related parameters. The difference between the methods is in the identification algorithm and the structure of the model. Therefore it is important to generate a proper model of components since the methods are developed based on fundamental understanding of physics. The interest in the modeling of a filed component, like pneumatic servo, control valve, i.e. came to the attention of researchers as a crucial concern like in [45], where a set of nonlinear differential equations representing the system dynamics based on physics are derived. For example in [46], derivations of similar nonlinear models have been presented in many recent publications, in which a detailed mathematical model of dual action pneumatic actuators controlled with proportional spool valves and two nonlinear force controllers based on the sliding mode control theory were developed. Besides modelling, there are also a series of notable researches that have been performed for FDD of component, i.e. pneumatic actuator. For instance, reference [2] develops an interval observers based passive fault detection method and apply it to a control valve in the DAMADICS benchmark problem. Authors in [47] introduce a state space sliding-stem control valve model in order to utilize an advanced nonlinear model predictive control strategy to compensate for the effects of friction. Other nonlinear modeling approaches involves using neural networks or fuzzy logic, such as in [48][49]. For example, in [49], the Adaptive Neuro-Fuzzy Inference System (ANFIS) model is used to detect and diagnose the occurrence of various faults in pneumatic valve used in the cooler water spray system. And work [63] introduces the application of neural networks for the identification and fault diagnosis of process valves and actuators.

A major difficulty of component level based diagnosis methodology is the lack of dynamics information of the global system. It is because the component level diagnosis method focuses only on managing the subsystems that only use the local information, i.e. states and outputs of this subsystem. However, none of these subsystems knows the system completely. For example, as shown in [9], a fault in a sensor subsystem may propagate their effects to the regulated variables and subsequently disturb other process variables through feedback control loops. The deleterious consequence of such disturbances is that the related actuators and plant equipment would not be able to operate at the designed optimal conditions and their expected lifetime may be shortened. Therefore a more effective way is to diagnose local faults online during the operation of the device, utilizing information of both local and global system, i.e. states of this subsystem while outputs of the overall process. Another challenge when researching FDD methods locally is getting data from the subsystem being observed to develop and validate these methods. For example, direct access to actuators is often not possible or difficult via physical measurements due to distances or rough environment. For each component subsystem, its corresponding local FDD system is designed by utilizing local measurements, thus sensors have to be installed to all the primary variables of the field devices to make faults of these field devices observable. From the view point of academic value, this is not a big problem while from the

view point of the engineering value, it is rather complicated. Installing additional sensors into the field devices leads to very complicated and expensive systems where deep expertise concerning the operation of the device is required from monitoring system designers. Moreover, even if the output of the field device (e.g. actuator) is available for measurement, considering the noisy output of the sensor of the field device, the numerical differentiation would be too noisy. The noisy control input made from these signals, not only could damage the field device, but also would make less accuracy in tracking and then instability in the control scheme. As a result, false alarms are easily generated and maintaining such a system requires a lot of resources. Furthermore, some parameters are not available for directly measurement, for instance, as a common actuating signal, concentration in chemical process cannot be measured through physical sensors.

1.2.2 Challenges and Trends in FDD

Incorporating safety issues into the design process is a rather contradictory problem, however, selling safety is not an easy problem in modern economy where the actors of the economy are mostly interested in maximizing their profits. In order to push decision makers of the economy towards the acceptance of safety regulations, and to encourage a volunteer approach to the consideration of those problems, it is necessary to develop techniques and application methodologies which produce safe and secure systems at affordable prices, and in parallel, to develop analysis and evaluation tools in order to quantify, prove and certify the above mentioned systems performances, that is to say, to increase the confidence measures of the application of the new safe intensive technologies.

Although many different fault diagnosis methods have been developed from various industries, neither the aforementioned system level based nor component level based fault detection and diagnosis methods are however sufficient alone to achieve effective diagnosis to handle all the requirements for an engineering problem since all methods have their characteristic strengths and weaknesses. Eventually, a diagnostic tool is expected by which a means of increasing productivity by identifying potential component as well as system-wide faults is provided. The only pragmatic solution is to have a thorough investigation of the weaknesses of individual methods and build an application dependent method to fully utilize their strengths.

1-) Lack capability of root cause analysis of a detected fault by system level based methodology

Because of the lack of information of internal dynamics of local component, current system level based advanced FDD methods can detect some symptoms of the component without having the capability to pinpoint the real root cause of the fault or localize the problem for repairing work. For example, stiction is said to be a common root cause of flow control loop oscillation in [8], while to the diagnosis of flowrate oscillation in process plants, almost all the approaches that have been made are from the point of view of plant level, not from field devices. This means that only process variables are used for diagnosis and methods are carried out on the system level, thus flowrate oscillation can be detected but the root cause, stiction, cannot be identified.

2-) Delay of detection by system level based methodology

An abnormal deviation of an internal variable inside the field device may not be observable until some internal variable saturates and field device performance is affected. After field device performance is affected by the internal faults, these faults can then be detected through process variables. But then the detection happens too late to keep process performance at an optimal level and to have time to prepare repair work.

3-) Lack capability of monitoring the overall system by component level based methodology

At the moment, more detailed field devices performance analysis can be done by using local measurement. This may not be an effective method for analysis, because the connectivity of a continuous process means that local disturbances often propagated plant wide. A more effective method is to perform the diagnosis locally during the operation of the device with information on the process globally.

4-) Challenges of availability of local measurement by component level based methodology

There have been significant research activities in the development of new methodologies for component FDD. They are typically based on supervision of the available local measured variables. In order to obtain these measurements, special sensors have to be installed. However, the problem of availability of these sensors installation has received less attention, especially from the view point of safe and secure measures at affordable prices. Moreover, direct accesses to a field device, i.e. actuator, is sometimes not permitted due to reasons like distance. Even if the output of a field device is available for measurement, considering the noisy output of the sensor of the field device, the numerical differentiation would be too noisy. The noisy control input made from these signals, not only could damage the field device, but also would make less accuracy in tracking and then instability in the control scheme.

In summary, there is a need for a FDD algorithm which is carried out advanced FDD methods capable of root cause diagnosis at local component level as well as system supervision at global plant level. In the literature review such a method that fulfilled the requirements was not found and therefore it was necessary to develop a new method.

1.3 Objectives of the Thesis

Motivated by the above considerations, this thesis is concerned with the challenges of applying system inversion and model based FDD techniques theory to handle the joint problem of fault diagnosis locally and performance monitoring globally. Since early detection of component malfunctions plays a fundamental role in advanced corporate management and in predictive maintenance planning, the major objective of the thesis is to detect incipient/abrupt faults resources of the components operation by diagnosing the failed component subsystem locally, thus in an attempt to prevent the development of possibly global malfunctions of the system liable to cause performance degradation or even

destruction. However, as mentioned above, both system level diagnosis and component level diagnosis have the weaknesses and strengths. As a consequence of these difficulties, the analysis and synthesis tasks cannot be solved efficiently in a single step diagnosis by “conventional” methods. As a solution, we try to develop a hybrid approach that combines different methods, thus, the weaknesses of individual methods can be compensated and more accurate diagnosis results obtained. For that, it is then to decompose the overall system into several subsystems and develop the FDD algorithm from the view point of both local and global system, the algorithm of design is illustrated in Fig. 1.3.

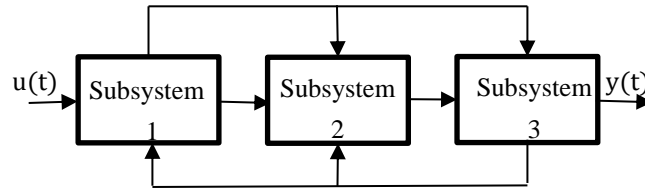


Fig 1.3 System decomposition and interconnections

As shown in Fig. 1.3, this thesis addresses fault diagnosis from a lower level with component subsystem of the plant (i.e. actuator) and deal generally with global system supervision to meet the growing need. The role of the developed performance monitoring and fault diagnosis system is to utilize the measured data to enhance the economics and safety of the interconnected dynamic system. The information that can be obtained from the developed system will include only the performance of critical parameter, such as temperature of continuous chemical reactor, and manipulated variables of the component such as the input of the reactor main control valve. The attempt is to explain how the behavior of overall output can be interpreted to identify subcomponent faults in component subsystem, so as to carry out advanced FDD algorithm for recognizing root causes of detected faults. In this way the faults can be detected through detecting changes in the operation points of the internal variables of subcomponent that was observed by analyzing the behavior of the internal variables. Ideally, this local intelligent FDD system can be part of the top level based monitoring system and can identify locally all the factors or the problems limiting the efficiency of the local process.

The advantages of using multilevel based diagnosis can be found from either economy or reliability standpoints. On one hand, this system will enable individual component to monitoring internal dynamics locally to improve plant efficiency and diagnose potential fault resources to locate malfunction when operation performance of global system degrades or have measurement faults. This reduces the complexity of the centralized or distributed monitoring system because the dimensionality problem, the number of sensors, wires, and diagnosis loops connected to the monitoring system is reduced. Since when the system is too large to be dealt with by centralized control, it is computationally efficient to use only local information, i.e. local states or outputs, to make the control decision. On the other hand, the obtained information is assumed to be only global output, this can be more realistic and technical availability because field devices are normally remote from the control room and additional sensors may cause reliability and economical problem. Except for a few, most researchers in fault diagnosis are paying more attention to the academic value than the engineering

value, therefore this consideration bridges the gap between the theoretical research on computational intelligence and the engineering design in performance monitoring and fault diagnosis.

In order to achieve the objectives, there are several tasks that the new nonlinear FDD schemes need to study. The first intention is to develop a reasonable system structure for the FDD algorithm, by which local faults can be distinguished globally. The second intention is to establish a complete observer based FDD framework for local nonlinear subsystems. In the following, the concrete objectives are presented.

1.3.1 Form an Invertible Interconnected System Structure

As mentioned above, a modern control system can be analyzed at different levels down to the component level in estimating the reliability of the whole plant. Therefore the first consideration is to answer the question of how to decompose the given control problem into manageable sub-problems, thus forming a dynamic system structure. Due to the extremely important status and increasing complex dynamics of actuator, in this thesis, we mainly focus on internal dynamics supervision of actuator. Therefore we develop an interconnected dynamic system by considering that actuator is viewed as subsystem connected with the process subsystem in series. And through the overall system, the only available measurement is the output of the terminal process subsystem. We then consider the problem that arises when the output from the low level nonlinear subsystem is not available directly, but instead available via a second nonlinear subsystem. That is, the output from the low level nonlinear subsystem acts as the input to a high level subsystem, from which output measurement is in turn available. This situation results in a cascade interconnection that is illustrated in Fig. 1.4.

As shown in Fig.1.4, an interconnected system Σ is considered which consists of two subsystems: actuator Σ_a and process Σ_p subsystems. The vector u represents the input vector of the actuators subsystem, which is also the input of the series system, v is the fault vector related to parameter variations of actuator subcomponent or external disturbances, u_a is the actuators output vector, also the input of process subsystem and y is the output vector of the process subsystem, also the output of the overall series system. The basic idea is to identify the fault v at local level, while monitoring dynamics of the overall plant at global level.

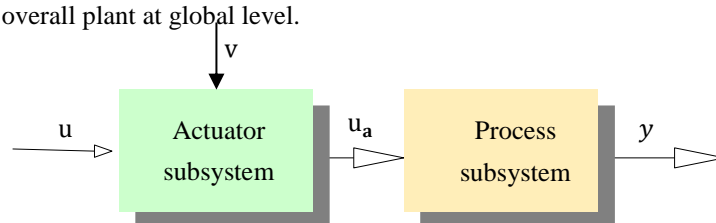


Fig. 1.4 An interconnected system structure

A key feature, opportunity and technical challenge of the scheme is to obtain the conditions by which the information (useful input u or faults v) issued by actuator subsystem can completely be transmitted to the final terminal, and have distinguishable effects on the output of the process system y . In this way, we can recognize actuator faults in local subcomponent while utilizing the measurable output y of the

process system. With respect to this consideration, if v is viewed as unknown input in the system, this can be seen as problem of input observability. And input or fault observability is equivalent to left invertibility of the system. In [60], input can be uniquely recovered from output and the initial state if dynamical system is left invertible.

We then consider a left invertible interconnected nonlinear system structure by which actuator is viewed as subsystem connected with the process subsystem in cascade manner, thus identifying component faults with advanced FDD algorithm in the subsystem. The left invertibility of the interconnected system is required for ensuring faults occurring in actuator subsystem can be distinguished globally. In this case, the performance of the overall interconnected system and fault occurrence are recognized by a system level based diagnosis algorithm while several independent local diagnosis subsystems are responsible for potential fault candidates of internal component. These two algorithms together perform the monitoring and diagnosis function of the overall interconnected system. The interconnected system is described by the following modelling statements.

1-) Process subsystem modelling

Model based FDD makes use of mathematical model for the purpose of system supervision. The goal within these methods is to generate symptoms that react only to faults in the system being monitored. These symptoms can be based, for example, on the difference between the model outputs and corresponding measured sensor signals from the system being monitored. However, a perfect complete mathematical model of a physical system is not available. Hence, one of the major concerns in the designing failure detection systems is detection performance, i.e., the ability to detect and identify faults promptly with minimal delays and false alarmed even in the presence of uncertainty. It is practically impossible to detect the failures with unlimited sensitivity. Obviously, finding a tradeoff between the sensitivity and disturbances attenuation of the methods is an important design issue.

Assuming the MIMO process subsystem is on input affine nonlinear system which is a common considerations involving system inverse, and is described by (1.1):

$$\Sigma_p: \begin{cases} \dot{x} = f(x) + \sum_{i=1}^m g_i(x)u_a \\ y = h(x, u_a) \end{cases} \quad (1.1)$$

where the state of the process subsystem vector $x \in M$, an n -dimensional real connected smooth manifold, e.g. \mathcal{R}^n . f, g_i are smooth vector field on M , $u_a \in \mathcal{R}^m$ is the input of process subsystem, which is also the output of the actuator and which we assume to be inaccessible and want to estimate on the basis of measures that taken on the evolution of the system, $y \in \mathcal{R}^p$ is overall system output. If initial conditions are specified, the relevant equation $x(t_0) = x_0$ is added to the system.

2-) Component subsystem modelling

The main objective of component modelling is to provide a detailed mathematical model for a filed device, i.e. electro-pneumatic actuator, which accurately represents the behavior of a real component,

including the inherent nonlinear characteristics and can be simplified in terms of computability, to be suitable for diagnostic purposes. Although compared with the number of publications on modelling of a process plant, the number of publications that include modelling aspects of field devices is much lower, it has been possible to analytically model dynamics of many kinds of actuator, such as control valve modelling in [52], serve motor in [53]. Their nonlinearities have been identified and estimated through selected parameters. The models that were derived have been verified with measurements and the modeling error is found to be acceptable for the fault simulations. Typical types of faults candidates have been simulated and the impacts on the internal variables of performance analyzed.

Normally, an actuator subsystem can be described by (1.2):

$$\Sigma_a: \begin{cases} \dot{x}_a = f_a(x_a, u, \theta_{fa}) \\ u_a = h_a(x_a, u, \theta_{fs}) \end{cases} \quad (1.2)$$

where $x_a \in \mathcal{R}^n$ is the state, $u \in \mathcal{R}^l$ is the input, $u_a \in \mathcal{R}^m$ is the output of the actuator subsystem, which is also the input of the process subsystem, $\theta_{fa} \in \mathcal{R}^q$ represents the actual subsystem parameters (i.e., when no faults are present in the system), $\theta_{fa} = \theta_{fa0}$ where θ_{fa0} is the nominal parameter vector (understanding "fault" as an unpermitted parameter deviation in the system), $\theta_{fs} \in \mathcal{R}^q$, represents the parameters in the output equation (if a sensor fault occurs $\theta_{fs} \neq \theta_{fs0}$, where θ_{fs0} represent the nominal parameters in the output equation).

Thus an interconnected system Σ is then constructed by these two subsystems Σ_a and Σ_p subsystems whereby the input is vector of u while output vector is y .

Assumption 1.1: The input vector of both subsystem u_a and u are locally essentially bounded function: $u_a(\cdot) \in [t, \infty) \rightarrow \mathfrak{R}^m$, $u(\cdot) \in [t, \infty) \rightarrow \mathfrak{R}^l$, if two inputs differ on a set of measure zero, i.e. almost everywhere (a.e), then they are considered to be equal.

If fault v is as integration of either parameters fault θ_{fa}, θ_{fs} or other disturbance signals, a fault mode of (1.2) is then obtained:

$$\Sigma_a: = \begin{cases} \dot{x}_a = f(x_a, u) + \sum_i^m g_{ai}(x_a, u)v_i \\ u_a = h_a(x_a, u) + \sum_i^m l_{ai}(x_a, u)v_i \end{cases} \quad (1.3)$$

Where g, l are analytic functions of the system subject to multiple, possible simultaneously faults. The $v(t)$ is the fault signal (v_1, \dots, v_m) whose element $v_i: [0, +\infty) \rightarrow \mathcal{R}$ are arbitrary functions of time.

Remark 1.1: the fault $\sum_i^m g_{ai}(x_a, u)v_i$ represents the parameters fault in θ_{fa} or external disturbance while $\sum_i^m l_{ai}(x_a, u)v_i$ represents the parameters faults in θ_{fs} or external disturbance. Effect of faults on outputs is independent.

And the detectability of one fault in nonlinear system (1.3) can be defined as:

Definition 1.1: the fault $v_i, i = 1, \dots, m$, is said to be non-detectable if for $v_i \neq 0$ the relation

$$u_a(x_{a0}, x_a, u, 0) = u_a(x_{a0}, x_a, u, 0, \dots, v_i, \dots, 0)$$

is satisfied; if not, the fault v_i is detectable.

Definition 1.2: the fault $v_i, i = 1, \dots, m,$ is said to be detectable and has independent effect on the system output y if the series system is invertible.

1.3.2 Performance Monitoring of the Interconnected System

A main task of the proposed strategy is to solve the problem of performances supervision of the interconnected system through available measurements. Performance supervision includes accurately estimate online the states vector of both subsystems. The problem of state observation is then addressed for invertible interconnected nonlinear systems that are modeled by two nonlinear interconnected series association. It is computationally efficient to use only local information, i.e. local inputs and outputs, to design a local observer for each subsystem independently and check the stability of the overall system. In this case, the observer can estimate the states precisely without any other uncertainties. However, the major difficulty is that the state observation can only rely on the output of the global system, i.e. the process at the terminal boundary. In particular, the connection point between the subsystems is not accessible to measurements. Instead, it acts as an input to the process subsystem from which physical measurement is in turn available. This is because the connection is the output of the actuator subsystem where the measurement is assumed not available. In this case, indirect measurements have to be used to infer the interconnection status using an estimation procedure from the available measurements.

The difficulty of states reconstruction for the interconnected system is then obvious since it can be seen that the unavoidable inaccurate estimation of interconnection may prevent the estimation error of the overall observer from reaching zero value. In order to achieve the robust estimation goals, as well as overcome the difficulties, we develop an interconnected observer design methodology for the resulting interconnected system, based on estimating the unavailable interconnection together with the states of both subsystems. The observer structure of the system is illustrated in Figure 1.5 with two interconnected estimators.

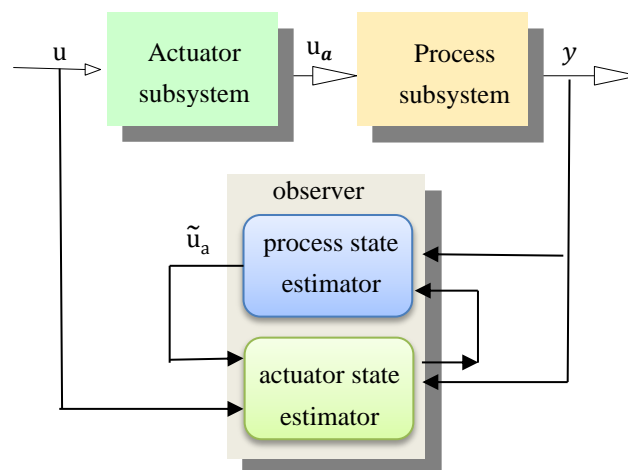


Fig 1.5 observer structure for interconnected system

The main idea of the interconnected observer design is as follows: in the first aspect, the unknown information of the interconnection is extended as new states of the process subsystem whose expression can be achieved by computing derivatives output expression of actuator subsystem, forming

a new process subsystem. For the states estimation of each subsystem of the interconnected system, it is proposed the use of the global observer using the state estimation of the other subsystem, and we insure the asymptotic stability of the overall estimator which is formed by the gathering of all the observers.

1.3.3 Multi-level Fault Diagnosis and Root Cause Analysis

Another major objective of the thesis focuses on the problem of model based fault detection and diagnosis (FDD) and root cause analysis (RCA) for a multivariable interconnected dynamic system. In the proposed multilevel based FDD architecture, a FDD component is designed for each subsystem of the interconnected system. For each subsystem, the performance may be affected by parameter variations, external disturbances, interconnection from other subsystems, and modelling uncertainty arising from structure uncertainty. The FDD is designed to overcome the problems associated with modeling errors that has to be robust, i.e., is able to distinguish between model uncertainties and failure modes and separate the effects of unmolded dynamics or uncertain knowledge of the system parameters, thus avoiding excessive false alarms or missed detections.

Therefore, in this method the faults involved are parameter variations and external disturbances which can be detected through detecting changes in the operation points of the internal variables that are observed by analyzing the behavior of the internal variables. Its corresponding local FDD component is designed by utilizing local measurements and estimation information from neighboring components subsystems that are directly interconnected to the particular subsystem under consideration. A novel fault detection and isolation scheme is then developed and some of its properties, such as the fault detectability and isolability conditions are rigorously investigated.

a-) Observer design for inverse system

In the first place, the input reconstruction method based on the dynamic inverse system may cause the reconstruction to be unavailable due to the initial state disturbance, drift and other factors. In order to eliminate these unfavorable factors, the input estimation value provided by the interconnected system, together with the dynamic inverse system, can be used to construct an observer for the inverse system. As shown in Fig. 1.6, the input of the observer is the measurement y , its estimated output is the \tilde{u}_a , the reference output is \hat{u}_a made by the previous interconnected observer. If convergence is expected then, there should be $\tilde{u}_a = \hat{u}_a = u_a$. While if there is fault detected, the RCA filters are triggered, where output used by the filter is obtained by system inversion based input reconstruction. This input reconstruction value is available now since disturbance, drift have already eliminated during observer operation.

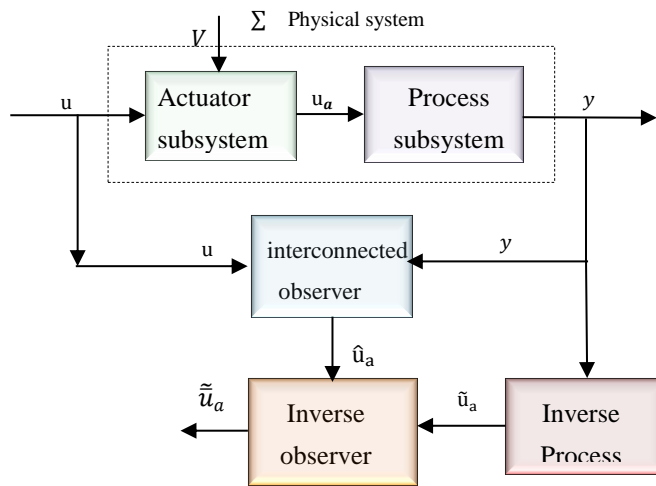


Fig 1.6 observer for inverse system of process subsystem

b-) RCA filter design

The attempt is to explain how the behavior of overall output can be interpreted to identify subcomponent faults in actuator subsystem, so as to carry out advanced FDD algorithm for recognizing root causes analysis of faults. As shown in Fig.1.7, the overall objective is to identify the occurrence of the fault v_i in (1.3) independently from each other whilst monitoring the overall plant at both local and global level, as required for reliable operation of complex and high interconnected process system. Fault v_i refers to the parameter variations which are related with special physical meaning, e.g. v_i represents fault caused by leakage or valve clogging of an actuator. To realize these causes of an actuator fault is defined as root cause analysis (RCA) in this work. We assume to feed the FDD strategy with input u and output u_a of actuator subsystem at local level, so as to achieve root cause analysis. However, online diagnosis of actuator component is often achieved by a remote supervisory diagnostic system, therefore, to a large extent, it is impractical to measure u_a in realistic industrial condition, so u_a is supposed to be inaccessible in this work. Besides, in order to monitor the plant at a global level, information of global level should be included when FDD function is performed at local subsystem. It became apparent that the FDD algorithm design of an interconnected system with multilevel based consideration requires that the interconnection be treated as special signals. If u_a can be estimated from the global level measurement y uniquely, then the above two problems can be solved. In that way, the residual generator of advanced FDD strategy performs some kind of validation of the nominal relationships of the system, using the actual input u , and output \tilde{u}_a reconstructed from measured output y . Hence, a means of monitoring and diagnosis of the overall plant at both local and global level is provided, which results in improved fault localization and provides better predictive maintenance aids.

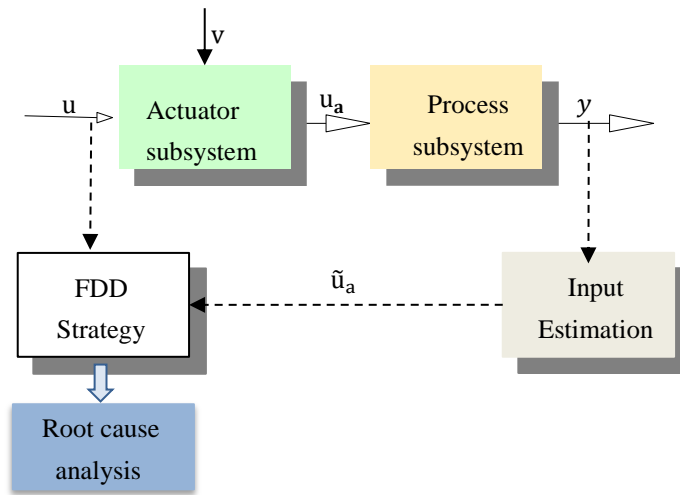


Fig.1.7 FDD algorithm for component FDD and RCA

As mentioned above, invertibility of the interconnected system can be a solution for guaranteeing that the information of actuators subsystem has distinguishable effects on system output. Moreover, an essential requirement of the combination of individual actuator with an advanced diagnostic capability to perform FDD functions is the availability and reliability of the output of the actuator subsystem u_a , which is also the input of the process system. This problem is considered as input reconstruction problem, which can also be viewed as problem of system inversion, as shown in Fig.1.7.

In summary, if the overall cascade system is invertible, fault vector v has distinguishable effect on system output vector y . While if process subsystem is invertible, u_a can be uniquely reconstructed by output vector y , in that case, reconstructed \tilde{u}_a and fault vector v also has one to one relationship. Then, one can utilize advanced FDD strategy in actuator subsystem while use the output vector y of the interconnected system to identify v , thus achieving FDD at local level while monitoring the whole system at global level. Above all, the key problem is to provide condition for guaranteeing invertibility of the overall cascade system and individual subsystems.

1.4 Contributions and Challenges of the Thesis

We propose a left invertible interconnected nonlinear system structure with a dynamic inversion based input estimation laws, forming a novel model based multilevel based FDD algorithm. This algorithm provides a systematic solution to performance monitoring and fault diagnosis for nonlinear dynamic system. The new system structure, together with the fault diagnosis algorithm design, is the first to emphasize the importance of root cause analysis of field devices fault, as well as the influences of local internal dynamic on the global dynamics. The developed multi-level model based fault diagnosis algorithm is then a first effort to combine the strength of the system level and the component level model based fault diagnosis. With the achievements of the above mentioned objectives, faults will be detected more quickly and fault location will be more precise, while there will be less number of false alarms. The primary advantages of the proposed FDD algorithm over the traditional methodology include improved control performance, low cost, reduced computation at resource requirements, reduced wiring requirements, simple installation and maintenance, and system agility.

The following original contributions are made in this thesis:

1-) Create the invertible interconnected nonlinear system structure

We propose a left invertible interconnected nonlinear system structure which guarantees that faults occurred in field devices subsystem will affect the measured output of the global system uniquely and distinguishably.

2-) Provide the condition of invertibility of the overall interconnected dynamic system

We prove that the left invertibility of individual subsystem is the necessary and sufficient condition which ensures invertibility of the interconnected system.

3-) Output estimation for unmeasured field devices

Output of the field device is supposed inaccessible, it is realistic due to remote distance or physical availability considerations. By viewing this problem as unknown input of process subsystem, then a kind of unknown input reconstruction method which employs the combination of system inversion and sliding mode observer is proposed.

4-) Observer design for performance monitoring of the overall interconnected system

We develop an observer design methodology for the proposed interconnected nonlinear system. This observer is capable of estimating the states of each subsystem, thus components subsystem and the overall systems can be monitored and diagnosed under desired parameters which can reduce service costs, improve the effectiveness of maintenance support teams, and preventive maintenance programs.

5-) FDD algorithm for root cause analysis of a component fault

A major contribution is to utilize the global output to identify root cause of a subcomponent fault locally. That is to identify root cause of the detected faults on individual component system using information of the entire plant during operation. This identification problem can not only take place before problems become too serious so that to prevent major repairs and production breakdowns, but also take place online considering influence of the process, so as to monitor performance of the plant.

1.5 Thesis Outlines

This thesis is divided into nine chapters. The first three chapters serve as introductory material. The rest of the chapters summarize the contribution and research results of this study. The first chapter describes motivations, objectives and contribution of the thesis.

Chapter 2 gives an overview of fault detection and diagnosis (FDD) and presents some existing methods for FDD in nonlinear systems. It begins with the definitions of basic concepts such as faults, failures, fault detection etc. A classification of FDD techniques, with a brief discussion on each approach, is also presented in this chapter. An appropriate attention is paid to observer based methods, their robustness and sensitivity issues are elaborated. The chapter also presents FDD methods for

nonlinear systems, most commonly used observers for FDD in nonlinear systems are described in a bit details. State of the art methods for FDD in interconnected nonlinear systems are also presented.

Chapter 3 provides a general background to system inversion of linear and nonlinear model, and special attention is given to the non-minimum phase system. It contains some important concepts and definitions of left invertibility and the formal problem statement. The main results on methods of computing system inversion are presented. In addition, we review some existing research works focusing on the application of system inversion, including the areas of parameter identification, fault diagnosis and input reconstruction, etc.

Chapter 4 develops a left invertible interconnected nonlinear system structure. It first defines inversion of interconnected nonlinear system and form the problem statement of invertibility of the interconnected system. A necessary and sufficient condition is given which requires the invertibility of individual subsystems. After that we develop a complete procedure for checking invertibility of the given system. A simple example is provided to illustrate the proposed methods and to show its effectiveness.

Chapter 5 studies observers design procedure for estimating states of the proposed systems structure. The problem of state observation is addressed for interconnected nonlinear systems that are modeled by two subsystems connected in a cascade manner. The aim is to accurately estimate online the state vector of two subsystems. The major challenge is that the state observation must only rely on the global system output, because the connection point between the subsystems is not accessible to measurements. The observation problem is dealt with by designing an interconnected observer which is a combination of individual state estimators. Sufficient conditions are formally established that ensure the observer exponential convergence. In addition, the developed interconnected observer will provide initial condition for the input reconstructor and local fault filter once FD & RCA procedure is triggered by any fault

Chapter 6 introduces input reconstruction as a process where the inputs to a system are estimated using the measured system output. We consider three methods for achieving input reconstruction despite the presence of non-minimum phase zeros. One way to achieve this goal is to invert the system model and cascade delays to guarantee that the inverse is proper. The standing issue in input reconstruction lies in the inversion of non-minimum phase systems, since the inverse model is unstable. The second one is to reconstruct the input using differential algebra techniques. The last one is based on a high gain second order sliding mode observer which is considered to exactly estimate the derivatives of the output vectors in a finite time. Then, by using the estimates of output derivatives, a kind of algebraic input reconstruction method is proposed.

Chapter 7 presents a multi-level based FDD&RCA method for a class of interconnected nonlinear systems, in which faults caused by sensors, actuators and process are taken into account in the unified framework. Sensor measurements, together with estimation by extended high gain observers are

processed; aim at identifying sensor faults and providing adequate estimation to substitute faulty measurements. Then reliable measurements are fed to several banks of interval filters to generate several banks of residuals for each subsystem in the interconnected system, each bank of residuals is sensitive to a particular process parameter variables. By evaluating these residuals, root cause analysis of a detected fault is achieved. A novel FDD scheme is then devised, and the fault detectability and isolability conditions are rigorously investigated, characterizing the class of faults in each subsystem that are detectable and isolable by the proposed FDD&RCA method.

Chapter 8 gives the application of the multi-level based FDD&RCA method developed in Chapter 7 to the intensified HEX/Reactor system. The intensified HEX/Reactor system has high nonlinearities and is, therefore, proper used as a benchmark to test nonlinear control and FDD algorithms. After describing the intensified HEX/Reactor system, a fault detection filter is used to generate residual signal. Then several banks of interval parameter filters are designed and threshold is computed to give RCA of the detected actuator faults. The simulation results are presented which show that all the faults including sensor faults, actuator faults and component faults are successfully diagnosed and fault causes are identified correctly. Both abrupt and incipient fault situations are presented.

Chapter 9 summarizes and concludes the overall work described by the thesis and makes suggestions and recommendations as to how the research can be further developed in the future.

CHAPTER 2 MODEL BASED FAULT DETECTION AND DIAGNOSIS

TECHNIQUES

In this Chapter, a critical review is performed on the technical elements of fault detection and diagnosis (FDD) techniques with a special attention to model based FDD. First, fundamental terminologies, such as fault, failure, fault detection, and fault isolation are introduced. Then different types of faults and their effects on the performance of processes are explained. A widely accepted classification of FDD techniques is presented with a particular focus on the state of the art of quantitative model based FDD techniques. Most commonly used evaluation functions and threshold selection approaches are described. Subsequently, a review of the historical development of the observer based FDD technique is introduced in detail, the major issues and tools in its framework and roughly highlights the topics are addressed in this chapter. Finally, popular FDD methodologies for interconnected nonlinear system are reviewed.

2.1 Basic Concepts

The importance of fault detection and diagnosis (FDD) has been realized since the invention of machines. In the beginning, the condition of systems is determined by using human senses such as vision, hearing and smell, however, these senses are not enough to notice all changes in more complex systems. Therefore, devices to measure quantities, sensors, were developed, aim at saving extra resource and achieving more precise and quick detection of faults or some parts or location that may not be accessible to, or dangerous for human beings. When measurements become available, the next problem is, how to use the information provided by the sensors, to determine if a system is working well or not. Therefore advanced methods of supervision are developed and widely used for fault detection and diagnosis. To achieve this purpose, it is important to establish what events can be classified as a fault.

Definition of a fault given by [54] is widely accepted. A fault is defined as an unpermitted deviation of at least one characteristic property or parameter of a system from the acceptable/usual/standard behavior. It is the result of a defect in a component or subsystem which leads to degrade the functionality and performance of the system. A permanent fault may lead to a failure and terminate the ability of a subsystem or the whole system to perform its required function. From the view point of mathematical model, faults can be modeled as external inputs and/or parameter deviations which change the system characteristics. Similarly, uncertainties and disturbances can also be mathematically modeled as parameter deviation and/or external input as faults. In addition, disturbances and uncertainties have effects on the process similar to that of faults. However, unlike faults, disturbances are unavoidable and are present even during the normal operation of the process, so they should be taken into account in the control system design. Faults, by contrast, are considered as more severe changes by which the affects cannot be overcome by the design of the controller of the system.

Therefore it is necessary to detect the faults which may change the control system from the normal operation to a faulty mode.

In the following section, basic definitions of fault detection and isolation (FDD), such as faults, uncertainties, disturbances, and the descriptions of fault detection, fault isolation and fault analysis/identification and some existing methods for FDD in nonlinear systems are presented in detail.

2.1.1 Definitions of the Terminology

The terminology used in this thesis is more closely related to that proposed by [54]. The following list clarifies some expressions utilized in this work.

1-) Type of faults

A fault in a system is an external input that causes a deviation from the normal behavior of the system. Faults can be categorized from different aspects. Based on the physical location of their occurrence in the system, faults can generally be categorized into three types: component fault, actuator fault, and sensor fault. With respect to the way faults are modelled, faults can be categorized based on the way they are added to the system as additive and multiplicative faults, and based on the time behavior of faults, they can be classified as abrupt or incipient faults. Each of these faults and their effects are briefly described below.

A) Definition based on location of occurrence

(1) Component fault

These are the faults which appear in the components of the process and are categorized as process faults. Process fault alters the physical parameters of the process which, in turn, leads to changes of the normal system dynamics, e.g. leakage and loads. All faults that cannot be categorized as sensor or actuator faults are considered as component faults. They can be modeled as additive component faults or multiplicative component faults. An additive component fault causes changes in the system outputs independent of known inputs, unknown input signals are well described as additive faults. A multiplicative component fault is expressed as changes in process parameters. For example, in a continuous heat exchanger system, fouling may result in a component fault.

The common reasons for these faults are often due to structural damages, usually wear and tear, aging of components etc. Some examples of component faults are leakages in tanks, breakages or cracks in gearbox system, change in friction due to lubricant deterioration etc. Component faults may result in instability of the process. Therefore, it is extremely important to detect these faults.

(2) Actuator fault

Actuators are the components that are among the most critical and vital parts of the modern control system which are required to transform control signals into proper actuation signals, such as torques and forces, to drive the system. An actuator fault represents the discrepancy between the input

command of an actuator and its actual output. That means the final control element that gets activated, due to a malfunction and can drive the whole system into a state of fault. For instance, in an aircraft control system, control surface damage can be considered as an actuator fault. Actuators faults behave as partial or total (complete) loss of control action. An example of a completely lost actuator is a “stuck” actuator that produces no (controllable) actuation regardless of the input applied to it. Total actuator fault can occur, for instance, as a result of a breakage, cut or burned wiring, shortcuts, or the presence of outer body in the actuator. Partially failed actuator produces only a part of the normal (i.e. under nominal operating conditions) actuation. It can result from, e.g. hydraulic or pneumatic leakage, increased resistance or fall in the supply voltage. A fault in an actuator may result in higher energy consumption to total loss of control [7], and therefore a special attention is paid on the determination of this kind of fault. Examples of actuator faults include stuck-up of control valves, faults in pumps, motors etc. The actuator faults can be classified into four types [7], as shown in Fig. 2.1, namely: (a) lock-in-place, (b) hard-over failure, (c) float, and (d) loss-of-effectiveness. These faults may be formally represented as follows:

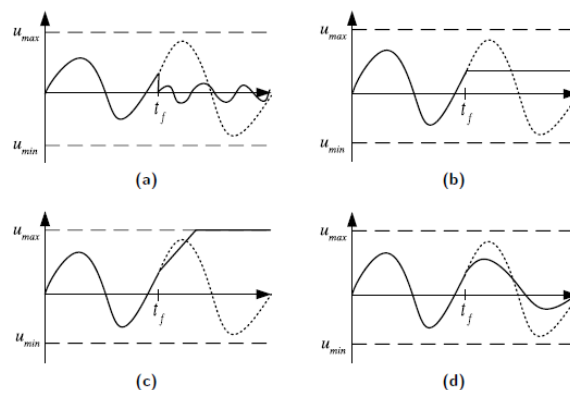


Fig. 2.1 Common types of actuator faults:

(a) lock-in-place, (b) hard-over failure, (c) float, and (d) loss-of-effectiveness

(3) Sensor fault

A sensor fault represents the deviation between the measured and the actual value of a plant’s output variable. Sensor faults can also be subdivided into partial and total. Total sensor faults produce information that is not related to the value of the measured physical parameter due to broken wires, lost contact with the surface, etc. Partial sensor faults produce reading that is related to the measured signal in such a way that useful information could still be retrieved. This can, for instance, be a gain reduction so that a scaled version of the signal is measured, a biased measurement resulting in a (usually constant) offset in the reading, or increased noise. These are faults occurring in measuring devices and are often best described as additive faults, e.g. bias. There are however situations where a multiplicative description is better, e.g. sticking or complete failure. Typical examples of sensor faults are listed in [7], as shown in Fig.2.2: (a) bias; (b) drift; (c) performance degradation (or loss of accuracy); (d) sensor freezing and (e) calibration error. Actuator faults and sensor faults are commonly modeled as additive faults in the system.

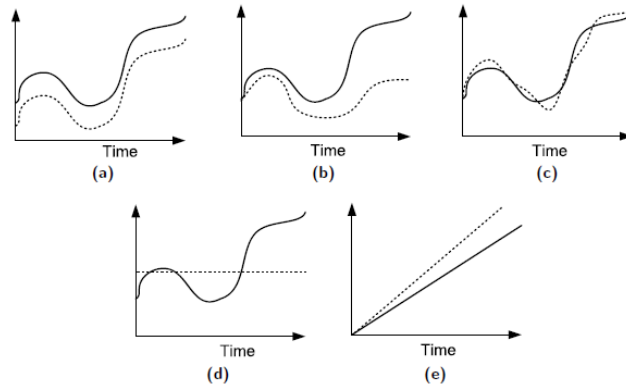


Fig. 2.2 Common types of sensor faults:

(a) bias; (b) drift; (c) performance degradation (or loss of accuracy); (d) sensor freezing; (e) calibration

B) Definition based on behavior of fault

In [55], faults can be distinguished by shape (systematic or random) according to the extension of the fault (local or global) or by their behavior over time. Moreover, according to the time profiles of faults, they can be classified as abrupt, incipient or intermittent fault, as shown in Fig. 2.3, where the notation t_f is the time of fault occurrence:

(a) Abrupt fault: An abrupt fault is a nearly instantaneous occurring fault, i.e., step-like change. Abrupt faults have more severe affects and may result in damage of equipment. However, fortunately abrupt faults are easier to detect.

$$f(t - t_f) = \begin{cases} \delta & t \geq t_f \\ 0 & t < t_f \end{cases}$$

(b) Incipient faults: An incipient fault is slowly developing; the magnitude of an incipient fault develops over a period of time. They are often modelled as a drift or time varying change in the parameters of a system. Incipient faults result in degradation of equipment. Their slowly changing behavior makes it difficult to detect.

$$f(t - t_f) = \begin{cases} \delta(1 - e^{-\alpha t}) & t \geq t_f \\ 0 & t < t_f \end{cases}$$

(c) Intermittent fault: In a system, the symptoms of an intermittent fault only show up at some time intervals or operating conditions, not all the time.

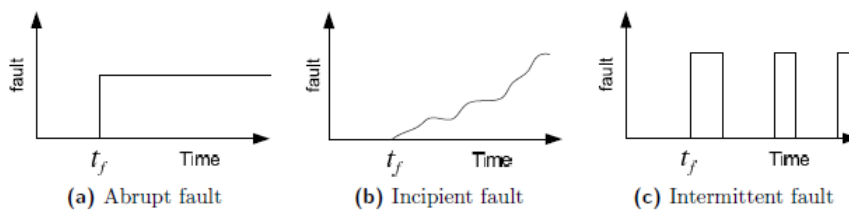


Fig. 2.3 Types of fault based on behavior

2-) Functions

The FDD procedure monitors the system and generates information about the abnormal behavior of its components, thus achieving the purpose of detecting faults and determining their location and significance. In general, the FDD procedure consists of three main steps namely fault detection, fault isolation and fault identification.

(1) Fault Detection

Fault detection is the process of determination of the occurrence and the time of the occurrence in a system. Fault detection consists of designing a residual generator that produces a residual signal enabling one to make a binary decision as to whether a fault occurred or not.

(2) Fault Isolation

The function of fault isolation is to exactly locate the reason and/or the origin of fault. The step of fault isolation ensures that we are able to retrieve some information about the fault such as fault type and/or location,

(3) Fault Identification

Fault identification aims at finding the magnitude and approximate time behavior of the fault.

(4) Fault Diagnosis

Fault diagnosis consists of determination of the kind, size, location, and the time of the occurrence of a fault. It includes fault detection and identification.

(5) Monitoring

Monitoring is a continuous online task of determining the conditions of a physical system, by recording information, recognizing and indicating anomalies of the system behavior.

3-) Models

(1) Quantitative model.

Quantitative model uses static and dynamic relations among systems variables and parameters in order to describe a system's behavior in quantitative mathematical terms.

(2) Qualitative model.

Qualitative model uses static and dynamic relations among systems variables and parameters in order to describe a system's behavior in qualitative terms such as causalities or if-then rules.

(3) Diagnostic model.

Diagnostic model describes a set of static or dynamic relations which link specific input variables - the symptoms - to specific output variables - the faults.

4-) Properties

Two important attributes that a fault detection and diagnosis (FDD) algorithm needs to possess are: few

missed detections and low false alarm rate. Next, we introduce some important properties for evaluating the performance of fault diagnosis schemes, including robustness, fault detectability and isolability.

(1) Robustness is the ability of the scheme to operate in the presence of noise, disturbance, and modeling errors, with few false alarms.

(2) Detectability and isolability are characterized by the class of faults which can be successfully detected and isolated. A successful fault diagnosis scheme should be able to detect and isolate faults of reasonably small sizes.

2.1.2 Classification of Fault Detection and Diagnosis Techniques

The idea of FDD is based on the fact that, though detection of change does not necessarily correspond to a failure, the faulty operation of the system is always preceded by certain changes in the dynamics. The fault detection and diagnosis implies the continuous monitoring of the whole process, including the sensors, actuators and control equipments. The simplest fault detection and diagnosis method is to monitor the magnitude and the trend of individual signals. If the magnitude exceeds the design limit or the trend deviates the expected behavior, a fault is then detected. Although this scheme is simple, it can be applied to simple processes with the aid of experienced operators for fault isolation.

The development of FDD theory and method has already been active since the early 1970's. As a result, a number of detection and diagnosis methods have been developed. Several authors have reviewed and classified these methods: early reviews of FDD methods have been published for example by [56][57] and more recently FDD methods have been comprehensively surveyed and classified by [16][17][18]. In the sequel, a rough classification of these techniques is presented as either data-driven or model-based.

1-) Hardware redundancy based FDD

One traditional method of FDD, mainly instrumental fault diagnosis (IFD) one, is hardware redundancy. The essential idea of this methodology can be realized by reconstruction of the process components using more than two components such as sensors, actuators, controllers, and computers to perform the same function. The fault detection is achieved by comparing the deviation between the actual process output and the output of redundant process component. If one component does not perform its function as designed, then a voting logic and a switching mechanism can be carried out to detect, identify, and isolate the malfunctioned component, as shown in Fig.2.4:

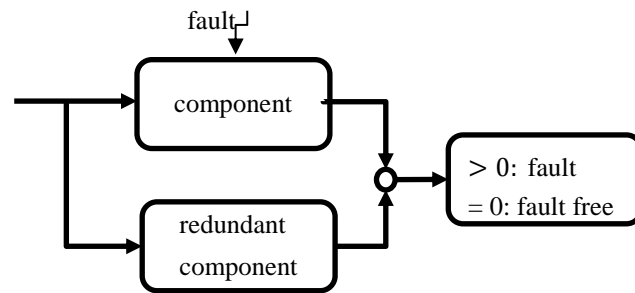


Fig. 2.4 Schematic description of the hardware redundancy scheme

Generally speaking, duplicating the actuators in the system in order to achieve increased fault tolerance is often not an option due to cost and sizes reasons. While because of the smaller sizes, sensors can be duplicated in the system to increase the fault tolerance. For instance, by using three sensors to measure the same variable one may consider it reliable enough to compare the readings from the sensors to detect faults in (one and only one) of them. The so-called “majority voting” method can then be used to pinpoint the faulty sensor. In [18], a section about voting techniques can be found along with several references. This approach usually implies significant increase in the related costs. Hardware redundancy is widely used in safety critical systems such as nuclear power plants and aircrafts. Some publications about hardware redundancy were presented in the second half of the 60s and the first half of the 70s. For example, aerospace task, flight control systems, etc. [4].

The main advantages of hardware redundancy is high reliability and direct fault isolation. However, in many situations, the application of hardware redundancy may not be possible or desirable, since the major problem of the hardware redundancy is in terms of volume, weight, the extra equipment, maintenance cost in addition to the extra space. In other situations, such as with actuators, direct access to certain variables is often not possible via physical measurements. Moreover, equal sensors installed at the same time have a tendency to become faulty almost simultaneously, since they have similar useful length of life. Thus its application is restricted to a number of key components which have a very high safety requirement. For example, in the aircraft industry, using hardware redundancy is a proven concept to diagnose sensor faults. Vital sensors are tripled or even quadrupled and faults in these sensors are diagnosed by using voting schemes.

2-) Analytical redundancy based FDD

Another kind of system redundancy is called analytical redundancy which is to reconstruct the process behavior accomplished by the functional relationships governed by physical laws in a process system [59]. In the context of analytical redundancy, the information about the fault is to compare the measured values with their estimates delivered by redundant relationships. The difference between the measured process variables and their estimates is called residual, which can be used as a fault signature for FDD. We generally define the redundant relationships as model. Therefore analytical redundancy based fault diagnosis is also called model based fault diagnosis methodology, which is defined as a systematic approach to generate residual quantities and analyze the residual properties such that the potential faults can be detected, identified and isolated. Based on what form of model is used for

achieving the purpose of residual generation, model based fault diagnosis scheme can further be divided into two categories. The mode can be quantitative model, an analytical model represented by set of differential equations, or it can be qualitative model, a knowledge-based model represented by, for example, neural networks, digraphs, experts systems, fuzzy rules etc.

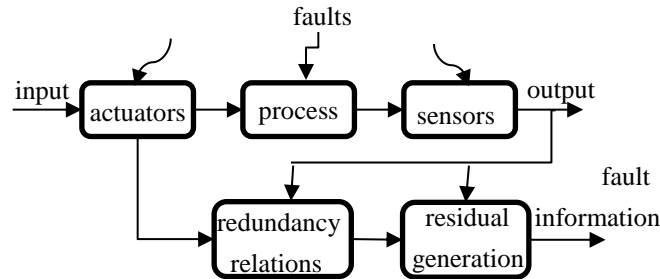


Fig. 2.5 Schematic description of the analytical redundancy scheme

The quantitative model based approaches utilize the deepest knowledge of the process, and therefore, are the most capable approaches for fault diagnosis given that the mathematical model of the process is available. Several early survey articles have been presented over the years on fault diagnosis utilizing a quantitative process model, e.g. [54] [60] [61]. Recent surveys can be found in [16][53]. Some books on the subject are e.g. [59] [55] Another possibility next to the quantitative model based methodologies referred to knowledge based fault diagnosis algorithms. Knowledge based model approaches do not need full analytical modeling, therefore, are more suitable in information-poor systems or in situations where the mathematical model of the process is difficult to obtain or is too complex [7]. This is the case, for example, in chemical processes which are difficult to model analytically. The main advantage of these methods is that they do not require a precise analytical model. A comprehensive study of these methods can be found in survey papers [17] [60] and recent books [62]. The main restriction of the so-called knowledge based FDD method is that they are depending on knowledge acquisition from the system in form of training data sets [60]. In practice these sets are difficult to obtain due to the fact that they must provide data from the system while the considered faults occur. Indeed, in a real running system it is hardly possible to convince the owner of a plant to simulate all possible faults. When knowledge based systems can be trained sufficiently they can be utilized to estimate measurements based on the available signal information, hence, provide redundancy.

A novel advantage of analytical redundancy based fault diagnosis is that no additional hardware is needed for fault detection and isolation since the intuitive idea is to replace the hardware redundancy by a process model which is used to cross check process variables. These algorithms can be implemented on some digital computer and hence avoided the disadvantages related to the hardware redundancy based fault detection techniques. Besides the analytical model based approaches are usually faster, as well as on-line implementation is easier, hence they are more suitable for processes with fast dynamics. Moreover since the redundancy provided by functional relationships has the same reliability as a processing computer, the reliability of analytical redundancy is much higher than traditional hardware redundancy. Another advantage is that it is applicable to IFD (instrument fault

diagnosis) as well as to AFP (actuator fault diagnosis) and to CFD (component diagnosis), while hardware redundancy is mainly applicable to IFD. Furthermore, the most significant contribution of analytical redundancy to fault diagnosis, which many researchers do not stress, is that the generated fault signatures are fully decoupled from the operation conditions if the developed functional relationships can cover entire operation regime. Given strengths, the field of model based FDD is well-studied.

3-) Signal processing based FDD

The essential idea of this approach is to get the information of the faults by collecting some properties of the measured signals [63]. Assuming that certain process signals carry information about the faults of interest in forms of symptoms, fault diagnosis can be achieved by suitable processing these signals, the symptoms can be such as the magnitudes of the time function, trend checking from the derivative, mean (arithmetic or quadratic) and variance, statistical moments of the amplitude distribution or envelope, spectral power densities of the frequency domain function, correlation coefficients, frequency spectral lines etc.

There are various approaches of signal processing. Several early survey articles have been presented in [57] [64] and book like [63]. Limit checking of absolute value of the measurements and limit checking of derivative (trend) of the measurements are the two most simple and widely used approaches in signal processing based schemes. Application of signal based methodologies can be found in various industry, such as mechanical machine. However, the drawback is that fault can only be detected when it grows enough to cross the limits. Moreover, signal processing based fault diagnosis approaches are only used for processes working in the steady state or with slow dynamics, not suitable for dynamic systems with transient behavior [8].

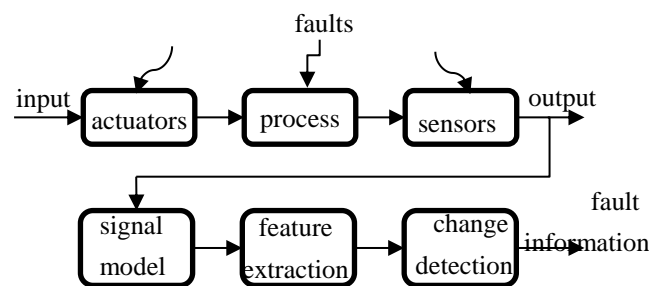


Fig. 2.6 Schematic description of the signal processing based scheme

4-) Comparison between different methods

In summary, signal processing based methods can be the option and useful when the mathematical model of a linear or nonlinear system is not available. It is because all signal processing based methods need data from both healthy and faulty operating conditions of the system under consideration. Therefore, it is difficult to design a generic signal processing based fault diagnosis method applicable to a wide range of systems. Moreover, collecting measurements in faulty conditions can be very costly and in some cases even impossible. By contrast, model based methods minimize the need for a priori

data and can perform online, but they require accurate mathematical model of the system. In fact, this is the fundamental difference between model based fault diagnosis and signal based fault diagnosis such as spectral analysis and pattern recognition. For signal based fault diagnosis, fault signatures need to be extracted from representative fault data, which are difficult to obtain in most situations. Whatever, among fault detection schemes, model based FDD techniques make use of the best knowledge of the monitored process for the purpose of system supervision. Therefore, model based FDD schemes are said to be the most capable approaches due to the advantages of low cost, fast detection, ability to deal with fast dynamical systems, when a process model is available and the requirement of FDD performance is relatively high. Nevertheless, the two abovementioned classes of fault diagnosis have become closer, as researchers have recently been tried to combine both methods, in order to eliminate the disadvantages of each method and construct more reliable and functional fault diagnosis schemes. For instance data, if available, can be utilized to tune the system model and also to determine robust fault detection thresholds. In both cases, fault diagnosis is done whereas prognosis is still in its infancy.

2.2 Quantitative Model-Based Fault Detection and Diagnosis Techniques

Most methods are covered by the term quantitative model based fault detection and diagnosis and there exists a wide variety of approaches, e.g. the observer-based approach [65][66], the parity space approach [67][68], and the parameter estimation approach [69][70]. A detailed description of the term model based FDD is given in [71]. Several survey articles have been presented over the years on fault diagnosis using a quantitative process model, e.g. [54] [57][16]. Some books on the subject are also available [55][63][59]. Additionally models can be grouped as linear or nonlinear based on their capability to deal with a mathematical relationship between physical quantities, depending on the problem at hand the most suitable models are chosen. The field of model based FDD for linear systems is well-studied, key references can be found in [61]. For nonlinear systems there also exist several model based FDD methods [31][23]. Especially the observer based approach has gained a lot of interest recently.

2.2.1 Introduction of Quantitative Model-based FDD Scheme

Quantitative model based FDD can be defined as the detection, isolation and characterization of faults in component of a system by comparing the available system measurements with estimates of these measurements using the mathematical model. The reflected inconsistencies between nominal and faulty system operation is called residual, and fault detection and diagnosis can be achieved by inspecting the residual. When an exact process model is available, the residual is only due to noise and disturbances. So the residual magnitude is zero or close to zero in the fault free case and become non zero as a result of a fault in the process. The procedure of creating the residual signal is called residual generation, while the procedure of checking the residual is called residual evaluation. Therefore model based FDD are composed of two parts: residual generation and residual evaluation. Fig2.7 illustrates the schematic of model based FDD.

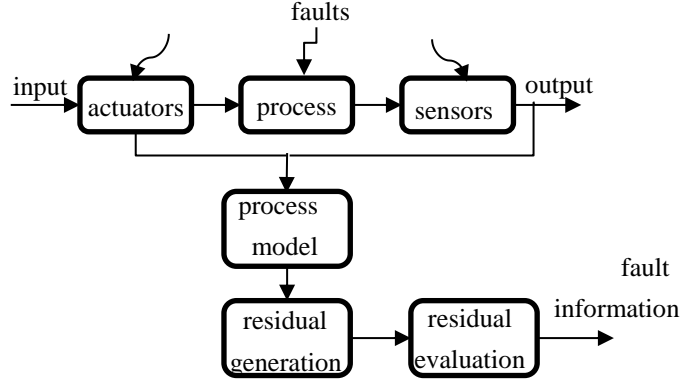


Fig. 2.7 Schematic description of the model based scheme

The residual generation step contains an estimator which uses a quantitative process model and derives an estimate of the process output. The purpose is to generate a fault indicating signal (residual) which is capable of reflecting the possible fault information of the analyzed system. The residual generation is therefore a procedure for extracting fault symptoms from the system, with the fault represented by the residual signal, thus the residual signal should ideally carry only the fault information. To guarantee reliable FDD, the loss of fault information in residual generation should be as small as possible. However, since modelling error and unknown disturbances are inevitable for technical process, the generated residual signal is usually non-zero even in the fault-free case. So a post processing of the residuals which extracts the information about the fault of interests from the residual signals is needed, which is called residual evaluation. The residuals are examined for the likelihood of fault. The residual evaluation step examines the residual signal or a function of it with a threshold for the likelihood of fault. The residual evaluation module has to detect, using adequate tests, when a given residual is indeed distinguishably different from zero. Residual generation and residual evaluation builds the core of the model based fault detection and diagnosis technique.

2.2.2 System and Fault Model for FDD

In order to simulate the behavior of the process components and control devices, an important issue is to build up a mathematical model of the system. While for the purpose of diagnosis of sensor, actuator, and process faults, the fault effects on the physical system should be explicitly represented by appropriate fault models. This explicit proper mathematical representation of fault effects, so that it can facilitate fault diagnosis such that the generated residuals will behave as designed.

Most of the real systems are nonlinear in nature, the process dynamics of a nonlinear system can be given by:

$$\begin{cases} \dot{x}(t) = f(x(t), u(t), \theta(t), \omega(t)) \\ y(t) = h(x(t), u(t), \theta(t)) \end{cases} \quad (2.1)$$

where $x(t) \in \mathcal{R}^n$ is the state, $u(t) \in \mathcal{R}^m$ is the input, $y(t) \in \mathcal{R}^p$ is the output of the system, $\theta(t) \in \mathcal{R}^l$ represents the system parameters (i.e., when no faults are present in the system, $\theta(t) = \theta_0$), where θ_0 is the nominal parameter vector (understanding "fault" as an unpermitted parameter deviation in the

system), and $\omega(t)$ represents modelling mismatches (if the model of the system is perfectly known, $\omega(t) = 0$).

If the sensor dynamic is ignored, let $y'(t) \in \mathcal{R}^p$ be the actual sensor outputs and $y_0(t) \in \mathcal{R}^p$ be the expected one (fault free), then the fault model for sensor faults can be generally described as follows:

$$y'(t) = (I - \Gamma(t))y_0(t) + v \quad (2.2)$$

where $\Gamma(t) = \text{diag}(\alpha_1(t), \alpha_2(t), \dots, \alpha_p(t))$, $(I - \Gamma(t))y_0(t)$ represents the effect of multiplicative sensor faults, and $v = \text{diag}(v_1, v_2, \dots, v_p)$ corresponds to the effect of an additive sensor fault as constant offset, the i th sensor is faulty if $\alpha_i(t) \neq 1$ or $v_j \neq 0$.

Case 1. $\Gamma(t) = 0, v \neq 0$, bias fault;

Case 2. $\Gamma(t) = I, v \neq 0$, freezing;

Case 3. $\Gamma(t) \neq 0, v = 0$, lost of accuracy;

Case 4. $\Gamma(t) = I, v = 0$, calibration;

Case 5. $\Gamma(t) = 0, v = 0$ drift.

If the actuator dynamics is ignored, let $u'(t) \in \mathcal{R}^m$ be the actual output of the actuators and $u_0(t) \in \mathcal{R}^m$ be the expected one (fault free), then the fault model for an actuator can be generally described as follows:

$$u'(t) = \Omega(t)u_0(t) + \varepsilon \quad (2.3)$$

$\Omega(t) = \text{diag}(\mu_1(t), \mu_2(t), \dots, \mu_m(t))$, $\Omega(t)u_0(t)$ represents the effect of a multiplicative actuator fault, and $\varepsilon = \text{diag}(\varepsilon_1, \varepsilon_2, \dots, \varepsilon_m)$ corresponds to the effect of an additive actuator fault as constant offset, the i th actuator is faulty if $\mu_i(t) \neq 1$ or $\varepsilon_j \neq 0$.

Case 1. $\Omega(t) = I, \varepsilon \neq 0$, actuator bias fault;

Case 2. $\Omega(t) = 0, \varepsilon \neq 0$, actuator blocked;

Case 3. $\Omega(t) \neq I, \varepsilon = 0$, actuator lost of effectiveness;

Case 4. $\Omega(t) = 0, \varepsilon = 0$, float.

Obviously, the actual mapping between the actuator input $u_0(t)$ and the actuator output $u'(t)$ can be easily represented by changing (2.3) accordingly. Once the actual process inputs and outputs $u'(t)$ and $y(t)$ (usually not available for $u'(t)$) are measured by the input and output sensors, the general model FDD theory can be treated as an observation problem of the knowledge only of the measured sequences $u'(t)$ and $y(t)$ [69].

If a process fault results in a change in the system parameters, the model for the fault is given by:

$$\theta' = \theta_0 + f_\theta \quad (2.4)$$

Where $\theta'(t) \in \mathcal{R}^1$ is the actual parameter vector, and in a fault-free system, its nominal parameter vector is regarded as $\theta_0(t) \in \mathcal{R}^1$. While a system with fault is called post-fault system, a parameter vector difference f_θ denotes a fault.

2.2.3 Residual Generation Method

Residual generator transforms the fault symptoms from measurement space to a lower dimensional feature space, it plays an important role in model based fault diagnosis techniques. In order to generate residuals with the desired properties for FDD, various residual generation techniques have been developed in the last several decades. Although these techniques are related to each other and become equivalent in certain cases, they do have very different characteristics in terms of complexity, flexibility, and applicability. The most representative used analytical model based approaches for residual generation include the observer based approach, the parity equations approach and the parameter estimation approach.

1-) Observer based residual generation

Observers are computational algorithms designed to estimate unmeasured state variables due to the lack of appropriate estimating devices or to replace high priced sensors in a plant. The main idea of observer based residual generation is achieved by comparing measurements from process with their estimates generated through observers [63]. The weighted estimation error is then used as residuals for the purpose of FDD [71], the residual is normally zero, and becomes non zero as a result of fault, disturbance, noise or model uncertainties. Therefore the generated residual signal should be insensitive to noise, disturbance and model uncertainties, but sensitive to faults, so that a fault can be detected when the residual signal is not zero or close to zero. This can be done by using further available knowledge about the system or by using robust fault detection techniques. While for the purpose of isolating and identifying faults, these methods usually use a bank of state estimators where each one is sensitive to a fault or a set of faults and insensitive to other faults.

In the past few decades, the problems of nonlinear system observability and observer design have received considerable interests for systems that can be described by ordinary differential equations (ODEs). There are possibly three reasons for this particular attention to observer based methods. The first one is due to associated advantages of observer based approaches, e.g., quick detection, requiring no excitation signal, possibility of on-line implementation etc. Secondly, other model based approaches which include parity space approach and parameter identification approach are, under certain conditions or assumptions, a specific form of the observer based approaches. Thirdly, control engineers are more familiar with the concepts of observer design. There are various approaches for designing observers. Details are described in section 2.3.

2-) Parity equations based residual generation

The parity equation based method is one of the earliest approaches used for residual generation in technical systems. The main idea is to check the consistency of the parity equations of the system by

using the measurement; while the parity equations are derived from the system model or transformed version of the state space model. That means the mathematical model of the process is rearranged to obtain the parity equations which are algebraic equations that indicate an explicit relation between input and output time-sequence data vector. These parity relations can in principle be either based on direct redundancy or on temporal redundancy. Direct redundancy exploits relationships among instantaneous outputs of sensors and temporal redundancy exploits relationships among the histories of sensor outputs and actuator inputs [72]. Contributions of parity relation based FDD for nonlinear systems can be found in [73][72][31]. In [74], it is presented a parity space approach based on the inverse model of input output nonlinear systems. In [73], the parity space approach for linear systems is generalized to nonlinear systems described by TS fuzzy models. The parity space approach to fault diagnosis can significantly extend its application when temporal redundancy is utilized [73].

There is a close relationship between parity space approach and observer based approach. As shown in [59], parity space approach leads to certain types of observer structures and is therefore structurally equivalent to the observer based approach, even though the design procedures are different. Parity relations are therefore a special form of observers, called the dead-beat observers (i.e. observers having all the poles at origin). Compared to observer based approaches, parity space approaches are more sensitive to measurement and require the model to be known accurately, and therefore are especially suitable for additive faults.

3-) Parameter estimation based residual generation

As the name suggests, the essential of the parameter estimation based residual generation method is a procedure of on-line parameter identification. It is assumed that faults in systems are often reflected by variation of physical parameters such as length, mass, damping, stiffness and capacities, etc. Parameters are estimated on-line repeatedly using the input and the output of the system. Then the estimated parameters can be used to compare with the parameters of the reference model obtained in fault free condition. If the estimated parameter values deviate from their nominal values, then decisions about occurrence of faults are made. There are several parameter estimation techniques including least squares (LS), recursive least squares (RLS), extended least squares (ELS), etc. Literature [69] has shown how parameter estimation methods can be used for detecting process faults in continuous time systems and more FDD approaches based on parameter estimation can be found in [70] while applications to engineering industries can be found in [47] [63] .

An advantage of parameter estimation approach is that with only one input and one output signal, several parameters can be estimated which give a detailed picture on internal process quantities [15]. Another advantage of the method is that it yields the size of the deviations of process parameters which is very useful for fault analysis [11]. Moreover, parameter estimation based approaches need only the structure of the process, the requirements are less strict since the parameters to be estimated do not have to be known exactly. However, sufficient input excitation is required to achieve good estimation performance which may not be always available.

Parameter identification approaches have many similarities to observer based approaches. Compared to observer based and parity relation based methods, parameter estimation methods are more flexible in how faults can affect the system. Therefore, parameter estimation methods are more suitable for multiplicative faults detection, especially for multiplicative component fault detection, although it can also detect sensor and actuator faults.

2.2.4 Residual Evaluation Method

After residual generation, the second step in model based fault detection and diagnosis scheme is residual evaluation. Residual evaluation is a decision making stage which performs appropriate statistical testing on the generated residuals to make a decision on fault diagnosis, the proper scheme for residual checking play a significant role in the satisfactory performance of FDD scheme.

In ideal situations where existence of no disturbances or their effects on the residual signal is completely eliminated, no modeling uncertainties and the initial conditions of the observer are the same as that of the process, the residual signal will be zero. In that case, any deviation of residual from zero will indicate the presence of faults. However, these ideal situations are never attained and there are always modelling errors, initial conditions of the observer may be different from that of the process. These reasons cause the residual signal to deviate from zero even in the absence of faults. It may block the determination of occurrence for the likelihood of faults and a decision rule is then required to determine if any faults have occurred. The purpose of residual evaluation is the decision rule to decide the occurrence of faults even in the presence of disturbances and uncertainties. The evaluation of the residue should answer the following questions: 1. is there a fault? 2. if so, what fault is present?

Based on the type of system under consideration, the evaluation schemes can be roughly divided into statistical based methods and norm based methods. For stochastic systems, the statistical properties like mean, variance, likelihood ratio (LR), generalized likelihood ratio (GLR) are used for the evaluation of residuals [4]. For deterministic systems, the norm based residual evaluation is preferred, where different kinds of norm like L2, peak and also Root Mean Square value (RMS) are used. Besides requiring less on-line computation, norm based schemes also allow a systematic way for threshold computation.

2.3 Observer Based Fault Detection and Diagnosis Approach

2.3.1 A Brief Description of the Observers

Among all the FDD approaches, observer based methods are the most popular methods to be researched and applied [37]. Observers are mathematical frameworks used as powerful tools to estimate unmeasured states variables from a minimum set of measurements in dynamic linear and nonlinear systems. A fundamental characteristic of any observer is that it does not need to be initialized with the actual initial conditions of the state variables to study the dynamics of the system [7]. Furthermore, two statements are desirable for any observer design: 1-) If the observer is provided with the actual initial condition and if the measurement noise is negligible, then the estimation of the state can be considered exact and the estimated state becomes the true state (i.e., the estimation error is zero

all the time); 2-) If the observer is provided with an initial condition different from the real, then the estimated state converges eventually to the true state (i.e., the estimation error converges towards zero in a finite time).

It should be noted that there is a difference between observers used for the purposes of control and for the purpose of FDD. The observers designed for control are state observers, i.e., they estimate states which are not measured. In contrary, the observers designed for FDD are output observer, i.e., these observers generate estimation of the measured states. Generally, the existence conditions for diagnostic observers are much more relaxed than that for a state observer. Full state observers like fault detection filter are also widely used for residual generation, the extra design freedom is used to achieve fault isolation, unknown input decoupling etc. A special form is the fault detection filter, which generates estimation of all the states, irrespective of whether they are measured or not. In this case, these can be used both for control and FDD purpose.

Considerable attention has been paid in the literature to the construction of observers for nonlinear systems. Some survey articles in the area are e.g. [66]. Considerable researches on fault detection and diagnosis using observer based theory have been carried out recently including, e.g. the high-gain observer [75], sliding-mode observers [76] Luenberger-like observers [77], adaptive observer [78], unknown input observer [79]. For example, in [80], a high-gain observer for uniformly observable systems is derived and sliding mode observers are presented in [26]. While [81] presents a nonlinear adaptive estimator for fault detection. The application of observers in industry could be widely found like, in chemical industry, water treatment, aircraft, nuclear plant, wind tube engine etc. A survey of some observer design techniques for nonlinear systems is presented in the following.

2.3.2 Different Observer Design Methods for Nonlinear System

In order to achieve an optimal residual generation, considerable efforts have been devoted to develop observer based residual generator which fulfill the following two requirements: (1) robust to model uncertainties, disturbance and sensor noises; (2) sensitive to faults.

1-) Nonlinear identity observer

This approach to fault diagnosis was first proposed by Henry and Frank [66], the use of this approach for the detection and isolation of component faults, see also [82]. A more general class of faults in [66].

The starting point is the nonlinear model (2.1) and the following observer structure.

$$\begin{aligned}\hat{\mathbf{x}}(t) &= \mathbf{f}(\hat{\mathbf{x}}(t), \mathbf{u}(t), \boldsymbol{\theta}_0(t), 0) + \mathbf{K}(\hat{\mathbf{x}}, \mathbf{u})(\mathbf{y}(t) - \hat{\mathbf{y}}(t)) & (2.5) \\ \hat{\mathbf{y}}(t) &= \mathbf{h}(\hat{\mathbf{x}}(t), \mathbf{u}(t)) \\ \mathbf{r}(t) &= \mathbf{y}(t) - \hat{\mathbf{y}}(t)\end{aligned}$$

where $\mathbf{r}(t)$ represents residual, the design of the observer is under the assumption that there is no faults and no modeling uncertainties are present.

Defining the estimation error $e(t) = x(t) - \hat{x}(t)$, the error dynamics can be written as:

$$\dot{e}(t) = F(\hat{x}(t), u(t), \theta_0(t), 0)e(t) - K(\hat{x}(t), u(t))H(\hat{x}(t), u(t), \theta_0(t), 0)e(t) \quad (2.6)$$

$$r(t) = H(\hat{x}(t), u(t))e(t)$$

where $F(\hat{x}(t), u(t), \theta_0(t), 0) = \partial f(x(t), u(t), \theta_0(t), 0)/\partial x(t)$,

$$H(\hat{x}(t), u(t), \theta_0(t), 0) = \partial h(\hat{x}(t), u(t))/\partial x(t).$$

The gain matrix $K(\hat{x}(t), u(t))$ can be developed in such a way that the error dynamics $\dot{e}(t) = 0$ is asymptotically stable. In some situations, for example in Lipschitz nonlinear systems, a constant matrix will guarantee the stability [83]. For instance, when $h(x(t), u(t)) = Cx(t)$, then the matrix $K(\hat{x}(t), u(t))$ takes the form

$$K(\hat{x}(t), u(t)) = P^{-1}\hat{F}(\hat{x}(t), u(t))C^TQ$$

where the symmetric positive definite matrix $P = P^T > 0$ should be assigned such that:

$$K^TP(\partial f(x(t), u(t), \theta_0(t), 0)/\partial x(t))K|_{\hat{x}=x} < 0$$

where K is the highest rank right orthogonal matrix to C and

$$\hat{F}(\hat{x}, u) = \text{diag} \left\{ \frac{1}{2} \sum_{j=1}^n |\psi_{ij} + \psi_{ji}| \right\}_{i=1, \dots, n}$$

where ψ_{ij} is the ij^{th} element of the matrix $P(\partial f(x(t), u(t))/\partial x(t))|_{\hat{x}=x}$ and Q is a matrix satisfying $C^TQC - I \geq 0$.

2-) Extended Luenberger observer

Luenberger observer is one of the basic state estimator for linear system and is used for fault detection in linear systems. For nonlinear systems, one can linearize the nonlinear model at an operating point and then apply the Luenberger observer. A similar approach for state estimation and its application to fault detection has been proposed in [84]. However, if the operating region is too wide, the linearized model will deviate largely from the nonlinear model, particularly, if the system is operating away from the linearizing point. Therefore, over the years, research in the design of observers has encounter challenges due to the requirements of high accuracy and good prediction performances [85]. Many observers today are simply modifications and extended versions of the classical Luenberger observer. The idea of the extended Luenberger observer is to linearize the model around current estimate of states $\hat{x}(t)$, instead of a fix point (e.g. $x = 0$), and then apply the Luenberger observer. This type of observer is suitable for less complex linear systems with relatively simpler computational methods. While because of the requirements of repetitive calculation of observer gain (which means more on line computations) and the linearization errors, the extended Luenberger observer is rarely used in practice.

Consider, for example, the nonlinear system as:

$$\dot{x}(t) = f(x(t), u(t)), \quad x(0) = x_0 \quad (2.7)$$

$$y(t) = h(x(t), u(t))$$

where $x \in \mathcal{R}^n$ denotes the vector of state variables, $u = [u_1, \dots, u_m] \in \mathcal{R}^m$ denotes the vector of constrained input variables, $y \in [y_1, \dots, y_p]^T \in \mathcal{R}^p$ denotes the vector of output variables. $f(x) \in \mathcal{R}^n$ is a nonlinear vector function, $f(x)$ and $h(x)$ are assumed to be sufficiently smooth on their domains of definition.

Then an extended Luenberger observer is

$$\dot{\hat{x}}(t) = f(\hat{x}(t), u(t)) + K(\hat{x}(t), u(t)) (y(t) - h(\hat{x}(t), u(t))), \quad \hat{x}(0) = \hat{x}_0 \quad (2.8)$$

$$\hat{y}(t) = h(\hat{x}(t), u(t))$$

Where $K(\hat{x}, u)$ is the observer gain which is computed at each time instant in such a way that the eigenvalues of $((\partial f(x, u)/\partial x) - K(\hat{x}, u)(\partial h(x, u)/\partial x))$ are stable. The detailed study can be found in [86].

3-) Nonlinear unknown input observer (NUIO)

The origins of NUIOs can be traced back to the early 1970s, it is one of the most common approaches of robust observers which can tolerate a degree of model uncertainty and hence increase the reliability of fault diagnosis. The main idea of NUIOs is to decouple the residual signal from the unknown disturbances, it was introduced by the pioneering work [82]. Considerable contribution has been made in the observer design and improvement like in [87] Besides, a large amount of knowledge by using these techniques for model based fault diagnosis has been accumulated through the literature, such as [79].

Let us consider a nonlinear system can be decoupled as the following structure:

$$\dot{x}(t) = Ax(t) + B(y(t), u(t)) + Ed(t) + K(x(t), u(t))f(t) \quad (2.9)$$

$$y(t) = Cx(t) + K_s(x(t), u(t))f_s(t)$$

where $x(t) \in \mathcal{R}^n$, $u(t) \in \mathcal{R}^m$, $y(t) \in \mathcal{R}^p$, $d(t) \in \mathcal{R}^q$ denote respectively the state, the input, the output and the unknown input vectors, $f(t)$ represents the component or the actuator faults and $f_s(t)$ represents the sensor faults.

Then the observer is given by:

$$\dot{\hat{x}}(t) = F\hat{x}(t) + J(y(t), u(t)) + Gy(t) \quad (2.10)$$

$$r(t) = L_1\hat{x}(t) + L_2y(t)$$

For the observer to be decoupled from the unknown inputs $d(t)$ and sensitive to fault vector $f(t)$, following conditions on observer matrixes are required [82]:

$$TA - FT = GC, \quad \text{where } F \text{ is stable}$$

$$J(y(t), u(t)) = TB(y(t), u(t))$$

$$L_1T + L_2C = 0, \quad TE = 0$$

$$k\{TK(x, u)\} = \text{rank}\{K(x, u)\}$$

$$\text{rank} \left(\begin{bmatrix} G \\ L_2 \end{bmatrix} \right) = \text{rank}(K_s(x(t), u(t)))$$

Provided the above requirements are satisfied, the estimation can be defined as $e \triangleq Tx - \hat{x}$, the dynamics of the residual obey the following equations:

$$\dot{e}(t) = Fe(t) - GK(x(t), u(t))f(t) + TK_s(x(t), u(t))f_s(t) \quad (2.11)$$

$$r(t) = L_1e(t) + L_2K_s(x(t), u(t))f_s(t)$$

The class of NUIO focuses only on disturbances or fault detection related variables during the estimation process. They are mostly suitable for estimating disturbances and faults, which provide early warning to operators prior to causing disruption to the process units. The drawback of this approach is the hard existing conditions and the poor fault detectability. Moreover, the class of systems covered by this technique is very limited. There are some methods which can transform other nonlinear model to the form suitable for unknown input observer design approach; however, the existence conditions for such transformations are very restrictive. Even if the existence conditions are satisfied, finding the transformations involves the solution of higher order partial differential equations [8]. A direct extension of the UIO results in linear systems to the nonlinear case was considered in [66]. The approach takes advantage of the structure of the system model, which is assumed to be in observable canonical form. In this case, a constant state transformation could be used (as in the linear case), and a complete design procedure can be achieved.

4-) The disturbance decoupling nonlinear observer (DDNO)

The disturbance decoupling nonlinear observer (DDNO) proposed in [88] can be considered as an alternative to the NUIO approach, considering a more general class of systems. The basic idea was the same as for the NUIO, but a nonlinear state transformation based technique instead of a linear one is used. Apart from a relatively large class of systems for which they can be applied, even if the nonlinear transformation is possible it leads to another nonlinear system and hence the observer design problem remains open.

The class of systems that can be treated with this approach is described by:

$$\dot{x}(t) = A(x(t), u(t)) + E(x(t), u(t))\omega(t) + K(x, u)f(t) \quad (2.12)$$

$$y(t) = C(x(t), u(t))$$

where $\omega(t)$ represents modelling mismatches due to uncertain model parameters (if the model of the system is perfectly known, $\omega(t) = 0$), $f(t)$ represents the component or the actuator faults.

To decouple the states from disturbances, a nonlinear state transformation $z(t) = T(x(t))$ is used and the transformed system becomes:

$$\dot{T}(x(t)) = \frac{\partial T(x(t))}{\partial x(t)} (A(x(t), u(t)) + E(x(t), u(t))\omega(t) + K(x(t), u(t))f(t)) \quad (2.13)$$

The transformation should be such that the transformed system becomes unaffected by disturbances but still reflects the effect of faults. The desired transformation can be selected as:

$$\frac{\partial T(x(t))}{\partial x(t)} E(x(t)) = 0 \quad (2.14)$$

If such a transformation exists, the transformed system can be described by:

$$\dot{z}(t) = \frac{\partial T(x(t))}{\partial x(t)} (A(x(t), u(t)) + K(x(t), u(t))f(t)) \quad (2.15)$$

$$y^*(t) = C^*(z(t), u(t), y(t))$$

where the output has been transformed into a new form which has no longer the effect of disturbances, instead the new output depends only on the state z , the input u and the original output y . Authors in [88] have also discussed a special case when the disturbance distribution matrix is also dependent on u . In that case the required transformation will also depend on u .

After the transformation is achieved, the next step is to design an observer for the reduced system (2.15) using any observer design method, e.g., it can use nonlinear identity observer approach.

5-) High gain observer

High gain observer approach is developed for the input affine nonlinear systems based on a nonlinear transformation described in [83]. See also [89] for more advanced developments. Based on the transformed system model, a nonlinear observer can be designed where observer gain is obtained by solving a linear algebraic equation. This class of observer is designed for process systems whose dynamics are described by ordinary differential equations (ODEs) and are quite straight forward to implement. It can be applied to a large class of nonlinear systems and the observer design is carried out in a systematic way. However, a drawback of high gain observer is the high sensitivity of the nonlinear transformation to model uncertainties. Further, another drawback is the peaking phenomenon due to the very high observer gain, because the high-gain observer is based on the idea of selecting a sufficiently large gain in such a way as to dominate the nonlinear contribution to the dynamics of the estimation error. However, such a large gain may cause destabilization in the loop when the high gain observer is used in cascade with a feedback regulator.

Such an observer is a dynamic system with a copy of the original dynamics and a correction term based on the output error, i.e., the difference between the current output and the output “predicted” by the observer itself.

The class of nonlinear systems covered by the approach is represented by:

$$\dot{x}(t) = A(x(t)) + g(x(t)) + \sum_{i=1}^m u_i \psi_i(x) \quad (2.16)$$

$$y(t) = Cx(t)$$

Where $A = \begin{bmatrix} 0 & 1 & \dots & 0 \\ \vdots & & \ddots & \vdots \\ 0 & 0 & \dots & 0 \end{bmatrix}$, $g(x) = \begin{pmatrix} 0 \\ \dots \\ g_n(x) \end{pmatrix}$, $C = [1, 0, \dots, 0]$, $\psi_i(x) = [\psi_1(x), \dots, \psi_n(x)]$

With the assumption that $g(x)$ and ψ_i are globally Lipschitz, an observer is of the form:

$$\hat{x}(t) = A(\hat{x}(t)) + g(\hat{x}(t)) + \sum_{i=1}^m u_i \psi_i(\hat{x}(t)) - S_\theta^{-1} C^T (C\hat{x}(t) - y(t)) \quad (2.17)$$

where S_θ is the unique solution of the Lyapunov algebraic equation:

$$\theta S_\theta + A^T S_\theta + S_\theta A - C^T C = 0 \quad (2.18)$$

The high gain observer design approach was extended to a more general class of nonlinear systems in [95]. The class of systems is:

$$\dot{x}(t) = A(t)x(t) + \psi(t, u, x) \quad (2.19)$$

$$y(t) = Cx(t)$$

Where $A = \begin{bmatrix} 0 & a_1(t) & \dots & 0 \\ \vdots & & \ddots & \vdots \\ 0 & 0 & \dots & 0 \end{bmatrix}$, $c = [1, 0, \dots, 0]$ and the i th component $\psi_i(t, u, x)$ is such that:

$$\psi_i(t, u, x) = \psi_i(t, u, x_1, \dots, x_i)$$

Furthermore, the following two assumptions are satisfied: ψ is globally Lipschitz with respect to x and t , locally with respect to u ; $a_i, i = 1, \dots, n - 1$ are known differentiable functions with unknown derivatives, and there exist $\epsilon > 0, M' > 0$ such that, for every $t \geq 0, \epsilon \leq |a_i(t)| \leq M$ and $\left| \frac{d}{dt} a_i(t) \right| \leq M', \text{ for } i = 1, \dots, n - 1.$

Then an observer for (2.19) is of the form:

$$\hat{\dot{x}} = A(t)\hat{x} + \psi(t, u, \hat{x}) - \Lambda^{-1} S_\theta^{-1} C^T (C\hat{x} - y) \quad (2.20)$$

where S_0 is the unique solution of (2.18) and Λ is then an $n \times n$ matrix:

$$\Lambda^{-1} = \text{diag} \{1, a_1(t), a_1(t)a_2(t), \dots, a_1(t) \dots a_{n-1}(t)\}$$

6-) Adaptive nonlinear observer (ANO)

One problem of the observer based methods for fault diagnosis is their weakness in detecting slowly developing faults, especially when model uncertainties are present [82][90]. To overcome this difficulty, an adaptive observer proposed in [90] could be a solution. Adaptive observers are based on online adaption for joint estimation of state and some parameters (or for state estimation only, despite the presence of some unknown parameters) [19][25]. Early works on adaptive observers for linear systems have been developed in the 70s. The design for nonlinear case is from the early 90s. Nonlinear adaptive observer can be achieved for the nonlinear systems whose dynamics can be linearized by coordinate change and output injection [91], or it can also be accomplished by some Lyapunov functions satisfying particular conditions instead of linearization [92]. Adaptive observers provide direct and indirect methods for fault diagnosis if the estimated parameters are related to faults. They have been utilized for fault diagnosis by different authors, such as [22][20]. For example in [20], a nonlinear observer is used in order to detect sensor and actuator additive fault in a waste water treat process, and the observer's performance is improved with online adaptation. While in [19], an observer is proposed which allows not only detect and isolate additive fault ,but also non-additive faults, each observer is designed to estimate one parameter in addition to the states.

Considering a nonlinear system described in [92] by:

$$\begin{cases} \dot{x}(t) = f(x(t), u(t)) + g(x(t), u(t))\theta(t) \\ y(t) = h(x) \end{cases} \quad (2.21)$$

where $x(t) \in \mathcal{R}^n$ denotes the states, $y(t) \in \mathcal{R}^p$ is the output vector of the system is, $u(t) \in \mathcal{R}^m$ is the measurable bounded input vector and $\theta(t) \in \mathcal{R}^1$ is a vector of unknown parameters.

The adaptive observer is in two steps, the first one is to transform the system in nonlinear adaptive observer form:

$$\begin{cases} \dot{y}(t) = \alpha(y(t), z(t), u(t)) + \beta(y(t), z(t), u(t))\theta(t) \\ \dot{z}(t) = \gamma(y(t), z(t), u(t)) \end{cases} \quad (2.22)$$

where $y(t) \in \mathcal{R}^p$ is the output vector of the system which is also the measurable states, $z(t) \in \mathcal{R}^r$ is the vector of the unmeasurable states. $\beta(y(t), z(t), u(t))$ is globally bounded. $\alpha(y(t), z(t), u(t))$ and $\gamma(y(t), z(t), u(t))$ are globally Lipschitz functions with respect to $z(t)$, and uniformly with respect to $(y(t), u(t), t)$.

The second step is the observer design:

$$\begin{cases} \dot{\hat{y}}(t) = \alpha(y(t), \hat{z}(t), u(t), t) + \beta(y(t), \hat{z}(t), u(t))\hat{\theta}(t) - \kappa_y(\hat{y}(t) - y(t)) \\ \dot{\hat{z}}(t) = \gamma(y(t), \hat{z}(t), u(t)) \\ \dot{\hat{\theta}}(t) = -\kappa_\theta \beta^T(y(t), \hat{z}(t), u(t))(\hat{y}(t) - y(t)) \end{cases} \quad (2.23)$$

where constants $\kappa_y > 0$ and $\kappa_\theta > 0$ are the gains of the observer. Generally, these observer gains are positive and they can have different values. However, it is recommended to take $\kappa_y < \kappa_\theta$. Such that for any $\hat{y}(0)$, $\hat{z}(0)$, any $y(0), z(0)$ and any measurable bounded $u(t)$, the estimation errors $\|\hat{y}(t) - y(t)\|$ and $\|\hat{z}(t) - z(t)\|$ asymptotically go to zero when t tends to infinity, while $\|\hat{\theta}(t) - \theta(t)\|$ remains bounded. Moreover, if $\beta^T(y(t), \hat{z}(t), u(t))$ is persistently exciting, and its time derivative is bounded, then $\|\hat{\theta}(t) - \theta(t)\| \xrightarrow[t \rightarrow \infty]{} 0$.

If there are no unmeasurable states, a reduced order asymptotic state observer is obtained by:

$$\begin{cases} \dot{\hat{y}}(t) = \alpha(y(t), u(t), t) + \beta(y(t), u(t))\hat{\theta}(t) - \kappa_y(\hat{y}(t) - y(t)) \\ \dot{\hat{\theta}}(t) = -\kappa_\theta \beta^T(y(t), u(t))(\hat{y}(t) - y(t)) \end{cases} \quad (2.24)$$

7-) Sliding mode observer

The sliding mode observers (SMO) are vastly applied to fault diagnosis in both linear and nonlinear systems with uncertainties, such as linear system in [37], as well as in nonlinear systems in [26]. The inherent property of sliding mode observer (SMO) is that it is normally insensitive to any uncertainty or external disturbance signals which are implicit in the input channels that are bounded by a known Lipschitz nonlinear function. Subsequently, this characteristic makes it suitable for state estimation and fault detection for nonlinear systems whose dynamics include a linear part and a nonlinear part which is Lipschitz with respect to system states. Designing a sliding mode observer consists in two steps: (1) the design of a sliding surface such that the system possesses the desired performance when it is restricted to the surface; (2) the design of a variable structure control law which drives the system trajectories to the sliding surface in finite time and maintains a sliding motion on it thereafter. As the trajectories reach the sliding surface, the estimations become insensitive to the external disturbances. Therefore the sliding mode observer can force the output estimation error to converge to zero in finite time, while the observer states converge asymptotically to the system states. The applications of SMO are concerned with the use of sliding mode ideas for fault diagnosis, reconstruction and how this information may be used in a simple way to provide a fault tolerant control scheme[30]. The limitation of this approach is its requirement of sufficient measurements and the chattering phenomenon caused by the nonlinear feedback in the observer. In below, we describe the major steps involved in the design of sliding mode observer. The discussion is based on the results from [93].

Consider the class of nonlinear systems can be transformed into triangular input form:

$$\begin{cases} \dot{x}_1 = x_2 + g_1(x_1, u) \\ \dot{x}_2 = x_3 + g_2(x_1, x_2, u) \\ \dots = \dots \\ \dot{x}_{n-1} = x_n + g_{n-1}(x_1, x_2, \dots, x_{n-1}, u) \\ \dot{x}_n = f_n(x_1, x_2, \dots, x_n) + g_n(x_1, x_2, \dots, x_n, u) \\ y = x_1 \end{cases} \quad (2.25)$$

where $x(t), u(t)$ and $y(t)$ are bounded state vector in finite time, bounded input vector and the output vector respectively. $g_i(\cdot, 0) = 0$, for $i = 1, \dots, n$.

A sliding mode observer can be generated as:

$$\begin{cases} \dot{\hat{x}}_1 = \hat{x}_2 + g_1(x_1, u) + \lambda_1 \text{sign}(x_1 - \hat{x}_1) \\ \dot{\hat{x}}_2 = \hat{x}_3 + g_2(x_1, \tilde{x}_2, u) + \lambda_2 \text{sign}(\tilde{x}_2 - \hat{x}_2) \\ \dots = \dots \\ \dot{\hat{x}}_{n-1} = \hat{x}_n + g_{n-1}(x_1, \tilde{x}_2, \dots, \tilde{x}_{n-1}, u) + \lambda_{n-1} \text{sign}(\tilde{x}_{n-1} - \hat{x}_{n-1}) \\ \dot{\hat{x}}_n = f_n(x_1, \tilde{x}_2, \dots, \tilde{x}_n) + g_n(x_1, \tilde{x}_2, \dots, \tilde{x}_n, u) + \lambda_n \text{sign}(\tilde{x}_n - \hat{x}_n) \end{cases} \quad (2.26)$$

Where

$$\tilde{x}_i = \hat{x}_i + \lambda_{i-1} \text{sign}(\tilde{x}_{i-1} - \hat{x}_{i-1}), i = 2, \dots, n-1 \quad (2.27)$$

The manifolds are effectively a sequential consideration of a series of first-order dynamics, it is easily seen by forming the error dynamics for $e = x - \hat{x}_i$:

$$\begin{cases} \dot{e}_1 = e_2 - \lambda_1 \text{sign}(x_1 - \hat{x}_1) \\ \dot{e}_2 = e_3 + g_2(x_1, x_2, u) - g_2(x_1, \tilde{x}_2, u) - \lambda_2 \text{sign}(\tilde{x}_2 - \hat{x}_2) \\ \dots = \dots \\ \dot{e}_{n-1} = \hat{x}_n - g_{n-1}(x_1, \tilde{x}_2, \dots, \tilde{x}_{n-1}, u) - \lambda_{n-1} \text{sign}(\tilde{x}_{n-1} - \hat{x}_{n-1}) \\ \dot{e}_n = f_n(x_1, x_2, \dots, x_n) - f_n(x_1, \tilde{x}_2, \dots, \tilde{x}_n) + g_n(x_1, x_2, \dots, x_n, u) - g_n(x_1, \tilde{x}_2, \dots, \tilde{x}_n, u) - \lambda_n \text{sign}(\tilde{x}_n - \hat{x}_n) \end{cases} \quad (2.27)$$

It can be verified that for sufficiently large λ_1 , a sliding mode is attained on $e_1 = 0$ in a finite time and it follows that $e_2 = \lambda_1 \text{sign}(x_1 - \hat{x}_1)$, which with (2.27) yields $\tilde{x}_2 = x_2$.

Then the observation error dynamics become:

$$\begin{cases} \dot{e}_1 = 0 \\ \dot{e}_2 = e_3 - \lambda_2 \text{sign}(\tilde{x}_2 - \hat{x}_2) \\ \dots = \dots \\ \dot{e}_{n-1} = \hat{x}_n - g_{n-1}(x_1, \tilde{x}_2, \dots, \tilde{x}_{n-1}, u) - \lambda_{n-1} \text{sign}(\tilde{x}_{n-1} - \hat{x}_{n-1}) \\ \dot{e}_n = f_n(x_1, x_2, \dots, x_n) - f_n(x_1, \tilde{x}_2, \dots, \tilde{x}_n) + g_n(x_1, x_2, \dots, x_n, u) - g_n(x_1, \tilde{x}_2, \dots, \tilde{x}_n, u) - \lambda_n \text{sign}(\tilde{x}_n - \hat{x}_n) \end{cases}$$

The manifolds are reached sequentially and $\tilde{x}_i - \hat{x}_i$ converges to zero if the $\tilde{x}_j - \hat{x}_j$ with $j < i$ have already converged to zero.

2.3.2 Observer Schemes

Using a single observer is not sufficient for fault isolation. For this purpose several observer schemes can be used [94] to detect and isolate faults in dynamic processes. The most popular two are the Dedicated Observer Scheme (DOS) and the Generalized Observer Scheme (GOS).

1-) Dedicated Observer Scheme

A well-known scheme is the dedicated observer scheme [59]. The basic idea of the dedicated observer scheme is to have a bank of observers where each observer only depends on one fault and is approximately decoupled from all of the other faults and from all disturbances [4]. It was first introduced by [95] for IFD (instrument fault diagnosis). For IFD, it consists of a set of observers each of which is driven by a different single sensor output. Each of these observers then estimates the full output vector, or if this is not possible, part of the output vector. The number of observers equals the number of outputs (sensors). For AFD, each observer uses one input and all the outputs. In this case, multiple residual generators are designed with each observer excited by a single input. Therefore, each residual generator is sensitive to only one actuator fault. It should be mentioned that the dedicated observer scheme allows detecting and isolating multiple faults by analysis of the residuals. As shown in Fig. 2.8.

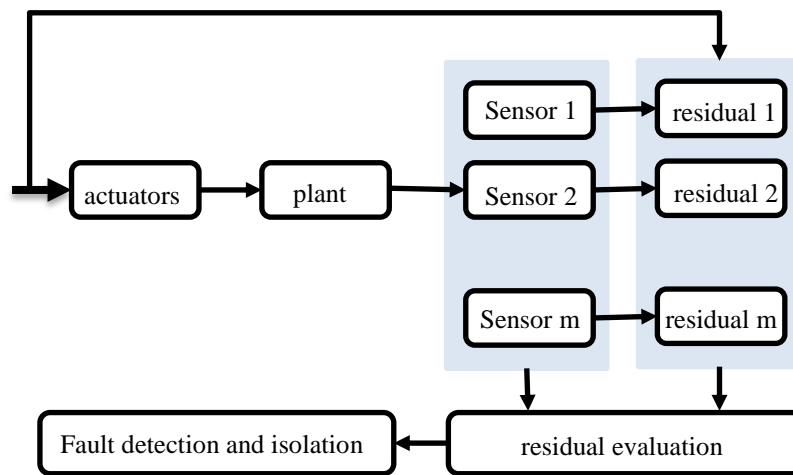


Fig. 2.8 Schematic of Dedicated Observer Scheme

2-) Generalized Observer Scheme

Another well-known scheme is the generalized observer scheme [59]. The main idea of the generalized observer scheme is to design the observer which is sensitive to all fault candidates but the one the observer involved. In the schemes, the FDD architectures consist of a reduced bank of N observers, where N is the number of fault candidates. Then i th residual is designed be sensitive to all faults but the i th one. For IFD, the i th observer uses all the inputs and M outputs but the i th one. While for AFD the i th observer is connected to all inputs except the i th. The decision function is as follows: if the i th residual is zero (or below a certain threshold) and all the remaining residuals are nonzero (or above their corresponding thresholds), then a decision on the occurrence of the i th fault is made.. The generalized observer scheme can be used for localization of single faults. As compared to dedicated observer scheme, in this design scheme, each observer is excited by all the system outputs but one. Because of its structure, the generalized observer scheme is less sensitive to modeling errors and disturbances than the dedicated observer scheme. As shown in Fig. 2.9.

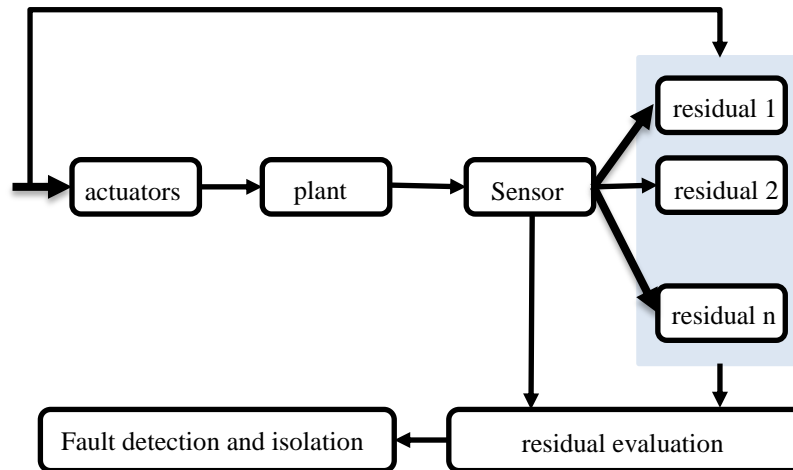


Fig. 2.9 Schematic of Generalized Observer Scheme

2.4 Fault Detection and Diagnosis Approach of Interconnected System

2.4.1 Introduction

Another important problem in the area of automatic control is related to the interconnected systems. The notion of interconnected systems is introduced to describe complex systems consisting of subsystems interacting on each other. A complex system can be defined as a system composed of a number of interconnected dynamic units whose interaction enforces the collective behavior of a system. Several practical systems, e.g. power generation and distribution systems, telecommunication networks, traffic networks, exhibit complex and spatially distributed dynamics and are referred to as large scale interconnected systems [96]. The study of interconnected systems plays a significant role in the development of stability theory of dynamic systems, as it allows investigating the stability property of a complex system by analyzing its less complicated components.

Recently, significant research works have been done in the area of interconnected systems. Most of the results focus on the control problem [97]. There have been many applications of a centralized scheme of interconnected systems control in different areas of the engineering field. Examples of such systems including multi-machine power system, robots, chemical process control systems etc. Due to the extensive efforts that are required in transmitting the entire system measurements for a centralized scheme which are not suitable for distributed systems, decentralized control of distributed systems by using local subsystem states is introduced. Many researchers in the field of large scale interconnected systems are devoted to decentralized robust control strategies, the advantages of using decentralized control can be found from either economy or reliability standpoints. When the system is too large to be dealt with by centralized control, it is computationally efficient to use only local information, i.e. local states or outputs, to make the control decision. Involved techniques are such as observer based control schemes [98], stepping based control algorithm [99], sliding mode control algorithm [100], unbiased observers based [101], adaptive control [102], decentralized adaptive output-feedback [103], decentralized observer based [104], reduced-order control [105]. Like in [100], a decentralized output feedback control strategy based on sliding mode techniques is proposed for a class of nonlinear large

scale interconnected systems with matched and mismatched uncertainties. The primary advantages of distributed over the traditional centralized control strategies include improved control performance, low cost, reduced computation resource requirements, reduced wiring or communication bandwidth requirements, simple installation and maintenance, and system agility.

In order to achieve reliable and safe operations of interconnected systems, the design of FDD and accommodation schemes is also a crucial step. Suitable FDD schemes are capable of ensuring that a fault at any given location can be detected at an incipient stage in order to prevent catastrophic failure of the overall system. There have been significant research activities in the development of new methodologies of FDD in interconnected systems. Until recently, centralized fault diagnosis approaches were the main topic of investigation and a variety of FDD methods have been developed. These FDD schemes need to own the capability to access to all the measurements available and the objective is to detect and isolate faults occurring in any part of the system. To guarantee this access availability, each subsystem requires transmitting information about actuators and sensors to a centralized FDD station that detects and isolates faults over the network. Many centralized fault accommodation schemes have been introduced in the above section. However, in practice, due to the constraints on computational capabilities, wiring, and/or communication bandwidth, it is very difficult to address the problem of diagnosing faults in interconnected distributed systems using a centralized architecture. In centralized FDD approaches, intelligence of monitored systems is at the top level of the process plant. When this centralized schematic is used, sensors have to be installed to all the primary variables of the field devices to make fault candidates observable. While installing additional sensors into the field devices leads to very complicated and expensive systems where deep expertise concerning the operation of the device is also required from monitoring system designers. Increasing complexity of these systems have also led to faulty alarms and maintaining such a system requires a lot of resources.

In recent years though, advances in sensing and communications, as well as to overcome these limitations, has motivated the investigation of FDD in interconnected system not that only focus on centralized fault diagnosis approaches, but also the focus of the research activities is directed mostly towards the development of hierarchical [106], decentralized [107], distributed [108] FDD schemes. The term distributed describes a FDD scheme whose structure is analyzed as being constituted by multiple subsystems that interact with neighboring subsystems. This is in contrast with the term decentralized FDD scheme, whose structure is considered as made of multiple subsystems that do not interact with each other, and of course with the term centralized, where a subdivision in distinct subsystems is not possible, as every part of the system interacts with every other one [109]. The difference between the concepts of centralized, decentralized and distributed systems can be easily understood by looking at Fig. 2.10, where a pictorial representation is given.

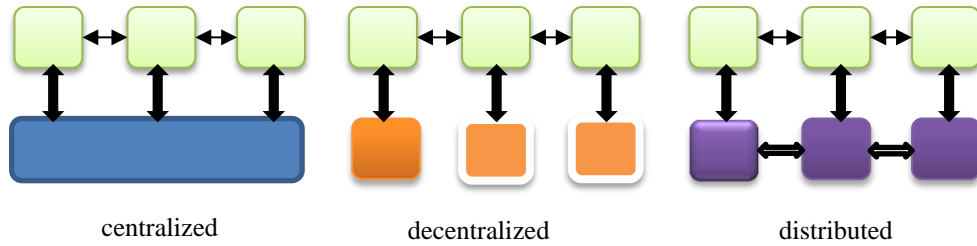


Fig. 2.10 Schematic of different structures: physical interconnection between subsystems is represented by black arrows, communication and measuring channels are represented by white arrows

Issues such as economic cost and reliability of communication links can be considered, thus providing impetus to develop and use a more advanced scheme. Traditional FDD schemes may not be applied to interconnected systems, since not all measurements are available in every node. In [110], the diagnosis problem is formulated and both a centralized and decentralized architectures are developed and compared. Obviously, distributed control and monitoring is more suitable than centralized for large-scale interconnected dynamical systems, such as power networks and multi-agent systems, due to the lower complexity and less use of network resources. Many factors contribute to this formulation such as the large scale nature of the system to be monitored, its spatial distribution, and the unavailability to access to certain parts of the system from a remote monitoring component and therefore local diagnosis should be performed. In fact, in many cases, the architecture of the underlying subsystems that are inherently decentralized and distributed makes the development of a distributed/decentralized FDD framework a necessity.

2.4.2 Distributed and Decentralized Fault Detection and Isolation

As previously mentioned, large scale interconnected systems require distributed or decentralized schemes, which motivated researchers to work on distributed approaches for fault diagnosis. In recent years, the problem of distributed or decentralized FDD for interconnected nonlinear system has attracted significantly increasing attention. In this case, the system is no longer diagnosed by a single monitor but several independent local monitors which together perform the FDD function of the overall system. Distributed/decentralized monitoring and control offers many advantages over centralized control, such as enhanced reliability, flexibility and efficiency.

In the literature of fault diagnosis of interconnected nonlinear systems, by assuming that the interconnection functions are known and the entire system states or entire estimated states are available at all subsystems, distributed/decentralized fault diagnosis schemes have been proposed, like in [153]. By using overlapping decomposition [111], a large scale system is decomposed into a set of subsystems which are interconnected by unknown nonlinear functions and distributed fault diagnosis scheme is introduced by assuming the entire state vector is available. Bank of adaptive observers, using only measurements and information from neighboring subsystems are used to detect and isolate faults in interconnected subsystems in [154]. In [108], a distributed fault detection scheme for process and sensor faults are developed by investigating the propagation of the fault effects to neighboring subsystems. In [97], a distributed sensor fault detection scheme is proposed for a class of

interconnected input output nonlinear systems where only the measurable part of state variables are directly affected by the interconnections between subsystems, but the estimator design is conducted under some potentially restrictive conditions and deals only with the fault detectability issue. Application of distributed FDD, e.g. power networks which is with inherent decentralized nature, can be found. In [112], it addresses the problem of distributed unknown input observers based FDD for a network of nodes with double integrator dynamics, whose interactions are described by a distributed control law. On the other hand, decentralized fault diagnosis schemes in [7] are introduced for interconnected systems by assuming the same conditions in distributed method are satisfied. In [113], a robust decentralized actuator fault detection and estimation scheme is proposed for a class of nonlinear interconnected systems using sliding mode observer. While in [59] a bank of decentralized observers is built where each observer contains the model of the entire system and receives both measurements from the local subsystem and information transmitted from other observers. Literature [114] presents a decentralized fault detection filter using game theory for a special large scale system where the interconnection terms are functions of the system outputs only.

Similar to current distributed/decentralized control approaches, these FDD methods are not completely distributed or decentralized since they still require the interconnection functions to be known and the entire state vector to be available at all subsystems. However, although availability of all the state information at each subsystem can help in an accurate diagnosis, the entire system state are typically not always fully available for practical systems. Some state variables may be difficult or costly to measure and sometimes have no physical meaning and thus cannot be measured at all [100]. Moreover, it is very expensive and time consuming to gather and process all the measured system states from a distributed large scale system at one place, even if this is possible, the information will be delayed and outdated. In practice, only a part of the states are available.

Motivated by the aforementioned observations, the need for a pure decentralized FD scheme which only uses local measurements with partial state measurement at each subsystem is expected. The objective is to design and analyze a distributed FDD approach, where a local fault detection agent is associated with each subsystem and receives local measurements and partial information from neighboring fault detection agents [108]. More specifically, the FDD scheme is designed in such a way that a process fault occurring in a subsystem can only be detected by its corresponding detection agent, whereas a sensor fault occurring in a subsystem may also be detected by the detection agents of the neighboring subsystems it affects. Decentralized diagnosis of interconnected systems by using only local subsystem states has been introduced recently [162]. For example, in [115], the authors propose a decentralized fault diagnosis and fault accommodation scheme by using only the local states at each local fault detector. Work [96] designs a decentralized fault diagnosis scheme for interconnected nonlinear systems by using local fault detectors (LFD) which consists of a nonlinear observer with an incorporated online approximator (IOA). The IOA is used to estimate the unknown part of the subsystem dynamics, i.e. interconnection term and possible fault function, so that each LFD monitors a

single subsystem by making use of the local information or states alone. A number of new developments in the design of pure distributed FDD for interconnected system can be found in the literature. For instance, in [116], the distributed fault detection scheme is based on local fault filtering schemes with each one assigned to monitor one subsystem and provide a decision regarding its health. A nonlinear observer-based approach is developed in [117] for distributed fault detection of a class of interconnected input-output nonlinear systems by relaxing the assumption of the availability of all the state measurements. In [118], authors present a distributed fault detection and isolation (FDI) strategy for a team of networked robots that builds on a distributed controller-observer schema. By means of a local observer, each robot can estimate the overall state of the team and it can use such an estimate to compute its local control input to achieve global tasks.

2.5 Summary

This chapter introduces the fundamental concepts in FDD with focus on nonlinear systems. Definitions of elementary nomenclature such as fault, failure, fault detection, fault identification and fault isolation are provided. A classification of FDD schemes is presented elaborating the main features of each approach. A particular attention is paid to observer-based fault detection schemes, their robustness properties are discussed and several approaches developed over the past for robust residual generation are introduced. At the end, some state of the art fault detection techniques for interconnected nonlinear systems are presented.

CHAPTER 3 INTRODUCTION TO SYSTEM INVERSION

This chapter gives a background to system inversion of linear and nonlinear systems with a particular focus on nonlinear system. First, we will review the related definitions and notations such as zero dynamics, Lie bracket, right and left invertibility, etc. Then the representation and inversion of linear system will be considered. Stability of the inversion and its connection to minimum and non-minimum phase systems will also be reviewed. Nonlinear systems will be considered in a similar manner and difficulties with stable inversion will be highlighted. This chapter ends with a short summary on related works with system inversion including system control, parameter identification, unknown input reconstruction and fault detection and diagnosis (FDD) problems.

3.1 Introduction

System inversion is one of the fundamental issues from a theoretical and practical viewpoint and has been extensively studied for over fifty years. The first systematic result relevant to the inverse systems was pioneered by Brockett and Mesarovic (1965). After that, the inversion problems were widely studied, in particular to characterize certain structural properties of systems. See for instance, in the classic linear systems theory, the works of [119][120]; for nonlinear systems [121][122]; for infinite dimensional systems [123], and for descriptor systems [124]. System inversion is a general concept in systems theory where left and right system inversions are two different aspects that appear in the literature, see e.g.[125]. From the system dynamics point of view, left inversion is mainly related to the system zeros, and a minimal left inversion gives a structure of the zero-dynamics of a system. Right-inversion relates to the input output decoupling problem and is sometimes referred to as the decoupling controller problem in control theory. Left and right invertibilities, as well as inversion procedures and algorithms, have been widely studied in the literatures. A good compendium of left and right invertibility of both linear and nonlinear systems can be found in [120].

For left invertibility, the problem has been a long studied problem in the systems literature. Many works on invertibility of linear dynamical system [120][126]. Necessary and sufficient conditions were obtained in [120] for the existence of a linear time invariant dynamical system that, when cascaded with the original system, produces as its output the input to the original system. With respect to nonlinear dynamic systems, in [127] invertibility of nonlinear continuous time systems, in [125] the notion of differential algebraic invertibility, and in [121] a geometric invertibility are discussed. For certain classes of nonlinear state space systems, one can find algorithms (and also sufficient or necessary conditions) of invertibility, see e.g. [128]. In [126] the left invertibility problem for switched linear systems is discussed, followed that nonlinear system is investigated in [36]. These conditions are given in terms of a rank condition on matrices made up of either the system matrices or the system Markov parameters. Although the existence conditions and properties of system inversion have been intensively studied, determining the inverse of a nonlinear model is not always a trivial thing even if it exists. With respect to the above mentioned researches, there are only few of them that supplies

computational algorithms of inverse dynamic. To achieve this purpose, the work [129] gives an algorithm to calculate the inverse and the zero dynamics. Another solution proposed for such problem, is to determine the class of nonlinear dynamical systems which are input output linearizable. Necessary and sufficient geometrical conditions have been stated [15][16]. Moreover, the paper [130] supplies a new algorithm to compute the dynamic inversion for an affine MIMO nonlinear control systems with regular characteristic matrix as well as singular matrix. While in [131], the left inverse system with minimal order and its algorithms of discrete time nonlinear systems are studied in a linear algebraic framework.

In recent years, dynamic inversion methods can be found in many interesting applications, such as aerospace and aviation, feedforward control, fault detection, system identification, signal processing problems, cryptography, electrical networks etc. Generally speaking, left inverse systems are typically used to observe internal variables and to reconstruct unknown exogenous signals directly acting on the system [120]. Right inverse systems are typically used for reference tracking and disturbance rejection. As far as systems input output decoupling is concerned, a controller insuring input output decoupling can be based on a right inverse of the controlled system. From a technological point of view, an important domain of application of left invertibility is the one corresponding to model based failure detection and isolation. Indeed, when failures are modeled as unknown exogenous signals, the failures detector is essentially a left inverse of the monitored system. The applicability of system inversion to fault detection in linear time invariant systems was first demonstrated in [132]. Followed in [133], it is shown how fault detection of both linear and nonlinear systems can be viewed as an input reconstruction process. Reference [120] developed failures detection schemes which overpass the limitations characterizing classical observer based failures detection methodologies.

Before stating the inverse dynamic of the systems, let us start with a review of some background from differential geometry and differential algebra needed to understand within the rest of this chapter.

3.2 Some Definitions and Notations

1-) Left and Right Inverse

Left and right inverse are two different concepts that appear in the system inversion literature. Loosely speaking, a left inverse for the original system would be a dynamic system which, driven by the process output (and its derivatives), reconstructs the applied input. A right inverse would then be a dynamic system which, driven by a desired output trajectory, produces the input necessary to obtain this trajectory.

In this respect, one can distinguish between the two notions of inverse systems as follows:

Left inverse: The left inverse reconstructs the input from the output of the plant, its derivatives, and the state variables of the inverse. Given a left invertible system, $\Sigma : U \rightarrow Y$, a left inverse $\Sigma_L^{-1} : Y \rightarrow U$, is a system satisfying $\Sigma_L^{-1}(\Sigma(u(\cdot))) = u(\cdot)$, as shown in Fig. 3.1.

Right inverse: The right inverse produces the input history that is required to obtain a particular output (i.e. an ideal feedforward controller) using the plant output and the state variables of the inverse. Given a right invertible system, $\Sigma: U \rightarrow Y$, a right inverse, $\Sigma_R^{-1}: Y \rightarrow U$, is a system satisfying $\Sigma(\Sigma_R^{-1}(\bar{y}(\cdot))) = \bar{y}(\cdot)$, as shown in Fig. 3.2.

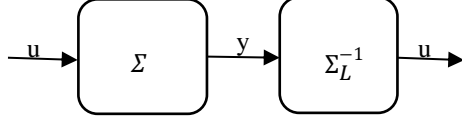


Fig. 3.1 Left inverse

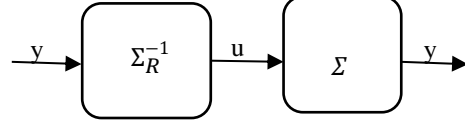


Fig. 3.2 Right inverse

2-) Left and Right Invertibility

Left invertibility is about uniquely finding the input, given the output and right invertibility is about finding one input sequence (not necessarily unique) such that the output is equal to a desired reference signal. Roughly speaking, the definition of left invertibility requires that any difference in the input must result in a difference in the following output symbols, at most in a time equal to the invertibility time. The system right invertibility (or functional controllability) denotes its property of reproducing at the output any arbitrary function, starting from the zero state and after some delay, provided that a suitable control input is applied.

For linear systems these two concepts can easily be explained in terms of the transfer matrix $G(s)$ of the system. One says that the (p, m) -matrix $G(s)$ is left-invertible if there exists a rational (m, p) -matrix $L(s)$ such that $L(s)G(s) = I_m$, whereas $G(s)$ is right-invertible if there is a rational (m, p) -matrix $R(s)$ such that $G(s)R(s) = I_p$.

Left and right invertibility of a linear system is often treated in a state space formulation among others. Let us for completeness also consider an LTI system described by a state space formulation:

$$\begin{cases} \dot{x}(t) = Ax(t) + Bu(t) & x(0) = x_0 \\ y(t) = Cx(t) + Du(t) \end{cases} \quad (3.1)$$

where $x \in \mathfrak{R}^n, u \in \mathfrak{R}^m, y \in \mathfrak{R}^p$ denote respectively the state, the input and the output of the system. The matrixes A, B, C, D are with appropriate dimensions.

The transfer function is given by:

$$G(s) = C(sI - A)^{-1}B$$

For nonlinear systems there are various attempts to analyze invertibility, see e.g. [121] where differential geometric methods are used, and [134] where noncommutative generating power series are the basic tools.

To give a formal definition, we consider a continuous time state space model:

$$\begin{cases} \dot{x}(t) = f(x(t)) + g(x(t))u(t) \\ y(t) = h(x(t)) \end{cases} \quad (3.2)$$

where $x \in X \subset \mathfrak{R}^n$, $u \in U \subset \mathfrak{R}^m$, $y \in Y \subset \mathfrak{R}^p$ denote respectively the state, the input and the output of the system. The mappings f, g_1, \dots, g_m which characterize the dynamics of the system are \mathfrak{R}^n -valued mappings defined on the open set X , i.e., $f(x), g_1(x), \dots, g_m(x)$ correspond to the values at a specific point $x \in X$ in the state space. The functions h_1, \dots, h_p are real valued functions defined on X , and $h_1(x), \dots, h_p(x)$ correspond to the values taken at a specific point x which characterize the output of the system. These mappings may be represented in the form of n -dimensional vectors of real-valued functions of the real variables x_1, \dots, x_n , as:

$$f(x) = \begin{bmatrix} f_1(x_1, \dots, x_n) \\ f_2(x_1, \dots, x_n) \\ \vdots \\ f_n(x_1, \dots, x_n) \end{bmatrix}, g_i(x) = \begin{bmatrix} g_{1i}(x_1, \dots, x_n) \\ g_{2i}(x_1, \dots, x_n) \\ \vdots \\ g_{ni}(x_1, \dots, x_n) \end{bmatrix}, h_i(x) = h_i(x_1, \dots, x_n)$$

In the following, \mathcal{R}^+ denotes the set of non-negative integers, a reference function $r(\cdot)$ is used to represent the desired output. Following is the definition for both left and right invertibility, as defined in [135].

Definition 3.1: A system is said to be left invertible at time k , if, for every $l \in \mathcal{R}^+$, there exists an integer $\sigma \in \mathcal{R}^+$, such that the input can be uniquely determined over the interval $[k-l, k]$ by the knowledge of the initial state $x(k-l)$ and of the output y over the interval $[k-l, k+\sigma]$.

Definition 3.2: A system is said to be right invertible at time k , if, for every $l \in \mathcal{R}^+$, $x(t_0) \in X$, and the reference function $r(\cdot) \in Y$ is defined over the interval $[k, k+l+1]$, there exists an integer $\sigma \in \mathcal{R}^+$ and an input u defined over the interval $[k-\sigma, k+l]$ such that for the initial state $x(k-\sigma) = x_0$, the output $y(j) = r(j)$, for all $j \in [k, k+l+1]$.

As will be clear in the following chapters, we have to consider cases where we can uniquely find the input given the output when the inversion is used for input distinguishable problems. Left inverse and left invertibility is therefore important in our considerations. However, it can be noted, in the case of a square system with an equal number of inputs and outputs, the notions of right and left inverse become identical. A realization of the inverse operator can then be interpreted as a right or a left inverse, depending on the context.

3-) Manifolds

A manifold is a topological space, usually denoted M , which has special properties that are useful for the results that follow. Most notably, a manifold is locally Euclidean. Consider the mapping of a point x in some neighborhood U of M to a point $\phi(x)$ in some open subset of \mathfrak{R}^n , the mapping ϕ and its inverse (ϕ^{-1}) are assumed to be C^∞ functions. We can define a coordinate chart as the pair (U, ϕ) , it is often useful to represent ϕ as a set (ϕ_1, \dots, ϕ_n) , where $\phi_i: U \rightarrow \mathfrak{R}$ is called the i th coordinate function. The set real number $(\phi_1(p), \dots, \phi_n(p))$ is called the set of local coordinates of x in the coordinate chart (U, ϕ) .

4-) Vector Fields

A vector map associates a point $x = (x_1, \dots, x_n)$ on an open subset of \mathfrak{R}^n with the vector in \mathfrak{R}^m :

$$f(x_1, \dots, x_n) = \begin{bmatrix} f_1(x_1, \dots, x_n) \\ f_2(x_1, \dots, x_n) \\ \vdots \\ f_m(x_1, \dots, x_n) \end{bmatrix}$$

A scalar map or function merely maps some open subset of \mathfrak{R}^n to \mathfrak{R} . A vector fields, $f(x)$, on \mathfrak{R}^n is the mapping which assigns to every point $x \in M$ a tangent vector $f(x)$ in the tangent space to M .

The mappings $f(x), g_1(x), \dots, g_m(x)$ of the system models (3.2) are smooth mappings in their arguments assigning to each point $x \in X$ a vector of \mathfrak{R}^n , i.e., $f(x), g_1(x), \dots, g_m(x), h_1(x), \dots, h_p(x)$ according to (3.2). Therefore they are referred to smooth vector fields defined on X .

5-) Lie Derivative

A co-vector field that will be used more frequently in the following parts of this work is the so called differential of the real-valued function λ . This co-vector field, denoted $d\lambda$ is defined as the $1 \times n$ row vector whose i – th element is the partial derivative of λ with respect to x_i . Its value at a point x is therefore:

$$d\lambda(x) = \left[\frac{\partial \lambda}{\partial x_1} \quad \frac{\partial \lambda}{\partial x_2} \quad \dots \quad \frac{\partial \lambda}{\partial x_n} \right]$$

or simply $d\lambda(x) = \partial\lambda/\partial x$.

Consider the real-valued function λ and a vector field f both defined on X . The derivative of λ along smooth field f is defined to be Lie Derivative. The notion we use is $L_f\lambda(x)$.

The Lie Derivative is equal to the value of the tangent vector $f(x)$ at point x . In local coordinates, it is in fact, the inner product, written as:

$$L_f\lambda(x) = \langle d\lambda(x), f(x) \rangle = \frac{\partial \lambda}{\partial x} f_i(x) = \left[\frac{\partial \lambda}{\partial x_1} \quad \dots \quad \frac{\partial \lambda}{\partial x_n} \right] \begin{bmatrix} f_1(x_1, \dots, x_n) \\ \vdots \\ f_n(x_1, \dots, x_n) \end{bmatrix} = \sum_{i=1}^n \frac{\partial \lambda}{\partial x_i} f_i(x)$$

The following notation is used for repeat Lie Derivatives:

$$L_f(L_f\lambda(x)) = L_f^2\lambda(x).$$

Continuing a recursion by differentiating λ k –times along f satisfies:

$$L_f^k\lambda(x) = \frac{\partial(L_f^{k-1}\lambda(x))}{\partial x} f(x), \quad \text{with } L_f^0\lambda(x) = \lambda(x)$$

Repeated use of this operation by extending the scope of the operation, the derivative of λ first along the vector field f and then along a vector field g is defined as:

$$L_g L_f\lambda(x) = \frac{\partial(L_f\lambda(x))}{\partial x} g(x)$$

6-) Lie algebra

A vector space V over R of all smooth vector fields on a manifold X is a Lie algebra, if in addition to its vector space structure, it is possible to define a binary operator on V : $[V, V] \equiv V \times V \rightarrow V$, called a product and written $[\cdot, \cdot]$, which has the following properties:

the operator is skew commutative: $[v, \omega] = -[v, \omega]$

the operator is bilinear over

$$[\alpha_1 v_1 + \alpha_2 v_2, \omega] = \alpha_1 [v_1, \omega] + \alpha_2 [v_2, \omega]$$

the operator satisfies the Jacobi identity:

$$[v, [\omega, z]] + [\omega, [z, v]] + [z, [v, \omega]] = 0$$

where α_1, α_2 are real numbers and v, ω, z are real vector fields.

7-) Lie Bracket

The binary operator $[\cdot, \cdot]$ on $V(X)$ satisfying the above properties is defined as the Lie bracket. With the motivation of the use of Lie theory, a second type of operation on co-vector fields that is important to introduce here involves two vector fields f and g , both defined on X . From these a new vector field can be constructed, noted $[f, g]$ and defined as:

$$[f, g](x) = \frac{\partial g}{\partial x} f(x) - \frac{\partial f}{\partial x} g(x) \quad (3.3)$$

at each x of X , in local coordinates, where the expressions:

$$\frac{\partial g}{\partial x} = \begin{bmatrix} \frac{\partial g_1}{\partial x_1} & \dots & \frac{\partial g_1}{\partial x_n} \\ \vdots & \ddots & \vdots \\ \frac{\partial g_n}{\partial x_1} & \dots & \frac{\partial g_n}{\partial x_n} \end{bmatrix}, \quad \frac{\partial f}{\partial x} = \begin{bmatrix} \frac{\partial f_1}{\partial x_1} & \dots & \frac{\partial f_1}{\partial x_n} \\ \vdots & \ddots & \vdots \\ \frac{\partial f_n}{\partial x_1} & \dots & \frac{\partial f_n}{\partial x_n} \end{bmatrix}$$

are the Jacobian matrices of the mappings g and f , respectively. The vector field defined in (3.3) is called the Lie product (or Lie bracket) of g and f . It is a fundamental property of Lie brackets that although they appear to be second order differential operators they are in fact first order because of the cancellation of the second order partial derivatives. To be more specific, the Lie bracket of two vector fields is always a vector field.

The notation that is typically employed for the operator is as follows:

$$\text{ad}_f^0 g(x) \equiv g(x)$$

$$\text{ad}_f^1 g(x) \equiv [f, g](x)$$

$$\text{ad}_f^2 g(x) \equiv [f, [f, g]](x) = [f, \text{ad}_f^1 g](x)$$

The importance of the notion of Lie bracket of vector fields and Lie algebras is very much related to their applications in the study of nonlinear systems of type (3.1). It is interesting to note the interpretation of the Lie derivative and Lie Bracket for a linear dynamical system is very much related to the study of nonlinear system.

In this case, considering (3.1) and (3.2), assume that:

$$f(x) = Ax, \quad g(x) = Bx, \quad h(x) = Cx$$

the repeat Lie derivative of the output function $h(x)$ along the $f(x)$ vector is given by:

$$L_f^k h(x) = CA^k x$$

Thus, one obtains the rows of the observability matrix of the linear system.

Apply the Lie derivative to the output function $h(x)$ along $g(x)$, proceeded by repeat derivatives along $f(x)$, one then obtain the Markov parameters for the linear system:

$$L_g L_f^k h(x) = CA^{k-1} Bx$$

Finally, consider the Lie Bracket of $f(x)$ and $g(x)$ vector fields:

$$\text{ad}_f^1 g(x) = [f, g](x) = [BA - AB]x$$

$$\text{ad}_f^k g(x) = [f, \text{ad}_f^k g](x) = (-1)^k A^k B$$

In this case, we obtain the columns of the controllability matrix of the linear system multiplied by $(-1)^k$.

Application of the theory of Lie groups, Lie algebras and their representations is a rapidly growing field of modern mathematics which occurs in the solution of problems in many fields of applied mathematics and physics. Recent approaches of applied Lie theory are motivated basically by control theory. During the period from the early 60's to the late 70's, for example, several research papers appeared that made use of Lie algebraic techniques to study controllability of nonlinear differential equations. These early results paved the way to a systematic use of these techniques in other system theoretic studies. There is another perhaps more important motivation behind the application of Lie theory to nonlinear problems. By embedding the original nonlinear problem in the framework of matrix Lie groups and associated Lie algebra, it is possible to reduce some system theoretic questions to problems which can be solved by using standard tools of linear algebra. Abstractly, a Lie algebra L represents a new kind of vector space to the problems which is equipped with a product $[x, y]$, which is called Lie product or Lie bracket in the sequel, satisfying certain axioms.

8-) Zero and Zero Dynamics

Zeros and zero dynamics of dynamical systems are of fundamental important notions in the analysis and inverse representation of the systems [136]. The concept of zero dynamics of a nonlinear system

was introduced about thirty years ago by Isidori, then in a series of papers, see e.g. [137]. As it will be found, the name zero dynamics is due to its relation to output zeroing and its relation to transmission zeros. Zero dynamics describes the internal behavior of a dynamical system where initial conditions and inputs are chosen in such a way to force the output to be identically zero, as introduced in [137].

As illustrated in [130], broadly speaking, the inverse dynamic of an input output dynamical system involves its decomposition into an external part, that enables an explicit relationship between inputs and outputs, and an internal part that is governed by its dynamics without input. This last dynamics provides naturally the so-called zero dynamics when the external variables are maintained at zero. From an analysis point of view, internal stability is a key issue for the practical application of the inverse system. For the single input single output (SISO) linear dynamical system the inverse dynamic has been completely characterized by its transfer function. It was also solved within the SISO nonlinear case by a full order realization. However, it is not an easy task when you dealing with a MIMO nonlinear dynamical system. Several researches have dealt with this problem, for example, the concept of zero dynamics was connected to the inverse dynamic, and in addition, it is settled by input output linearization via a feedback thus removing the dynamics of zero. From the system dynamics point of view, left inversion is mainly related to the system zeros, and a minimal left inversion gives a structure of the zero dynamics of a system [137]. It is now understood that a meaningful characterization of zeros in a MIMO setting goes beyond the zeros of the individual transfer functions between the inputs and outputs; it involves the concept of transmission zeros, which can be defined as the poles of the inverse system.

For the brief characterization of this principle consider the following problem and the corresponding definition, as describe in [137], consider a state space system of the form:

$$\begin{cases} \dot{x} = f(x, u) \\ y = h(x) \end{cases} \quad (3.4)$$

It is assumed that the origin $x = 0, u = 0$ is an equilibrium point for this system ($\dot{x} = 0$) and that $h(0) = 0$. Let, furthermore, the point x_0 in the state space of (3.3) such that $f(x_0, 0) = 0$ and $h(x_0) = 0$. Thus, if the initial state of (3.4) at time $t = 0$ is equal to x_0 , moreover, the input $u(t)$ is zero for all $t \geq 0$, then also the output $y(t)$ is zero for all $t \geq 0$.

Definition 3.3: The system dynamics described by (3.4) restricted to the set of initial conditions described above is called the zero output constrained dynamics or shortly, the zero dynamics. To be more specific, the zero dynamics identifies the set of all pairs consisting of an initial state x_0 and an output function $h(x)$ which produce an identically zero output.

3.3 Left Inversion of Linear system

Studying inversion of linear systems servers as a good introduction to inversion of nonlinear systems. In the following part, it will be shown how linear and nonlinear system inversion can be interpreted in a familiar manner. The problem of calculating a realization of the inverse has a straightforward solution

in the case of linear systems. A linear model can be described by a transfer function, a state space realization or an impulse response. There are, therefore, potentially many different notions of inversion that can be used in developing techniques for inverting systems, e.g., [135][120].

These are mainly two powerful tools studied from the two principal frameworks of the linear systems theory, namely: the Transfer Function Matrix (TFM) approach, in which the argument of the considered signals is “s”, and the Time Domain (TD) approach, in which the argument of the considered signals is “t”, as shown in [120].

Let us note that a system is causal if, for every choice of t_0 , the output sequence value at $t = t_0$ depends only on the input sequence values for $t \leq t_0$.

3.3.1 Input Output Description of Linear System

Given a transfer function description of a linear system, one can easily calculate a realization for the inverse of its transfer function (SISO case) or transfer matrix (MIMO case).

Consider the LTI system Σ given in (3.1), the input output representation of Σ can be given in the form of:

$$G(s) = C(sI - A)^{-1}B$$

$$y(s) = G(s)u(s)$$

Here $G(s)$ is referred to as the transfer function. The zeros of the transfer function are given as the roots of:

$$C(sI - A)^{-1}B = 0$$

and the poles are given by:

$$\det(sI - A) = 0$$

The input and output behavior of an LTI system can be completely defined by its transfer function together with its region of convergence (ROC). ROC is in fact a ring centered at the origin and it will be bounded by some of the poles. If the system is stable then the ROC includes the unit circle. Also, if the system is causal, the ROC must be outside the poles with the largest magnitude. Hence, for a system to be both stable and causal all the poles need to be inside the unit circle. We say that the system with casual zeros is with minimum phase. We will only consider stable minimum phase linear system, meaning that the ROC includes the unit circle.

In this case, the transfer function has a corresponding inverse system denoted $G^{-1}(s)$. The (left) inverse $G^{-1}(s)$ satisfies the identity:

$$G^{-1}(s)y(s) = G^{-1}(s)G(s)u(s)$$

with $G^{-1}(s)G(s) = I$. It means that the input $u(t)$ can be uniquely identified by the output function $y(t)$ and the left inverse $G^{-1}(s)$.

Remarks: Not all systems have inverses. For example, an ideal low pass filter does not have an inverse since there is no way to recover the frequency components above the cutoff frequency that are set to zero by the ideal low pass filter. Thus, a condition for a system to be invertible is that there is one to one correspondence between the input and the output.

3.3.2 State Space Description of Linear System

Left and right invertibility of a linear system is often treated in a state space formulation among others [138]. The left inversion of continuous time linear system on state space form is of the topic of [119][127]. There are two major approaches to the problem: one is the algebraic approach where conditions are obtained in terms of matrix rank equalities [126]; the other is the geometric approach that is based on the invariant properties of subspaces [120].

An algebraic approach relies on the observation that differentiating output function y reveals extra information about input function u . Let us also consider an LTI system described by a state space formulation in (3.1), denote by c_i the rows of the matrix C . The derivatives of the measurement vector y can be written as:

$$\begin{aligned} y^{(1)} &= C\dot{x} = CAx + CBu \\ y^{(2)} &= CA^2x + CABu + CB\dot{u} \\ &\vdots \\ y^{(k)} &= CA^kx + CA^{k-1}Bu + \dots + CBu^{(k-1)}, \quad \text{for } k \geq 0 \end{aligned}$$

If there exists a relative degree r_i which is exactly the number of times the output function $y(t)$ is to be differentiated in order to have the value $u(t)$ of the input explicitly appearing in the equations, such that:

$$c_i A^k B = 0, \quad \text{and} \quad c_i A^{r_i-1} B \neq 0, \quad \text{for all } k < r_i - 1$$

and

$$\text{rank} \begin{bmatrix} c_1 A^{r_1-1} \\ \vdots \\ c_p A^{r_p-1} \end{bmatrix} = m$$

Then one can construct the equations:

$$\begin{bmatrix} y_1^{(r_1)} \\ \vdots \\ y_p^{(r_p)} \end{bmatrix} = \begin{bmatrix} c_1 A^{r_1-1} \\ \vdots \\ c_p A^{r_p-1} \end{bmatrix} x + \begin{bmatrix} c_1 A^{r_1-1} B \\ \vdots \\ c_p A^{r_p-1} B \end{bmatrix} u \quad (3.5)$$

Obviously, from the representation (3.5) the input variable u can be obtained by inversion. The inverse system of (3.1) can be represented in the possible non-minimal state space form, for more details in [139]:

$$\begin{cases} \dot{\eta} = A_{\text{inv}}\eta + B_{\text{inv}}v_{\text{inv}} \\ u = C_{\text{inv}}\eta + D_{\text{inv}}v_{\text{inv}} \end{cases} \quad (3.6)$$

where (3.6) describes the inverse dynamics and the vector v_{inv} contains the measurements and its derivatives in the respective orders as:

$$v_{\text{inv}} = [y_1 \quad \dots \quad y_1^{(r_1)} \quad \dots \quad y_p \quad \dots \quad y_p^{(r_p)}]$$

If the realization of the inverse system is minimal, then A_{inv} gives the so-called zero dynamics of (A, B, C) . Throughout this paper it will be assumed that the zero dynamics of the system is asymptotically stable, that is the considered system is minimum phase. If this condition does not hold, the system inversion based method presented here does not give a feasible solution to the problem.

3.4 Inversion of Nonlinear System

Linear models cannot always describe physical phenomena. Nonlinear models, on the other hand, offer a wide range of models. In a nonlinear setting however, there is no explicit input output representation of a system (only in the sense of an abstract operator) [137]. Consequently, the calculation of a realization of the inverse becomes a highly nontrivial problem, which necessarily has to be addressed in a state space framework. The contributions to stable inversion of non-minimum phase nonlinear systems can be found in [127][51][137]. There are also two major approaches to the problem: one is the algebraic approach where conditions are obtained in terms of matrix rank equalities [125]; the other is the geometric approach that is based on the invariant properties of subspaces [121]. For multiple-input multiple-output (MIMO) nonlinear systems, the problem of left inversion is revisited and explicit formulas are derived for the full-order and the reduced inverse system. The reduced left inverse naturally leads to an explicit calculation of the unforced zero dynamics of the system and the definition of a concept of forced zero dynamics. These concepts generalize the notion of transmission zeros for MIMO linear systems in a nonlinear setting.

Similar to linear case, let us give the definition of relative degree and the concept of minimum phase first, since these concepts are related to the stability of the inverse. The concepts of minimum, non-minimum and also maximum are related to zero dynamics. According to [140], a continuous system is denoted minimum phase if the zero dynamics is asymptotically stable. And a system with unstable zero dynamics is, thus, not minimum phase and therefore denoted non-minimum phase. A similar definition can be found in [135], a system is considered to be non-minimum phase if there exists a stable feedback that can hold the system output identically zero, while the zero dynamics become unstable.

In this work we are concerned with the continuous time deterministic nonlinear systems described in (3.2) by ordinary differential equations in which the control appears affine.

Given a nonlinear dynamic system described in (3.2), the relative degree r_i is an integer which satisfies:

$$\begin{aligned} L_{g_j} L_f^k h_i(x) &= 0, \quad \text{for } j = 1, \dots, m; i = 1, \dots, p; \text{ and } k < r_i - 1 \\ L_{g_j} L_f^{r_i-1} h_i(x) &= 0 \end{aligned}$$

assuming that the matrix:

$$A(x) := \begin{bmatrix} L_{g_1} L_f^{r_1-1} h_1(x) & \dots & L_{g_m} L_f^{r_1-1} h_1(x) \\ \vdots & \ddots & \vdots \\ L_{g_1} L_f^{r_p-1} h_p(x) & \dots & L_{g_m} L_f^{r_p-1} h_p(x) \end{bmatrix} \quad (3.7)$$

is nonsingular at $x = x_0$ or, equivalently:

$$\text{rank } A(x_0) = m$$

In the case of a general MIMO system described by (3.2), the issue of left invertibility is extremely involved by work [127] where it suggested an algorithm for the construction of a left inverse by recursively differentiating the output map. Given the outputs y_i for the system described by (3.2), and calculating expressions for their derivatives until the control vector appears explicitly, we get:

$$\begin{aligned} y_1^{(r_1)} &= L_f^{r_1} h_1(x) + \sum_{i=1}^m L_{g_i} L_f^{r_1-1} h_1(x) u \\ &\vdots \\ y_m^{(r_m)} &= L_f^{r_m} h_m(x) + \sum_{i=1}^m L_{g_i} L_f^{r_m-1} h_m(x) u \end{aligned}$$

the above set of equations can be solved for the input vector u to obtain subject to the dynamics:

$$\begin{cases} \dot{x} = f(x) + g(x) A(x)^{-1} \left(\begin{bmatrix} \frac{d^{r_1} y_1}{dt^{r_1}} \\ \vdots \\ \frac{d^{r_m} y_m}{dt^{r_m}} \end{bmatrix} - \begin{bmatrix} L_f^{r_1} h_1(x) \\ \vdots \\ L_f^{r_m} h_m(x) \end{bmatrix} \right) \\ u = A(x)^{-1} \left(\begin{bmatrix} \frac{d^{r_1} y_1}{dt^{r_1}} \\ \vdots \\ \frac{d^{r_m} y_m}{dt^{r_m}} \end{bmatrix} - \begin{bmatrix} L_f^{r_1} h_1(x) \\ \vdots \\ L_f^{r_m} h_m(x) \end{bmatrix} \right) \end{cases} \quad (3.8)$$

The equation (3.8) can be referred to as a 1-step algorithm to obtain an inverse. Noted that some models are extremely hard to invert, e.g., when there are more inputs than outputs.

3.5 Some Related Work

Inversion of linear and nonlinear systems is successfully applied to many interesting areas, such as unknown input reconstruction, fault diagnosis, system identification and pre-forward system control. Here we will give a brief introduction on some of the works presented in these areas.

3.5.1 Inversion for Unknown Input Reconstruction

Systems with unknown inputs, mainly in connection with the increasing demand for sophisticated, enhanced reliability control systems in safety critical fields like aerospace, underwater robotics, power plants and chemical or petrochemical plants, have received considerable attention, see e.g. [141][142][35]. The unknown inputs may represent unknown external drivers, input uncertainty, or instrument faults. In most cases, it is either too expensive or perhaps not possible to measure these unknown inputs; for instance, the cutting force is often unavailable in machine tool applications. The problem of estimating unknown inputs is therefore motivated in part by such situations and has been the object of a fair amount of research efforts in the last decades.

Input reconstruction is the process of using the output of a system to estimate its input. The issue of simultaneously observing states and inputs has been investigated, see e.g.[143][144]. However, when addressed the problem without observing the whole state, the input reconstruction problem has a clear physical meaning. This is because it is rarely the case that an estimation of the whole state is required in practical applications, e.g. controller design as well as for the synthesis of fault diagnosis schemes. Left invertibility is important for recovering unknown inputs where the close relation of input reconstruction with the inverse problem was recognized by many authors earlier, see, e.g., [124]. The reconstruction of unknown inputs under the assumption that the initial state of the system is either known or zero is addressed by left inversion, a long studied problem in the systems literature [145][146]. Inverse systems entail a number of problems. Any non-minimum phase zeros of the original system will become unstable poles of the inverse system. However, the issue of internal stability of the resulting cascade system was subsequently addressed in [14], which considers both left inversion and the dual problem of right inversion. From then on, the issue of internal stability and the effect of non-minimum-phase zeros on input reconstruction were addressed within the context of right inversion along with the related notions of non-causal inversion, preview, pre-action, and steering along zeros [123].

The input reconstruction problem corresponds to formulation of a re-constructor whose inputs are the measurements of the original system and whose outputs converge to the inputs of the original system. This approach is an application of dynamic inversion to filtering which is dual to the concept of dynamic inversion for control. The analysis of the interaction between input and state, on the one hand, and between state and output, on the other hand, is of a fundamental importance in solving the input reconstruction problem. Key tools for the analysis of such interactions are the notions of input reconstructability, left invertibility, the relative degree and zero dynamics of the representation of a dynamical system. In the problem of input reconstruction, the first task consists of an evaluation of observability of inputs, thus distinguishing whether the changes of the input of a dynamic system are reflected as changes at the output [147]. Roughly, input observability means that the change of inputs in a dynamic system can reflect itself in the change of measurements. If a system is input observable, the input reconstruction problem consists in the synthesis of a device or a mechanism which has as

input the measured outputs, and it should take place as output a signal that should converge to the observable input.

By using an algebraic state space approach, the elaboration of an inversion algorithm for LTI systems (3.2) that can be used for detector design represented as minimum order stable linear dynamic systems. As shown in [124], the input reconstruction problem is in fact to find an estimator in the form:

$$\begin{cases} \dot{z}(t) = F_1 z(t) + F_2 y(t) \\ \hat{u}(t) = G_1 z(t) + \sum_{i=0}^p G_{2,i} y^{(i)}(t) \end{cases} \quad (3.9)$$

where $\hat{u} \rightarrow u$ for arbitrary y and x_0 of the system (3.2). $y^{(i)}$ denotes the i th derivative of y . The number p is known as the index of the estimator. So, the existence of the derivatives of y up to order p is assumed. The convergence speed of $\hat{u} \rightarrow u$ is required to be arbitrarily assignable. Nevertheless, a remark on the case that the convergence speed cannot arbitrarily be assigned will be given at a suitable point. The design of the estimator consists of finding all coefficient matrices in equations (3.9) and determining the lowest index p .

The linear structure allows the results to be carried forward in a simpler form and easier computational procedure to be developed for the derivation of the inverse system. In fact, while in the nonlinear case it will be necessary to use structural properties of the system such as relative degree and zero dynamics, for linear time invariant systems it is possible to relate the inverse to some structure independent problems such as the purely algebraic approach presented in this chapter. The notion of relative degree and zero dynamics has been introduced above.

Consider a MIMO nonlinear system of the form of (3.2), with finite relative orders $r_i, i = 1, \dots, m$, and nonsingular characteristic matrix $A(x)$ as (3.7). Then, the dynamic system is a realization of the inverse of the original system. Define the following change of the coordinates:

$$\begin{aligned} \xi_i &= [\xi_i^1, \xi_i^2, \dots, \xi_i^{r_i}] = [\phi_i^1(x), \phi_i^2(x), \dots, \phi_i^{r_i}(x)] \\ &= [h_i(x), L_f h_i(x), \dots, L_f^{r_i-1} h_i(x)] \quad i = 1, \dots, m \\ \xi &= [\xi_1, \xi_2, \dots, \xi_m] = [\phi_1(x), \phi_2(x), \dots, \phi_m(x)] \\ \eta &= [\phi_{r+1}(x), \phi_{r+2}(x), \dots, \phi_n(x)] \\ y &= [\xi_1^1, \xi_2^1, \dots, \xi_m^1] \end{aligned}$$

By application new local coordinates transformation proposed in [122], it is always possible to find the function $\phi_{r+1}(x), \phi_{r+2}(x), \dots, \phi_n(x)$, thus

$$\begin{aligned} \Phi(x) &= [\phi_1(x), \phi_2(x), \dots, \phi_m(x), \phi_{r+1}(x), \dots, \phi_n(x)] \\ x &= \Phi^{-1}(\xi, \eta) \end{aligned}$$

Then input vector u can be obtained by means of the output vector y and its derivatives. The inversion based algebraic polynomial (3.8), however, requires the computation of successive derivatives of outputs, which might be unrealistic in practical applications where measurements suffer noise and disturbances. Estimations techniques are then employed to tackle this problem, approaches include sliding mode observer, reduced-order observers geometric techniques, and differential algebra techniques.

$$\hat{u} = A \left(\Phi^{-1}(\hat{\xi}, \hat{\eta}) \right)^{-1} \left(\begin{bmatrix} \hat{\xi}_1^{(r_1)} \\ \vdots \\ \hat{\xi}_m^{(r_m)} \end{bmatrix} - \begin{bmatrix} L_f^{r_1} h_1(\Phi^{-1}(\hat{\xi}, \hat{\eta})) \\ \vdots \\ L_f^{r_m} h_m(\Phi^{-1}(\hat{\xi}, \hat{\eta})) \end{bmatrix} \right) \quad (3.10)$$

Input reconstruction is an ill posed problem so that any reconstruction algorithm must introduce a penalization parameter $\alpha > 0$ and reconstruct a candidate approximant u_α of the input u . The point is to prove that, under suitable assumptions, u_α converges to u for $\alpha \rightarrow 0^+$.

3.5.2 Inversion for FDI Purpose

Another interesting area is inversion based FDI. Although the solution of various types of inverse problems became particularly important in control and system theory in the classical age of control sciences, the feasibility of the idea for solving various detection problems was first appeared in the work [132]. Additional issues of inverse computation for the FDI problem can be found, e.g., in [148] [35], as well as in [149][133]. The main idea is to use input observers to reconstruct inputs to the system based on a dynamic model and measurements. The estimated inputs are then compared to the commanded inputs to assess the health of sensors and actuators, as shown in [133][147]. This approach is based on system inversion techniques developed for either input observers (left inversion) or preview control (right inversion). Furthermore, this approach will make not only the detection and isolation but also the estimation of the fault signals possible. On-line dynamic inversion based FDI methods were successfully applied to many interesting problems, such as in aerospace and aviation, real power converter, switching electrical networks, chemical reactors, aircraft longitudinal dynamics, etc.

With respect to the FDI problem via system inversion, the basic concepts and the existence of FDI filters are closely related to system invertibility, which is the backbone of this approach [147]. As a starting point, the basic concepts as the detectability of one fault, fault separability, the detectability of each faults, and simultaneous separability, can be expressed in term of system invertibility. Very briefly, in inversion based detection filter design the goal is to find the left inverse of the fault-to-output residual transfer function such that the fault estimation error transfer function is diagonal. This approach is based on the existence of the left inverse and arrives at detector architectures whose outputs are the fault signals while the inputs are the measured system inputs and outputs and possibly their time derivatives.

In order to introduce this idea, consider the following disturbance free linear control system subject to faults given instates space form as:

$$\begin{cases} \dot{x}(t) = Ax + Bu + Lv \\ y(t) = Cx + Du + Mv \end{cases} \quad (3.11)$$

where $x \in \mathcal{R}^n$, is the state vector, $u \in \mathcal{R}^r, y \in \mathcal{R}^p$ are the inputs and the measured outputs, respectively. It is noted again that the fault signal $v \in \mathcal{R}^q$ can represent both actuator and sensor failures, in general, as reflected in the structure of the matrices L, M . The goal is to detect the presence of the components of the fault signal independently from each other.

The residual generation problem is viewed as an inverse problem and is aimed at being solved by dynamic system inversion which we expect to have in the general form, as shown in [132]:

$$\begin{cases} \dot{\bar{x}}(t) = \bar{A}\bar{x} + B_u \xi_u + B_y \xi_y \\ v(t) = \bar{C}\bar{x} + D_u \xi_u + D_y \xi_y \end{cases} \quad (3.12)$$

where the elements of the vectors ξ_u, ξ_y consist of the input and output signals and also their time derivatives of the appropriate order as:

$$\begin{aligned} \xi_y &= [y \quad \dot{y} \quad \dots \quad \ddot{y}]^T, \\ \xi_u &= [u \quad \dot{u} \quad \dots \quad \ddot{u}]^T \end{aligned}$$

One of the advantages of the inversion approach discussed in this chapter is that the extension of the idea to some classes of nonlinear systems (bilinear and input affine) is possible. It will be shown that, by using this concept, linear and nonlinear problems can be treated in the same theoretical framework and the methodology presented can be easily generalized to nonlinear systems. As soon as the results for linear systems were obtained, the corresponding results for nonlinear systems can be regarded as natural generalizations of the linear case.

System representation (3.2) can be extended with additional inputs which may represent faults and other unknown external excitations. One possible form of this extension can be written in the form

$$\begin{cases} \dot{x}(t) = f(x, u) + \sum_{i=1}^m g_i(x, u)v_i \\ y_j(t) = h_j(x, u) + \sum_{i=1}^m l_{ij}(x, u)v_{ij}, \quad 1 \leq j \leq p \end{cases} \quad (3.13)$$

Where $x \in \mathcal{R}^n, u \in \mathcal{R}^r, y \in \mathcal{R}^p$ are the states, the inputs and the measured outputs, respectively. f, g, h, l are functions smooth in their arguments, l_i are real valued functions defined on X and $v(t)$ is the fault signal $(v_1, \dots, v_m)^T$ whose elements $v_i: [0, +\infty) \rightarrow \mathbb{R}$ are arbitrary bounded functions of time. The fault signals v_i can represent both actuator and sensor failures, in general. The goal is to detect the occurrence of the components v_i of the fault signal independently of each other and identify which fault component specifically occurred.

In this kind of approach, a detector, i.e., another dynamic system is constructed with outputs v and with inputs u, y and possibly their time derivatives which, in the most general form, can be thought of:

$$\begin{cases} \dot{\zeta}(t) = \varphi(\zeta, y, \dot{y}, \dots, u, \dot{u}, \dots) \\ v(t) = \omega(\zeta, y, \dot{y}, \dots, u, \dot{u}, \dots) \end{cases} \quad (3.14)$$

with the state variable $\zeta(t)$ assuming φ, ω are arbitrary analytic time functions. The filter reproduces the fault signal at its output that is zero in normal system operation, while it differs from zero if a particular fault occurs. The detector should satisfy a number of requirements. It should distinguish among different failure modes v_i , e.g., between two independent faults in two particular actuators. Moreover, it is aimed to completely decouple the faults from the effect of disturbances and also from the input signals. Note that for LTI systems the filter (3.12), accomplishing these requirements, traditionally serves as a robust residual generator which assign the fault effects and the disturbances into disjoint subspaces in the detector output space.

Along with the discussion of this chapter, linear and nonlinear problems will be treated in parallel to each other. Results for linear time invariant (LTI) systems will always be viewed as special cases of the results obtained for the nonlinear problems specified by the general system model (3.2).

The relationship of nonlinear system models (3.2) to linear systems (3.1) can be established provided that $f(x), g_i(x), h_j(x), l_i(x)$ are linear functions of x , i.e., $f(x) = Ax$, $g_i(x) = b_i$, $h_j(x) = c_jx$, $l_i(x) = d_i$ for some $n \times n$ matrix A and $b_i \in \mathcal{R}^n \times 1, c_j \in \mathcal{R}^1 \times n, d_i \in \mathcal{R}^p \times 1, i = 1, \dots, n, j = 1, \dots, p$. The system representation (3.1) characterized above can be written in the form

$$\begin{cases} \dot{x}(t) = A_0x(t) + \sum_{i=1}^k \alpha_i(t)A_i x(t) + \sum_{i=1}^m u_i(t)B_i x(t), x(0) = x_0 \in \mathcal{R}^n \\ y(t) = Cx(t) \end{cases} \quad (3.15)$$

assuming $A_0, A_i \in \mathcal{R}^{n \times n}$ are linearly independent constant real matrices. We assume $f: \mathcal{R}^n \rightarrow \mathcal{R}^n, g: \mathcal{R}^n \rightarrow \mathcal{R}^{m \times n}, h: \mathcal{R}^n \rightarrow \mathcal{R}^p$ (and also $\alpha_i(t)$) to be smooth (analytic) mappings. Note that the output $y(t)$ of the systems (3.2) and (3.13) which is affine in the inputs depends only on the state $x(t)$. The systems written either in the form of (3.2) and (3.13) describe a large number of physical systems of interest in many engineering applications, including fault detection and isolation.

3.5.3 Inversion for System Identification

Problems of reconstructing unknown characteristics of dynamical systems through measurements of a part of the phase coordinates are embedded into the theory of inverse problems of dynamics. Systems identification has attracted significant interests and still an active area, see e.g. [135]. Representation of system models can be achieved in many ways; it is common categorized into Black box, grey box and white box. When considering system identification, we will focus on the case where the model structure is given, e.g. based on a prior physical knowledge of the system. The purpose of identification is to use the knowledge of the model to predict future outputs or to design a controller that, applied to the system, stabilize or improves the performance of a system [135]. The identification process, represented in Fig.3.3, considers the input output time histories from real or simulated data and by means of an algorithm, linear or nonlinear model can be obtained. In system identification, the goal is

to achieve as good a model as possible to explain the behavior of y by a prediction or simulation $\hat{y}(t|\theta)$, which depends on estimated model parameters and the input u . This is done using measured data, usually input data, $u(t)$, and output data $y(t)$. Commonly used identification methods for linear models are, e.g., prediction error methods, maximum likelihood and spectral based methods.

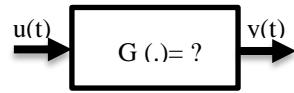


Fig.3.3 identification process

To simplify the discussion, we will start by looking at LTI dynamical systems. The model estimation is done in open loop and under the assumption that the output was created according to:

$$y(t) = G_0(q)u(t) + H_0(q)e_0(t) \quad (3.16)$$

where G_0 is the true system, H_0 is the true noise dynamics and e_0 is a white noise sequence. In system identification, the goal is often to find the minimizing argument of a function of the prediction error $\varepsilon(t, \theta)$

$$\begin{aligned} \hat{\theta} &= \arg \min_{\theta} \frac{1}{N} \sum_{t=1}^N \varepsilon(t, \theta)^2 \\ &= \arg \min_{\theta} \frac{1}{N} \sum_{t=1}^N [y(t) - \hat{y}(t|\theta)]^2 \end{aligned}$$

where $y(t)$ is the measured output and $\hat{y}(t|\theta)$ is the predicted output, given the model parameters θ . Here, we use a fixed noise model $H_{* \equiv 1}$ such that the prediction is described by $\hat{y}(t|\theta) = G(q, \theta)$.

3.5.4 Inversion for Control Purpose

Control of a system can be described as determining the input such that the outputs follows as closely as possible a desired reference signal, despite disturbance or errors in the model. Dynamic inversion is one of the most popular methods for controlling minimum phase nonlinear systems [122]. It is well known that right inversion is strictly connected to perfect tracking [123]. The difference between these inversion approaches is that control uses a right inverse whereas estimation uses a left inverse of the system.

In the context of the control of nonlinear systems, the problem of inversion arises when one wishes to control the output of a control system to track a desired trajectory. One must then “invert” the control system in order to obtain a state trajectory and control which will produce the desired output. Inversion-based feedforward controllers (e.g., [129][123]) have been used for output tracking in a variety of applications, for example, in aircraft and aerospace systems, and flexible structures. Recent successes in using non-causal inverses for systems with non-minimum phase dynamics have further renewed the interest in inversion-based feedforward controllers.

CHAPTER 4 INVERTIBILITY OF INTERCONNECTED SYSTEM

In this chapter, we address the invertibility problem of interconnected system, which is the problem of recovering the input of local subsystem uniquely given an output of the global system and initial states. The interconnected system involves two cascade nonlinear systems. In solving the invertibility problem, we give a necessary and sufficient condition for an interconnected system to be invertible, which says that the individual subsystems should be invertible. When the individual subsystems are invertible, we present an algorithm for finding inputs of local subsystems that generates the given global output in a finite interval. Numerical examples are included to confirm the proposed algorithm.

4.1 Introduction of Interconnected System

Interconnections are very common in control systems. In many applications, input output systems are interconnected to form more complex systems. The system or process that is to be controlled, commonly referred to as the plant, may itself be the result of interconnecting various sorts of subsystems in series, in parallel, and in feedback. For example, many practical control applications often include electrical power systems, nuclear reactors, chemical process control systems, transportation systems, computer communication, economic systems and so on. In addition, the plant is interfaced with sensors, actuators and the control system.

Classical system theory introduces inputs, outputs, and signal-flow graphs. Inputs serve to capture the influence of the environment on the system; outputs serve to capture the influence of the system on the environment, while output-to-input assignments, such as series and feedback connection, serve to capture interconnections. A system is thus viewed as transmitting and transforming signals from the input channel to the output channel, and interconnections are viewed as pathways through which outputs of one system are imposed as inputs to another system. Interconnected system poses challenging problems both in modeling and computation. The development of the nonlinear dynamic process model either requires large amounts of identification data or deep physical insight for rigorous modeling. Laws that govern physical phenomena, however, merely impose relations on the system variables, while interconnection means that variables are shared among subsystems. For example, the gas law states how the variables of interest temperature, volume, and mass are related. This law does not, however, state that some of the variables generate the others. The interconnection of two physical devices means that certain variables associated with the first device are set equal to certain variables associated with the second device. Connecting two pipes of two hydraulic systems means that the pressure and flow in the first pipe at the interconnection point are set equal to the pressure and flow in the second pipe at the interconnection point. After interconnection, the two hydraulic systems share the pressure and flow variables. Describing the nature of the composite system and providing some explicit description of it are generally nontrivial problems especially when the subsystems are nonlinear.

The study of interconnected systems plays a significant role in the development of stability theory of dynamic systems, as it allows one to investigate the properties of a complex system by analyzing its

less complicated components. By an interconnected system, we mean a system that consists of interacting subsystems either due to physical phenomena or due to analytic purpose. The motivation for this assumption is two fold. On one hand, physical plants are made up of parts, which can be identified as different subsystems, and this structural feature can facilitate the control design. On the other hand, even if the system does not present these physical boundaries, it might be useful to decompose it into mathematical subsystems which have no obvious physical identity. The notion “interconnected system” is concerned more with interactions. In this case, if there are interconnections between subsystems, the overall system can be referred to as an “interconnected system”. Several practical systems such as power generation and distribution systems, telecommunication networks, traffic networks, etc., exhibit complex and spatially distributed dynamics and are referred to as large scale interconnected systems [97]. Moreover, each subsystem can also be viewed as composed of dynamic subsystems connected in series since each component itself is a dynamic system. For example, a typical system has at least three cascade subsystems: sensor, process and actuator subsystems. The three parts function properly for the whole system to operate properly. In all situations, the global plant and/or each subsystem can be analyzed at different levels down to the component level in estimating the reliability of the whole plant.

Interconnected systems have been a focus of ongoing research and results related to stability, controllability, observability, and invertibility of such systems have been published, see e.g. [122] [101][150]. As illustrated in [150], several dynamics subsystems can be distinguished and delays generally arise in the processing of information transmission. This can cause instability and oscillation in these systems. Therefore many studies have been devoted to the analysis of stability of these systems, e.g. in [122], it has proved that an interconnected system is input to state stable if both subsystems are input to state stable. In addition to the problem of stability, the area of controllability of an interconnected system is also attracting more and more attention, and there have been many applications of networked control system in different areas of the engineering field. Examples of such systems including automotive control systems, cooperative control of unmanned vehicles, power generation and distribution systems, etc. Composition products arise in many forms when systems are interconnected to produce new systems. Certain elements of this problem are well understood by other means. For example, the composition of analytic functions is introduced in most texts addressing power series [151]; Cascade interconnections between a nonlinear system and a linear time-invariant dynamical system are analyzed in [152], and between an PDE and ODE can be found in [153]; The composition of two Fliess operators was considered in [154]; Bilinear system interconnections in [155].

One way to study the properties of interconnected systems is to consider that the plant is composed of subsystems connected in cascade manners. Generally speaking, in practice, it is very difficult to address the problem of analyzing cascade interconnected systems using a centralized architecture because of the constraints on computational capabilities and communication bandwidth. Consequently, in recent years, the area of distributed or decentralized methods has attracted increasing attention. However, because of the interactions among subsystems and the limitation of information that is

available for each subsystem, the problem of distributed analyzing is much more challenging. Therefore it is interesting to concern the problem that whether we can prove that under some condition, the effect in lower subsystems can be distinguished in higher subsystems thus avoiding full measurements of local subsystem. This consideration can be viewed as invertibility problem since an important aspect of the motivation of invertibility is to prove the distinguishability of the input or unknown input. While the property of distinguishability of two variables refers to their capacity to generate identifiable output signals for a given system. Several notions of distinguishability or invertibility may be encountered in the literature, see e.g. [120][125][51]. For example, Vu and Liberzon introduced the problem of invertibility of switched linear systems in [126]. They characterize the ability to determine the active mode of the system from the input and output data. The idea was further extended to nonlinear system in [51] and applied to fault diagnosis in [156].

Specifically, this chapter is concerned with the construction of the necessary and (or) sufficient condition so that given initial states, the control inputs are capable of generating distinguishable outputs of an interconnected system with two subsystems. The problem statement is analogous to the classical invertibility problem for non-interconnected systems. The problem is that whether we can prove that under some conditions, the inputs in lower subsystem have distinguishable impacts on higher subsystem.

The chapter is organized as follows: The required notations and some background on the invertibility of nonlinear system are given in Section 4.2. Section 4.4 is devoted to definition for invertibility of an interconnected dynamic systems followed by the formal problem statement of invertibility of non-interconnected dynamic systems in section 4.3. After that, we give conditions to validate involved definitions in Section 4.5. This characterization is used in Section 4.6 to establish simple dynamic inverse computation procedure for the interconnected system and numerical examples are implemented to confirm the effectiveness in section 4.7. Finally, some remarks and conclusions are highlighted in Section 4.8.

4.2 Basic Notion of Mappings and Differential Algebra

In fact, for every control system, we have an input output map, and the left invertibility of the dynamical system basically refers to the injective and surjective of this map. Moreover, differential algebra is often related with computation algorithm of dynamic inverse. Therefore we first recall some basic notions about composition mapping, invertible mapping and differential algebra. Whenever possible, the same notation will be used for any given composition product, and the specific definition will be evident from the context. Further details can be found in [137][139] and references therein.

1-) Composition of Mappings

For any set V , U , Y , let mapping $\alpha: V \rightarrow U$ and mapping $\beta: U \rightarrow Y$ be two given mappings. Composition is the combination of two or more mappings to form a single new mapping.

Definition 4.1: For any set V , U , Y , let mapping $\alpha: V \rightarrow U$ and mapping $\beta: U \rightarrow Y$, the composition of

mapping α followed by β is the mapping $\beta \circ \alpha: V \rightarrow Y$, denoted by $\beta \circ \alpha(x) = \beta(\alpha(x))$, for all $x \in V$.

As shown in Fig. 4.1:

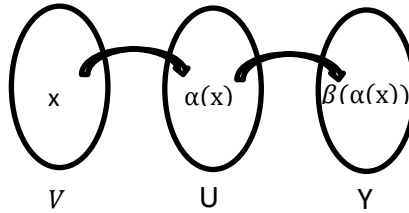


Fig. 4.1 Composition of mappings

In the following two statements, we discuss the question of either composing two onto mappings or two one-to-one mappings.

Theorem 4.1: For any set V, U, Y , and any mappings $\alpha: V \rightarrow U$ and $\beta: U \rightarrow Y$.

- 1-) If both α and β are injective, then composition mapping $\beta \circ \alpha$ is also injective.
- 2-) If both α and β are surjective, then composition mapping $\beta \circ \alpha$ is also surjective.

Proposition 4.1: Let $f: U \subset \mathbb{R}^n \rightarrow \mathbb{R}^m, U$ open be differentiable at x_0 and $g: \mathbb{R}^m \rightarrow \mathbb{R}^k$ be differentiable at $y_0 = f(x_0)$. Then the composition mapping $F(x) = g \circ f(x) = g(f(x)), F: \mathbb{R}^n \rightarrow \mathbb{R}^k$ is differentiable at x_0 and

$$F'(x_0) = g'(f(x_0))f'(x_0)$$

2-) Invertible Mappings

In this section we consider special kind of mappings which have the property that for each output value we can work out way backwards to find the unique input that produced it.

Definition 4.2: For set U, Y , a mapping $\beta: Y \rightarrow U$ is the inverse of a mapping $\alpha: U \rightarrow Y$, if and only if the composition mapping $\beta \circ \alpha = i_U$ and $\alpha \circ \beta = i_Y$. The mapping α is said to be invertible if it has an inverse.

Theorem 4.2: For set U, Y , if a mapping $\alpha: U \rightarrow Y$ is invertible, then its inverse is unique, denoted by α^{-1} .

The following theorem characterizes those mappings that are invertible.

Definition 4.3: For set U, Y , a mapping $\alpha: U \rightarrow Y$ is one to one (injective) if $\forall x, y \in A, \alpha(x) = \alpha(y) \rightarrow x = y$; and it is onto (surjective) if $\forall y \in B, \exists x \in A, \alpha(x) = y$

Definition 4.4: a mapping α is called bijective if it is both injective and surjective.

Theorem 4.3: For set U, Y , a mapping $\alpha: U \rightarrow Y$ is invertible if and only if it is bijective.

Theorem 4.4: For set U, Y , if a mapping $\alpha: U \rightarrow Y$ is invertible, then its inverse α^{-1} is also invertible with $(\alpha^{-1})^{-1} = \alpha$.

Theorem 4.5: For set V, U, Y , let two mappings $\alpha: V \rightarrow U$ and $\beta: U \rightarrow Y$, if α and β are both

invertible, then the composition mapping $\beta \circ \alpha$ is invertible with inverse $(\beta \circ \alpha)^{-1} = \alpha^{-1} \circ \beta^{-1}$.

Proof: supposed that both α and β are invertible, then $\alpha^{-1} \circ \alpha = i_U$, $\beta^{-1} \circ \beta = \alpha \circ \alpha^{-1} = i_U$ and $\beta \circ \beta^{-1} = i_Y$.

Thus, for any $y \in Y$, we have:

$$\begin{aligned} [(\beta \circ \alpha) \circ (\alpha^{-1} \circ \beta^{-1})](y) &= [\beta \circ (\alpha \circ \alpha^{-1}) \circ \beta^{-1}](y) \\ &= \beta \circ (i_U(\beta^{-1}(y))) \\ &= \beta \circ \beta^{-1}(y) \\ &= i_Y(y) = y \end{aligned}$$

It follows that $(\beta \circ \alpha) \circ (\alpha^{-1} \circ \beta^{-1}) = i_Y$. Similarly, one can show that $(\alpha^{-1} \circ \beta^{-1}) \circ (\beta \circ \alpha) = i_U$. Therefore, according to Definition 4.2, $\beta \circ \alpha$ is invertible with inverse $\alpha^{-1} \circ \beta^{-1}$.

Definition 4.5: A function $f: \mathfrak{R}^n \rightarrow \mathfrak{R}^m$ is said to be one-to-one (or injective) if $f(x) \neq f(\tilde{x})$ whenever $x \neq \tilde{x}$; it is said to be onto (or surjective) if, for every $y \in \mathfrak{R}^m$, there exists an $x \in \mathfrak{R}^n$ such that $f(x) = y$. If f is both one-to-one and onto, then it is called a one-to-one correspondence (or bijection). Bijections are invertible functions; that is, if f is bijective, then there exists a unique f^{-1} such that $f^{-1}(f(x)) = x$ for all $x \in \mathfrak{R}^n$ and such that $f(f^{-1}(y)) = y$ for all $y \in \mathfrak{R}^m$.

3-) Differential Algebra Notions

Some definitions of differential algebra are given. Further details can be found in [122][157] and references therein.

Let \mathcal{L} and \mathcal{K} be differential fields. A differential field extension \mathcal{L}/\mathcal{K} is given by \mathcal{L} and \mathcal{K} , such that: (1) \mathcal{K} is a subfield of \mathcal{L} and (2) the derivation of \mathcal{K} is the restriction to \mathcal{K} of the derivation of \mathcal{L} .

Definition 4.6: An element is said to be differentially algebraic with respect to the field k if it satisfies a differential algebraic equation with coefficients over k :

Example Let $\mathfrak{R}\langle e^{at} \rangle / \mathfrak{R}$ a differential field extension, where $\mathfrak{R} \subset \mathfrak{R}\langle e^{at} \rangle$, $x = e^{at}$ is a solution of $P(x) = \dot{x} - ax = 0$ (a is a constant).

Definition 4.7: An element is said to be differentially transcendental over k , if and only if, it is not differentially algebraic over k .

Definition 4.8: let a set of element of \mathcal{L} as $\xi = (\xi_1, \dots, \xi_n)$, if there exists an algebraic differential polynomial $P(\xi, \dot{\xi}, \ddot{\xi}, \dots) = 0$ with coefficients in \mathcal{K} , then ξ is called differentially \mathcal{K} -algebraically dependent, otherwise ξ is defined as \mathcal{K} -algebraically independent.

Definition 4.9: Any set of elements of \mathcal{L} which is differentially \mathcal{K} - algebraically independent and maximal with respect to inclusion forms a differential transcendence basis of \mathcal{L}/\mathcal{K} . Two such bases have the same cardinality. This is called the differential transcendence degree of \mathcal{L}/\mathcal{K} and denoted by $\text{difftrd}^\circ(\mathcal{L}/\mathcal{K})$.

Definition 4.10: Let $\mathcal{G}, \mathcal{K}(u)$ be differential fields. A nominal dynamic consists of a finitely generated differential algebraic extension $\mathcal{G}/\mathcal{K}(u)$, ($\mathcal{G} = \mathcal{K}(u, \xi)$, $\xi \in \mathcal{G}$). Any element of \mathcal{G} satisfies an algebraic differential equation with coefficients over \mathcal{K} in the components of u and their time derivatives.

Definition 4.11: Any unknown variable x in a dynamic is said to be algebraically observable with respect to $\mathcal{K}(u, y)$ if x satisfies a differential algebraic equation with coefficients over \mathcal{K} in the components of u, y and a finite number of their derivatives. Any dynamic with output y is said to be algebraically observable if, and only if, any state variable has this property.

4.3 Inversion of Nonlinear Interconnected System

4.3.1 Interconnected System Modelling

Composition products arise in many forms when systems are interconnected to produce new systems. Their particular form depends on the nature of the systems involved. In solving the modelling problems, we need to take into consideration the following questions:

Do we, system theorists, get the physics right?

Do our basic model structures adequately translate physical reality?

Does the way in which we view interconnections respect the physics?

In this work, cascade connections involving two classes of analytic nonlinear input output subsystems are considered. As shown in Fig.4.2, an interconnected system Σ is considered which consists of two subsystems: actuator Σ_a and process Σ_p subsystems.

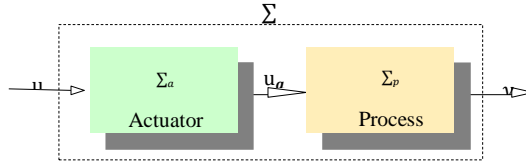


Fig. 4.2 Interconnected system structure

Assuming that the MIMO process subsystem is an input affine nonlinear system, and is described by (4.1):

$$\Sigma_p \begin{cases} \dot{x} = f(x) + g(x)u_a, & x(t_0) = x_0 \\ y = h(x, u_a) \end{cases} \quad (4.1)$$

where $x \in \mathcal{X} \subseteq \mathfrak{R}^n$ is the state of the process subsystem, $y \in \mathcal{Y} \subseteq \mathfrak{R}^p$ is the output of the global system, which is also the output of the process subsystem. $u_a \in \mathcal{U}_a \subseteq \mathfrak{R}^m$ is the input of the process subsystem, which is also the output of the actuator subsystem. u_a is inaccessible and is to reconstruct by measurements of y . f and g are smooth vector fields on \mathfrak{R}^n and h is smooth vector field on \mathfrak{R}^p . f, g, h are algebraic functions respectively.

An input affine structure is also assumed for the actuator subsystem by (4.2):

$$\Sigma_a: \begin{cases} \dot{x}_a = f_a(x_a) + g_a(x_a)u, & x_a(t_0) = x_{a0} \\ u_a = h_a(x_a) \end{cases} \quad (4.2)$$

where $x_a \in \mathcal{X}_a \subseteq \mathfrak{R}^n$ is the state, $u \in \mathcal{U} \subseteq \mathfrak{R}^l$ is the input, $u_a \in \mathcal{U}_a \subseteq \mathfrak{R}^m$ is the output of the actuator subsystem, which is also the input of the process subsystem. f_a and g_a are smooth vector fields on \mathfrak{R}^n and h is smooth vector field on \mathfrak{R}^m . f_a, g_a, h_a are algebraic functions respectively.

Thus an interconnected cascade system Σ is then constructed by these two subsystems Σ_a and Σ_p whereby the input is vector u while output vector is y .

Theorem 4.6: as demonstrated in [122], consider the cascade interconnected system Σ composed of the two subsystems Σ_a and Σ_p , if both subsystems are input to state stable, then the composite system Σ :

$$\Sigma: u \rightarrow \begin{bmatrix} x \\ x_a \end{bmatrix};$$

is input to state stable.

System (4.1) and (4.2) describe causal input output systems, we assume that the maps:

$$H_p: \mathfrak{R}^n \times \mathfrak{R}^m \rightarrow \mathfrak{R}^n \text{ and } h: \mathfrak{R}^n \times \mathfrak{R}^m \rightarrow \mathfrak{R}^p, H_a: \mathfrak{R}^n \times \mathfrak{R}^l \rightarrow \mathfrak{R}^n \text{ and } h_a: \mathfrak{R}^n \times \mathfrak{R}^l \rightarrow \mathfrak{R}^m$$

are analytic over an open subset of \mathfrak{R}^{n+m} and \mathfrak{R}^{n+l} . To avoid singularities, we have the following assumption on system (4.1) and (4.2).

Assumption 4.1: the maps H_p, h define submersion, i.e.

$$\begin{aligned} \text{rank} \frac{\partial H_p}{\partial(x, u_a)} &= n, & \text{rank} \frac{\partial H_p}{\partial u_a} &= m, & \text{rank} \frac{\partial h}{\partial x} &= p \\ \text{rank} \frac{\partial H_a}{\partial(x_a, u)} &= n, & \text{rank} \frac{\partial H_a}{\partial u} &= l, & \text{rank} \frac{\partial h}{\partial x_a} &= m \end{aligned}$$

over an open subset of \mathfrak{R}^{n+m} and \mathfrak{R}^{n+l} .

Considering interconnected system depicted by (4.1) and (4.2), the basic idea in this work is to prove invertibility of this interconnected system. The invertibility characterizes in this context the ability to identify the input u of the local subsystem from output data of the global system y . Thus, the motivation of invertibility here is in fact to study the distinguishability of the input at local level through their impacts on final product at the global level. The property of distinguishability of two inputs refers to their capacity to generate different output signals, and studies of distinguishability deals with the determination of necessary and (or) sufficient conditions that allow to test whether or not two different inputs are distinguishable.

4.3.2 Inversion of Interconnected System

In this section, we develop the required notations and provide some background on the invertibility of nonlinear system. Based on that, we develop the definition for invertibility of an interconnected

dynamic systems followed by the formal problem statement. After that, we give conditions to validate involved definitions. Finally, inverse computation procedure is discussed.

1-) Nonlinear inverse system

The primary objectives of invertibility are input identifiability, and several notions have been discussed in the literature. For example, for the purpose of FDI problem, the fault signal can be considered as unknown input, the motivation of invertibility is in fact input detectability and isolability that is to recognize the possible location and determination of the faults present in a system and the time of their occurrences. The tasks of fault detection and isolation are to be accomplished by reconstructing the unknown input through the output variables.

This section takes care to recall system inverse of dynamic systems. Let us start off by reviewing classical definitions of invertibility for non-interconnected systems. For simplicity, both subsystems are considered with the form as (4.1). For that, consider the input output map of process subsystem $H_p: \mathcal{U}_a \rightarrow \mathcal{Y}$ for input function space \mathcal{U}_a and the corresponding output function space generated by \mathcal{Y} . H_p maps an input $u_a(\cdot)$ to the output $y(\cdot)$ generated by the system driven by $u_a(\cdot)$ with an initial condition x_0 . Let us now proceed to the formal definition of invertibility for a nonlinear dynamical system as given in [122].

Definition 4.12: Fix an output set \mathcal{Y} and consider an arbitrary interval $[t_0, T)$, the system (4.1) is invertible at a point $x_0 := x(t_0) \in \mathcal{X}$ over \mathcal{Y} , if for every $y_{[t_0, T)} \in \mathcal{Y}$, the equality $H_{p(x_0)}(u_{a1[t_0, T)}) = H_{p(x_0)}(u_{a2[t_0, T)}) = y$ implies that $\exists \varepsilon > 0$, such that $u_{a1[t_0, t_0 + \varepsilon)} = u_{a2[t_0, t_0 + \varepsilon)}$. The system is strongly invertible at a point x_0 if it is invertible for each $x \in \mathcal{N}(x_0)$, where \mathcal{N} is some open neighborhood of x_0 . The system is strongly invertible if there exists an open and dense sub-manifold \mathcal{M} (called inverse sub-manifold) such that $\forall x_0 \in \mathcal{X}$, the system is strongly invertible at x_0 .

In fact, by definition 4.12, invertibility at x_0 is equivalent to saying that $u_{a1[t_0, t_0 + \varepsilon)} \neq u_{a2[t_0, t_0 + \varepsilon)}$ for all $\varepsilon \in (0, T - t_0)$ implies that $H_{p(x_0)}(u_{a1[t_0, T)}) \neq H_{p(x_0)}(u_{a2[t_0, T)})$.

This notion was captured by Hirschorn in [127]. We will now generalize this notion of invertibility to the interconnected systems.

2-) Nonlinear inverse interconnected system

As shown in Fig.4.3, we concern with the following question: what is the condition on the subsystems of an interconnected system so that, given an initial states and the corresponding output y generated with some input u , we can recover the input u uniquely? The problem statement is analogous to the classical invertibility problem for non-interconnected nonlinear systems. The inversion of an interconnected system can be thought of doing the composition invertible mapping and individual input recovery.

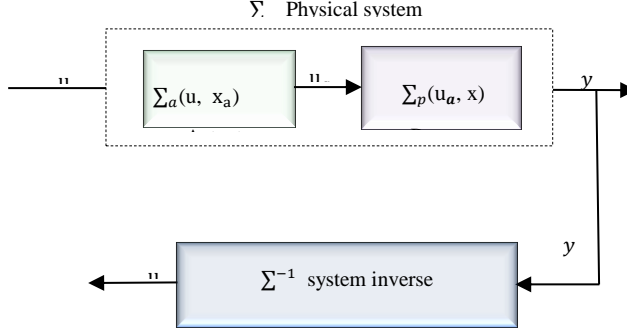


Fig. 4.3 inversion of interconnected system

Considering the input output map of process subsystem $H_p: \mathcal{U}_a \rightarrow \mathcal{Y}$ for input function space \mathcal{U}_a and the corresponding output function space generated by \mathcal{Y} . H_p maps an input $u_a(\cdot)$ to the output $y(\cdot)$ generated by the system driven by $u_a(\cdot)$ with an initial condition x_0 . In addition, the input output map of actuator subsystem is $H_a: \mathcal{U} \rightarrow \mathcal{U}_a$ for some input function space \mathcal{U} and the corresponding output \mathcal{U}_a . H_a maps an input $u(\cdot)$ to the output $u_a(\cdot)$ generated by the system driven by $u(\cdot)$ with an initial condition x_{a0} .

Define composition maps $H_a \circ H_p: \mathcal{U} \rightarrow \mathcal{Y}$ as input output map of the interconnected system, which maps an input $u(\cdot)$ to the output $y(\cdot)$ generated by the system driven by $u(\cdot)$ with initial conditions (x_{a0}, x_0) . We say that an interconnected system is invertible if unknown input $u(t)$ can be recovered from the knowledge of the output $y(\cdot)$, part of the state and the initial state (x_{a0}, x_0) . We now first extend the definition of invertibility to an interconnected system.

Definition 4.13: Fix an output set \mathcal{Y} and consider an arbitrary interval $[t_0, T)$, the interconnected system described by (4.1) and (4.2) is invertible at a point $(x_{a0}, x_0) := x(t_0) \in \mathcal{X}$ over \mathcal{Y} , $x_a(t_0) \in \mathcal{X}_a(t_0)$ over \mathcal{U}_a , if for every $y_{[t_0, T)} \in \mathcal{Y}$, the equality:

$$(H_a \circ H_p)_{(x_{a0}, x_0)}(u_{1[t_0, T)}) = (H_a \circ H_p)_{(x_{a0}, x_0)}(u_{2[t_0, T)}) = y_{[t_0, T)}$$

implies that $\exists \varepsilon > 0$, such that $u_{1[t_0, t_0 + \varepsilon)} = u_{2[t_0, t_0 + \varepsilon)}$. The system is strongly invertible at a point (x_{a0}, x_0) if it is invertible for each $x_a \in \mathcal{N}_a(x_{a0})$, $x \in \mathcal{N}(x_0)$, where $(\mathcal{N}_a, \mathcal{N})$ is some open neighborhood of (x_{a0}, x_0) . The system is strongly invertible if there exists an open and dense sub-manifold \mathcal{M}_a of $\mathcal{X}_a, \mathcal{M}$ of \mathcal{X} , such that $\forall (x_{a0}, x_0) \in (\mathcal{M}_a, \mathcal{M})$, the system is strongly invertible at (x_{a0}, x_0) .

The invertibility formulated in Definition 4.13 may fail to hold in two ways:

- (a) either because there exists two different inputs u_1, u_2 that yield the same $u_{a1} = u_{a2}$;
- (b) or even if two different inputs u_1, u_2 produce two different u_{a1}, u_{a2} , but they may yield the same output y .

The former one refers to be non-invertibility of actuator subsystem while the latter possibility is due to non-invertibility of process subsystem.

4.4 On the Condition of Invertibility of Interconnected System

As the systems under consideration are interconnected systems, classical inversion techniques can no longer be sufficient and hence we need to develop new tools for guaranteeing invertibility of interconnected dynamic systems in this chapter. As mentioned above, the inversion of an interconnected system can be thought of doing the composition invertible mapping and individual input recovery. Consequently, the basic idea for solving the invertibility problem is first to do the composition mapping by utilizing the relationship among the outputs and the states of the subsystems, and then use the nonlinear structure algorithm for the corresponding subsystem to recover the input.

From Definition 4.13, non-invertibility of either subsystems results in non-invertibility of the interconnected system. We now give a sufficient and necessary condition on the subsystem dynamics so that the interconnected system is invertible for set $\mathcal{U}, \mathcal{U}_a$ and \mathcal{Y} .

Theorem 4.7: Consider the interconnected system Σ which consists of two subsystems: actuator Σ_a and process Σ_p subsystems depicted by (4.1) and (4.2), and an output set \mathcal{Y} . The interconnected system is invertible at (x_0, x_{a0}) over \mathcal{Y} , if and only if each subsystem actuator Σ_a and process Σ_p is invertible at x_{a0} over \mathcal{U}_a , and x_0 over \mathcal{Y} respectively.

Proof: Considered H_a as the input output mapping of actuator Σ_a subsystem, while H_p is the input output mapping of process Σ_p subsystem. Then the input output mapping of the interconnected system is the composition $H_a \circ H_p$.

a-) (Sufficiency): invertibility of a dynamic system refers to bijective of the input output mapping. Since both subsystems are invertible, the corresponding mapping H_a and mapping H_p are bijective mapping. Moreover, composition of two bijective mappings is a bijective mapping, so input output mapping $H_a \circ H_p$ of the cascade system is bijective. Thus, the cascade interconnected system is invertible.

b-) (Necessity): We now show that if any of the subsystems is not invertible at (x_0, x_{a0}) , then the interconnected system Σ is not invertible.

For one hand, supposed that the process subsystem Σ_p is not invertible, while the actuator subsystem Σ_a is invertible. Then for the actuator subsystem (4.2), fix an output set \mathcal{U}_a and consider an arbitrary interval $[t_0, T)$, there exists two distinct inputs for $\exists \varepsilon > 0$ $u_1 \neq u_2$ on $[t_0, t_0 + \varepsilon)$, that may yield two distinct outputs $H_{a(x_{a0})}(u_{1[t_0, T)}) = u_{a1[t_0, T)}$, $H_{a(x_{a0})}(u_{2[t_0, T)}) = u_{a2[t_0, T)}$, $u_{a1[t_0, T)} \neq u_{a2[t_0, T)}$. However, for the process subsystem (4.1), fix an output set \mathcal{Y} , these two distinct inputs $u_{a1} \neq u_{a2}$ on $[t_0, t_0 + \varepsilon)$ may produce two equal output $H_{p(x_0)}(u_{a1[t_0, T)}) = H_{p(x_0)}(u_{a2[t_0, T)}) = y_{[t_0, T)}$. Therefore, for the series system, these two distinct inputs $u_1 \neq u_2$ on $[t_0, t_0 + \varepsilon)$ may result in two equal outputs:

$$(H_a \circ H_p)_{(x_{a0}, x_0)}(u_{1[t_0, T)}) = (H_a \circ H_p)_{(x_{a0}, x_0)}(u_{2[t_0, T)}) = y_{[t_0, T)}$$

Thus, it implies that the interconnected system Σ is not invertible at (x_0, x_{a0}) over $(\mathcal{U}_a, \mathcal{Y})$.

For the other, supposed that the process subsystem Σ_p is invertible, while the actuator subsystem Σ_a is not invertible. Then for the actuator subsystem Σ_a in (4.2), fix an output set \mathcal{U}_a and consider an arbitrary interval $[t_0, T)$, there exists two distinct inputs for $\exists \varepsilon > 0$ $u_1 \neq u_2$ on $[t_0, t_0 + \varepsilon)$, that may yield two equal outputs $H_{a(x_{a0})}(u_1|_{[t_0, T)}) = u_{a1|_{[t_0, T)}}$, $H_{a(x_{a0})}(u_2|_{[t_0, T)}) = u_{a2|_{[t_0, T)}}$, $u_{a1|_{[t_0, T)}} = u_{a2|_{[t_0, T)}}$. Even if, the process subsystem Σ_a in (4.1) is invertible, these two distinct inputs $u_{a1} = u_{a2}$ on $[t_0, t_0 + \varepsilon)$ can only precede one output $H_{p(x_0)}(u_{a1|_{[t_0, T)}}) = H_{p(x_0)}(u_{a2|_{[t_0, T)}}) = y|_{[t_0, T)}$. However, for the series interconnected system, these two distinct inputs $u_1 \neq u_2$ on $[t_0, t_0 + \varepsilon)$ result in two equal outputs:

$$(H_a \circ H_p)_{(x_{a0}, x_0)}(u_1|_{[t_0, T)}) = (H_a \circ H_p)_{(x_{a0}, x_0)}(u_2|_{[t_0, T)}) = y|_{[t_0, T)}$$

Thus, it implies that the interconnected system Σ is not invertible at (x_0, x_{a0}) over $(\mathcal{U}_a, \mathcal{Y})$. ■

Theorem 4.8: Consider the interconnected system Σ which consists of two subsystems: actuator Σ_a and process Σ_p subsystems depicted by (4.1) and (4.2), and an output set \mathcal{Y} . The interconnected system is strong invertible at (x_0, x_{a0}) over \mathcal{Y} , if and only if each subsystem actuator Σ_a and process Σ_p is strong invertible at x_{a0} over \mathcal{U}_a , and x_0 over \mathcal{Y} respectively.

Remark 4.1: For the interconnected system, if all the subsystems are globally invertible, then it is possible to recover the inputs uniquely over the time interval $[t_0, T)$. Also, note that T may be arbitrarily large if the state trajectories do not exhibit finite escape time.

After verifying the invertibility of individual subsystems, we will be able to construct an interconnected inverse system that can recover the original input uniquely from the global measurement, by which implies that each original input affect the global output distinguishably. In fact, if a system is invertible, the structure algorithm allows us to express the input as a function of the output, its derivatives and possibly some states, see, e.g. in [122].

4.5 Invertibility Checking

In this section, we address the computational aspect of the concepts introduced in previous sections and develop algebraic criteria for checking the invertibility of interconnected systems. As illustrated in Theorem 4.7, the first condition asks for invertibility of individual subsystems, and it will be verified by the output differential rank. To put everything into perspective, we provide appropriate background related to the invertibility of nonlinear systems and use it to develop the concept of functional reproducibility.

System invertibility problems are of great importance from theoretical and practical viewpoint and have been studied extensively for fifty years. The systematic study of invertibility for nonlinear systems began with the work [127] where Silverman's structure algorithm to multiple input multiple-output (MIMO) nonlinear systems was generalized. Then reference [158] modified the algorithm to cover a larger class of systems. Literatures related with extension of this algorithm can be found in [137][121][125]. As mentioned above, there are potentially many different notions of

inversion that can be used in developing techniques for inverting systems. Let us begin this section recalling the following basic concepts related with left invertibility:

1-) Input output mapping

The left invertibility is the problem of injective and bijective of the input output map, e.g. invertibility of the dynamical system (4.1) basically refers to the injective of the input output map H_p . Roughly speaking, the definition of left invertibility requires that any difference in the input must result in a difference in the following output symbols, at most in a time equal to the invertibility time. A control system is invertible when the corresponding input output map is injective. Thus given an output function one can, in theory, recover the control which was applied.

As a first approach, an input output system Σ from inputs \mathcal{U} into outputs \mathcal{Y} is left invertible if there exists an input output system Σ^{-1} from inputs \mathcal{Y} into outputs \mathcal{U} , such that the cascade system $\Sigma \Sigma^{-1}: \mathcal{U} \rightarrow \mathcal{Y} \rightarrow \mathcal{U}$ is the identity. In our mainly algebraic setting, it is supposed that \mathcal{U} , \mathcal{Y} are good class of functions equipped with an algebraic structure, for example, those are differential vector space.

Definition 4.14: A system Σ from inputs \mathcal{U} into outputs \mathcal{Y} is left invertible if there exists an input output system Σ^{-1} from inputs \mathcal{Y} into outputs \mathcal{U} , and a differential polynomial $P(u, \dot{u}, \dots, y, \dot{y}, \dots)$, such that if $y = \Sigma(u)$, then $\Sigma^{-1}(y) = u$, for all pairs $(u, y) \in \mathcal{U} \times \mathcal{Y}$, if:

$$P(u, \dot{u}, \dots, y, \dot{y}, \dots) \neq 0$$

2-) Differential output rank

In differential algebraic setting, left invertibility (as our case) can be expressed in terms of the differential output rank of the system, see [159][3][147]. We have some definitions concerning the differential output rank of a system as the following statements.

Definition 4.15: The differential output rank ρ of a system is equal to the differential transcendence degree of the differential extension $k\langle y \rangle$ over the differential field k , i.e.: $\rho = \text{difftrd}^{\circ} k\langle y \rangle / k$

Property 4.1: The differential output rank ρ of a system is smaller or equal to $\min(m, p)$

$$\rho = \text{diff tr } d^{\circ} k\langle y \rangle / k \leq \min(m, p)$$

where m, p are the total number of inputs and outputs respectively.

The differential output rank ρ is also the maximum number of outputs that are related by a differential polynomial equation with coefficients over \mathcal{K} (independent of x and u).

A practical way, for certain simple cases, to determine the differential output rank is by taking into account all possible differential polynomials of the form

$$P_r(y_1, y_2, \dots, y_m, \dot{y}_1, \dot{y}_2, \dots, \dot{y}_m, \ddot{y}_1, \ddot{y}_2, \dots, \ddot{y}_m, \dots) = 0 \quad (4.3)$$

and if it is possible to find r independent relations of the form, then the differential output rank is given by $\rho = p - r$, that is to say, there exist only $p-r$ independent outputs.

Theorem 4.9: A system is left-invertible if, and only if the differential output rank ρ is equal to the total number of inputs, e.g. $\rho = m$ in (4.1).

That is, if the differential output rank is equal to the number of the inputs, the system is invertible. This implies that the number of outputs must be greater, or equal to the number of inputs.

Remark 4.2: If a subsystem has more inputs than outputs, then it cannot be (left) invertible. On the other hand, if it has more outputs than inputs, then some outputs are redundant (as far as the task of recovering the input is concerned), therefore the case of input and output dimensions being equal perhaps, is the most interesting case.

Remark 4.3: For the interconnected system, the case of input and output dimensions being equal in each subsystem, as well as the overall system, perhaps, is the most interesting case.

4.6 Computing the Inverse Dynamics

4.6.1 Inverse of Interconnected Nonlinear System

We now have a toolset to check the invertibility conditions given in Theorem 4.7. If these conditions are satisfied and the interconnected system is strongly invertible, an interconnected inverse system can be constructed to recover the input from given output and initial state.

Considering the interconnected input output system Σ with two subsystems Σ_a and Σ_p from inputs \mathcal{U} into outputs \mathcal{Y} , its composition input output map is $H_a \circ H_p$. If the interconnected system is left invertible, there exists an input output system Σ^{-1} from inputs \mathcal{Y} into outputs \mathcal{U} , the inverse composition map is defined as $(H_a \circ H_p)^{-1}$, such that the cascade system $\Sigma \Sigma^{-1}: \mathcal{U} \rightarrow \mathcal{Y} \rightarrow \mathcal{U}$ is the identity. In our mainly algebraic setting, it is supposed that \mathcal{U} , \mathcal{Y} are good class of functions equipped with an algebraic structure, for example, those are differential vector space. Then the inverse of the interconnected system defined as in Theorem 4.10.

Theorem 4.10: Consider the interconnected system Σ which consists of two subsystems: actuator Σ_a and process Σ_p subsystems, and an input-output set $(\mathcal{U}, \mathcal{Y})$. If the interconnected system is strong invertible at (x_0, x_{a0}) over $(\mathcal{U}_a, \mathcal{Y})$, then the inverse interconnected system can also be an interconnected system with input output set $(\mathcal{Y}, \mathcal{U})$, as follows:

$$(H_a \circ H_p)^{-1} = H_p^{-1} \circ H_a^{-1}$$

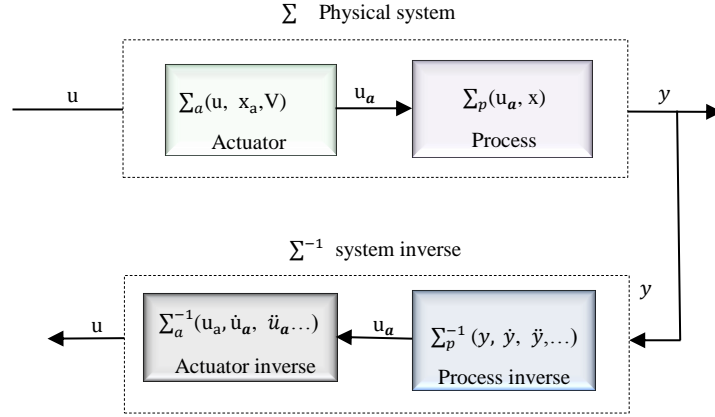


Fig. 4.4 interconnected inverse system scheme

As shown in Fig.4.4, the inverse of an interconnected system can also be considered as an interconnected system which consists of inverse of individual subsystem connected in series. The output of the inverse interconnected system is the original input of the interconnected system, by which implies that each original input affect the global output distinguishably.

4.6.2 Structure Algorithm

The main purpose of this section is to present a procedure to compute inverse dynamics of input affine interconnected nonlinear system. In fact, if a system is invertible, the structure algorithm allows us to express the input as a function of the output, its derivatives and possibly some states. More details are given in [122]. Invertibility of the control systems, affine in the input can be solved by algorithms within the framework of output differentiating and elementary linear algebra. The algorithms in [122] will be reconsidered and structured in order to obtain more systems which are invertible and to point out the real nature of the invertibility conditions. The main computational tool for studying the problem is in an algebraic.

If a system is differentially left invertible, the input can be recovered from the output by means of a finite number of ordinary differential equations. As the dynamical subsystem (4.1), the realization of its inverse dynamic can be expressed as the following form (4.4):

$$H_p^{-1}: \begin{cases} \dot{\eta} = \varphi(\eta, y, \dot{y}, \dots) \\ u_a = \omega(\eta, y, \dot{y}, \dots) \end{cases} \quad (4.4)$$

where η is a function of sub-state of the state x to be determined. It represents also the internal state that does not have a relationship with inputs. Its determination is a crucial issue on the inverse dynamic.

As the dynamical subsystem (4.2), the realization of its inverse dynamic which is also the inverse of the interconnected system can be expressed as the following form (4.5):

$$H_a^{-1}: \begin{cases} \dot{\eta}_a = \varphi_a(\eta_a, u_a, \dot{u}_a, \dots) \\ u = \omega_a(\eta_a, u_a, \dot{u}_a, \dots) \end{cases} \quad (4.5)$$

where η_a is a function of sub-state of the state x_a to be determined, u_a is the output of inverse process subsystem.

Since (4.4) and (4.5) may have the same structure, we only consider compute (4.4) for demonstration. This approach is based on the existence of the left inverse system whose outputs are the unknown input while the inputs are the measured system outputs and possibly their time derivatives. The existence of the left inverse determines the feasibility of the inversion based approach to the input reconstructor design. Therefore, we will study a series of problems concerned with the analysis of the properties of invertibility of dynamical systems. It will be seen that the point of departure of the invertibility analysis is the notion of relative degree of dynamical systems. The theory is developed for linear time invariant and nonlinear systems having vector relative degree. For more details, one can turn to [122].

Definition 4.16 (Relative degree of nonlinear systems): For invertible dynamic system described by (4.1), the relative degree r_i of the output y_i with respect to the input vector u_a is the smallest integer which is defined by:

$$(a) L_{g_j} L_f^{r_i-1} h_i(x) \neq 0; \quad 1 \leq j \leq m$$

$$(b) L_{g_j} L_f^k h_i(x) = 0; \quad 0 \leq k < r_i - 1, 1 \leq j \leq m$$

where $L_f(\cdot)$ and $L_g(\cdot)$ represent the Lie derivatives of a real function $h(x)$ along the vector field $f(x)$ and $g(x)$.

$$L_f^0 h_i(x) = h_i(x), \quad L_f^k h_i(x) = \frac{\partial(L_f^{k-1} h_i(x))}{\partial x} f(x) \quad \text{and} \quad L_{g_j} L_f^k h_i(x) = \frac{\partial(L_f^k h_i(x))}{\partial x} g_j(x).$$

Definition 4.17 (vector relative degree of nonlinear system): Based on the individual components r_i , the vector relative degree r of a multivariable linear system is defined as:

$$r = [r_1 \quad \cdots \quad r_p]$$

the multivariable nonlinear system (6.1) is said to have a vector relative degree r at a point x_0 if:

$$L_{g_j} L_f^k h_i(x) = 0; \quad 0 \leq k < r_i - 1, 1 \leq j \leq m \quad (4.6)$$

In this case, the matrix:

$$A(x) = \begin{bmatrix} L_{g_1} L_f^{r_1-1} h_1(x) & \cdots & L_{g_m} L_f^{r_1-1} h_1(x) \\ \vdots & \ddots & \vdots \\ L_{g_1} L_f^{r_m-1} h_m(x) & \cdots & L_{g_m} L_f^{r_m-1} h_m(x) \end{bmatrix} \quad (4.7)$$

is nonsingular or equivalently it has full rank:

$$\text{rank } A(x) = m$$

Definition 4.18 (total relative degree of nonlinear system): Based on the individual components r_i and vector relative degree, the total relative degree is defined as:

$$r = \sum_{i=1}^m r_i \quad (4.8)$$

For certain classes of nonlinear state space systems one can find computation algorithms and also sufficient or necessary conditions of system inversion, in order to obtain a differential algebraic polynomial of the input vector u_a by means of the output vector y through system inverse, see e.g.,[122][137].

Indeed, to derive an expression for $u_a(t)$ as a function of states and output in (4.1), following the inversion algorithm given by [122], we first need to compute the derivatives of $y_i, i = 1, \dots, m$. We have:

If $r_i = 1$, then:

$$\begin{aligned} y_i^{(1)} &= \frac{\partial h_i(x)}{\partial x} \dot{x}(t) \\ &= \frac{\partial h_i(x)}{\partial x} (f(x) + g(x) u_a) \\ &= L_f^1 h_i(x) + \sum_{j=1}^m L_{g_j}^1 L_f^0 h_i(x) u_{aj} \end{aligned}$$

If $r_i \neq 1$, then $L_{g_j}^1 L_f^0 h_i(x) = 0; 1 \leq j \leq m$

then we get:

$$y_i^{(1)} = L_f^1 h_i(x)$$

We should go on this differentia procedure, in general, for $k < r_i$, we have:

$$\begin{aligned} y_i^{(j)} &= L_f^j h_i(x) \\ &= \partial_x (L_f^{j-1} h_i(x) f(x)) + \sum_{s=0}^{j-2} \partial_{u_a^{(s)}} (L_f^{j-1} h_i(x)) u_a^{(s)} \quad j = 0, \dots, k, k < r_i \end{aligned}$$

Until when we reach the relative degree r_i , we then obtain::

$$y_i^{(r_i)} = L_f^{r_i} h_i(x) + \sum_{j=1}^m L_{g_j} (L_f^{r_i-1} h_i(x)) u_{aj} \quad i = 1, \dots, m$$

Given finite relative order r_1, \dots, r_m for (6.1) with respect to the output y , and if the total relative degree satisfied as:

$$r = \sum_{i=1}^m r_i = n$$

then calculating expressions for their derivatives, it can be referred to as a 1-step algorithm to obtain an inverse, we get:

$$\begin{bmatrix} y_1^{(r_1)} \\ \vdots \\ y_m^{(r_m)} \end{bmatrix} = \begin{bmatrix} L_f^{r_1} h_1(x) \\ \vdots \\ L_f^{r_m} h_m(x) \end{bmatrix} + \begin{bmatrix} L_{g_1} L_f^{r_1-1} h_1(x) & \dots & L_{g_m} L_f^{r_1-1} h_1(x) \\ \dots & \dots & \dots \\ L_{g_1} L_f^{r_m-1} h_m(x) & \dots & L_{g_m} L_f^{r_m-1} h_m(x) \end{bmatrix} u_a \quad (4.9)$$

the equation (6.8) can be solved for u_a to obtain:

$$u_a = \begin{bmatrix} L_{g_1} L_f^{r_1-1} h_1(x) & \dots & L_{g_m} L_f^{r_1-1} h_1(x) \\ \dots & \dots & \dots \\ L_{g_1} L_f^{r_m-1} h_m(x) & \dots & L_{g_m} L_f^{r_m-1} h_m(x) \end{bmatrix}^{-1} \cdot \left(\begin{bmatrix} y_1^{(r_1)} \\ \vdots \\ y_m^{(r_m)} \end{bmatrix} - \begin{bmatrix} L_f^{r_1} h_1(x) \\ \vdots \\ L_f^{r_m} h_m(x) \end{bmatrix} \right) \quad (4.10)$$

In this situation, there will be no internal dynamics and all the results will be finite time in nature.

However, normally, the total relative degree is assumed:

$$r = \sum_{i=1}^m r_i < n$$

In this case, the system given by (6.1) can be presented in a new basis that is introduced as follows.

Define the following change of the coordinates:

$$\begin{aligned} \xi_i &= [\xi_i^1, \xi_i^2, \dots, \xi_i^{r_i}]^T \\ &= [\phi_i^1(x), \phi_i^2(x), \dots, \phi_i^{r_i}(x)]^T \\ &= [h_i(x), L_f h_i(x), \dots, L_f^{r_i-1} h_i(x)]^T \quad i = 1, \dots, m \\ \xi &= [\xi_1, \xi_2, \dots, \xi_m] \\ &= [\phi_1(x), \phi_2(x), \dots, \phi_m(x)] \\ \eta &= [\phi_{r+1}(x), \phi_{r+2}(x), \dots, \phi_n(x)]^T \\ y &= [\xi_1^1, \xi_2^1, \dots, \xi_m^1] \end{aligned}$$

By application new local coordinates transformation proposed in [122], if the system hold the assumption of relative degree, it is always possible to find the function $\phi_{r+1}(x), \phi_{r+2}(x), \dots, \phi_n(x)$, thus :

$$\Phi(x) = [\phi_1(x), \phi_2(x), \dots, \phi_m(x), \phi_{r+1}(x), \dots, \phi_n(x)] \quad (4.11)$$

The mapping $\Phi(x)$ is a local diffeomorphism which means:

$$x = \Phi^{-1}(\xi, \eta) \quad (4.12)$$

Furthermore, according to [122], if the assumption is satisfied:

Assumption 4.4: the distribution is $\Gamma = \text{span} \{g_1 \ g_2 \ \dots \ g_m\}$ involutive, then, it is always possible to identify the function $\phi_{r+1}(x), \phi_{r+2}(x), \dots, \phi_n(x)$ in such a way that:

$$L_{g_j} \phi_i(x) = 0, i = r + 1, \dots, n, j = 1, \dots, m$$

$$\dot{\eta} = q(\xi, \eta)$$

Then input vector u_a can be obtained by means of the output vector y and its derivatives.

$$u_a = A(\Phi^{-1}(\xi, \eta))^{-1} \left(\begin{bmatrix} \xi_1^{(r_1)} \\ \vdots \\ \xi_m^{(r_m)} \end{bmatrix} - \begin{bmatrix} L_f^{r_1} h_1(\Phi^{-1}(\xi, \eta)) \\ \vdots \\ L_f^{r_m} h_m(\Phi^{-1}(\xi, \eta)) \end{bmatrix} \right) \quad (4.13)$$

4.7 Numerical Simulations

In this section, we present the results of a numerical simulation analysis performed to validate the effectiveness of the inverse interconnected system concepts presented in the previous sections. The main objective is to confirm by means of numerical simulations that the input of an invertible interconnected system can be recovered uniquely from measured output.

A case study is developed on an intensified HEX reactor. The pilot consists of three process plates sandwiched between five utility plates, two pneumatic control valves are used to control utility and process fluid. More relative information could be found in [160]. During the course of the simulation work, the aim is to prove that the pneumatic pressure of the actuators can be recovered by the measured outlet temperatures of the HEX reactor.

4.7.1 System Modelling

a-) Actuator Subsystem modelling

Pneumatic control valve is employed to act as actuator in this system. The main function of this pneumatic valve is to regulate the flow rate in a pipe line. By application of Bernoulli's continuous flow law of incompressible fluids, we have:

$$F = C_v f(X) \sqrt{\frac{\Delta P}{sg}}$$

where F is flow rate (m^3s^{-1}), ΔP is the fluid pressure drop across the valve (Pa), sg is specific gravity of fluid and equals 1 for pure water, X is the valve opening or valve "lift" ($X=1$ for max flow), C_v is valve coefficient (given by manufacturer), $f(X)$ is flow characteristic which is defined as the relationship between valve capacity and fluid travel through the valve. There are three flow

characteristics to choose from: linear valve control; quick opening valve control; equal percentage valve control. For linear valve, $f(X) = X$, the valve opening is related to stem displacement. In [1],[3], a pneumatic control valve has a dynamic model of the type:

$$p_c A_a = m \frac{d^2 X}{dt} + \mu \frac{dX}{dt} + kX$$

where A_a is the diaphragm area on which the pneumatic pressure acts, p_c is the pneumatic pressure, m is the mass of the control valve stem, μ is the friction of the valve stem, k is the spring compliance, and X is the stem displacement or percentage opening of the valve.

$$x_a^T = [x_{a1} \quad x_{a2} \quad x_{a3} \quad x_{a4}] = \left[X_1 \quad \frac{dX_1}{dt} \quad X_2 \quad \frac{dX_2}{dt} \right], \quad u^T = [u_1 \quad u_2] = [p_{c1} \quad p_{c2}], \quad u_a^T = [F_1 \quad F_2] = \left[C_v \sqrt{\frac{\Delta P_1}{sg}} X_1 \quad C_v \sqrt{\frac{\Delta P_2}{sg}} X_2 \right], \quad C = [c_1 \quad c_2 \quad c_3 \quad c_4] = \left[C_v \sqrt{\frac{\Delta P_1}{sg}} \quad 0 \quad C_v \sqrt{\frac{\Delta P_2}{sg}} \quad 0 \right].$$

the actuator subsystem is then described by four states, two inputs and two outputs, as:

$$\begin{cases} \dot{x}_a = \begin{bmatrix} 0 & 1 & 0 & 0 \\ -\frac{k_1}{m} & -\frac{\mu_1}{m} & 0 & 0 \\ 0 & 0 & 0 & 1 \\ 0 & 0 & -\frac{k_2}{m} & -\frac{\mu_2}{m} \end{bmatrix} x_a + \begin{bmatrix} \frac{A_a}{m} & 0 \\ 0 & 0 \\ 0 & \frac{A_a}{m} \\ 0 & 0 \end{bmatrix} u \\ u_a = \begin{bmatrix} C_v \sqrt{\frac{\Delta P_1}{sg}} & 0 & C_v \sqrt{\frac{\Delta P_2}{sg}} & 0 \end{bmatrix} x_a \end{cases} \quad (4.14)$$

b-) Process subsystem modelling

The heat exchanger reactor can be modeled as N ideally mixed interconnected tanks, the modelling of a given cell k is based on the mass and energy balances which describe the evolution of the characteristic values: temperature, mass, composition, pressure, etc. Consider the heat exchanger reactor system taken from [16], the dynamic equation governing the heat balance of the process fluid and the utility fluid are given by:

$$\dot{T}_p^k = \frac{UA}{\rho_p c_{pp} V_p} (T_u^k - T_p^k) + \frac{1}{V_p} (T_p^{k-1} - T_p^k) F_p$$

$$\dot{T}_u^k = \frac{UA}{\rho_u c_{pu} V_u} (T_p^k - T_u^k) + \frac{1}{V_u} (T_u^{k+1} - T_u^k) F_u$$

where ρ_p, ρ_u are density of the process fluid and utility fluid (in $\text{kg} \cdot \text{m}^{-3}$), V_p, V_u are volume of the process fluid and utility fluid (in m^3), c_{pp}, c_{pu} are specific heat of the process fluid and utility fluid (in $\text{J} \cdot \text{kg}^{-1} \cdot \text{K}^{-1}$), U is the overall heat transfer coefficient (in $\text{J} \cdot \text{m}^{-2} \cdot \text{K}^{-1} \cdot \text{s}^{-1}$). A is the reaction area (in m^2). F_p, F_u are mass flowrate of process fluid and utility fluid (in $\text{kg} \cdot \text{s}^{-1}$). T_p^{k-1} is the process fluid temperature of previous cell, for the cell 1, it is the inlet temperature of process fluid T_p^{in} . T_u^{k+1} is the utility fluid temperature of previous cell, for the cell N , it is the inlet temperature of utility fluid T_u^{in} .

For simplicity, we consider one cell model. Define the state vector as $x^T = [x_1, x_2]^T = [T_p, T_u]^T$, the control input $u_a^T = [u_{a1}, u_{a2}]^T = [F_p, F_u]^T$, the output vector of measurable variables $y^T = [y_1, y_2]^T = [T_p, T_u]^T$, then above two the equations can be rewritten in the following state-space form:

$$\begin{cases} \dot{x} = f(x) + \sum_{i=1}^2 g_i(x)u_a \\ y = h(x, u_a) \end{cases} \quad (4.15)$$

where $f(x) = \begin{pmatrix} f_1(x) \\ f_2(x) \end{pmatrix} = \begin{pmatrix} \frac{h_p A}{\rho_p C_p V_p} (T_{pi} - T_u) \\ \frac{h_u A}{\rho_u C_p V_u} (T_u - T_p) \end{pmatrix}$, and $g(x) = (g_1, g_2) = \begin{pmatrix} \frac{(T_{pi} - T_p)}{V_p} & 0 \\ 0 & \frac{(T_{ui} - T_u)}{V_u} \end{pmatrix}$,

$y_1 = x_1, y_2 = x_2$, T_{pi}, T_{ui} are the outputs of the previous cell, for the first cell, they are the inlet temperature of process fluid and utility fluid, besides, they are measured and are constant. It is worth noting that the exclusive consideration of such measurements is the usual case in an industrial environment.

Thus, an interconnected system is constituted by (4.14) and (4.15).

4.7.2 Checking Invertibility

As mentioned above, a key point to compute dynamic inverse via system inversion lies on the invertibility of the system, we address the computational aspect of the concepts by algebraic criteria introduced above. After that, by using eq. (4.13), we can represent the input of the system as a function of the output and its derivatives.

To check if the interconnected system, modelled by (4.14) and (4.15) is invertible, we have to check whether the output differential rank of each subsystem is equal to the number of the inputs.

1-) For process subsystem invertibility checking

There are two inputs in this work: flowrate of process fluid F_p and flowrate of utility fluid F_u which are denoted by u_{a1}, u_{a2} in (4.15) respectively. To compute the output differential rank, we first need to derive an explicit expression for the input in terms of the output y by computing the derivatives of y . When it comes to (4.15), two outputs are temperature of process fluid T_p and utility fluid T_u , which are denoted by y_1, y_2 in (4.15) respectively. As mentioned above, there are two inputs in this work, if the computed output differential rank is equal to the total number of inputs, then it refers that the process subsystem is invertible.

Step 1: Invertibility checking:

a-) differential all two outputs:

$$\begin{cases} \dot{y}_1 = a(y_2 - y_1) + \frac{u_{a1}}{V_p}(T_{pi} - y_1) \\ \dot{y}_2 = b(y_1 - y_2) + \frac{u_{a2}}{V_u}(T_{ui} - y_2) \end{cases} \quad (4.16)$$

b-) find all possible relations as the form given in (4.3).

There exists no any differential equation that output is independent of x and u_a , therefore, both outputs are differential dependent, $r=0$

c-) there are 2 outputs, therefore:

$$\rho = p - r = 2$$

Output differential rank is equal to the total number of inputs, and then the system is invertible.

2-) For the actuator subsystem invertibility checking

There are two inputs in actuator subsystem: the pneumatic pressures p_{c1} , p_{c2} which are denoted by u_1 u_2 in (4.14) respectively. By computing the derivatives of output vector u_{a1} , u_{a2} , invertibility of the actuator subsystem can be easily obtained.

4.7.3 Inverse System Representation

Step 1: Represents the inverse of the process subsystem as a function of the output and its derivatives:

Thanks to the invertibility of the system, we can compute the inverse of process subsystem (4.1) as a function of measured the output and its derivatives. According to (4.13), an expression for the two inputs can be derived as $\tilde{u}_a = [\tilde{u}_{a1} \quad \tilde{u}_{a2}]$:

$$\begin{cases} \tilde{u}_{a1} = \frac{V_p}{T_{pi}-y_1}(\dot{y}_1 - ay_2 + ay_1) \\ \tilde{u}_{a2} = \frac{V_u}{T_{ui}-y_2}(\dot{y}_2 - by_1 + by_2) \end{cases} \quad (4.17)$$

Step 2: Represents the inverse of the actuator subsystem as a function of the output and its derivatives:

According to Theorem 4.10, the inverse of an interconnected system is also an interconnected system. That is to say the input of the inverse actuator subsystem is in fact the output of the inverse process subsystem, then by computing successive derivatives of \tilde{u}_a , an expression for the two inputs can be derived as $u = [u_1 \quad u_2]$:

$$\begin{cases} u_1 = \alpha \cdot \beta_1 [\ddot{\tilde{u}}_{a1} + \gamma_{11}\dot{\tilde{u}}_{a1} + \gamma_{12}\tilde{u}_{a1}] \\ u_2 = \alpha \cdot \beta_2 [\ddot{\tilde{u}}_{a2} + \gamma_{21}\dot{\tilde{u}}_{a2} + \gamma_{22}\tilde{u}_{a2}] \end{cases} \quad (4.18)$$

Where $\alpha = \frac{m}{A_a}$, $\beta_i = 1/C_v \sqrt{\frac{\Delta P_i}{sg}}$, $i = 1, 2$, $\gamma_{11} = -\frac{k_1}{m}$, $\gamma_{12} = -\frac{\mu_1}{m}$, $\gamma_{21} = -\frac{k_2}{m}$, $\gamma_{22} = -\frac{\mu_2}{m}$

4.7.4 Numerical Simulation

The proposed invertibility algorithm was simulated with respect to actuator and process subsystems using the values given in Table 1. These constants, corresponding to a HEX exchanger reactor system having fast dynamics, were taken from [16]. The inlet temperatures T_{pi} and T_{ui} were 76°C and 15.6 °C respectively, the computed inlet flow rate of the utility fluid F_u is $4.22e^{-5}m^3s^{-1}$, and inlet flow rate of the process fluid F_p is constant $4.17e^{-6}m^3s^{-1}$, the computed value means the expected true values of the actuators. Parameters in actuator subsystem are: $m=2kg$, $A_a=0.029m^2$, $\mu=1500Ns/m$ and $k=6089 Ns/m$, pressure drop ΔP in utility fluid is 0.6MPa and 60KPa in process fluid.

TABLE I PHYSICAL DATA USED IN THE PILOT

Constant	description	Value	units
hA	overall heat transfer coefficient*reaction area	214.8	W. K ⁻¹
A	Reaction area	$4e^{-6}$	m ³
V_p	process fluid volume	$2.685e^{-5}$	m ³
V_u	utility fluid volume	$1.141e^{-4}$	m ³
ρ_p, ρ_u	fluid density	1000	kg. m ⁻³
c_{p_p}, c_{p_u}	specific heat of the fluid	4180	J. kg ⁻¹ . k ⁻¹
T_{ui}	utility fluid input	15.6	°C
T_{pi}	process fluid input	76	°C

The pneumatic pressures p_{c1} , p_{c2} are considered as the two inputs of the actuator subsystem, the values are 1MPa, 1.2Mpa for utility and process fluid respectively. The aim here is to check whether the recovered values of pneumatic pressures via the inverse interconnected system are consistent with the original values. To achieve this aim, two simulations are implemented. In case one, constant value is simulated, while in case 2, we considered there is an abrupt change in pneumatic pressure of utility fluid p_{c2} , simulation results are reported in Figs. 4.5-4.8

Case 1: constant pneumatic pressure p_{c1} , p_{c2}

In this case, we consider both pneumatic pressures p_{c1} , p_{c2} remain constant. The aim is to check whether inverse interconnected system can recover the original inputs (pneumatic pressure p_{c1} , p_{c2}) of the interconnected system correctly. Fig.4.5 demonstrates the reconstructibility of the inverse process subsystem using measured outlet temperature and Fig.4.6 corresponds to output of the inverse interconnected system using results of inverse process subsystem. Fig.4.5 together with Fig.4.6 confirms the reconstructibility of the interconnected system. As shown in Fig. 4.5, the black solid lines are the real values of both fluid flow rates while red dash lines represent the outputs of the inverse process system. It is illustrated in Fig. 4.5 that, after a short transient period, the values of red dash lines track the black solid lines correctly. Therefore the inverse process subsystem could recover its input with acceptable

accuracy. After then, the resulted outputs of the inverse process subsystem are fed to the actuator inverse subsystem to check the tracking capacities.

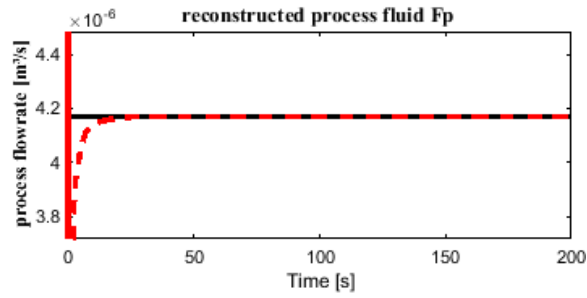


Fig.4.5a computed and reconstructed process fluid flow rate in case 1, black solid is the computed value while red dash curve is recovered by inverse system

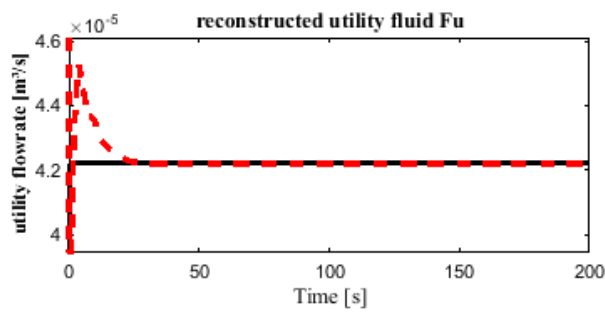


Fig.4.5b computed and reconstructed utility fluid flow rate in case 1, black solid is the computed value while red dash curve is recovered by inverse system

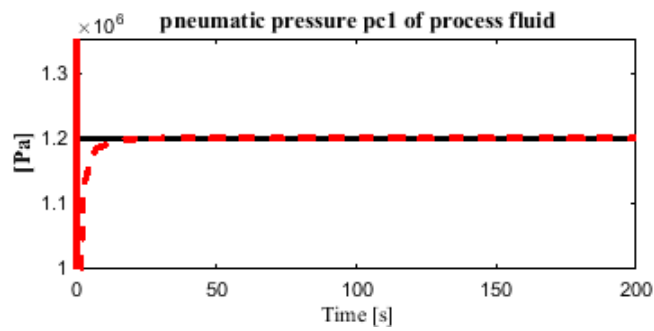


Fig.4.6a measured and recovered pneumatic pressured of process fluid flow rate in case 1, black solid line is the measured value while red dash line is recovered by inverse interconnected system

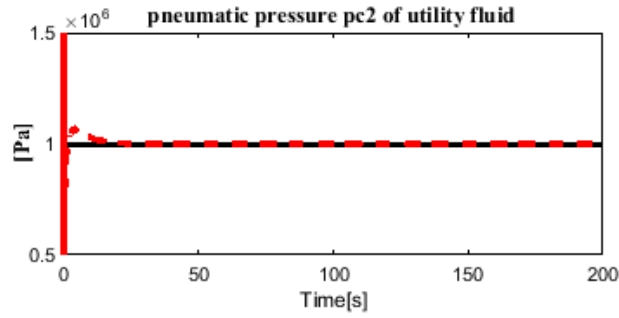


Fig.4.6b measured and recovered pneumatic pressured of utility fluid flow rate in case 1, black solid line is the measured value while red dash line is recovered by inverse interconnected system

As we can see from Fig.4.6, the recovered pneumatic pressure (red dash line), which are also the outputs of the inverse interconnected system, converge to the measured pneumatic pressure (black solid curve) after short transient time. Thus we can conclude that the input of an interconnected system can be recovered by the inverse system correctly if both subsystems are invertible. It implies that the interconnected system is invertible since the input can be recovered by the output correctly.

Case 2: constant pneumatic pressure p_{c1} , and varied pneumatic pressure p_{c2}

In this simulation, we intend to confirm that the inverse computation procedure is effective even the input is time varying. For that, we consider that the pneumatic pressure p_{c1} of process fluid remain constant also, however, the value of pneumatic pressure p_{c2} varies from 1Mpa to 1.05Mpa at time 80s. The simulation results are illustrated in Fig. 4.7 and Fig. 4.8.

It can be seen from Fig. 4.7 that both reconstructed fluid flow rates in red dash curves track the computed values after a short time. Due to change of pneumatic pressure p_{c2} at 80s, both reconstructed values fluctuated. Then reconstructed process fluid flow rate F_p converges back to its computed value again after several seconds. For the utility fluid flow rate F_u , we can see that the reconstructed value stables at a new level after transient. Since the reconstructed value is obtained by the inverse process subsystem via global measured temperature, it is obvious that changes of variables at local actuator subsystem have distinguishable impacts on global measured outputs which are in accordance with the assumption. The next task is to feed the inverse actuator subsystem with outputs of inverse process subsystem to identify the reconstructibility of the inverse interconnected system. The simulation results are shown in Fig. 4.8.

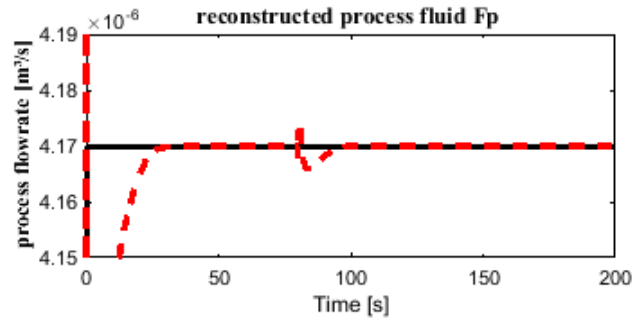


Fig.4.7a computed and reconstructed process fluid flow rate in case 2, black solid is the computed value while red dash curve is recovered by inverse system

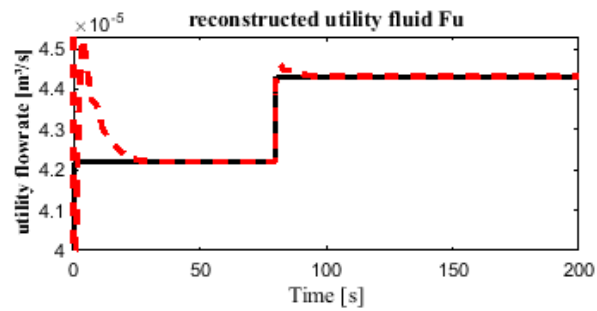


Fig.4.7b computed and reconstructed utility fluid flow rate in case 2, black solid is the computed value while red dash curve is recovered by inverse system

As we can see from Fig. 4.8, both reconstructed pneumatic pressure p_{c1} , p_{c2} in red dash lines follow up the measured values in black solid lines after short transient response. At time 80s, recovered pneumatic pressure p_{c1} of process fluid flow rate in Fig.4.8a varies at 80s due to the variation parameter pneumatic pressure p_{c2} , after then the curve tracks back its measured value in black solid line. The result is plotted in Fig. 4.8b for recovered pneumatic pressure p_{c2} of utility fluid flow rate. The recovered value in red dash line tracks the measured value, then at 80s, both measured and recovered values changes, and after short transient response time, they are overlapped again. It implies that the inputs of the interconnected system can be uniquely recovered by the inverse interconnected system, in other words, the inputs at local level have distinguishable influences at higher level if the interconnected system is invertible. However, it is also obviously that the computation bias is relatively important, it may even larger if measurement noise exists.

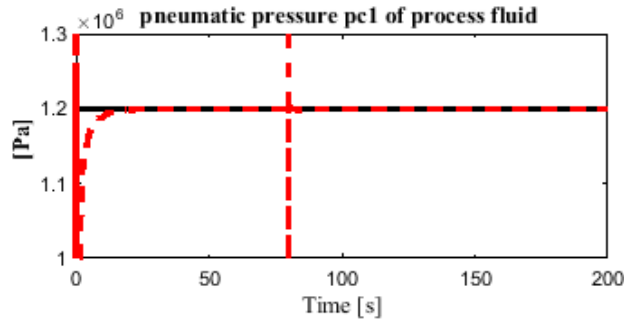


Fig. 4.8a measured and recovered pneumatic pressured of process fluid flow rate in case 2, black solid line is the measured value while red dash line is recovered by inverse interconnected system

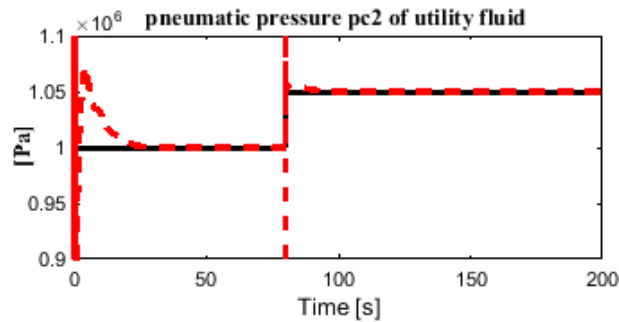


Fig. 4.8b measured and recovered pneumatic pressured of utility fluid flow rate in case 2, black solid line is the measured value while red dash line is recovered by inverse interconnected system

4.8 Summary

This chapter addresses the invertibility problem of interconnected nonlinear systems involving two nonlinear subsystems that affine in controls. The studied interconnected system can be formulated to describe as a composition map of two cascade connections. The problem is concerned with the ability to reconstruct the input at local level uniquely from given output and initial state. A necessary and sufficient condition for the invertibility of the interconnected nonlinear systems is given, which requires the invertibility of individual subsystems. When all the subsystems are invertible, we present an algorithm for finding inputs at local subsystem that generate a given output at global system. Detailed examples are included to illustrate these developed concepts.

Although large bias involves and large computation errors may appear especially when outputs are corrupted with noise, the particular aim is to confirm that the inputs at local level have distinguishable impacts at global level in case the interconnected system is invertible. In that case, it allows monitoring and analyzing the overall system at local subcomponent but using global information. For example, if we view failures at local component as unknown input, we can recognize different faults through their distinguishable impacts on global outputs, thus a combination of local intelligence with a more advanced diagnostic capability (combining fault monitoring and diagnosis at both local and global levels) to perform FDD functions is achieved.

CHAPTER 5 OBSERVER DESIGN FOR INVERTIBLE INTERCONNECTED SYSTEM

This chapter investigates the possibility to decompose a control system into an interconnection of actuator and process subsystems, and studies observers for such interconnected nonlinear system. This allows monitoring the properties of the interconnected system globally and locally. Specially, the interconnection between the two subsystems, which is the output of the actuator and also the input of the process, is assumed to be inaccessible. It is due to that, for the actuator, it can be uneconomic or unrealistic to measure its output. The practical meaning is as the following: for one hand, the measurement equipment or the running costs for this measurement may be very expensive; for the other, the measured value could be unreliable due to its rough operation environment.

5.1 Introduction

In practice, interconnected dynamical systems appear in many control applications whether naturally or intentionally due to control design. An interconnected system consists of a series of interconnected dynamical units, and therefore exhibits very complicate dynamics has received increasing treats in various fields of the real world, such as biology, sociology, World Wide Web, electrical power grids, and so on [161].

Over the past years, the interconnected complex system has received increasing attention. A large number of publications are focused on the problem of stabilization and control problems with satisfactory results. The literature concerning the complex dynamic networks which consist of a large number of interconnected units are relatively important, different kinds of methodologies are developed, like in [162][106]. For example in [163], an observer based controller scheme is designed to robustly drive a sensor-less Induction Motor (IM) even for the case of low frequencies with unknown load torque. And in [101], a functional observer based controller is derived to estimate directly a stabilizing control for a wide class of large scale systems, constituted by subsystems with interconnection terms between each other.

Compare to the literature concerning the purpose of synchronization, the purpose of better understanding the dynamics of each subsystem, as well as making use of this information for maintenances, the topic of states estimation and reconstruction of unknown input through available measurements has also received extensively attention in the literature, see e.g. in [152][27]. Note that a centralized observer may not be practical for the complex interconnected systems due to the complexity of implementation, and the state or parts of the state cannot be measured due to uneconomic measurement costs or physical circumstances like high temperatures, where no measurement equipment is available, for example.

A solution to overcome this difficulty is to decompose the complex systems into an interconnection of several subsystems so that the observers can be designed in a decentralized manner. A typical

approach of state estimation is to design observers for each subsystem individually and the overall estimator is formed by gathering all the observers. It is because, normally, nonlinear interconnected systems such as complex biological processes and power networks operate using local state information. This is due to the fact that global network states are generally unavailable, arrive with time delays, or require expensive infrastructure. Coupled with nonlinear interconnections, state disturbances, and sensor noise/attacks, the distributed state estimation problem is a challenging one. Therefore, distributed states observers are proposed for estimating the internal states of the nonlinear subsystems using measurement of inputs and outputs for each subsystem in many cases. For instance in [164], an observer is designed for the whole system from the separate synthesis of observers for each subsystem, assuming that for each of these separate designs, the states from the other subsystem are available. In [165], for each subsystem of the interconnected system, it is proposed the observer using the state estimation of the previous subsystem. In addition, a quasi-ISS/ISDS reduced-order observer for the whole system is designed considering interconnections quasi-ISS/ISDS reduced-order observers for each subsystem are derived in [166]. Existing observers for single nonlinear systems are normally employed for individual local systems in these approaches. In fact, in the last decades, the problem of state observation for single nonlinear system have intensively been investigated, resulting in various types of observers like high gain observer in [89][83], sliding mode observer in [167] , adaptive observer in [168],etc.

Notice that in most practical situations, the complete state measurements are not available for each subsystem, as explained in [150]. But with respect to the previous mentioned results, the availability of the states (or a functional of the states) of each subsystem is required. This problem is normally tackled by transforming unavailable information as unknown inputs (UI) through system augmentation in the literature. The problem of designing an observer for a multi-variable dynamic system partially driven by unknown inputs has been widely studied, as in [169]. Such observers can be of important use for systems subject to disturbances or with inaccessible inputs, or when dealing with the problem of fault diagnosis. Results are also available for interconnected systems subject to unknown inputs. Like in [161], the problems of both state estimation and unknown input reconstruction for uncertain complex networks are simultaneously discussed. What's more, in [170], distributed unknown input observers are proposed for estimating the internal states of the nonlinear subsystems using local measurement outputs. For each subsystem, the network configuration is exploited to formulate sufficient conditions for the estimation of the unknown input to arbitrary accuracy.

With respect to the above mentioned state observation problems, contributions dealing with the state observation problem for interconnected system subjected to unknown interconnections have received less extensively treats in the literature. Moreover, the proposed methodologies are often developed for a particular kind of interconnected system. A promising approach was reported in [153] where the problem of state observation is addressed for nonlinear systems modeled by an ODE–PDE series association. The aim is to accurately estimate online the state vector of the ODE subsystem and the

distributed state of the PDE element. This problem has also been studied for interconnected system formed by a nonlinear system followed by a linear system, like in [152]. Authors developed an observer design methodology for the resulting cascade nonlinear and linear interconnection, based on estimating the unavailable output together with the states of the linear system. The paper [150] proposes a functional observer for each subsystem of two interconnected system. The proposed observers are free of interconnection terms and the observation error is unbiased.

This chapter considers the issues of both state and unknown interconnection estimation for the interconnected system represented by two nonlinear associations connected in series. The aim is to accurately estimate online the states vector of each subsystem, as well as the unknown interconnection. One major difficulty is that the state observation must only rely on the output of the global system at the terminal subsystem making useless existing observers developed for separately nonlinear system. It is because the connection point between the subsystems is assumed not to be accessible to measurements. To cope with this difficulty, estimation via observer theory is employed. We extend the use of some classical observers to the interconnected dynamic system. For each subsystem of the interconnected system, it is proposed the use of the global observer using the state estimation of the other subsystem, and we insure the asymptotic stability of the overall estimator which is formed by the gathering of all the observers and estimators. Two underlying issues are worth to be highlighted to better understand the nature of the considered estimation problem. Firstly, the measurement output used in the observer of former subsystem is assumed not accessible; the solution is to replace it by an estimate via observer of latter subsystem. In fact, this unknown output is the unknown interconnection which is also the input of the latter subsystem. Secondly, in the latter subsystem, the estimated interconnection that provided for the previous subsystem is treated as an additional state, forming a new extended subsystem; and expression for the new state is obtained by computing derivatives of output equation of the previous subsystem, resulting in a function of input.

This chapter is organized as follows: the problem formulation is introduced in Section 5.2, where the type of dynamic units of the interconnected system is performed. The main objective is introduced. Section 5.3 contains all the results for the observer design with respect to interconnected systems. Some numerical simulation examples are given to illustrate the effectiveness of the proposed methods in section 5.4. Finally, conclusion is made in section 5.5.

5.2 Motivation and Problem Formulation

The problem of states observation is addressed for nonlinear systems that can be modeled by a nonlinear interconnected series association. The studied interconnected system consists of two interconnected nonlinear dynamical units, the actuator and the process subsystems, as shown in Fig.5.1. The partitioning of the overall system into two subsystems may stem from inherent physical divisions in a particular application, or it may be a convenient way to represent a system for design purposes. Both subsystems are considered as input affine type. The aim is to accurately monitor the states vector of both subsystems, as well as the interconnection. The idea is then to design an observer for the overall

system from the separate synthesis of observers for each subsystem, assuming that the states from the other subsystem are available.

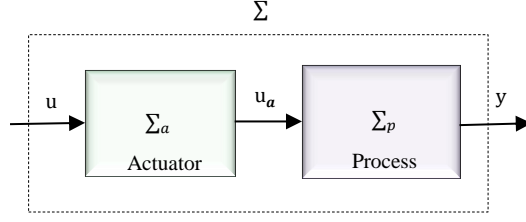


Fig 5.1 interconnected system structure

We consider a dynamical process subsystem as the form:

$$\Sigma_p: \begin{cases} \dot{x} = f(x) + g(x)u_a, & x(t_0) = x_0 \\ y = h(x, u_a) \end{cases} \quad (5.1)$$

where $x \in \mathfrak{R}^n$ is the state of the process subsystem, $y \in \mathfrak{R}^p$ is the output of the global system, which is also the output of the process subsystem. $u_a \in \mathfrak{R}^m$ is the input of process subsystem, which is also the output of the actuator subsystem. u_a is inaccessible and is reconstructed from measurements of y . f and g are smooth vector field on \mathfrak{R}^n and h is smooth vector field on \mathfrak{R}^p .

An input affine structure is also assumed for the actuator subsystem:

$$\Sigma_a: \begin{cases} \dot{x}_a = f_a(x_a) + g_a(x_a)u, & x_a(t_0) = x_{a0} \\ u_a = h_a(x_a, u) \end{cases} \quad (5.2)$$

where $x_a \in \mathfrak{R}^n$ is the state, $u \in \mathfrak{R}^1$ is the input, $u_a \in \mathfrak{R}^m$ is the output of the actuator subsystem, which is also the input of the process subsystem. f_a and g_a are smooth vector field on \mathfrak{R}^n and h is smooth vector field on \mathfrak{R}^m .

As introduced in [164], by considering models of physical process, we assume that inputs are bounded borelian functions and belong to some set $\mathcal{U}, \mathcal{U}_a$, that $u \subset \mathcal{U}$, and $u_a \subset \mathcal{U}_a$, the space of all bounded borelian function taking their values in $\mathcal{U}, \mathcal{U}_a$.

Considering interconnected system depicted by (5.1) and (5.2), it is desirable to monitor the performance of the interconnected system with aspect to individual subsystems and the overall system. One way to achieve this purpose is to have observers for each of the subsystems and the whole network. However, the major difficulty for employing the existing methods is to satisfy the assumption that inputs and outputs of each subsystem are available, since the connection point between the two blocks is not accessible to measurements. This is because the connection is the output of the actuator subsystem where measurements are either difficult to obtain due to physical reasons or the measurement is uneconomical since actuators are often far from the controller. Therefore the state observation in this work can only rely on the global system output i.e. the process state at the terminal boundary. As shown in Fig. 5.1, the particular aim in our design is to accurately estimate online the state vector x and x_a of each subsystem, as well as the unmeasured interconnection vector u_a using measurements of input u and output y .

Existing observers in the literature are not available for the purpose. To cope with this difficulty, we assume that design of the observer can be divided into one part to estimate the unknown interconnection, which is the input of the latter subsystem and output of the former subsystem, and a second part to estimate the state of the two subsystems. To achieve this purpose, we extend the use of some classical observers to the interconnected dynamic system. For each subsystem of the interconnected system, it is proposed the use of the global observer using the state estimation of the other subsystem, and we insure the asymptotic stability of the overall estimator which is formed by the gathering of all the observers.

5.3 Observer Design

The structure of the proposed observer is depicted in Fig. 5.2. It is a two level interconnected observer system which consists of two state estimators, the actuator and the process state estimators. The actuator state estimator deals with estimating the states in actuator subsystem. First, we assume that an observer with a corresponding quadratic-type Lyapunov function has already been designed for the actuator subsystem. We then consider the problem that arises when the output from the actuator subsystem is not available directly, but instead available via the second subsystem, the process subsystem. That is, the output from the actuator subsystem acts as the input to the process subsystem, from which measurement of the final product is in turn available. To get a solution for the unknown output of the actuator subsystem, the process state estimator is a coordinator dealing with interconnections by extending the interconnection as an additional state of the process subsystem. This process state estimator generates an input sequence which is applied to the actuator subsystem as estimation of its output. Then the overall observer estimates the states and interconnection of the interconnected system by using the estimates of the two estimators.

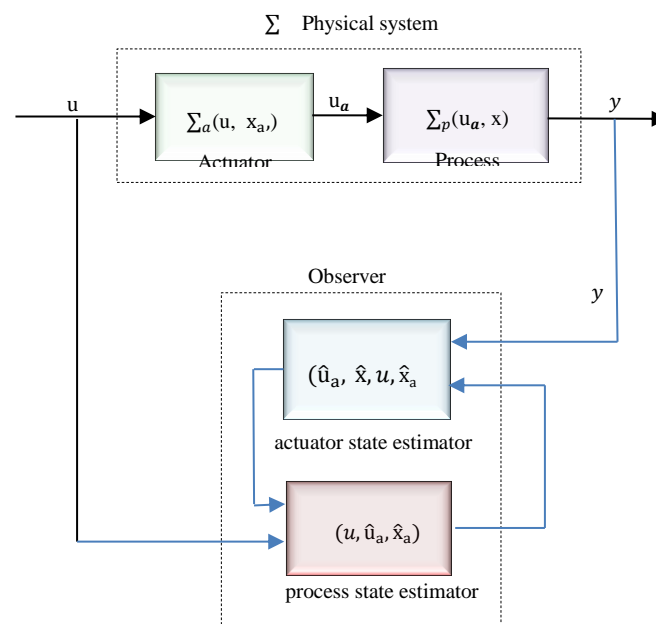


Fig. 5.2 structure of the proposed interconnected observer

As shown in Fig. 5.2, the main idea of the proposed interconnected observer design is as follows. First, an existing observer is supposed to be already available for the nonlinear subsystem Σ_a with measured output u_a , then we implement that observer using an estimate of u_a , denoted by \hat{u}_a . In order to produce such an estimate, we extend the state space of the process subsystem Σ_p to include u_a as an additional state. By computing derivatives of u_a in actuator subsystem, we can obtain an expression corresponding to time derivatives of the output u_a which is a function of u , derivatives of u and x_a . Then an observer is constructed for this extended process subsystem. State estimator of actuator subsystem, together with state estimator of process subsystem, a kind of interconnected observer designed method is then proposed for the studied interconnected nonlinear system. It must be pointed out that this work is significantly inspired by the works proposed in [152] and [171]. In [152], an observer for the nonlinear and linear system is investigated in which invertibility of the nonlinear system is not required and observer design is not utilized for fault detection purpose. The novelty of the presented approach in this work stems from that it deals with a nonlinear interconnected system which consists of two nonlinear subsystems connected in cascade manners; this is quite different from the one in [152]. In this work, we maintain the assumption of stabilities interconnections expression by computing derivatives of output in the previous subsystem as proposed in [152]. While for the part of extending unknown input as an extra state, the estimator is of the same structure form proposed in [171], but the time derivatives expression of unknown input differs. In [171], the unmeasured part is a known function with respect to states, inputs and noise, etc.

5.3.1 Observer Design for the Interconnected System

1-) Interconnected System Extension

Consider system depicted by (5.1) and (5.2) ,let:

$$\begin{aligned} x_u &\triangleq u_a \\ \dot{x}_u &= \dot{u}_a \\ \dot{x}_u &= \frac{\partial h_a}{\partial u}(u, x_a)\dot{u} + \frac{\partial h_a}{\partial x_a}(u, x_a)f_a(u, x_a) \\ &= \varepsilon(u, \dot{u}, x_a) \end{aligned}$$

A new interconnected system can be expressed by: $\Sigma = \Sigma_p + \Sigma_a + x_u$

$$\begin{cases} \dot{x} = f(x) + g(x)x_u \\ \dot{x}_u = \varepsilon(u, \dot{u}, x_a) \\ \dot{x}_a = f_a(x_a) + g_a(x_a)u \\ y = h(x) \\ x(t_0) = x_0; x_a(t_0) = x_{a0}; x_u = h_a(x_a) \end{cases}$$

Where input of the system is u , and output is y , u_a is an unmeasured state.

Then new actuator and new process subsystem can be expressed as:

$$\Sigma_p: \begin{cases} \dot{x} = f(x) + g(x)x_u \\ \dot{x}_u = \varepsilon(u, \dot{u}, x_a) \end{cases} \quad (5.3)$$

$$\Sigma_a: \dot{x}_a = f_a(x_a) + g_a(x_a)u \quad (5.4)$$

2-) an observer for new actuator subsystem

First, consider a converging observer for actuator subsystem (5.3) as the following form is admitted:

$$\begin{cases} \dot{\hat{x}}_a = f_a(\hat{x}_a) + g_a(\hat{x}_a)u + k_a(\varrho_a, \hat{x}_a)(h_a(\hat{x}_a) - u_a) \\ \dot{\varrho}_a = G_a(\hat{x}_a, u, \varrho_a) \end{cases} \quad (5.5)$$

Where k_a , G_a are smooth gain functions with respect to their arguments and yet to be defined. G_a is a subset of \mathfrak{R}^n . To this end, introduce the state estimation error as:

$$e_a := x_a - \hat{x}_a$$

Then subtracting corresponding equation of (5.3) and (5.5), we get the following error dynamics as:

$$\begin{cases} e_a := x_a - \hat{x}_a \\ \dot{e}_a(t, e_a) = f_a(x_a) + g_a(x_a)u - f_a(\hat{x}_a) - g_a(\hat{x}_a)u - K(u, \hat{x}_a, u_a) \end{cases}$$

Where $K(u, \hat{x}_a, u_a) = k_a(\varrho_a, \hat{x}_a)(h_a(\hat{x}_a) - u_a)$.

In order to formulate a solution to the convergence of the observer, we need the following assumption 5.1 with respect to error Lyapunov function introduced in [164]. This error Lyapunov function shows the equivalence of the existence of an error Lyapunov function and the existence of a converging observer.

Assumption 5.1: for any $u \in \mathcal{U}$, $(t, e_a) \in \mathcal{A}$. $\mathcal{C}(\mathcal{R}^+, \mathcal{R})$, there exists a continuously differentiable function V_a and positive constants $\alpha, \beta, \gamma_1, \gamma_2$, satisfies:

$$\begin{cases} (a) \gamma_1 \|e_a\|^2 \leq V_a(t, e_a) \leq \gamma_2 \|e_a\|^2 \\ (b) \frac{\partial V_a}{\partial t}(t, e_a) + \frac{\partial V_a}{\partial e_a}(t, e_a)\dot{e}_a \leq \alpha \|e_a\|^2 \\ (c) \left\| \frac{\partial V_a}{\partial e_a}(t, e_a) \right\| \leq \beta \|e_a\| \end{cases}$$

The observer defined by (5.5) is an exponential observer if Assumption 5.1 is satisfied, such that:

$$\lim_{t \rightarrow \infty} e_a(t) = 0$$

$$\int_0^\infty e_a(t) < \infty$$

The observer in (5.5) could be implemented on condition that u_a is accessible, but it is not the fact in the case. Since u_a in our design represents the output of the actuator subsystem which is assumed unmeasured, therefore we have to replace u_a with an estimated \tilde{u}_a by the available measurements.

Suppose that estimation of \tilde{u}_a is available, by substituting u_a as \tilde{u}_a , we can now implement observer (5.5) for actuator subsystem as the following form:

$$\begin{cases} \dot{\hat{x}}_a = f_a(\hat{x}_a) + g_a(\hat{x}_a)u + k_a(\varrho_a, \hat{x}_a)(h_a(\hat{x}_a) - \tilde{u}_a) \\ \dot{\varrho}_a = G_a(\hat{x}_a, u, \varrho_a) \end{cases} \quad (5.6)$$

Denote $K(u, \hat{x}_a, \tilde{u}_a) = k_a(\varrho_a, \hat{x}_a)(h_a(\hat{x}_a) - \tilde{u}_a)$.

We seek again estimation error by subtracting corresponding equation in (5.3) and (5.6), thus yielding the new error dynamics as follows:

$$\begin{aligned}
\dot{\tilde{e}}_a(t, \tilde{e}_a) &= f_a(x_a) + g_a(x_a)u - f_a(\hat{x}_a) - g_a(\hat{x}_a)u - K(u, \hat{x}_a, \tilde{u}_a) \\
&= f_a(x_a) + g_a(x_a)u - f_a(\hat{x}_a) - g_a(\hat{x}_a)u - K(u, \hat{x}_a, u_a) + K(u, \hat{x}_a, u_a) - K(u, \hat{x}_a, \tilde{u}_a) \\
&= \dot{e}_a(t, e_a) + K(u, \hat{x}_a, u_a) - K(u, \hat{x}_a, \tilde{u}_a)
\end{aligned} \tag{5.7}$$

In order to ensure exponential stability of the error dynamics (5.7), we need an assumption regarding the sensitivity of $K(u, \hat{x}_a, u_a)$ with respect to changes in u_a . In particular, since output of actuator subsystem \tilde{u}_a used in observer (5.6) is in fact a virtual measurement which is estimated by output of the process subsystem, thus estimation error becomes unavoidable. This estimation error can be viewed as bounded disturbance to the real output of the actuator subsystem u_a . Therefore the basic problem addressed in this work is the design of nonlinear observer that possesses robustness to the disturbance affecting the real output. The following Assumption 5.2 provides a sufficient condition for achieving this purpose. This subject of following statement is inspired by [8] and proven in Appendix 5.1.

Assumption 5.2: for any $u \in \mathcal{U}$, $(t, \hat{x}_a, \hat{u}_a) \in \mathcal{A}$. $\mathcal{C}(\mathcal{R}^+, \mathcal{R})$, there exists a real constant γ_3 satisfies:

$$\|K(u, \hat{x}_a, u_a) - K(u, \hat{x}_a, \hat{u}_a)\| \leq \gamma_3 \|u_a - \hat{u}_a\| \tag{5.8}$$

In addition to asking that the state estimation error e_a converges to 0 in the absence of disturbances, we want it to still converge to 0 if a disturbance is present but converge to 0, and to remain bounded if the disturbance is bounded. Therefore Assumption 5.2 implies that the definition of $\dot{\tilde{e}}_a(t, \tilde{e}_a)$ in (5.7) is not affected.

Theorem 5.1: if Assumption 5.1 and Assumption 5.2 are satisfied, then the observer described in (5.6) is an exponential observer for the actuator subsystem described in (5.2).

The proof is given in Appendix 5.2.

Let us discuss this property with high gain observer as an example to confirm Theorem 5.1. Relative proof is placed in Appendix 5.3 and Appendix 5.4.

Assume without any loss of generality, the studied invertible system (5.3) can be transformed into the following form:

$$\begin{cases} \dot{\chi}_1 = A_1 \chi_1 + \Theta_1(\chi_1, u) \\ u_a = C_1 \chi_1 \end{cases} \tag{5.9}$$

$$\text{with } \chi_1^T = (\chi_{11} \quad \dots \quad \chi_{1n})^T, \quad A_1 = \begin{bmatrix} 0 & 1 & \dots & 0 \\ \vdots & \ddots & \ddots & \vdots \\ 0 & \dots & 0 & 1 \\ 0 & \dots & 0 & 0 \end{bmatrix}, \quad \Theta_1(\chi_1, u) = \begin{bmatrix} \Theta_1(\chi_{11}, u) \\ \vdots \\ \Theta_n(\chi_{11}, \dots, \chi_{1n}, u) \end{bmatrix}, \quad C_1 =$$

$$[1 \quad 0 \quad \dots \quad 0],$$

this transformation with the structure ensures the existence of a high gain observer for system (5.2) of the following structure, as shown in [89]:

$$\begin{cases} \dot{\hat{\chi}}_1 = A_1 \hat{\chi}_1 + \Theta_1(\hat{\chi}_1, u) - S_{\theta_1}^{-1} C_1^T (C_1 \hat{\chi}_1 - u_a) \\ 0 = \theta_1 S_{\theta_1} + A_1^T S_{\theta_1} + S_{\theta_1} A_1 - C_1^T C_1 \end{cases} \quad (5.10)$$

Where define $\Delta_{\theta_1} = \begin{bmatrix} 1 & 0 & \dots & 0 \\ 0 & \theta_1^{-1} & \ddots & 0 \\ \vdots & \ddots & \ddots & 0 \\ 0 & \dots & 0 & \theta_1^{-(n-1)} \end{bmatrix}$, then $S_{\theta_1} = \frac{1}{\theta_1} \Delta_{\theta_1} S_{1_1} \Delta_{\theta_1}$ and $S_{1_1} = S_{\theta_1|\theta=1}$.

By defining estimation error $e_1 := \hat{\chi}_1 - \chi_1$, we then obtain the error dynamics from (5.7) as:

$$\dot{e}_1(t, e_1) = (A_1 - S_{\theta_1}^{-1} C_1^T C_1) e_1 + \Theta_1(\hat{\chi}_1, u) - \Theta_1(\chi_1, u) \quad (5.11)$$

By defining $V_1(e_1) = \frac{1}{\theta_1} e_1^T S_{\theta_1} e_1$, the following convergence of the error dynamics is obtained and the proof of which is given in Appendix 5.3. That:

$$\dot{V}_1(e_1) \leq -\theta_1 V_1 + 2n\theta \frac{\lambda_{\max}(S_{1_1})}{\lambda_{\min}(S_{1_1})} V_1 \quad (5.12)$$

Set $\theta_1^* = 2n\theta \frac{\lambda_{\max}(S_{1_1})}{\lambda_{\min}(S_{1_1})}$, then by taking $\theta_1 > \theta_1^*$, it results that Assumption 5.1 holds. The following lemma analyzes the conditions for the boundedness of estimation error dynamics of the subsystem.

Lemma 5.1: Assume that the subsystem (5.9) satisfies Assumptions 5.1. Then there exists $\theta_1^* > 0$, such that $\forall \theta_1 > \theta_1^*$, the error dynamics (5.11) will remain bounded.

Now, let consider that u_a in (5.10) is inaccessible and is replaced by its estimates \tilde{u}_a , then the observer for system (5.2) is expressed in terms of variables \tilde{u}_a and $\hat{\chi}_1, u$. Thus the observer (5.10) becomes the following structure:

$$\begin{cases} \dot{\hat{\chi}}_1 = A_1 \hat{\chi}_1 + \Theta_1(\hat{\chi}_1, u) - S_{\theta_1}^{-1} C_1^T (C_1 \hat{\chi}_1 - \tilde{u}_a) \\ 0 = \theta_1 S_{\theta_1} + A_1^T S_{\theta_1} + S_{\theta_1} A_1 - C_1^T C_1 \end{cases} \quad (5.13)$$

By defining estimation error as $\tilde{e}_1 := \hat{\chi}_1 - \chi_1$ and subtracting corresponding equation in (5.9) and (5.13), one can obtain the error dynamics equation which is the same as the structure proposed in (5.7) and (5.11):

$$\begin{aligned} \dot{\tilde{e}}_1(t, \tilde{e}_1) &= A_1 \hat{\chi}_1 + \Theta_1(\hat{\chi}_1, u) - S_{\theta_1}^{-1} C_1^T (C_1 \hat{\chi}_1 - \tilde{u}_a) - (A_1 \chi_1 + \Theta_1(\chi_1, u)) \\ &= \dot{e}_1 + S_{\theta_1}^{-1} C_1^T (u_a - \tilde{u}_a) \end{aligned} \quad (5.14)$$

Our purpose is to prove the convergence of the observer (5.13) where output u_a is substituted by its estimate \tilde{u}_a . We have to confirm that if estimation \tilde{u}_a satisfied Assumption 5.2, then convergence of (5.14) is guaranteed. To achieve this purpose, define the positive Lyapunou function $\tilde{V}_1(\tilde{e}_1)$ as:

$$\tilde{V}_1(\tilde{e}_1) = \frac{1}{\theta_1} \tilde{e}_1^T S_{\theta_1} \tilde{e}_1 \quad (5.15)$$

Now the convergence of observer (5.13) is obtained by calculating time-derivation of (5.15). Specific related proven procedure is given in Appendix 5.4. The final result is as follows:

$$\dot{\tilde{V}}_1(\tilde{e}_1) \leq -\theta_1 V_1 + 2nq \frac{\lambda_{\max}(S_{1_1})}{\lambda_{\min}(S_{1_1})} V_1 + \frac{1}{\lambda_{\min}(S_{1_1})} \sqrt{V_1} \|u_a - \hat{u}_a\| \quad (5.16)$$

Therefore by choosing $\theta_1^* = \left(2nq \frac{\lambda_{\max}(S_{1_1})}{\lambda_{\min}(S_{1_1})} + \frac{1}{\lambda_{\min}(S_{1_1})} \right)$, the right side of the above inequality is negative. It implies that Theorem 5.1 holds.

2-) an observer for new process subsystem

In order to produce an observer for the process subsystem which is with unknown inputs, we have solved this problem by extending this unknown input as an additional state, and propose an observer for the extended system.

According to [152], we define a function $\varepsilon(u, \dot{u}, x_a)$ with respect to the time derivative of the output u_a in (5.4).

$$\varepsilon(u, \dot{u}, x_a) = \frac{\partial h_a}{\partial u}(u, x_a) \dot{u} + \frac{\partial h_a}{\partial x_a}(u, x_a) f_a(u, x_a) \quad (5.17)$$

Assumption 5.3: For any $u \in \mathcal{U}$, $(t, \hat{x}_a) \in \mathcal{A}$. $\mathcal{C}(\mathcal{R}^+, \mathcal{R})$, there exists a real constant γ_4 satisfies that:

$$\|\varepsilon(u, \dot{u}, \hat{x}_a) - \varepsilon(u, \dot{u}, x_a)\| \leq \gamma_4 \|x_a - \hat{x}_a\|$$

Similar to Assumption 5.2, Assumption 5.3 implies global Lipchitz-type condition on function ε , and it can also be replaced by local smoothness condition since u, \dot{u}, x_a are bounded in physical problem.

Consider system (5.3), define $z = [z_1 \ z_2] = [x \ x_u]$, then system (5.3) can be extended as:

$$\begin{cases} \dot{z}_1 = f_1(z_1, u) + g_1(z_1, u)z_2 \\ \dot{z}_2 = \varepsilon(u, \dot{u}, x_a) \\ y = z_1 \end{cases} \quad (5.18)$$

Where $f_1(z_1) = f(x, u)$, $g_1(z_1, u) = g(x, u)$, we can organize an observer for system (5.18) as follows:

$$\begin{cases} \dot{\hat{z}}_1 = f_1(\hat{z}_1, u) + g_1(\hat{z}_1, u)\hat{z}_2 - H_{z_1}(\hat{y} - y) \\ \dot{\hat{z}}_2 = \varepsilon(u, \dot{u}, \hat{x}_a) - H_{z_2}(\hat{y} - y) \\ \hat{y} = \hat{z}_1 \end{cases} \quad (5.19)$$

System (5.18) can be expressed as in a condensed form:

$$\begin{cases} \dot{z} = l(z_1)G(z_1)z + F(z_1) + \bar{\varepsilon}(u, \dot{u}, x_a) \\ y = Cz \end{cases} \quad (5.20)$$

Where: $G(z_1) = \begin{pmatrix} 0 & g_1(z_1) \\ 0 & 0 \end{pmatrix}$, $F(x_1) = \begin{pmatrix} f_1(z_1) \\ 0 \end{pmatrix}$, $C = (I_n \quad 0)$, $\bar{\varepsilon}(u, \dot{u}, x_a) = [0 \quad \varepsilon(u, \dot{u}, x_a)]^T$, I_n is $n \times n$ identity matrix, $l(z_1)$ is a scalar real function with respect to their arguments and $\alpha_1 \leq |l(z_1)| \leq \beta_1$.

Supposed the assumptions defined in [171] related boundedness of the states, signals, functions etc. are satisfied, an extended high gain observer for the system (5.20) can be given in the following way:

$$\begin{cases} \dot{\hat{z}} = l(\hat{z}_1)G(\hat{z}_1)\hat{z} + F(\hat{z}_1) + \bar{\varepsilon}(u, \dot{u}, \hat{x}_a) + H(\hat{z}_1)(\hat{y} - y) \\ \hat{y} = C\hat{z} \end{cases} \quad (5.21)$$

Where: $H = [H_{z_1} \quad H_{z_2}]^T = \Lambda^{-1}(\hat{z}_1)S_\theta^{-1}C^T$, $\Lambda(\hat{z}_1) = \begin{bmatrix} 1 & 0 \\ 0 & G_1(\hat{z}_1) \end{bmatrix}$, S_θ is the unique symmetric positive definite matrix satisfying the following algebraic Lyapunov equation:

$$\theta S_\theta + A^T S_\theta + S_\theta A - C^T C = 0 \quad (5.22)$$

Where $A = \begin{bmatrix} 0 & I \\ 0 & 0 \end{bmatrix}$, $\theta > 0$ is a parameter defined by (5.22) and the solution of (5.22) is:

$$S_\theta = \begin{bmatrix} \frac{1}{\theta} I & -\frac{1}{\theta^2} I \\ -\frac{1}{\theta^2} I & \frac{2}{\theta^3} I \end{bmatrix}$$

Then, the gain of estimator can be given by:

$$H = \Lambda^{-1}(\hat{z}_1)S_\theta^{-1}C^T = \Lambda(\hat{z}_1) \begin{bmatrix} 2\theta I \\ \theta^2 G_1^{-1}(\hat{x}_1) \end{bmatrix} \quad (5.23)$$

Theorem 5.2: If Assumption 5.3 is satisfied, by proper choosing a relatively high gain tuner θ , the system (5.21) becomes a converging observer for the system described in (5.20) which is a transformed form of the process subsystem described in (5.1).

The proof is given in Appendix 5.5. The proof goes along the lines of the proof of Theorem 1 in [171] with corresponding changes according to definition of expression for unknown input in (5.17) and properties defined in Assumption 5.3.

3-) Synthesis Observers

System (5.6), together with (5.21), constitutes the observer for the studied interconnected system depicted by (5.4) and (5.20), as follows:

$$\begin{cases} \dot{\hat{x}}_a = f_a(\hat{x}_a, u) + g_a(\hat{x}_a)u + k_a(g_a, \hat{x}_a)(h_a(\hat{x}_a) - \hat{z}_2) \\ \dot{\hat{z}} = l(\hat{z}_1)G(\hat{z}_1)\hat{z} + F(\hat{z}_1) + \bar{\varepsilon}(u, \dot{u}, \hat{x}_a) + H(\hat{z}_1)(\hat{y} - y) \end{cases} \quad (5.24)$$

Where virtual measurement \tilde{u}_a in (5.6) is replaced by its estimation \hat{z}_2 . The observer estimation errors satisfy the following equation:

$$\tilde{e}_a = \hat{x}_a - x_a, e(t) = \hat{z}(t) - z(t) \quad (5.25)$$

5.3.2 Observer Analysis

The observer (5.24) has been designed so that the dynamics of the corresponding error system (5.25) are governed as:

$$\begin{cases} \dot{\tilde{e}}_a(t, \tilde{e}_a) = \dot{e}_a(t, e_a) + K(u, \hat{x}_a, u_a) - K(u, \hat{x}_a, \hat{u}_a) \\ \dot{e}(t, e) = (l(\hat{z}_1)G(\hat{z}_1) + H(\hat{z}_1)C)e + (l(\hat{z}_1)G(\hat{z}_1) - l(z_1)G(z_1))z(t) + F(\hat{z}_1, u) - F(z_1, u) - e_{\tilde{e}}(t, \tilde{e}_a) \end{cases} \quad (5.26)$$

To analyze the system (5.26), our purpose is to study the stability of the error dynamics.

Proposition 5.1: If the Assumptions 5.1-5.3 are satisfied, then a relatively high values of θ can be chosen that the error dynamics governed in (5.26) is exponentially stable.

Proof: The objective is to analysis the stability of the error dynamics, to achieve this purpose, by using V_a and V_z defined Theorem 5.1 and Theorem 5.2, the following Lyapunov function candidate is constructed:

$$V(t, \tilde{e}_a, e) = V_a(t, \tilde{e}_a) + V_z(t, e) \quad (5.27)$$

Then time derivation of $V(t, \tilde{e}_a, e)$ yields:

$$\begin{aligned} \dot{V}(t, \tilde{e}_a, e) &= \underbrace{\frac{\partial V_a}{\partial t}(t, \tilde{e}_a) + \frac{\partial V_a}{\partial e_a}(t, e_a)\dot{e}_a(t, e_a) + \frac{\partial V_a}{\partial e_a}(t, e_a)(K(u, \hat{x}_a, u_a) - K(u, \hat{x}_a, \hat{u}_a))}_{\text{term 1}} \\ &+ \underbrace{\frac{\partial V_z}{\partial t}(t, e) + \frac{\partial V_z}{\partial e_z}(t, e)\dot{e}(t, e)}_{\text{term 2}} \end{aligned} \quad (5.28)$$

Let us analyze the different terms on the right side of (5.28), starting with term 1 and using results in Theorem 5.1:

$$\begin{aligned} \frac{\partial V_a}{\partial t}(t, \tilde{e}_a) + \frac{\partial V_a}{\partial e_a}(t, e_a)\dot{e}_a(t, e_a) + \frac{\partial V_a}{\partial e_a}(t, e_a)(K(u, \hat{x}_a, u_a) - K(u, \hat{x}_a, \hat{u}_a)) \\ \leq -\alpha V_a + \gamma_2 \gamma_3 \sqrt{V_a} \|u_a - \hat{u}_a\| \\ \leq -\alpha V_a + \gamma_2 \gamma_3 \sqrt{V_a} \|\hat{z}(t) - z(t)\| \\ \leq -\alpha V_a + \gamma_2 \gamma_3 \sqrt{V_z} \sqrt{V_a} \end{aligned}$$

In turn, the term 2 on the right side of (5.28) develops as follows:

$$\frac{\partial V_z}{\partial t}(t, e) + \frac{\partial V_z}{\partial e_z}(t, e)\dot{e}_a(t, e) \leq (-\theta\alpha_1 + \eta_1)V_z + \frac{\eta_2}{\theta} \sqrt{V_z} \sqrt{V_a}$$

Then, the overall inequality yields:

$$\dot{V}(t, \tilde{e}_a, e) \leq -\alpha V_a + \gamma_2 \gamma_3 \sqrt{V_z} \sqrt{V_a} + (-\theta\alpha_1 + \eta_1)V_z + \frac{\eta_2}{\theta} \sqrt{V_z} \sqrt{V_a} + \frac{\eta_2}{\theta} \sqrt{V_z} \sqrt{V_a} \quad (5.29)$$

Now, set $V_a^* = \alpha V_a$, $V_z^* = (-\theta\alpha_1 + \eta_1)V_z$ and $V^* = V_a^* + V_z^*$.

Please note that:

$$\begin{aligned} V^* &\geq (\theta\alpha_1 - \eta_1)V_z, \\ V_a^* + V_z^* &\geq 2\sqrt{V_a^*}\sqrt{V_z^*} \\ &= 2\sqrt{\alpha(\theta\alpha_1 - \eta_1)}\sqrt{V_z}\sqrt{V_a} \end{aligned}$$

Thus:

$$\sqrt{V_z}\sqrt{V_a} \leq \frac{1}{2\sqrt{\alpha(\theta\alpha_1 - \eta_1)}}V^*$$

It is easy to get that inequality (5.29) yields to:

$$\begin{aligned} \dot{V}(t, \tilde{e}, e_a) &\leq -V^* + \frac{1}{2\sqrt{\alpha(\theta\alpha_1 - \eta_1)}}\left(\gamma_2\gamma_3 + \frac{\eta_2}{\theta}\right)V^* \\ &\leq -(\theta\alpha_1 - \eta_1)\left(1 - \frac{1}{2\sqrt{\alpha(\theta\alpha_1 - \eta_1)}}\left(\gamma_2\gamma_3 + \frac{\eta_2}{\theta}\right)\right)V \end{aligned}$$

Now, it suffices to choose θ such that $\left(1 - \frac{1}{2\sqrt{\alpha(\theta\alpha_1 - \eta_1)}}\left(\gamma_2\gamma_3 + \frac{\eta_2}{\theta}\right)\right) \geq 0$.

This ends the proof ■.

Theorem 5.1: Letting the gain of the observer be selected as in Proposition 5.1, there exists a scalar θ^* , such that for all $\theta \geq \theta^*$, then the interconnected observer depicted by (5.25) denotes an observer for interconnected system depicted by (5.3) and (5.4) with an exponential error convergence.

5.3.3 Particular example: two high gain observers interconnected

In this section, the above interconnected observer design method is confirmed by choosing two high gain observers for actuator and process subsystems as an example.

Following the system (5.13) and (5.21), the observer for interconnected system depicted in (5.9) and (5.20) is then developed as follows:

$$\begin{cases} \dot{\hat{\chi}}_1 = A_1\hat{\chi}_1 + \theta_1(\hat{\chi}_1, u) - S_{\theta_1}^{-1}C_1^T(C_1\hat{\chi}_1 - \hat{z}_2) \\ \dot{\hat{z}} = l(\hat{z}_1)G(\hat{z}_1)\hat{z} + F(\hat{z}_1) + \bar{e}(u, \dot{u}, \hat{x}_a) + H(\hat{z}_1)(c\hat{z}_1 - y) \end{cases}$$

The observer estimation errors satisfy the following equation:

$$\tilde{e}_1 = \hat{\chi}_1 - \chi_1, e(t) = \hat{z}(t) - z(t)$$

To analysis the stability of the error dynamics, by using V_a and V_z defined as:

$$V_1(\tilde{e}_1) = \frac{1}{\theta_1}\tilde{e}_{11}^T S_{\theta_1} \tilde{e}_{11} \text{ and } V_z(t, e) = \tilde{e}^T S_1 \tilde{e}$$

The following Lyapunov function candidate is constructed:

$$V(t, \tilde{e}_1, e) = V_1(t, \tilde{e}_1) + V_z(t, e)$$

Then time derivation of $V(t, \tilde{e}_1, e)$ is calculated as follows, the detailed calculation is placed in Appendix 5.6:

$$\dot{V}(t, \tilde{e}_1, e) \leq -\left(1 - \frac{1}{2\sqrt{(\theta_0 - \kappa)(\theta_0\alpha_1 - \eta_1)}}\left(\rho + \frac{\eta_2}{\theta_0}\right)\right)V^* \quad (5.30)$$

Where $\theta_0 = \max\{\theta_1, \theta\}$, $\kappa = 2n\rho \frac{\lambda_{\max}(S_{11})}{\lambda_{\min}(S_{11})}$, $\rho = \frac{1}{\lambda_{\min}(S_{11})}$, then it follows that :

Thus by appropriately choosing such that $\left(1 - \frac{1}{2\sqrt{(\theta_0 - \kappa)(\theta_0\alpha_1 - \eta_1)}}\left(\rho + \frac{\eta_2}{\theta_0}\right)\right) \geq 0$ is guaranteed, the convergence of the observer is obtained.

5.4 Numerical Simulation

In this section, we present the results of a numerical simulation analysis performed to validate the effectiveness of the interconnected observer presented in the previous sections. The main objective is to confirm by means of numerical simulations that the interconnected observer given by (5.24) can be designed as software sensors for monitoring the performance of heat exchangers reactor system. Furthermore, the results obtained through the implementation of the observers can be analyzed in order to conclude existence of actuator fault and to provide initial value for FD (fault diagnosis) and RCA (root cause analysis) observer in faulty situation.

A case study is developed on an intensified HEX reactor. The pilot consists of three process plates sandwiched between five utility plates, two pneumatic control valves are used to control utility and process fluid. More relative information could be found in [160]. Moreover, the outlet fluid flow rates of the control valves are assumed unmeasured according to realistic. Therefore during the course of the simulation work, the proposed observers are designed for estimating unmeasured inlet flows u_a and monitoring performance in the Hex reactor from available measurements. The measurements involve the inlet outlet temperatures of the Hex reactor and the pneumatic pressure of the actuators. It essentially aims at estimating unmeasured inlet flows u_a whose variation may relate to decrease of overall heat transfer coefficient. And overall heat transfer coefficient analysis conveys a full description of heat transfer rate evolution. Thus, any reduction observed in heat transfer rates may be directly related to heating performance degradation. Accordingly, the information obtained from the monitoring of u_a can readily provide a strong support base to determine when a preventive or a corrective maintenance is necessary for preserving or restoring the heat transfer rates in processes.

5.4.1 System Modelling

1-) Actuator subsystem modelling

As introduced in Chapter 4, the actuator system model can be described as :

$$x_a^T = [x_{a1} \quad x_{a2} \quad x_{a3} \quad x_{a4}] = \left[X_1 \quad \frac{dx_1}{dt} \quad X_2 \quad \frac{dx_2}{dt} \right], \quad u^T = [u_1 \quad u_2] = [p_{c1} \quad p_{c2}],$$

$$u_a^T = [F_1 \quad F_2] = \left[C_v \sqrt{\frac{\Delta P_1}{sg}} X_1 \quad C_v \sqrt{\frac{\Delta P_2}{sg}} X_2 \right], \quad C = [c_1 \quad c_2 \quad c_3 \quad c_4] = \left[C_v \sqrt{\frac{\Delta P_1}{sg}} \quad 0 \quad C_v \sqrt{\frac{\Delta P_2}{sg}} \quad 0 \right].$$

the actuator subsystem is then described by four states, two inputs and two outputs, as:

$$\begin{cases} \dot{x}_a = \begin{bmatrix} 0 & 1 & 0 & 0 \\ -\frac{k_1}{m} & -\frac{\mu_1}{m} & 0 & 0 \\ 0 & 0 & 0 & 1 \\ 0 & 0 & -\frac{k_2}{m} & -\frac{\mu_2}{m} \end{bmatrix} x_a + \begin{bmatrix} \frac{A_a}{m} & 0 \\ 0 & 0 \\ 0 & \frac{A_a}{m} \\ 0 & 0 \end{bmatrix} u \\ u_a = \begin{bmatrix} C_v \sqrt{\frac{\Delta P_1}{sg}} & 0 & C_v \sqrt{\frac{\Delta P_2}{sg}} & 0 \end{bmatrix} x_a \end{cases} \quad (5.31)$$

2-) Process subsystem modelling

As in chapter 4, define the state vector as $x^T = [x_1, x_2]^T = [T_p, T_u]^T$, the control input $u_a^T = [u_{a1}, u_{a2}]^T = [F_p, F_u]^T$, the output vector of measurable variables $y^T = [y_1, y_2]^T = [T_p, T_u]^T$, then above two the equations can be rewritten in the following state-space form:

$$\begin{cases} \dot{x} = f(x) + \sum_{i=1}^2 g_i(x) u_a \\ y = h(x, u_a) \end{cases} \quad (5.32)$$

where $f(x) = \begin{pmatrix} f_1(x) \\ f_2(x) \end{pmatrix} = \begin{pmatrix} \frac{h_p A}{\rho_p c_{p,p} V_p} (T_{pi} - T_u) \\ \frac{h_u A}{\rho_u c_{p,u} V_u} (T_u - T_p) \end{pmatrix}$, and $g(x) = (g_1, g_2) = \begin{pmatrix} \frac{(T_{pi} - T_p)}{V_p} & 0 \\ 0 & \frac{(T_{ui} - T_u)}{V_u} \end{pmatrix}$,

$y_1 = x_1, y_2 = x_2$, T_{pi}, T_{ui} are the outputs of the previous cell, for the first cell, they are the inlet temperature of process fluid and utility fluid, besides, they are measured and are constant. It is worth noting that the exclusive consideration of such measurements is the usual case in an industrial environment.

By using (5.17), we can obtain a function for the derivatives for u_a :

$$\begin{aligned} \dot{u}_a = \varepsilon(u, \dot{u}, x_a) &= \frac{\partial h_a}{\partial u}(u, x_a) \dot{u} + \frac{\partial h_a}{\partial x_a}(u, x_a) f_a(u, x_a) \\ &= \begin{pmatrix} C_v \sqrt{\frac{\Delta P_1}{sg}} & 0 & C_v \sqrt{\frac{\Delta P_2}{sg}} & 0 \end{pmatrix} x_a + \begin{pmatrix} \frac{A_a}{m} C_v \sqrt{\frac{\Delta P_1}{sg}} & \frac{A_a}{m} C_v \sqrt{\frac{\Delta P_2}{sg}} \end{pmatrix} u \end{aligned} \quad (5.33)$$

Define the state vector as $x_1^T = [x_{11}, x_{12}]^T = [T_p, T_u]^T$, unmeasured state $x_2^T = [x_{21}, x_{22}]^T = [u_{a1}, u_{a2}]^T = [F_p, F_u]^T$, the output vector of measurable variables $y^T = [y_1, y_2]^T = [T_p, T_u]^T$, then the equation (5.32) and (5.33) can be rewritten in the following state-space form:

$$\begin{cases} \dot{x}_1 = G_1(x_1) x_2 + g_1(x_1, u) \\ \dot{x}_2 = \varepsilon(u, \dot{u}, x_a) \\ y = x_1 \end{cases} \quad (5.34)$$

$$\text{Where, } G_1(x_1) = \begin{pmatrix} \frac{(T_{pi}-x_{11})}{V_p} & 0 \\ 0 & \frac{(T_{ui}-x_{12})}{V_u} \end{pmatrix}, \text{ and } f_1(x) = \begin{pmatrix} \frac{h_p A}{\rho_p C_{p_p} V_p} (x_{11} - x_{12}) \\ \frac{h_u A}{\rho_u C_{p_u} V_u} (x_{12} - x_{11}) \end{pmatrix}.$$

In this case, the full state of the studied system is given as:

$$\begin{cases} \dot{x} = G(x_1)x + F(x_1, u) + \bar{\varepsilon}(t) \\ y = Cx \end{cases} \quad (5.35)$$

$$\text{Where } x = \begin{bmatrix} x_1 \\ x_2 \end{bmatrix}, G(x_1) = \begin{pmatrix} 0 & G_1(x_1) \\ 0 & 0 \end{pmatrix}, F(x_1, u) = \begin{pmatrix} f_1(x, u) \\ 0 \end{pmatrix}, C = (I \quad 0), \bar{\varepsilon}(t) = \begin{pmatrix} 0 \\ \varepsilon(t) \end{pmatrix}$$

5.4.2 Observer Design

1-) observer 1 for actuator subsystem

In this model, outputs are considered as unmeasured and are substituted by its estimation proposed in observers 2, then, an extended high gain observer of the form (5.6) for system (5.31) is given by:

$$\begin{cases} \hat{\dot{x}}_a = \begin{bmatrix} 0 & 1 & 0 & 0 \\ -\frac{k_1}{m} & -\frac{\mu_1}{m} & 0 & 0 \\ 0 & 0 & 0 & 1 \\ 0 & 0 & -\frac{k_2}{m} & -\frac{\mu_2}{m} \end{bmatrix} \hat{x}_a + \begin{bmatrix} \frac{A_a}{m} & 0 \\ 0 & 0 \\ 0 & \frac{A_a}{m} \\ 0 & 0 \end{bmatrix} u - \begin{bmatrix} k_1 \\ k_2 \\ k_3 \\ k_4 \end{bmatrix} [C\hat{x}_a - \hat{x}_2] \\ \hat{u}_a = \begin{bmatrix} C_v \sqrt{\frac{\Delta P_1}{sg}} & 0 & C_v \sqrt{\frac{\Delta P_2}{sg}} & 0 \end{bmatrix} \hat{x}_a \end{cases} \quad (5.36)$$

2-) observer 2 for process subsystem

It should be noted that the original system (5.32) has been augmented with the differential equation $\dot{u}_a = \varepsilon(u, \dot{u}, x_a)$, that is to say the unknown inputs are treated like an unmeasured state. Then, it is possible to design an observer of the form (5.21) for the system by (5.35) as follows:

$$\begin{cases} \hat{\dot{x}}_1 = \begin{pmatrix} \frac{(T_{pi} - \hat{x}_{11})}{V_p} & 0 \\ 0 & \frac{(T_{ui} - \hat{x}_{12})}{V_u} \end{pmatrix} \hat{x}_2 + \begin{pmatrix} \frac{h_p A}{\rho_p C_{p_p} V_p} (\hat{x}_{11} - \hat{x}_{12}) \\ \frac{h_u A}{\rho_u C_{p_u} V_u} (\hat{x}_{12} - \hat{x}_{11}) \end{pmatrix} - \begin{pmatrix} 2\theta \\ 2\theta \end{pmatrix} (\hat{y} - y) \\ \hat{\dot{x}}_2 = \begin{pmatrix} C_v \sqrt{\frac{\Delta P_1}{sg}} & 0 & C_v \sqrt{\frac{\Delta P_2}{sg}} & 0 \end{pmatrix} \hat{x}_a + \begin{pmatrix} \frac{A_a}{m} C_v \sqrt{\frac{\Delta P_1}{sg}} & \frac{A_a}{m} C_v \sqrt{\frac{\Delta P_2}{sg}} \end{pmatrix} u - \begin{pmatrix} \theta^2 \frac{h_p A}{\rho_p C_{p_p} V_p} (\hat{x}_{11} - \hat{x}_{12}) \\ \theta^2 \frac{h_u A}{\rho_u C_{p_u} V_u} (\hat{x}_{12} - \hat{x}_{11}) \end{pmatrix} (\hat{y} - y) \\ \hat{y} = \hat{x}_1 \end{cases} \quad (5.37)$$

It should be remarked that although F_p, F_u undergo different initial trajectories in each observer; they will converge to their “true values” as time t tends to infinity.

5.4.3 Numerical Simulations Results

In order to test the performance of the proposed observers, two numerical simulations were carried out. Considering the actuator and process model given by (5.31) and (5.35), observers 1 (5.36) and observer 2 (5.37) were designed for estimating unmeasured inlet flows F_p, F_u , and monitoring performance final

product T_p, T_u in the Hex reactor from available measurements. These measurements involve the inlet outlet temperatures of the hex reactor and the pneumatic pressure p_{c1}, p_{c2} of the actuators.

Two cases were considered. In Case 1, constant inlet flows F_p, F_u are considered in both utility and process fluid actuators. By contrast, in Case 2, F_p, F_u are considered as time-varying individually and simultaneously respectively. Observers 1 and 2 were simulated with respect to actuator and process subsystems using the values given in chapter 4. These constants, corresponding to a HEX exchanger reactor system having fast dynamics, were taken from [16]. The inlet temperatures T_{pi} and T_{ui} were 76°C and 15.6°C respectively. Parameters in actuator subsystem are: $m=2\text{kg}$, $A_a = 0.029\text{m}^2$, $\mu = 1500\text{Ns/m}$ and $k=6089\text{Ns/m}$, P_c for utility fluid is 1MPa , 1.2Mpa for process fluid, pressure drop ΔP in utility fluid is 0.6MPa and 60KPa in process fluid.

Case 1: Both inlet fluid flow rates F_p, F_u are constant

The objective of this series of simulations is to prove the convergence of the observers in the common situation in which both fluid flow rates remain constant over a long time. The computed inlet flow rate of the utility fluid F_u is $4.22e^{-5}\text{m}^3\text{s}^{-1}$, and inlet flow rate of the process fluid F_p is constant $4.17e^{-6}\text{m}^3\text{s}^{-1}$, the computed value means the expected true values of the actuators. The initial conditions of the process model were: $T_p^0 = 80^\circ\text{C}$ and $T_u^0 = 20^\circ\text{C}$ respectively, while those of the observers were: $\hat{T}_p^0 = \hat{T}_u^0 = 30$. The discrepancies between the initial conditions of the process and that of the observers are reasonable and realistic considering that temperature is a process variable that can be easily measured. In order to evaluate the observer performance against uncertainties on the knowledge of fluid flow rate, the initial value of the estimates were $\hat{F}_p^0 = \hat{F}_u^0 = 0$ in both observers. This assumption represents a relatively rough situation in practical engineering world, however, simulation results show an encouraging results. The tuning parameters were $k_1 = k_3 = 100, k_2 = k_4 = 0.15$ (for Observer 1) respectively, and $\theta = 80$ (for Observer 2).

The results of the estimation of outlet temperature T_p and T_u are reported in Fig. 5.3 and Fig. 5.4 respectively. The dash curve corresponds to the estimates obtained using Observer 1, and solid line is the measured temperature. It can be seen that the convergence of the estimated \hat{T}_p and \hat{T}_u proves to be fast (in several seconds). This fact is not surprising because, actually T_p and T_u are the measured outputs of the overall system.

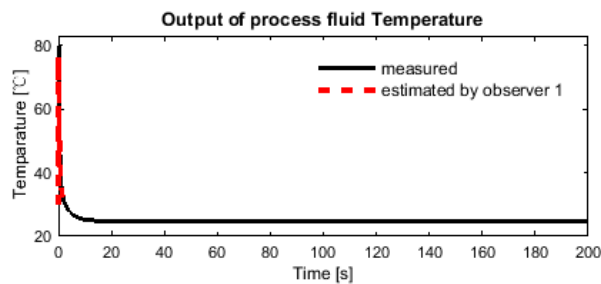


Fig. 5.3 output of process fluid temperature, solid line is the measured value T_p , while dash line is the estimated value \hat{T}_p by observer 1

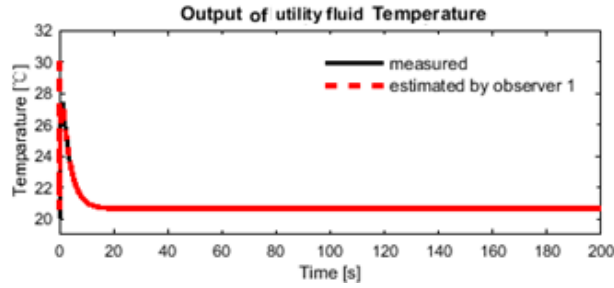


Fig. 5.4 output of utility fluid temperature , solid line is the measured value T_u , while dash line is the estimated value \hat{T}_u using observer 1

The main contribution of the proposed method is the capacity that it can estimate the unknown connection of an interconnected system by the final measured outputs, where the unknown connection represents the inlet fluid flow rate F_p , F_u in the Hex reactor system. Fig.5.5 and Fig 5.6 give the encouraged results. Fig. 5.5 shows the computation F_p and estimation of process fluid flow rate \hat{T}_u using Observer 2. Fig. 5.6 shows the computation F_u and estimation \hat{F}_u of utility fluid flow rate using Observer 2 respectively. As expected, \hat{F}_p and \hat{F}_u follow different trajectories before they converge towards the “true value” (computed value) in a relatively short transient period. For process fluid, after less than 5s, the two curves overlapped, and it takes about 1s for the utility fluid. In both fluids, these differences are caused by their varied initial values. However, it is proved that if adequate values of the tuning parameters k and θ are selected, no matter the degree of deviation of the initial value of \hat{F}_p^0 and \hat{F}_u^0 from the simulated value in the system model, convergences are guaranteed. Larger values of these tuning parameters ensure a smaller convergence time while smaller values have the opposite effect. However, large tuning values should be avoided since the observer may become too sensitive to measurement noise in real-time applications. According to the above analysis, we can readily conclude that the proposed interconnected observer works effectively on the designed purposes with proper tuning parameters.

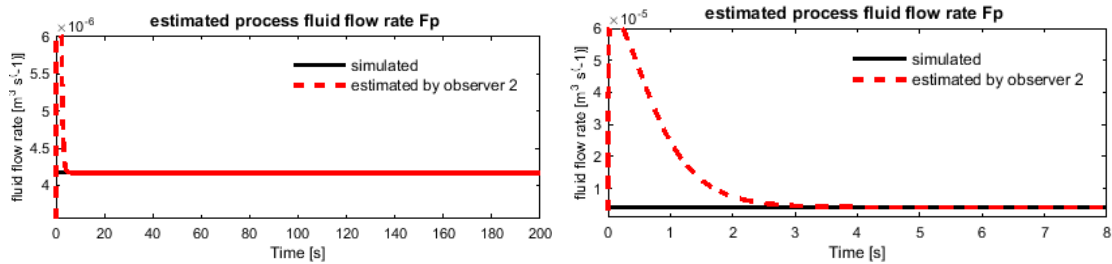


Fig. 5.5 the computation and estimation of process fluid flow rate. Solid line is the computed value F_p ; dash line is the estimated one \hat{F}_p by Observer 2.

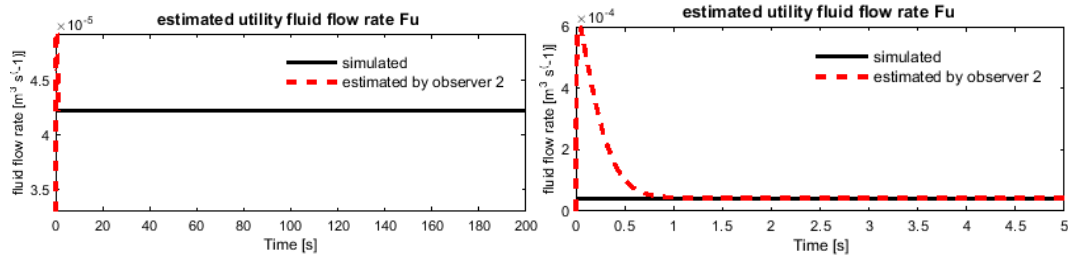


Fig. 5.6 the computation and estimation of utility fluid flow rate. Solid line is the computed value F_u ; dash line is the estimated one \hat{F}_u by Observer 2.

Case 2: single and/or simultaneous variation of the fluid flow rates parameters changes

The present computations are executed to get an accurate screening of the variation of the observer estimate, by corroborating if it is in agreement with the simulated fluid flow rates, which undergo either an abrupt change (prompted in essence by an unexpected parameter fault) or a gradual variation (essentially due to a degradation problem). The degradation can be attributed to, for example, aging or erosion which is modeled and recognized as parameter changes in the actuator subsystem. Two situations were considered in this case, single fluid variation is expected firstly and simultaneous changes follow after.

In the first situation, the parameters effects were taken into account in the following way. An initial value of $F_u = 4.22e^{-5}m^3s^{-1}$, and $F_p = 4.17e^{-6}m^3s^{-1}$ were considered, followed by an abrupt change at F_u . The reason caused this change is due to variation of parameter ΔP with the value from 0.6 MPa to 0.4Mpa at time $t = 60s$. Several factors can be attributed to this kind of variation, for instance, valve clogging or unexpected pressure drop across the control valves. This simulation was carried out using the same constants used in the previous simulation (Table 1) and the same values of T_{pi} and T_{ui} , as well as T_p^0 and T_u^0 respectively. The initial conditions of both observers, as well as the observer parameters (k_1 , k_2 , k_3 , k_4 and θ) were the same as the previous ones. No error was assumed in measuring T_p and T_u .

The simulation results are illustrated in Fig. 5.7- Fig.5.10. Fig 5.7 and Fig. 5.8 verify the tracking capacities of observer 1 on the outlet temperature. The dash line denotes the estimated fluid temperature through observer 1 while solid line represents the measured values. As shown in Fig 5.7 and Fig. 5.8, it demonstrates that after short transient response, both estimated values \hat{T}_p and \hat{T}_u converge to the measurement T_p and T_u with readily accuracy. The measured value in the two curves drop about 0.2 °C and 0.15 °C on process and utility fluid respectively at 60s, these variations are influenced by variation of actuator parameter ΔP_1 which is in accordance with the assumption. In addition, we can see from the Figs. 5.7 and 5.8 that the estimated outputs in dash line follow up the measured solid after a short convergence time at $t=60s$.

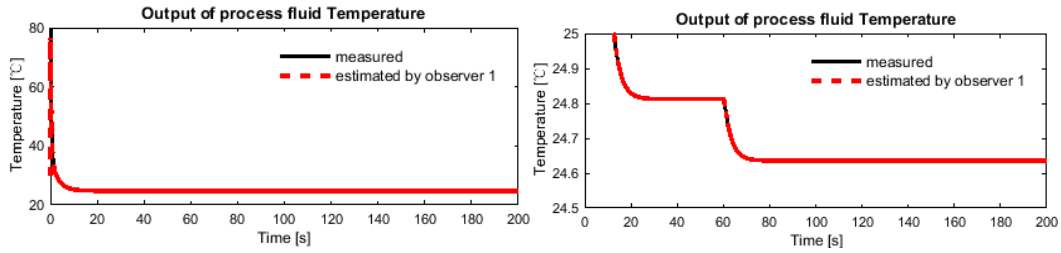


Fig. 5.7 outlet temperature of process fluid, solid line is the measurement T_p while dash line is estimated one \hat{T}_p by observer 1

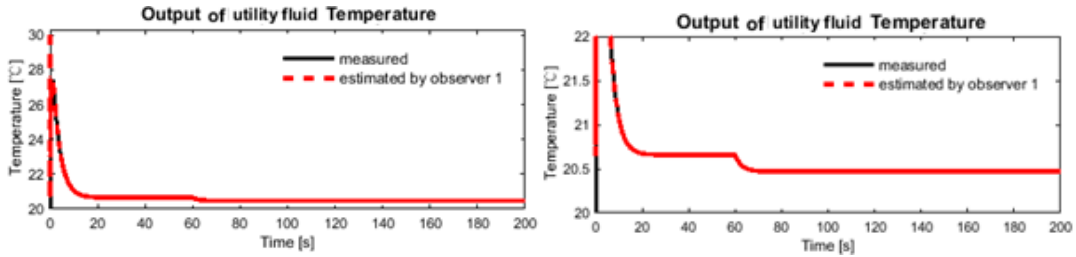


Fig. 5.8 outlet temperature of utility fluid, solid line is the measurement T_u while dash line is estimated value \hat{T}_u by observer 1

Fig. 5.9 shows the simulated and estimated result of process fluid flow rate. The dashed curve corresponds to \hat{F}_p generated by Observer 2, while the solid curve corresponds to simulated value F_p . It can be seen that once the observer converges, \hat{F}_p in dash line tracks well F_p in solid line and both curves remain constant after transient time. The similar result is plotted in Fig. 5.10 for utility fluid flow rate F_u , it illustrates that the estimated \hat{F}_u tracks its simulated value F_u after a relatively short transient period in spite of the time-varying nature of the actuator parameter ΔP_1 . Due to the variation parameter ΔP_1 at $t=60s$, both curves in Fig.10 jump and the estimated dash line tracks the simulated solid line again after about 1.5s. Moreover, we can see from the solid line that the impact of the variation of parameter ΔP_1 is to cause the outlet flow rate of utility fluid jumps from $4.22e^{-5}m^3s^{-1}$ to $4.4e^{-5}m^3s^{-1}$, that is the utility fluid flow rate increases $0.18 e^{-5}m^3s^{-1}$ because of drops of parameter ΔP_1 .

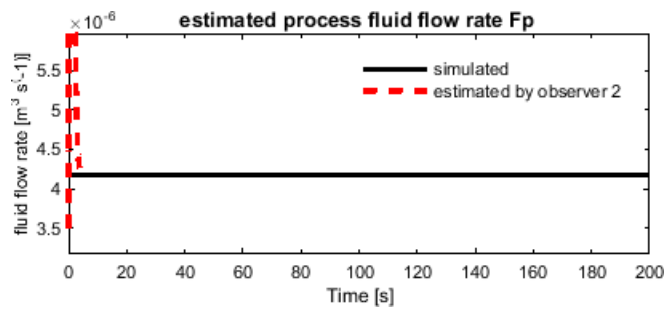


Fig. 5.9 the computation and estimation of process fluid flow rate; solid line is the computed value F_p , dash line is the estimated one \hat{F}_p by Observer 2.

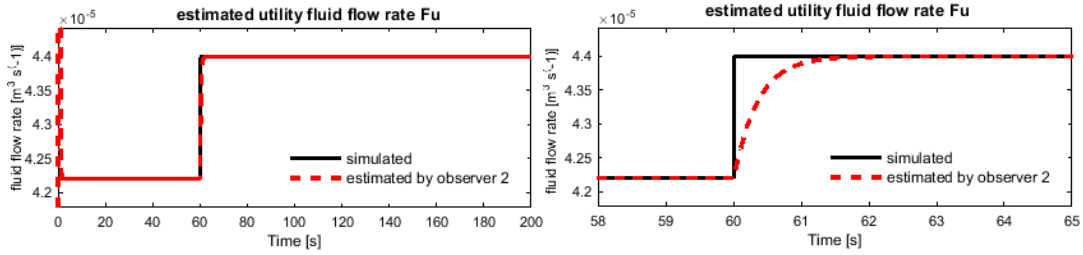


Fig. 5.10 the computation and estimation of utility fluid flow rate; solid line is the computed value F_u , dash line is the estimated one \hat{F}_u by Observer 2.

For the second situation, we consider that both fluid flow rates change simultaneously. In the first place, just as the previous case, an initial value of $F_u = 4.22e^{-5}m^3s^{-1}$, and $F_p = 4.17e^{-6}m^3s^{-1}$ were considered, then followed by an abrupt change of F_u caused by ΔP_1 from 0.6 MPa to 0.4MPa at $t = 60$ s. After that, at $t = 100$ s, F_p begins to deteriorate due to an increase of the parameter of the spring compliance k_2 in process fluid actuator. A main reason contributes to this change is due to erosion, and because of erosion, the gland packing of the valve may be loosen which leads to stem vibration. In the simulation, a value of $1,000\text{ nm}^{-1}$ is added to the spring compliance k_2 . These variations are illustrated in Fig. 5.11-Fig. 5.14.

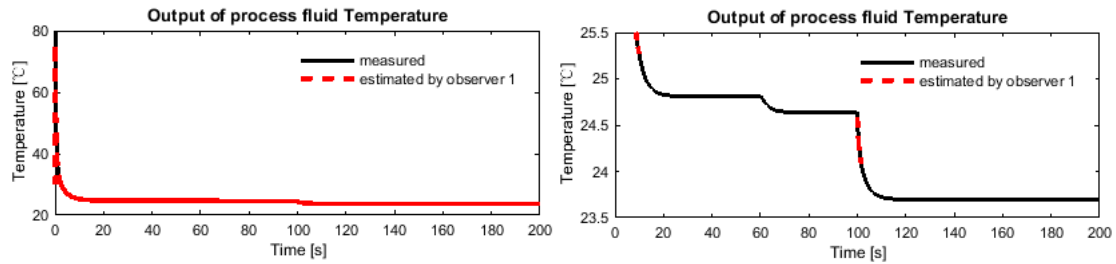


Fig. 5.11 outlet temperature of process fluid, solid line denotes measured value T_p while dash line is the estimated one \hat{T}_p by observer 1.

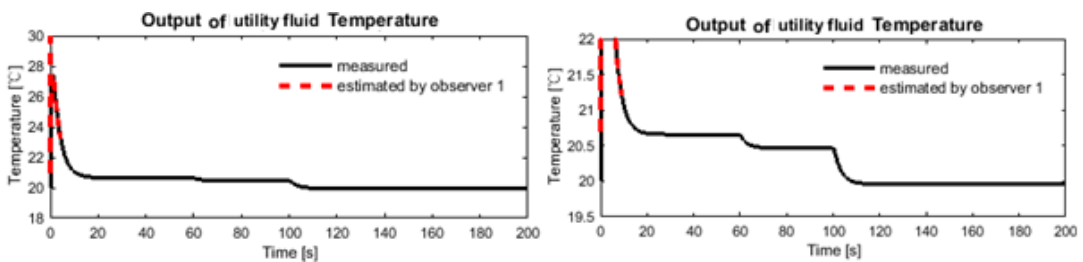


Fig. 5.12 outlet temperature of utility fluid, solid line denotes measured value T_u while dash line is the estimated one \hat{T}_u by observer 1.

From Fig. 5.11 and Fig. 5.12, after a short transient time, the estimated outlet fluid temperature \hat{T}_p and \hat{T}_u in dash line give an accurate estimation value to the measurement T_p and T_u in solid line. At 60s, the estimated \hat{T}_p unexpectedly decrease, and finally it stabilizes at a new level, a drop of 0.2 °C is occurred, then another drops happens at $t=100s$ before it reaches the new stable level with another 0.9 °C reduction. These decreases imply the influences of parameter changes in fluid actuators and no further variations illustrate no additional changes occurs. The similar result is obtained in the

estimated \hat{T}_u of utility fluid in Fig. 5.12. It is shown that, due to changes of ΔP_1 and k_2 , the measured T_u drops 0.2 °C and 0.5 °C at 60s, 100s respectively. The estimated \hat{T}_u in dash line tracks T_u after observer converges. The simulation curve indicates that the observer proposed is proper for tracking system performances.

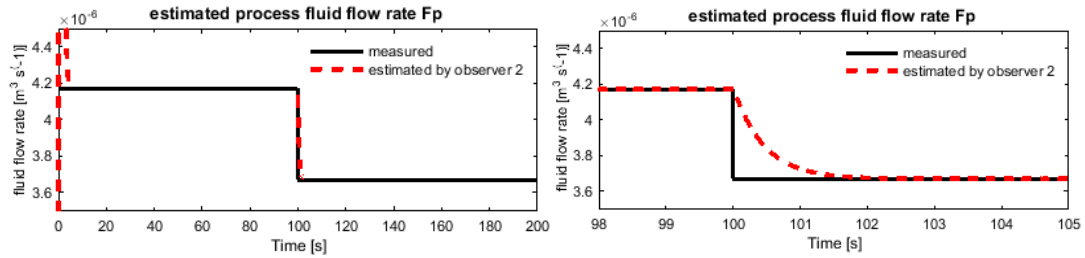


Fig. 5.13 the computation and estimation of process fluid flow rate; solid line is the computed value F_p , dash line is the estimated one \hat{F}_p via Observer 2.

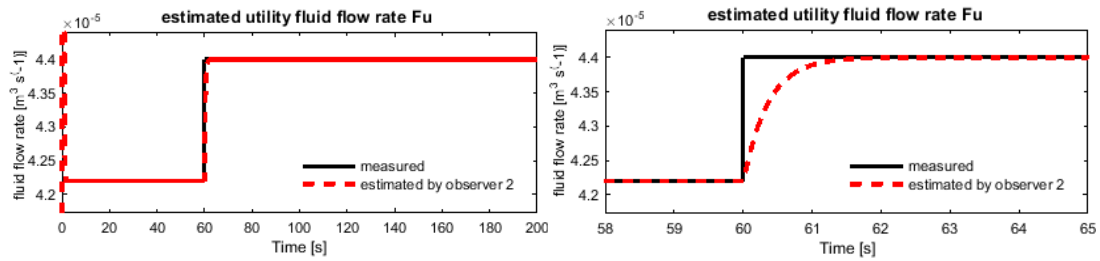


Fig. 5.14 the computation and estimation of utility fluid flow rate; solid line is the computed value F_u , dash line is the estimated one \hat{F}_u via Observer 2.

As shown in Fig.5.13, in the first place, the estimated process fluid flow rate \hat{F}_p in dash line converges to the simulated value F_p in solid line after transient response. After that, at 100s, the simulated F_p in solid line decrease unexpectedly, fortunately, the estimated value in dash curve gives a quick response to the variation, and it takes 1.5s to track F_p again. The decrease implies parameter changes in process fluid actuator which satisfied the assumption that k_2 changes at $t=100s$. Fig.5.14 demonstrates the results for utility fluid flow rate. At time 60s, as expected, the simulated utility fluid flow rate in solid line jumps due to the change of ΔP_1 . It also proves in Fig. 5.14 that the estimated utility fluid flow rate \hat{F}_p in dash line tracks well F_p in solid line. Now, it is clear that the proposed interconnected observer is effective even the unknown connection is time-varying either individually or simultaneously. Therefore the proposed observer proves the capacity of performance monitoring, as well as estimation of unknown connection of an interconnected system.

The performance evaluation of the proposed observers integrates system performances monitoring with unknown interconnection estimation for a pilot Hex reactor. At the first stage, the numerical simulations confirmed the convergence of the observers. Indeed, the results prove that the estimated values of \hat{T}_p (Figs. 3, 7, 11), \hat{T}_u (Figs. 4, 8, 12) and \hat{F}_p , \hat{F}_u (Figs. 5-6, 9-10) compare quite well with the measured and expected variables T_p , T_u , F_p and F_u , though neither F_p or F_u can be

measured. It is worth to note that even if F_p or F_u cannot be measured directly, the estimation of these parameters in terms of experimental temperatures exhibit a consistent and characteristic behavior in several respects, as already noted in Fig. 9-10: (a) As expected, at short times, the estimated fluid flow rates remain the same for a set of operation conditions. In practice, we expect both fluid flow rates are constant in order to obtain better final product. Any variation of this parameter due to aging or erosion can take some weeks or several months to appear. (b) Then, flow perturbations were programmed to study the sensibility of F_p or F_u to the parameters changes in the actuator subsystem. Each time, the corresponding response of F_p or F_u and the corresponding steady state values were observed. A further point to be discussed as a potential advantage is the fact that minimal information is demanded for achieving the observer computations. Summarizing, only limited knowledge on the system behavior is needed, no assumptions are necessary to initialize the estimation of F_p or F_u and no assumptions regarding the system dynamics are required. The encouraging results are obtained through the robustness performance of the proposed scheme. All the simulated situations have been correctly satisfied, leading to a desired performances monitoring and parameter estimation method.

5.5 Conclusion

This chapter considers the issues of both state estimation and unmeasured interconnection estimation for a class of invertible interconnected dynamic system. The aim is to design an interconnected observer that provides accurately estimates of states of each subsystem, as well as the interconnection. In particular, the interconnection signal is not supposed to be accessible to measurement. The unmeasured interconnection is the input of the process system, which is also the output of the actuator subsystem. To achieve the estimation purpose, firstly, an existing converging observer is extended to estimate the states of the actuator subsystem, in particular, the information of outputs of actuator system are replaced by their estimation through the observer proposed in process subsystem. Second, an extended high gain observer is considered to exactly estimate the states of the process subsystem subject to unknown inputs which is also the outputs of the actuator subsystem. The unknown inputs are treated as new states of the process subsystem. While through computing the derivatives of the output vectors in actuator subsystem, the unknown input can be expressed as a function of the inputs, derivatives of the inputs and the states of the actuator subsystem. Third, by using the estimates of the states and unmeasured interconnection, a kind of observer designed method is proposed for the studied invertible interconnected dynamic system, and convergence of the observer is studied. Finally, some numerical simulation examples are given to illustrate the effectiveness of the proposed methods.

A. Appendix 5.1: Proof of Assumption 5.2

Assumption 2 implies global Lipchitz-type condition on function K , although this condition seems restrictive, it becomes far less since u and u_a are bounded which is usually the case in physical situation. Moreover, this boundedness can be found by introducing saturation on the argument of g . According to [80], if u and u_a belong to compact set U, U_a , then the global Lipchitz-type condition on function K can be replaced by local smoothness for by using saturations.

Suppose that $K(u, \hat{x}_a, u_a)$ is locally Lipchitz continues on u_a , uniformly in (u, \hat{x}_a) on $U \times \mathbb{R} \times \mathbb{R}$.and suppose $\text{sat}(u_a) = u_a$ for $u_a \in U_a$, where $\text{sat}(u_a)$ is a component wise saturation with limits. We then replaced $K(u, \hat{x}_a, u_a)$ with $K(u, \hat{x}_a, \text{sat}(u_a))$, locally Lipchitz condition means that:

$$\|K(u, \hat{x}_a, \text{sat}(u_a)) - K(u, \hat{x}_a, \text{sat}(\hat{u}_a))\| \leq \gamma_3 \|u_a - \text{sat}(\hat{u}_a)\| \leq \gamma_3 \|u_a - \tilde{u}_a\|$$

Since the saturation is inactive on U_a , the definition of $\dot{\tilde{e}}_a(t, \tilde{e}_a)$ is not affected.

B. Appendix 5.2: Proof of Theorem 5.1

In order to show that the system described in (5.6) represents an exponential converging observer for (5.2), we need to make its corresponding error dynamics (5.7) coincide with Assumption 5.2 which has been proven to be an exponential condition for the existence of an observer.

Therefore by computing time derivation of V_a with respect to the trajectory \tilde{e}_a in (5.7), using (5.5), (5.7) and (5.8), it follows that:

$$\begin{aligned} \dot{V}_a(t, \tilde{e}_a) &= \frac{\partial V_a}{\partial t}(t, \tilde{e}_a) + \frac{\partial V_a}{\partial e_a}(t, e_a) \dot{e}_a(t, e_a) + \frac{\partial V_a}{\partial e_a}(t, e_a) (K(u, \hat{x}_a, u_a) - K(u, \hat{x}_a, \tilde{u}_a)) \\ &\leq -\alpha \|e_a\|^2 + \gamma_2 \gamma_3 \|e_a\| \|u_a - \tilde{u}_a\| \end{aligned}$$

where the right side of this inequality is negative if

- i-) $\alpha \geq \gamma_2 \gamma_3$ and $\|u_a - \tilde{u}_a\|$ is bounded, it results: $\dot{V}_a(t, \tilde{e}_a) \leq -(\alpha - \gamma_2 \gamma_3) \|e_a\|^2$
- ii-) $\|u_a - \tilde{u}_a\|$ converges to 0, it results: $\dot{V}_a(t, \tilde{e}_a) \leq -\alpha \|e_a\|^2$

This ends the proof.

C. Appendix 5.3: Proof of (5.12)

$$\text{Let } \Delta_{\theta_1} = \begin{bmatrix} 1 & 0 & \dots & 0 \\ 0 & \theta_1^{-1} & \ddots & 0 \\ \vdots & \ddots & \ddots & 0 \\ 0 & \dots & 0 & \theta_1^{-(n-1)} \end{bmatrix}, \text{ and } S_{\theta_1} = S_{\theta_1|\theta=1},$$

then we can obtain the following equalities:

$$\begin{aligned} S_{\theta_1} &= \frac{1}{\theta_1} \Delta_{\theta_1} S_{\theta_1} \Delta_{\theta_1}, \\ \Delta_{\theta_1} A_1 \Delta_{\theta_1}^{-1} &= \theta_1 A_1, \\ C_1 \Delta_{\theta_1} &= C_1 \Delta_{\theta_1}^{-1} = C_1 \end{aligned}$$

By defining error $e_1 := \hat{\chi}_1 - \chi_1$, we can obtain the error dynamics from (5.7) as:

$$\dot{e}_1(t, e_1) = (A_1 - S_{\theta_1}^{-1} C_1^T C_1) e_1 + \Theta_1(\hat{\chi}_1, u) - \Theta_1(\chi_1, u)$$

We set $\bar{e}_1 = \Delta_{\theta_1} e_1$, then:

$$\dot{\bar{e}}_1 = \Delta_{\theta_1} \left((A_1 - S_{\theta_1}^{-1} C_1^T C_1) e_1 + \Theta_1(\hat{\chi}_1, u) - \Theta_1(\chi_1, u) \right)$$

$$= \theta_1 (A_1 - S_{1_1}^{-1} C_1^T C_1) \bar{e}_1 + \Delta_{\theta_1} (\Theta_1(\hat{\chi}_1, u) - \Theta_1(\chi_1, u))$$

according to [80], define the positive Lyapunouv function $V_1(e_1)$ as :

$$V_1(e_1) = \frac{1}{\theta_1} e_1^T S_{\theta_1} e_1 = e_1^T \Delta_{\theta_1} S_{1_1} \Delta_{\theta_1} e_1 = \bar{e}_1^T S_{1_1} \bar{e}_1$$

$$\dot{V}_1(e_1) = 2\bar{e}_1^T S_{1_1} \Delta_{\theta_1} (A_1 - S_{\theta_1}^{-1} C_1^T C_1) e_1 + 2\bar{e}_1^T S_{1_1} \Delta_{\theta_1} (\Theta_1(\hat{\chi}_1, u) - \Theta_1(\chi_1, u))$$

A simple calculation gives:

$$\Delta_{\theta_1} (A_1 - S_{\theta_1}^{-1} C_1^T C_1) \Delta_{\theta_1}^{-1} = \theta_1 (A_1 - S_{1_1}^{-1} C_1^T C_1)$$

Thus we obtain:

$$\dot{V}_1(e_1) = 2\bar{e}_1^T S_{1_1} \theta_1 (A_1 - S_{1_1}^{-1} C_1^T C_1) \bar{e}_1 + 2\bar{e}_1^T S_{1_1} \Delta_{\theta_1} (\Theta_1(\hat{\chi}_1, u) - \Theta_1(\chi_1, u))$$

$$\text{Since } 2\bar{e}_1^T S_{1_1} A_1 \bar{e}_1 = \bar{e}_1^T (S_{1_1} A_1 + A_1^T S_{1_1}) \bar{e}_1 = \bar{e}_1^T (-S_{1_1} + C_1^T C_1) \bar{e}_1$$

Then

$$\dot{V}_1(e_1) = -\theta_1 \bar{e}_1^T S_{1_1} \bar{e}_1 - \theta_1 \|C_1 \bar{e}_1\|^2 + 2\bar{e}_1^T S_{1_1} \Delta_{\theta_1} (\Theta_1(\hat{\chi}_1, u) - \Theta_1(\chi_1, u))$$

On one hand, we have:

$$\|\Delta_{\theta_1} (\Theta_1(\hat{\chi}_1, u) - \Theta_1(\chi_1, u))\| \leq n\varrho \|\bar{e}_1\|$$

with ϱ is the Lipschitz constant with respect to $\Theta_1(\chi_1, u)$.

On the other hand:

$$\|\bar{e}_1\|^2 \leq 1/\lambda_{\min}(S_{1_1}) V_1$$

Then we obtain:

$$\begin{aligned} \dot{V}_1(e_1) &\leq -\theta_1 V_1 - \theta_1 \|C_1 \bar{e}_1\|^2 + 2n\varrho \lambda_{\max}(S_{1_1}) \|\bar{e}_1\|^2 \\ &\leq -\theta_1 V_1 + 2n\varrho \frac{\lambda_{\max}(S_{1_1})}{\lambda_{\min}(S_{1_1})} V_1 \end{aligned}$$

Set $\theta_1^* = 2n\varrho \frac{\lambda_{\max}(S_{1_1})}{\lambda_{\min}(S_{1_1})}$, then by taking $\theta_1 > \theta_1^*$, it results that Assumption 2 holds.

D. Appendix 5.4: Proof of (5.16)

By defining error $\tilde{e}_1 := \hat{\chi}_1 - \tilde{\chi}_1$,

we can obtain the error dynamics from Eqs. (5.7) and (5.11) as:

$$\begin{aligned} \dot{\tilde{e}}_1(t, \tilde{e}_1) &= A_1 \hat{\chi}_1 + \Theta_1(\hat{\chi}_1, u) - S_{\theta_1}^{-1} C_1^T (C_1 \hat{\chi}_1 - \hat{u}_a) - (A_1 \chi_1 + \Theta_1(\chi_1, u)) \\ &= A_1 \hat{\chi}_1 + \Theta_1(\hat{\chi}_1, u) - S_{\theta_1}^{-1} C_1^T (C_1 \hat{\chi}_1 - u_a) - (A_1 \chi_1 + \Theta_1(\chi_1, u)) + S_{\theta_1}^{-1} C_1^T (C_1 \hat{\chi}_1 - u_a) \\ &\quad - S_{\theta_1}^{-1} C_1^T (C_1 \hat{\chi}_1 - \tilde{u}_a) \\ &= (A_1 - S_{\theta_1}^{-1} C_1^T C_1) \tilde{e}_1 + \Theta_1(\hat{\chi}_1, u) - \Theta_1(\chi_1, u) + S_{\theta_1}^{-1} C_1^T (u_a - \tilde{u}_a) \\ &= \dot{e}_1 + S_{\theta_1}^{-1} C_1^T (u_a - \tilde{u}_a) \end{aligned}$$

Define the positive Lyapunouv function $\tilde{V}_1(\tilde{e}_1)$ as :

$$\tilde{V}_1(\tilde{e}_1) = \frac{1}{\theta_1} \tilde{e}_1^T S_{\theta_1} \tilde{e}_1 = \tilde{e}_1^T \Delta_{\theta_1} S_{1_1} \Delta_{\theta_1} \tilde{e}_1$$

Then:

$$\begin{aligned} \dot{\tilde{V}}_1(\tilde{e}_1) &= \frac{\partial \tilde{V}_1(\tilde{e}_1)}{\partial \tilde{e}_1} \dot{e}_1 + \frac{\partial \tilde{V}_1(\tilde{e}_1)}{\partial \tilde{e}_1} (S_{\theta_1}^{-1} C_1^T (u_a - \tilde{u}_a)) \\ &= 2\tilde{e}_1^T \Delta_{\theta_1} S_{1_1} \Delta_{\theta_1} (\dot{e}_1 + S_{\theta_1}^{-1} C_1^T (u_a - \tilde{u}_a)) \\ &= \dot{V}_1(e_1) + \frac{\partial \tilde{V}_1(\tilde{e}_1)}{\partial \tilde{e}_1} (S_{\theta_1}^{-1} C_1^T (u_a - \tilde{u}_a)) \end{aligned}$$

A simple calculation gives:

$$\begin{aligned} &\left\| \frac{\partial \tilde{V}_1(\tilde{e}_1)}{\partial \tilde{e}_1} (S_{\theta_1}^{-1} C_1^T (u_a - \tilde{u}_a)) \right\| \\ &\leq \left\| \frac{\partial \tilde{V}_1(\tilde{e}_1)}{\partial \tilde{e}_1} \right\| \left\| (S_{\theta_1}^{-1} C_1^T (u_a - \tilde{u}_a)) \right\| \\ &= \|2\tilde{e}_1^T \Delta_{\theta_1} S_{1_1} \Delta_{\theta_1}\| \|S_{\theta_1}^{-1} C_1^T\| \|u_a - \tilde{u}_a\| \\ &= \|2\Delta_{\theta_1} S_{1_1} \Delta_{\theta_1}\| \|\tilde{e}_1\| \|S_{\theta_1}^{-1} C_1^T\| \|u_a - \tilde{u}_a\| \\ &= \|2\tilde{e}_1^T \Delta_{\theta_1} S_{1_1} \Delta_{\theta_1} S_{\theta_1}^{-1} C_1^T (u_a - \tilde{u}_a)\| \\ &= \|2\Delta_{\theta_1} S_{1_1} \Delta_{\theta_1} S_{\theta_1}^{-1} C_1^T\| \|e_1\| \|u_a - \tilde{u}_a\| \\ &= \|2\Delta_{\theta_1} S_{1_1} \theta_1 S_{1_1}^{-1} C_1^T \Delta_{\theta_1}\| \|e_1\| \|u_a - \tilde{u}_a\| \\ &= \frac{2}{\theta_1^{n-1}} \|e_1\| \|u_a - \tilde{u}_a\| \\ &\leq \frac{1}{\lambda_{\min}(S_{1_1})} \sqrt{V_1} \|u_a - \tilde{u}_a\| \end{aligned}$$

Hence,

$$\dot{\tilde{V}}_1(\tilde{e}_1) \leq -\theta_1 V_1 + 2n\varrho \frac{\lambda_{\max}(S_{1_1})}{\lambda_{\min}(S_{1_1})} V_1 + \frac{1}{\lambda_{\min}(S_{1_1})} \sqrt{V_1} \|u_a - \tilde{u}_a\|$$

Thus:

i-) if $\|u_a - \tilde{u}_a\|$ converges to 0, let $\theta_1^* = 2n\varrho \frac{\lambda_{\max}(S_{1_1})}{\lambda_{\min}(S_{1_1})}$, then by taking $\theta_1 > \theta_1^*$, it results that

Assumption 2 holds which means convergence of the observer (5.13) holds.

ii-) if $\|u_a - \tilde{u}_a\|$ is bounded, let $\theta_1^* = \left(2n\varrho \frac{\lambda_{\max}(S_{1_1})}{\lambda_{\min}(S_{1_1})} + \frac{1}{\lambda_{\min}(S_{1_1})}\right)$, then by taking $\theta_1 > \theta_1^*$, it results

that Assumption 2 holds which means convergence of the observer (5.13) holds.

That ends the proof.

E. Appendix 5.5: Proof of Theorem 5.2

Before preceding the convergence proof of the observer, one introduces the following notations:

$$S_\theta = \frac{1}{\theta} \Delta_\theta S_1 \Delta_\theta$$

Where:

$$S_1 = S_{\theta|\theta=1} \quad \text{and} \quad \Delta_\theta = \begin{bmatrix} I_n & 0 \\ 0 & \frac{1}{\theta} I_n \end{bmatrix}$$

Now, followed by assumption defined in [22], $\Lambda^{-1}(\hat{z}_1)$ is invertible, and thus yields the following equalities

$$G(\hat{z}_1) = \Lambda^{-1}(\hat{z}_1) A \Lambda(\hat{z}_1)$$

$$C \Lambda(\hat{z}_1) = C$$

$$\text{Let} \quad \bar{S}_\theta(\hat{z}_1) = \Lambda^T(\hat{z}_1) S_\theta \Lambda(\hat{z}_1)$$

We then get:

$$\theta l(\hat{z}_1) \bar{S}_\theta(\hat{z}_1) + l(\hat{z}_1) G^T(\hat{z}_1) \bar{S}_\theta(\hat{z}_1) + l(\hat{z}_1) \bar{S}_\theta(\hat{z}_1) G(\hat{z}_1) - l(\hat{z}_1) C^T C = 0$$

To proof the Theorem 5.2, the estimation error is introduced as: $e(t) = \hat{z}(t) - z(t)$.

Then subtracting corresponding equation in (5.21) and (5.20), one gets the following error dynamics:

$$\begin{aligned} \dot{e}(t) &= l(\hat{z}_1) G(\hat{z}_1) \hat{z} + F(\hat{z}_1) + \bar{\varepsilon}(u, \dot{u}, \hat{x}_a) + H(\hat{z}_1)(C \hat{z} - y) - l(z_1) G(z_1) z - F(z_1) \\ &\quad - \bar{\varepsilon}(u, \dot{u}, x_a) \\ &= l(\hat{z}_1) G(\hat{z}_1)(e(t) - z(t)) + H(\hat{z}_1) C(e(t) - z(t)) - H(\hat{z}_1) C z(t) - l(z_1) G(z_1) z(t) \\ &\quad + F(\hat{z}_1, u) - F(z_1) + \bar{\varepsilon}(u, \dot{u}, \hat{x}_a) - \bar{\varepsilon}(u, \dot{u}, x_a) \\ &= (l(\hat{z}_1) G(\hat{z}_1) + H(\hat{z}_1) C) e + (l(\hat{z}_1) G(\hat{z}_1) - l(z_1) G(z_1)) z(t) + F(\hat{z}_1) - F(z_1) \\ &\quad + e_{\bar{\varepsilon}}(t, \tilde{e}_a) \end{aligned}$$

Where $e_{\bar{\varepsilon}}(t, \tilde{e}_a) = \bar{\varepsilon}(u, \dot{u}, \hat{x}_a) - \bar{\varepsilon}(u, \dot{u}, x_a)$.

Set $\tilde{e} = \Delta_\theta \Lambda(\hat{z}_1) e$, one can then gets:

$$\begin{aligned} \dot{\tilde{e}}(t) &= \theta l(\hat{z}_1) (A - S_1^{-1} C^T C) \tilde{e} + \dot{\Lambda}(\hat{z}_1) \Lambda^{-1}(\hat{z}_1) \tilde{e} + \Delta_\theta \Lambda(\hat{z}_1) (F(\hat{z}_1) - F(z_1)) \\ &\quad + \Delta_\theta \Lambda(\hat{z}_1) (l(\hat{z}_1) G(\hat{z}_1) - l(z_1) G(z_1)) z(t) - \Delta_\theta \Lambda(\hat{z}_1) e_{\bar{\varepsilon}}(t, \tilde{e}_a) \end{aligned}$$

To analyze the dynamics of the error system, the following positive Lyapunov function candidate is considered:

$$V_z(t, \tilde{e}) = \tilde{e}^T S_1 \tilde{e}$$

Convergence of the observer is described by the time-derivation of $V_z(t, e)$, then we obtain:

$$\begin{aligned} \dot{V}_z(t, e) \\ = 2\tilde{e}^T S_1 \dot{\tilde{e}} \end{aligned}$$

$$\begin{aligned}
&= \theta l(\hat{z}_1)(2\tilde{e}^T S_1 A \tilde{e} - 2\tilde{e}^T C^T C \tilde{e}) + 2\tilde{e}^T S_1 \dot{\Lambda}(\hat{z}_1) \Lambda^{-1}(\hat{z}_1) \tilde{e} 2\tilde{e}^T S_1 \Delta_\theta \Lambda(\hat{z}_1) (F(\hat{z}_1) - F(z_1)) \\
&\quad + 2\tilde{e}^T S_1 \Delta_\theta \Lambda(\hat{z}_1) \left((l(\hat{z}_1)G(\hat{z}_1) - l(z_1)G(z_1))z(t) \right) - 2\tilde{e}^T S_1 \Delta_\theta e_{\tilde{\varepsilon}}(t, \tilde{e}_a) \\
&= -\theta l(\hat{z}_1)V_z - \theta \|C\tilde{e}\|^2 + 2\tilde{e}^T S_1 \dot{\Lambda}(\hat{z}_1) \Lambda^{-1}(\hat{z}_1) \tilde{e} + 2\tilde{e}^T S_1 \Delta_\theta \Lambda(\hat{z}_1) (F(\hat{z}_1) - F(z_1)) \\
&\quad + 2\tilde{e}^T S_1 \Delta_\theta \Lambda(\hat{z}_1) \left((l(\hat{z}_1)G(\hat{z}_1) - l(z_1)G(z_1))z(t) \right) - 2\tilde{e}^T S_1 \Delta_\theta e_{\tilde{\varepsilon}}(t, \tilde{e}_a) \\
&\leq -\theta \alpha_1 V_z + 2\|S_1 \tilde{e}\| \|\dot{\Lambda}(\hat{z}_1) \Lambda^{-1}(\hat{z}_1)\| \|\tilde{e}\| + 2\|S_1 \tilde{e}\| \|\Lambda(\hat{z}_1)\| \|\Delta_\theta (F(\hat{z}_1) - F(z_1))\| \\
&\quad + 2\|S_1 \tilde{e}\| \|\Delta_\theta \Lambda(\hat{z}_1) \left((l(\hat{z}_1)G(\hat{z}_1) - l(z_1)G(z_1))z(t) \right)\| \\
&\quad + \frac{2}{\theta} \|S_1 \tilde{e}\| \|G(\hat{z}_1)\| \|e_{\tilde{\varepsilon}}(t, \tilde{e}_a)\| \\
&\leq -\theta \alpha_1 V_z + 2\mu \|S_1 \tilde{e}\| \|\tilde{e}\| + 2\rho \|S_1 \tilde{e}\| \|\Delta_\theta (F(\hat{z}_1) - F(z_1))\| \\
&\quad + 2\|S_1 \tilde{e}\| \|\Delta_\theta \Lambda(\hat{z}_1) \left((l(\hat{z}_1)G(\hat{z}_1) - l(z_1)G(z_1))z(t) \right)\| + \frac{2\tau\gamma_4}{\theta} \|S_1 \tilde{e}\| \|x_a - \hat{x}_a\|
\end{aligned}$$

Where $\mu = \sup_{t \geq 0} \|\dot{\Lambda}(\hat{z}_1) \Lambda^{-1}(\hat{z}_1)\|$, ρ is the up bounder of $\|\Lambda(\hat{z}_1)\|$, τ is given in assumptions in [171], $\|e_{\tilde{\varepsilon}}(t, \tilde{e}_a)\| \leq \gamma_4 \|x_a - \hat{x}_a\|$ as proposed in Assumption 5.3.

On one hand, we assume:

$$\|\Delta_\theta (F(\hat{z}_1) - F(z_1))\| \leq \|f_1(\hat{z}_1) - f_1(z_1)\| \leq \sigma \|\tilde{e}\|$$

Where σ denotes the lipschitz constant of $f_1(z_1)$.

Similarly,

$$\|\Delta_\theta \Lambda(\hat{z}_1) \left((l(\hat{z}_1)G(\hat{z}_1) - l(z_1)G(z_1))z(t) \right)\| = \|l(\hat{z}_1)G(\hat{z}_1)z_2 - l(z_1)G(z_1)z_2\| \leq \epsilon \|\tilde{e}\|$$

ϵ is positive constant depending on the upper bound of z_2 , thus,

$$\begin{aligned}
\dot{V}_z(t, \tilde{e}) &\leq -\theta \alpha_1 V_z + \eta_1 V_z + \frac{\eta_2}{\theta} \sqrt{V_z} \|x_a - \hat{x}_a\| \\
&\leq (-\theta \alpha_1 + \eta_1) V_z + \frac{\eta_2}{\theta} \sqrt{V_z} \|x_a - \hat{x}_a\|
\end{aligned}$$

Where $\eta_1 = (2\mu + 2\rho + 2\epsilon)\xi(S_1)$ with $\xi(S_1) = \sqrt{\lambda_{\max}(S_1)/\lambda_{\min}(S_1)}$, $\eta_2 = 2\tau\gamma_4\lambda_{\max}(S_1)$.

Thus:

i-) if $\|x_a - \hat{x}_a\|$ converges to 0, it results in $\dot{V}_z(t, \tilde{e}) \leq (-\theta \alpha_1 + \eta_1)V_z$, then by taking $\theta > \theta^* = \frac{\eta_1}{\alpha_1}$,

negative of the right side of the above inequality is obtained.

ii-) if $\|x_a - \hat{x}_a\|$ is bounded, it results in $\dot{V}_z(t, \tilde{e}) \leq (-\theta \alpha_1 + \eta_1 + \frac{\eta_2}{\theta})V_z$, then by choosing $\theta >$

θ^* such that $(\theta^* \alpha_1 - \eta_1 - \frac{\eta_2}{\theta^*}) \geq 0$, negative of the right side of the above inequality is obtained.

That ends the proof.

F. Appendix 5.6: Proof of (5.30)

The observer estimation errors satisfy the following equation:

$$\tilde{e}_1 = \hat{\chi}_1 - \chi_1, e(t) = \hat{z}(t) - z(t)$$

to analysis the stability of the error dynamics, to achieve this purpose, by using V_a and V_z defined as,

$$V_1(\tilde{e}_1) = \frac{1}{\theta_1} \tilde{e}_1^T S_{\theta_1} \tilde{e}_1 \text{ and } V_z(t, e) = \tilde{e}^T S_1 \tilde{e}$$

the following Lyapunov function candidate is constructed:

$$V(t, \tilde{e}_1, e) = V_1(t, \tilde{e}_1) + V_z(t, e)$$

Then time derivation of $V(t, \tilde{e}_1, e)$ yields:

$$\dot{V}(t, \tilde{e}_1, e) \leq -\theta_1 V_1 + 2n\varrho \frac{\lambda_{\max}(S_{1_1})}{\lambda_{\min}(S_{1_1})} V_1 + \frac{1}{\lambda_{\min}(S_{1_1})} \sqrt{V_1} \sqrt{V_z} + (-\theta\alpha_1 + \eta_1) V_z + \frac{\eta_2}{\theta} \sqrt{V_z} \sqrt{V_1}$$

Let $\theta_0 = \max\{\theta_1, \theta\}$, $\kappa = 2n\varrho \frac{\lambda_{\max}(S_{1_1})}{\lambda_{\min}(S_{1_1})}$, $\varrho = \frac{1}{\lambda_{\min}(S_{1_1})}$, then it follows that :

$$\begin{aligned} \dot{V}(t, \tilde{e}_1, e) &\leq -\theta_0 V_1 + \kappa V_1 + \varrho \sqrt{V_1} \sqrt{V_z} + (-\theta_0 \alpha_1 + \eta_1) V_z + \frac{\eta_2}{\theta_0} \sqrt{V_z} \sqrt{V_1} \\ &\leq -(\theta_0 - \kappa) V_1 + \left(\varrho + \frac{\eta_2}{\theta_0}\right) \sqrt{V_z} \sqrt{V_1} - V_z \end{aligned}$$

Now $V_1^* = (\theta_0 - \kappa) V_1$, $V_z^* = (\theta_0 \alpha_1 - \eta_1) V_z$ and $V^* = V_1^* + V_z^*$, such that

$$\begin{aligned} \dot{V}(t, \tilde{e}_1, e) &\leq -V^* + \frac{1}{2\sqrt{(\theta_0 - \kappa)(\theta_0 \alpha_1 - \eta_1)}} \left(\varrho + \frac{\eta_2}{\theta_0}\right) V^* \\ \dot{V}(t, \tilde{e}_1, e) &\leq -(\theta_0 \alpha_1 - \eta_1) \left(1 - \frac{1}{2\sqrt{(\theta_0 - \kappa)(\theta_0 \alpha_1 - \eta_1)}} \left(\varrho + \frac{\eta_2}{\theta_0}\right)\right) V \end{aligned}$$

Thus by appropriately choosing such that $\left(1 - \frac{1}{2\sqrt{(\theta_0 - \kappa)(\theta_0 \alpha_1 - \eta_1)}} \left(\varrho + \frac{\eta_2}{\theta_0}\right)\right) \geq 0$ is guaranteed, the convergence of the observer is obtained.

CHAPTER 6 INPUT RECONSTRUCTIONS BY MEANS OF SYSTEM INVERSION AND SLIDING MODE OBSERVER

This chapter studies input reconstruction for nonlinear dynamic system. Firstly, input reconstruction technique through direct system inversion is reviewed. Some challenges on application of system inversion based input reconstruction such as reliable computations of the successive outputs derivatives are addressed. A high gain sliding mode observer is proposed to exactly estimate and substitute these derivatives of outputs in the differential algebraic polynomial obtained via system inversion. Numerical simulations are presented to make a comparison of both procedures. Results show that the system inversion based method is proper in ideal situation if successive computations of derivatives are available, while sliding mode observer based method is more applicable in the presence of measurement noise.

6.1 Introduction

In traditional applications of identification, estimation and control, the input is generally assumed to be known, therefore input estimation or reconstruction is not required. But what happens when the input is unknown. Such a problem arises in systems subject to disturbances or with inaccessible inputs, since inputs in these systems are either too expensive or perhaps not accessible to direct measurement. Unknown inputs may represent unknown external drivers, input uncertainty, or instrument faults, such as the seismic excitations, the ambient wind loads, the moving traffic loads and the cutting force etc. In this case, traditional system identification techniques fail. Therefore the unknown input reconstruction or estimation is required in order to help us make better measures for realizing synchronization, stabilization control and fault tolerant. More specifically, when unknown inputs represent disturbances or the effects of system uncertainties, reconstruction or estimation can be used to improve the control system performance. Additionally, when unknown inputs represent the effect of actuator failures or plant components, reconstruction or estimation can be used for the purpose of FDI and FTC, and thereby enhance system reliability.

Systems with unknown inputs have received considerable attention in the literature. An active research area is a state reconstruction with known model equations and unknown inputs. The key point of this problem is to design an observer for a system partially driven by unknown inputs. The methods in the literature can be classified into two forms: either estimating of the partially unknown inputs or decoupling of the unknown inputs. For the former one, the idea is to augment the system to a new set of coordinates that include the unknown input vector as an additional component of the state, so that estimation techniques can be applied to the augmented system. This leads to various fundamental contributions with successful experimental evaluations on the observability and observer design including full-order observers [172], reduced-order observers [105], geometric techniques [133], adaptive observers [27], sliding mode observer [173]. Another technique for state estimation in the presence of unknown inputs rely on the decoupling of the unknown inputs through nonlinear

transformations and relative degree, see [174]. The problem amounts to design a filter of which the output is exactly decoupled from the control and disturbance inputs and it is known in the literature as the fundamental problem of residual generation. This disturbance decoupling approach has been considered in the case of nonlinear systems, like in [88]. A necessary condition has been given in the work [175]. The approach is made in differential geometric terms and it is shown that a solution to the problem of unknown input reconstruction can be characterized in terms of un-observability distributions. It is worth pointing out that the primary objective of this technique focus on reconstruct only the state variables [59].

In the above mentioned works, only the state estimation is conducted, leaving the unknown input estimation un-tackled. However, the unknown inputs impact numerous applications, ranging from machine tool control to cryptography, filtering, and coding. Therefore, it is of great importance to reconstruct the unknown input. The input reconstruction problem is distinct from, but closely related to, the problem of state observation subject to unknown inputs. In both problems, the inputs are unknown. However, unlike state observation problem, the problem of input reconstruction is a process where the inputs to a system are estimated using the measured system output, and possibly some modeling information from the system model. Although not as well known as the state estimation problem, input reconstruction has been studied for several decades, and interest continues up to the present time.

One approach to estimating unknown inputs is to use input observers to reconstruct inputs to the system based on a dynamic model and measurements. The relevant literature on this topic has its roots in system inversion theory developed as in [122]. The idea basically relies on the concept studied for example by [147] for LTI systems and considered by [119][136] for nonlinear systems. Basic issues concerning re-constructability of unknown input relates to the input observability that has been discussed earlier for linear systems such as e.g. in [124]. In the framework of nonlinear systems, the problem of input reconstruction using classical invertibility techniques has been studied before in [133]. In this work, the authors consider faults as additive unknown inputs to the system, and recover them as outputs of another dynamic system—the inverse system. Moreover, the problem of left invertibility of switched systems, recently introduced in [126], concerns with the recovery of switching signal and input using the knowledge of the output and the initial state. And the work was extended to nonlinear system by authors in [51]. In [176], it derives a re-constructor for 1-step-delay input and initial-state reconstruction, where the delay l accounts for the relative degree of the left invertible system. The condition of invertibility in these literatures is given in terms of a rank condition on matrices made up of either the system matrices or the system Markov parameters.

In these inversion based methods mentioned above, inversion, however, requires an exact and fully known analytical model, since the initial values of the state variables are assumed to be unknown. One difficulty that arises in system inversion is the presence of zeros. If the system has no zeros, then input reconstruction is possible even if the initial state is unknown and nonzero. However, if the system has zeros, then there exists an initial state such that, for some nonzero input, the output is identically zero,

as shown in [177]. Therefore the classical invertibility based method is limited by instabilities arising from non-minimum phase zeros. Beyond the problem associated with non-minimum-phase zeros, most input reconstruction techniques require an exact analytical model of the system, however many interesting input reconstruction problems do not have analytical representations. Another difficulty that arises in system inversion techniques is that many methods require the successive computation of time derivatives of the inputs and outputs of nonlinear systems from the computed control inputs and the noisy and disturbed output measurements [178]. However, numerical differentiation of these quantities may lead to serious computational errors. This problem is indeed known to be ill-posed that small perturbations of the signal may lead to large errors in the computed derivatives. Besides, these approaches require model transformations that lack generality.

A solution to overcome the limitations of system inversion lies on observer design where the literature is extensive, e.g. [34][27][38]. Many challenging observation problems have been investigated to this end thanks to high gain, sliding mode, back-stepping and adaptive control principles. For example, the paper [179] studies the problem of simultaneous input and state estimation for nonlinear dynamical systems with and without direct input output feedthrough using the classical Gauss–Newton method. Based on linear minimum-variance unbiased estimation, a five-step recursive filter with global optimality is proposed to estimate both the unknown input and the state in [180]. In [181], a novel Extended Kalman filter approach referred to as the General Extended Kalman filter with unknown inputs (GEKF-UI) is proposed to estimate the structural parameters and the unknown excitations (inputs) simultaneously.

In this chapter, the combination of both system inversion and sliding observer based input reconstruction for invertible nonlinear system is considered. We first state the objective of the chapter and introduce notation in section 6.2. We then provide a detailed illustration for input reconstruction procedure via dynamic inverse computation in section 6.3. While in order to avoid using any information of the derivatives of the output, a high gain second order sliding mode observer is considered to exactly estimate the derivatives of the output. A kind of algebraic unknown input estimation method is presented by combining both techniques in Section 6.4. We then demonstrate the effectiveness of the proposed methods by comparing these two methods using numerical simulation in section 6.5.

6.2 Problem Formulation

In the context of this work, it is assumed that, without loss of generality, the dynamic behavior of MIMO dynamical systems can be described by an input affine nonlinear state space model of the form (6.1):

$$\Sigma_p \begin{cases} \dot{x} = f(x) + g(x)u, & x(t_0) = x_0 \\ y = h(x, u_a) \end{cases} \quad (6.1)$$

where $x \in \mathcal{R}^n$ is the state of the system, $y \in \mathcal{R}^p$ is the output of the system. $u \in \mathcal{R}^m$ is the input of system, which is inaccessible and is reconstructed by measures of y . f and g are smooth vector field on \mathcal{R}^n and h is smooth vector field on \mathcal{R}^p .

The main objective addressed in this chapter is the design and analysis of an input re-structor for the classes of nonlinear input affine systems described in the general form of (6.1). That is to reconstruct u from measure y , and the initial condition x_0 . One can easily notice that the input reconstruction problem is closely linked to the problem of system inversion. Since the problem of input reconstruction can be viewed as problem of input observability while input observability is equivalent with left invertibility of system. As shown in reference [137], the input can be uniquely recovered from output and the initial state if dynamical system is left invertible. Therefore, in the problem of input reconstruction, the first task consists in evaluating the input observability, distinguishing whether the changes of the input of a dynamic system are reflected as changes at the output. If a system is input observable, the input reconstruction problem consists in the synthesis of a device or a mechanism which has as input the measured outputs, and it should take place as output a signal that should converge to the observable input.

First, let us start with a definition of the so-called observability and invertibility of a dynamic system, more detailed can be found in [124][137].

Definition 6.1: Consider the dynamical system in (6.1), the input $u(t)$ is said observable if that input can be distinguished from zero by the output $y(t)$, i.e., if $y(t) = 0$ for $t > 0$, implies $u(t) = 0$ for $t > 0$.

Remark 6.1: For any known initial condition $x(t_0) = x_0 = \xi$ with $\xi \in \mathcal{R}^n$, input observability implies left invertibility of (6.1).

Since the ideal solvability of this problem is equivalent to the left invertibility of system (6.1), therefore the key step is to ensure the invertibility of the system. In particular, the left invertibility condition requires the local injective of the input output map. If and only if the left invertibility condition is satisfied, it makes sense to proceed and to try to reconstruct the input function $u(t)$ from noisy measurements of $y(t)$. Thus, the first issue is to check whether the system of equations (6.1) defines a left invertible map. This task can be treated in both the differential algebraic and differential geometric framework in the literature, see as in [139].

We approach here the computational aspect of the concepts by algebraic criteria introduced in Chapter 4. The system under consideration is interconnected system, classical inversion techniques can no longer be used and hence we use newly developed tools of invertibility for interconnected dynamic systems in chapter 4. Also, by using information provided by the observer for interconnected system introduced in chapter 5, we obtain the initial conditions from the observer and hence do not require stability of the inverse system. In chapter 4, we employ the differential output rank to check system invertibility. Differential output rank is defined as the maximum number of outputs that are related by a

differential polynomial equation which is independent of x and u (state and input respectively). Details of differential output rank definitions can be, for example, found in [159]. A simple way to compute differential output rank of system (6.1) is defined by corollary 6.1.

Corollary 6.1: Supposed there are p outputs, and if there exists r possible differential polynomial equations of the form (6.2):

$$P_r(y_1, y_2, \dots, y_p, \dot{y}_1, \dot{y}_2, \dots, \dot{y}_p, \ddot{y}_1, \ddot{y}_2, \dots, \ddot{y}_p, \dots) = 0 \quad (6.2)$$

then the differential output rank ρ is defined as $\rho = p - r$, which implies $(p - r)$ independent outputs.

Theorem 6.1: A system is left-invertible if, and only if the differential output rank ρ is equal to the total number of inputs, e.g. $\rho = m$ in (6.1).

By verifying invertibility of the studied system, to solve the input reconstruction problem in the ideal situation, we obtain: (1) \mathbf{y} is known at any time t , together with its derivatives; (2) \mathbf{y} belongs to the image space of the input output map of the dynamical system (6.1). However, the technique may work well in ideal situations, but generally turns out difficult to implement in real engineering situation. This is because, in reality, the measured output may be affected either by disturbances or by measurement errors which may lead to serious computation errors in the computing derivatives. In fact, they may be subject to local minima and are often time consuming e.g. when each evaluation of the objective function needs the integration of complex nonlinear differential equations. Therefore, this is another consideration that is worth to be taken into account which is the reliability and availability of the successive computation of time derivatives of the output \mathbf{y} .

To avoid numerical differentiation, in this work, following an inversion based strategy, we propose an estimation procedure for nonlinear input affine systems exploiting estimated successive output derivatives. We employ a second order sliding mode observer to estimate the time derivatives of the output \mathbf{y} , thus avoiding the potential serious errors arise by the computation. The procedure takes advantage of the fact that sliding mode observation strategies possess attractive features such as robustness. By combining the left inversion and sliding mode observer, we propose a kind of algebraic unknown input estimation method. Detailed illustration of this procedure is presented in 6.4.

6.3 Input Reconstruction by System Inversion

This approach is an application of dynamic inversion to filtering which is dual to the concept of dynamic inversion for control. The difference between these inversion approaches is that control uses a right inverse whereas estimation uses a left inverse of the system. Broadly speaking, the inverse dynamic of an input output dynamical system involves its decomposition into an external part, that enables an explicit relationship between inputs and outputs, and an internal part that is governed by its dynamics without input.

6.3.1 Fundamentals

Key tools for the analysis are the notions of re-constructability, invertibility, the relative degree and zero dynamics of the representation of a dynamical system. In finding the left inverse of a nonlinear system, the idea is always to solve first the output zeroing problem, i.e., to find initial conditions and inputs consistent with the constraint that the output function $y(t)$ is identically zero for all times in a neighborhood, and to analyze the corresponding internal dynamics. This will provide an appropriate extension of the notion of zero dynamics to a system having relative degree. The analysis can be made either in algebraic or geometric way. For certain classes of nonlinear state space systems one can find algorithms (and also sufficient or necessary conditions) of invertibility, see e.g. in [122].

We review in this chapter some relevant aspects of this from view point of algebraic theory. In differential algebraic setting, left invertibility (as our case) can be expressed in terms of the differential output rank of the system, see in [32]. If a system is differentially left invertible, the input can be recovered from the output by means of a finite number of ordinary differential equations. As the dynamical system (6.1), the realization of its inverse dynamic can be expressed as the following form (6.3):

$$\begin{cases} \dot{\eta} = \varphi(\eta, y, \dot{y}, \dots) \\ u = \omega(\eta, y, \dot{y}, \dots) \end{cases} \quad (6.3)$$

where η is a function of sub-state of the state x to be determined. It represents also the internal state that does not have a relationship with inputs. Its determination is a crucial issue on the inverse dynamic.

This approach is based on the existence of the left inverse system whose outputs are the unknown input while the inputs are the measured system outputs and possibly their time derivatives. The existence of the left inverse determines the feasibility of the inversion based approach to the input re-constructor design. Therefore, we will study a series of problems concerned with the analysis of the properties of invertibility of dynamical systems. It will be seen that the point of departure of the invertibility analysis is the notion of relative degree of dynamical systems. The theory is developed for linear time invariant and nonlinear systems having vector relative degree. For more details, one can turn to [122].

Definition 6.2 (Relative degree of nonlinear systems): For invertible dynamic system described by (6.1), the relative degree r_i of the output y_i with respect to the input vector u is the smallest integer which is defined by:

$$(a) L_{g_j} L_f^{r_i-1} h_i(x) \neq 0; \quad 1 \leq j \leq m$$

$$(b) L_{g_j} L_f^k h_i(x) = 0; \quad 0 \leq k < r_i - 1, \quad 1 \leq j \leq m$$

where $L_f(\cdot)$ and $L_g(\cdot)$ represent the Lie derivatives of a real function $h(x)$ along the vector field $f(x)$ and $g(x)$.

$$L_f^0 h_i(x) = h_i(x) \quad , \quad L_f^k h_i(x) = \frac{\partial(L_f^{k-1} h_i(x))}{\partial x} f(x) \quad \text{and} \quad L_{g_j} L_f^k h_i(x) = \frac{\partial(L_f^k h_i(x))}{\partial x} g_j(x).$$

Definition 6.3 (vector relative degree of nonlinear system): Based on the individual components r_i , the vector relative degree r of a multivariable linear system is defined as:

$$r = [r_1 \quad \cdots \quad r_p] \quad (6.4)$$

the multivariable nonlinear system (6.1) is said to have a vector relative degree r at a point x_0 if:

$$L_{g_j} L_f^k h_i(x) = 0; \quad 0 \leq k < r_i - 1, \quad 1 \leq j \leq m \quad (6.5)$$

In this case, the matrix:

$$A(x) = \begin{bmatrix} L_{g_1} L_f^{r_1-1} h_1(x) & \cdots & L_{g_m} L_f^{r_1-1} h_1(x) \\ \vdots & \ddots & \vdots \\ L_{g_1} L_f^{r_m-1} h_m(x) & \cdots & L_{g_m} L_f^{r_m-1} h_m(x) \end{bmatrix} \quad (6.6)$$

is nonsingular or equivalently it has full rank:

$$\text{rank } A(x) = m$$

Definition 6.4 (total relative degree of nonlinear system): Based on the individual components r_i and vector relative degree, the total relative degree is defined as:

$$r = \sum_{i=1}^m r_i \quad (6.7)$$

6.3.2 The procedure of System Inverse Computation

For certain classes of nonlinear state space systems one can find computation algorithms and also sufficient or necessary conditions of system inversion, in order to obtain a differential algebraic polynomial of the input vector u by means of the output vector y through system inverse, see e.g., [122][137].

Indeed, to derive an expression for $u(t)$ as a function of states and output in (6.1), following the inversion algorithm given by [122], we first need to compute the derivatives of $y_i, i = 1, \dots, m$. We have:

If $r_i = 1$, then:

$$\begin{aligned} y_i^{(1)} &= \frac{\partial h_i(x)}{\partial x} \dot{x}(t) \\ &= \frac{\partial h_i(x)}{\partial x} (f(x) + g(x)u) \\ &= L_f^1 h_i(x) + \sum_{j=1}^m L_{g_j}^1 L_f^0 h_i(x) u_j \end{aligned}$$

If $r_i \neq 1$, then $L_{g_j}^1 L_f^0 h_i(x) = 0; \quad 1 \leq j \leq m$

then we get:

$$y_i^{(1)} = L_f^1 h_i(x)$$

We should go on this differentia procedure, in general, for $k < r_i$, we have:

$$\begin{aligned} y_i^{(j)} &= L_f^j h_i(x) \\ &= \partial_x (L_f^{j-1} h_i(x) f(x)) + \sum_{s=0}^{j-2} \partial_{u_a^{(s)}} (L_f^{j-1} h_i(x)) u^{(s)} \quad j = 0, \dots, k, k < r_i \end{aligned}$$

Until when we reach the relative degree r_i , we then obtain:

$$y_i^{(r_i)} = L_f^{r_i} h_i(x) + \sum_{j=1}^m L_{g_j} (L_f^{r_i-1} h_i(x)) u_j \quad i = 1, \dots, m$$

Given finite relative order r_1, \dots, r_m for (6.1) with respect to the output y , and if the total relative degree satisfied as:

$$r = \sum_{i=1}^m r_i = n$$

then calculating expressions for their derivatives, it can be referred to as a 1-step algorithm to obtain an inverse, we get:

$$\begin{bmatrix} y_1^{(r_1)} \\ \vdots \\ y_m^{(r_m)} \end{bmatrix} = \begin{bmatrix} L_f^{r_1} h_1(x) \\ \vdots \\ L_f^{r_m} h_m(x) \end{bmatrix} + \begin{bmatrix} L_{g_1} L_f^{r_1-1} h_1(x) & \dots & L_{g_m} L_f^{r_1-1} h_1(x) \\ \dots & \dots & \dots \\ L_{g_1} L_f^{r_m-1} h_m(x) & \dots & L_{g_m} L_f^{r_m-1} h_m(x) \end{bmatrix} u \quad (6.8)$$

the equation (6.8) can be solved for u to obtain:

$$u = \begin{bmatrix} L_{g_1} L_f^{r_1-1} h_1(x) & \dots & L_{g_m} L_f^{r_1-1} h_1(x) \\ \dots & \dots & \dots \\ L_{g_1} L_f^{r_m-1} h_m(x) & \dots & L_{g_m} L_f^{r_m-1} h_m(x) \end{bmatrix}^{-1} \cdot \left(\begin{bmatrix} y_1^{(r_1)} \\ \vdots \\ y_m^{(r_m)} \end{bmatrix} - \begin{bmatrix} L_f^{r_1} h_1(x) \\ \vdots \\ L_f^{r_m} h_m(x) \end{bmatrix} \right) \quad (6.9)$$

In this situation, there will be no internal dynamics and all the results will be finite time in nature, see in [182].

However, normally, the total relative degree is assumed:

$$r = \sum_{i=1}^m r_i < n$$

In this case, the system given by (6.1) can be presented in a new basis that is introduced as follows.

Define the following change of the coordinates:

$$\xi_i = [\xi_i^1, \xi_i^2, \dots, \xi_i^{r_i}]^T$$

$$\begin{aligned}
&= [\phi_i^1(x), \phi_i^2(x), \dots, \phi_i^{r_i}(x)]^T \\
&= [h_i(x), L_f h_i(x), \dots, L_f^{r_i-1} h_i(x)]^T \quad i = 1, \dots, m \\
&\xi = [\xi_1, \xi_2, \dots, \xi_m] \\
&= [\phi_1(x), \phi_2(x), \dots, \phi_m(x)] \\
&\eta = [\phi_{r+1}(x), \phi_{r+2}(x), \dots, \phi_n(x)]^T \\
&y = [\xi_1^1, \xi_2^1, \dots, \xi_m^1]
\end{aligned}$$

By application new local coordinates transformation proposed in [122], if the system hold the assumption of relative degree, it is always possible to find the function $\phi_{r+1}(x), \phi_{r+2}(x), \dots, \phi_n(x)$, thus :

$$\Phi(x) = [\phi_1(x), \phi_2(x), \dots, \phi_m(x), \phi_{r+1}(x), \dots, \phi_n(x)] \quad (6.10)$$

The mapping $\Phi(x)$ is a local diffeomorphism which means:

$$x = \Phi^{-1}(\xi, \eta) \quad (6.11)$$

Furthermore, according to [122], if the assumption is satisfied:

Assumption 6.1: the distribution is $\Gamma = \text{span} \{g_1 \quad g_2 \quad \dots \quad g_m\}$ involutive,

then, it is always possible to identify the function $\phi_{r+1}(x), \phi_{r+2}(x), \dots, \phi_n(x)$ in such a way that :

$$L_{g_j} \phi_i(x) = 0, i = r + 1, \dots, n, j = 1, \dots, m$$

$$\dot{\eta} = q(\xi, \eta)$$

Then input vector u can be obtained by means of the output vector y and its derivatives:

$$u = A(\Phi^{-1}(\xi, \eta))^{-1} \left(\begin{bmatrix} \xi_1^{(r_1)} \\ \vdots \\ \xi_m^{(r_m)} \end{bmatrix} - \begin{bmatrix} L_f^{r_1} h_1(\Phi^{-1}(\xi, \eta)) \\ \vdots \\ L_f^{r_m} h_m(\Phi^{-1}(\xi, \eta)) \end{bmatrix} \right) \quad (6.12)$$

6.4 Observer Based Input Estimation

The inversion based algebraic polynomial (6.12), however, requires the computation of successive derivatives of outputs, which might be unrealistic in practical applications where measurements suffer noise and disturbances. In most engineering problems, finding the derivative of a signal is normally avoided especially in the presence of noise. As highlighted in [183], in most cases, the problem of estimating the derivative of a signal is posed as an observer problem. Thus in order to avoid using any information of the derivatives of the output, a high gain second-order sliding mode observer is considered to exactly estimate the derivatives of the output. The main idea is as follows. First, a

high-gain second-order sliding mode observer is considered to exactly estimate the derivatives of the output vectors in a finite time. Then, by substituting output derivatives in (6.12), a kind of algebraic unknown input reconstruction method is proposed.

To avoid using any derivative information $\xi_i^j(t), 1 \leq i \leq m, 1 \leq j \leq r_i$ of measurement output directly $y_i = h_i(x)$, a high gain second-order sliding mode observer is considered to exactly estimate them in a finite time.

By construction:

$$\begin{aligned} y_i &= \xi_i^1 \\ \dot{\xi}_i^j &= \xi_i^{j+1}; 1 \leq j \leq r_i - 1 \\ \dot{\xi}_i^{r_i} &= L_f^{r_i} h_i(\Phi^{-1}(\xi, \eta)) + \sum_{j=1}^m L_{g_j} L_f^{r_i-1} h_i(\Phi^{-1}(\xi, \eta)) u_{aj}; j = r_i \end{aligned}$$

Following is structure of the observer:

$$\begin{aligned} \hat{y}_i &= \hat{\xi}_i^1 \\ \dot{\hat{\xi}}_i^j &= \hat{\xi}_i^{j+1} + \lambda_i^j |\hat{y}_i - y_i|^{1/2} \text{sgn}(\hat{y}_i - y_i); 1 \leq j \leq r_i - 1 \\ \dot{\hat{\xi}}_i^{r_i} &= \lambda_i^{r_i} |\hat{y}_i - y_i|^{1/2} \text{sgn}(\hat{y}_i - y_i); j=r_i \end{aligned} \quad (6.13)$$

Therefore, the following exact estimates are available in finite time:

$$\begin{aligned} \hat{\xi}_i &= [\hat{\xi}_i^1, \hat{\xi}_i^2, \dots, \hat{\xi}_i^{r_i}]^T \\ &= [\hat{\Phi}_i^1(x), \hat{\Phi}_i^2(x), \dots, \hat{\Phi}_i^{r_i}(x)]^T \quad i = 1, \dots, m \\ \hat{\xi} &= [\hat{\xi}_1, \hat{\xi}_2, \dots, \hat{\xi}_m] \\ &= [\hat{\Phi}_1(x), \hat{\Phi}_2(x), \dots, \hat{\Phi}_m(x)] \end{aligned}$$

According to [182], with some initial condition from the stability of the internal dynamics, a solution of $\hat{\eta}$ is obtained. And this solution converges asymptotically to an unknown solution that passes through a known ignition condition. That is to say, the asymptotic estimate $\hat{\eta}$ of η can be obtained locally:

$$\begin{aligned} \hat{\eta} &= q(\hat{\xi}, \hat{\eta}) \\ \hat{\eta} &= [\hat{\Phi}_{r+1}(x), \hat{\Phi}_{r+2}(x), \dots, \hat{\Phi}_n(x)]^T \end{aligned}$$

By application new local coordinates transformation proposed in [122], if the system hold the assumption of relative degree, it is always possible to find the function $\phi_{r+1}(x), \phi_{r+2}(x), \dots, \phi_n(x)$, thus :

$$\hat{\Phi}(x) = [\hat{\Phi}_1(x), \hat{\Phi}_2(x), \dots, \hat{\Phi}_m(x), \hat{\Phi}_{r+1}(x), \dots, \hat{\Phi}_n(x)] \quad (6.14)$$

The mapping $\Phi(x)$ is a local diffeomorphism which means:

$$x = \Phi^{-1}(\xi, \eta) \quad (6.15)$$

By using the estimates of output derivatives, a kind of algebraic unknown input reconstruction method is proposed.

$$\hat{u} = A(\Phi^{-1}(\xi, \hat{\eta}))^{-1} \left(\begin{bmatrix} \hat{\xi}_1^{(r_1)} \\ \vdots \\ \hat{\xi}_m^{(r_m)} \end{bmatrix} - \begin{bmatrix} L_f^{r_1} h_1(\Phi^{-1}(\xi, \hat{\eta})) \\ \vdots \\ L_f^{r_m} h_m(\Phi^{-1}(\xi, \hat{\eta})) \end{bmatrix} \right) \quad (6.16)$$

Based on the developments in this section, the following theorem is hold.

Theorem 6.2: Suppose that system (6.1) is locally detectable and the measured outputs are corrupted with noise which is a Lebesgue-measurable function of time with maximal magnitude ε : Then the higher-order sliding-mode observer ensures observation error accuracy of the order of $\varepsilon^{2/\bar{r}+1}$, $\bar{r} = \max(r_i), i = 1, \dots, m$.

6.5 Numerical Simulations

The main objective is to confirm the effectiveness of the input reconstruction techniques given in (6.12) and (6.16) by means of numerical simulations. Further, the results obtained through the implementation of both techniques are compared in order to conclude which is the one that best fits for applications involving heat exchanger reactor. A case study is developed to test the effectiveness of the proposed scheme on a pilot intensified HEX reactor. The pilot is made of three process plates sandwiched between five utility plates. More relative information could find in [160].

6.5.1 System Modelling and Input re-Constructor Design

1-) HEX reactor system model

As in chapter 4, The constants and physical data used in the pilot are given. The model is as follows:

define the state vector as $x^T = [x_1, x_2]^T = [T_p, T_u]^T$, the control input $u^T = [u_{a1}, u_{a2}]^T = [F_p, F_u]^T$,

the output vector of measurable variables $y^T = [y_1, y_2]^T = [T_p, T_u]^T$, then the above two equations can

be rewritten in the following state-space form:

$$\begin{cases} \dot{x}_1 = \frac{u_{a1}}{V_p} (T_{pi} - x_1) + a(x_2 - x_1) \\ \dot{x}_2 = \frac{u_{a2}}{V_u} (T_{ci} - x_2) + b(x_1 - x_2) \end{cases} \quad (6.17)$$

where $a = \frac{h_p A}{\rho_p c_p V_p}$, $b = \frac{h_u A}{\rho_u c_p V_u}$, $y_1 = x_1, y_2 = x_2$

The above model is just for one cell which may lead to moderate differences for the dynamic behavior of the realistic reactor. However, this will not affect the application and demonstration of the proposed algorithm on the reactor, encouraging results are got.

2-) System inversion based input reconstruction

As mentioned above, a key point to compute input via system inversion lies on the invertibility of the system, we address the computational aspect of the concepts by algebraic criteria introduced in Chapter 4. After that, by using eq. (6.12), we can represent the input of the system as a function of the output and its derivatives.

To check if the system, modelled by (6.17), is invertible, we have to check whether the output differential rank is equal to the number of the inputs. There are two inputs in this work: flowrate of process fluid F_p and flowrate of utility fluid F_u which are denoted by u_{a1}, u_{a2} in (6.17) respectively. To compute the output differential rank, we first need to derive an explicit expression for the input in terms of the output y by computing the derivatives of y . When it comes to (6.17), two outputs are temperature of process fluid T_p and utility fluid T_u , which are denoted by y_1, y_2 in (6.17) respectively. As above mentioned, there are two inputs in this work, if the computed output differential rank is equal to the total number of inputs, then it refers that the process subsystem is invertible.

Step 1: Invertibility Checking:

From chapter 4, the system is invertible.

Step 2: Represents the input of the process subsystem as a function of the output and its derivatives:

Thanks to the invertibility of the system, we can reconstruct the inputs as a function of the output and its derivatives. From the above equation, an expression for the two inputs can be derived as $\tilde{u}_a = [\tilde{u}_{a1} \quad \tilde{u}_{a2}]$:

$$\begin{cases} \tilde{u}_{a1} = \frac{V_p}{T_{pi}-y_1}(\dot{y}_1 - ay_2 + ay_1) \\ \tilde{u}_{a2} = \frac{V_u}{T_{ui}-y_2}(\dot{y}_2 - by_1 + by_2) \end{cases} \quad (6.19)$$

3-) Observer based input reconstruction

In order to avoid compute the derivatives, a high-gain second-order sliding mode observer is considered to exactly estimate them in a finite time.

By construction:

$$y_1 = T_p = \xi_1^1$$

$$y_2 = T_u = \xi_2^1$$

$$\xi_i^j = \xi_i^{j+1}, 1 \leq j \leq r_i - 1$$

$$\dot{\xi}_i^{r_i} = L_f^{r_i} h_i(\Phi^{-1}(\xi, \eta)) + \sum_{j=1}^m L_{g_i} L_f^{r_i-1} h_i(\Phi^{-1}(\xi, \eta)) u_{aj}; j = r_i$$

Following is structure of the observer:

$$\begin{aligned} \hat{y}_i &= \xi_i^1 \\ \dot{\xi}_i^j &= \xi_i^{j+1} + \lambda_i^j |\hat{y}_i - y_i|^{1/2} \text{sgn}(\hat{y}_i - y_i); 1 \leq j \leq r_i - 1 \\ \dot{\xi}_i^{r_i} &= \lambda_i^{r_i} |\hat{y}_i - y_i|^{1/2} \text{sgn}(\hat{y}_i - y_i); j=r_i \end{aligned}$$

Step 3: by using the estimates of output derivatives, a kind of algebraic unknown input reconstruction method is proposed.

$$\begin{cases} \hat{u}_{a1} = \frac{V_p}{T_{pi}-y_1} (\hat{\xi}_1^{j+1} - ay_2 + ay_1) \\ \hat{u}_{a2} = \frac{V_u}{T_{ui}-y_2} (\hat{\xi}_2^{j+1} - by_1 + by_2) \end{cases} \quad (6.20)$$

6.5.2 Simulation Results and Discussion

In order to test the performance of the proposed input reconstruction procedures, two numerical simulations were carried out. They consist in estimating the fluid flow rate from measurements of the inlet–outlet temperatures of the studied heat exchanger reactor. The input of the inlet flow rate of the utility fluid F_u is $4.22e^{-5} m^3 s^{-1}$, and inlet flow rate of the process fluid F_p is constant $4.17e^{-6} m^3 s^{-1}$. Both flow rate are assumed unmeasured. In Case 1, an ideal situation is considered which means the measured outputs are not corrupted by noise. In Case 2, the inlet outlet temperatures are considered being measured in the presence of disturbances.

Case 1 measurements not corrupted by noise

The objective of this series of simulations is to prove the convergence of the two input re-constructors given by (6.19) and (6.20) in the ideal situation in which measured temperature is not corrupted by noise. Considering the process model given by (6.17), input re-constructors designed by (6.19) and (6.20) were simulated using the values given in Table 1. These constants, corresponding to a heat exchanger reactor having fast dynamics, were taken from [20]. A value of $UA = 214.8 W.K^{-1}$ was considered. The inlet temperatures T_{ui} and T_{pi} were 15 °C and 76°C respectively. The initial conditions of the process model were $T_p^0 = 80^\circ C$ and $T_u^0 = 20^\circ C$ respectively. The results of the estimation of fluid flow rate F_p and F_u are reported in Fig. 6.1a and Fig.6.2b respectively.

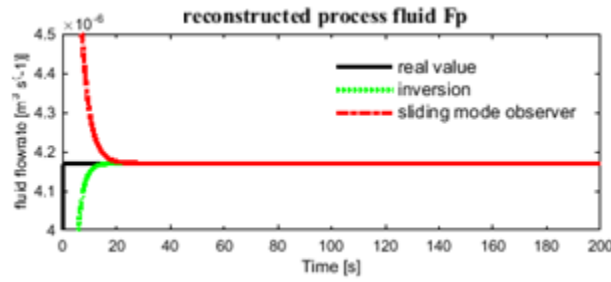


Fig 6.1a reconstructed process fluid flow rate in case 1, solid line is the referenced real value, the dash line is the reconstructed value through system inversion based method, and the dash dot line is the one reconstructed by sliding mode observer based method.

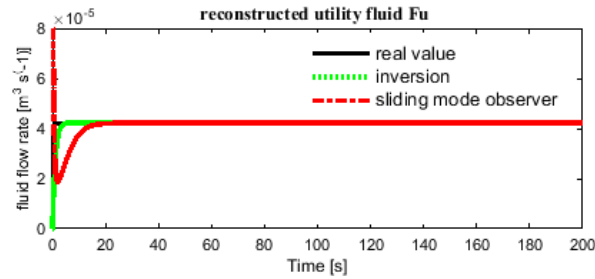


Fig. 6.1b reconstructed utility fluid flow rate in case 1, solid line is the referenced real value, the dash line is the reconstructed value through system inversion based method, and the dash dot line is the one reconstructed by sliding mode observer based method.

Fig. 6.1a and Fig.6.1b confirm the effectiveness of the proposed input estimators. The curves in solid line represent the real value of both fluid flow rate F_p and F_u , denoted as u_{a1} and u_{a2} . Then, we confirm the effectiveness of system inversion based input reconstruction method in dash line, while the curves in dash dot line are the estimations with the help of sliding mode observers. It can be seen from Fig. 6.1a and Fig.6.1b that the reconstructed inputs (both fluid flow rate \tilde{u}_{a1} , \tilde{u}_{a2}) by system inversion in dash line can track the simulation values u_{a1} and u_{a2} in solid line correctly after a short transient period. The similar encouraging results are obtained when the case is carried out to test the effectiveness of the proposed by sliding mode observer aided input reconstruction scheme. From Fig. 6.1a and Fig. 6.1b, \tilde{u}_{a1} , \hat{u}_{a1} and \tilde{u}_{a2} , \hat{u}_{a2} follow different trajectories before they converge towards the “real value” u_{a1} and u_{a2} . In both cases, convergence is guaranteed, and it is clear that convergence rate of system inversion based input reconstruction method is faster than that is in the sliding mode observer based method. Therefore, under ideal situation, on condition that the successive derivatives are available, direct computation of system inversion may be a better choice in reconstructing the unknown input of a dynamic system.

Case 2 measurements are corrupted by noise

The present computations are executed to get an accurate screening of the variation of the reconstructed values, by corroborating if it is in accordance with the simulated noise. To compare the robustness of the proposed schemes, different measurement noises power are considered in Case 2. Suppose that all

parameters and initial conditions are the same as Case 1, however, the output measurement y is corrupted by a colored noise. The colored noise is generated with a second order AR filter excited by a Gaussian white noise with zero mean and unitary variance. The standard deviation of the colored noise is differed as 0.01, 0.028 and 0.1 respectively. The purpose is to conclude which technique is more applicable in the present of noise. Simulation results are shown in the following Figs.6.2-6.4.

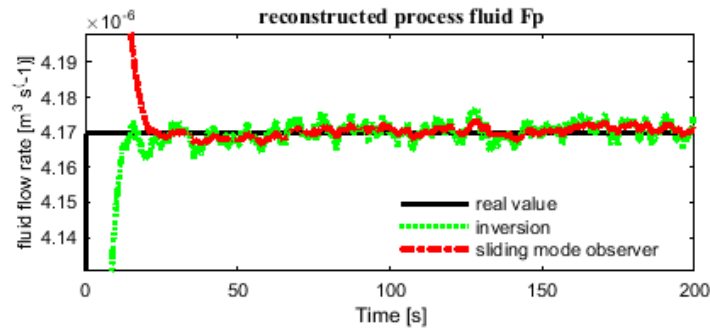


Fig. 6.2a reconstructed process fluid flow rate in case 2 where measurement noise power is 0.01. solid line is the referenced real value, the dash line is the reconstructed value through system inversion based method, and the dash dot line is the one reconstructed by sliding mode observer based method.

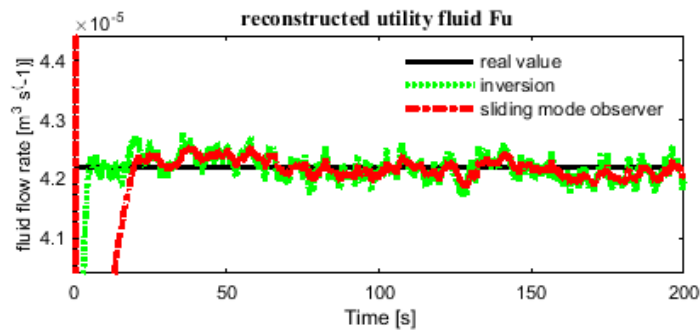


Fig 6.2b reconstructed utility fluid flow rate in case 2 where measurement noise power is 0.01. Solid line is the referenced real value, the dash line is the reconstructed value through system inversion based method, and the dash dot line is the one reconstructed by sliding mode observer based method.

Fig.6.2a and Fig. 6.2b show the simulation results of the reconstructed fluid flow rate when the measured temperatures are corrupted by a colored noise with noise power 0.01. The dashed curves corresponds to fluid flow rate $\tilde{u}_{a1}, \tilde{u}_{a2}$ generated by system inversion based method, while the curves of dash dot line correspond to fluid flow rate $\hat{u}_{a1}, \hat{u}_{a2}$ generated by sliding mode observe based method, it is worth noting that all the curves converge to the real value of the both fluid flow rate F_p and F_u , denoted as u_{a1} and u_{a2} . It can be seen from the Figs.6.3a and 6.3b that once the convergences are obtained, the reconstructed values track well real value in spite of the noise. In addition, no big difference is observed with respect to the two techniques.

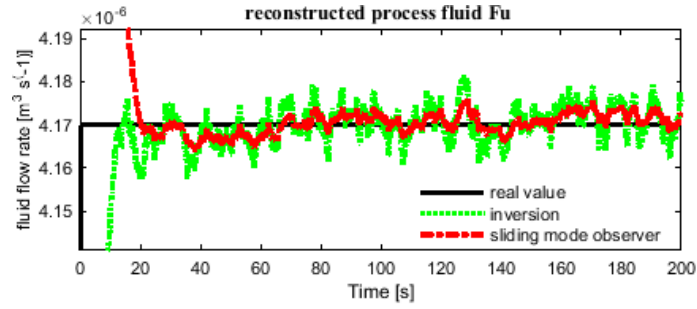


Fig. 6.3a a reconstructed process fluid flow rate in case 2 where measurement noise power is 0.028. Solid line is the referenced real value, the dash line is the reconstructed value through system inversion based method, and the dash dot line is the one reconstructed by sliding mode observer based method.

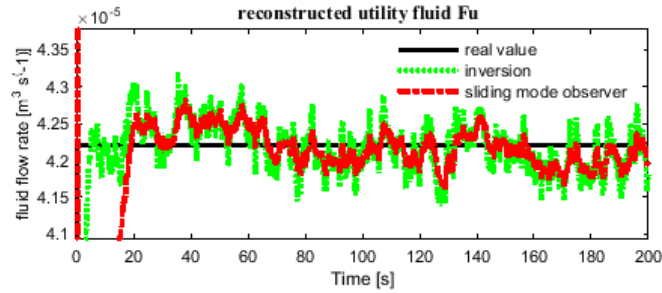


Fig. 6.3b a reconstructed utility fluid flow rate in case 2 where measurement noise power is 0.028. Solid line is the referenced real value, the dash line is the reconstructed value through system inversion based method, and the dash dot line is the one reconstructed by sliding mode observer based method.

Fig.6.3a and Fig. 6.3b show that the two unknown input reconstructed methods estimate the same value as the previous simulation. In this case, it is assumed the measured output is corrupted by noise with power 0.028 which is larger than the previous one, see Fig.6.2a and Fig.6.2b. Figs. 6.3a and 6.3b show the real fluid flow rate F_p and F_u in solid line and their estimates $\tilde{u}_{a1}, \tilde{u}_{a2}$ in dash line and $\hat{u}_{a1}, \hat{u}_{a2}$ in dash dot line respectively. They correspond to the results obtained using reconstructed method (6.19) and (6.20) respectively. It can be seen that the estimates converge well towards the simulated real values. Figs. 6.3a and 6.4b demonstrate that the two methods reconstruct the same value. As expected, the variations of $\tilde{u}_{a1}, \tilde{u}_{a2}$ in dash line and $\hat{u}_{a1}, \hat{u}_{a2}$ in dash dot line reflect the measurement noise on the operating conditions. While different from the previous simulation in Figs 3a and 3b where the noise power is 0.01, with the increase of measurement noise power (with noise power 0.028), the estimation error produced by system inversion based method is obviously larger than that is produced by sliding mode observer based method.

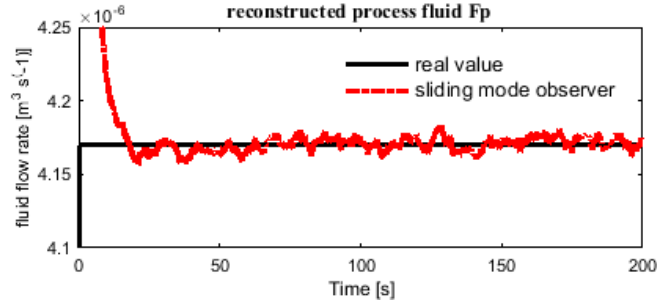


Fig. 6.4a a reconstructed process fluid flow rate in case 2 where measurement noise power is 0.1. Solid line is the referenced real value, and the dash dot line is the one reconstructed by sliding mode observer based method.

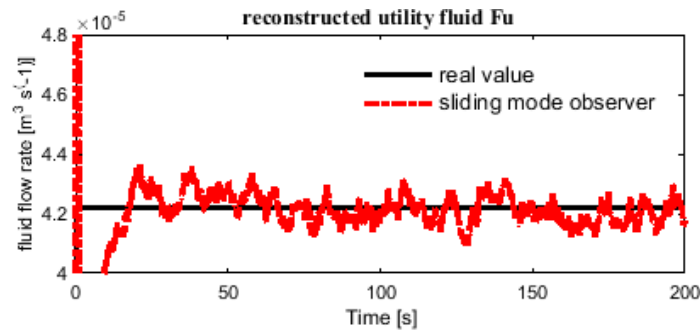


Fig. 6.4b a reconstructed utility fluid flow rate in case 2 where measurement noise power is 0.1. Solid line is the referenced real value, and the dash dot line is the one reconstructed by sliding mode observer based method.

In Fig.6.4a and Fig.6.4b, this study is similar with the previous simulations, see Figs. 6.2-6.3, but a more sever situation (with measurement noise power 0.1) is considered in implementation in order to test the robustness of the proposed methods. Two unknown input re-constructors are designed based on (6.19) and (6.20). Then, they were used to monitor the value of fluid flow rate F_p and F_u on a one-cell heat exchanger reactor modelled by (6.17). Unfortunately, the re-structor designed by system inversion cannot be plotted since sever computation error occurs. Therefore, as shown in Figs.6.4 and 6.4b, only the sliding mode observer based method still works well. Moreover, it can be seen that the estimated values \hat{u}_{a1} , \hat{u}_{a2} in dash dot curves could still coincide with the simulated value of F_p and F_u . This is an expected outcome with respect to the proposed methods. From this, we conclude that sliding mode observer based input reconstruction procedure is more suitable for estimating the unknown input of a dynamic system in the presence of noise.

6.6 Summary

In this paper, two unknown input reconstruction techniques for an invertible nonlinear system are presented, one based on direct system inversion computation, and the other is based on sliding mode observer. The main contribution of this chapter is the combination of system inversion capability with sliding mode observer advantages. A high gain sliding mode observer is proposed for the purpose exactly estimate derivatives of outputs which is used to substitute the successive outputs derivatives in

the differential algebraic polynomial obtained via system inverse. Numerical simulations are presented to make a comparison of both procedures. Results show that the approach achieves satisfactory performances in terms of unknown input reconstruction capabilities. Conclusion are made that system inversion based method is proper in ideal situation if successive computation of derivatives are available, while sliding mode observer based method is more applicable in the presence of measurement noise.

CHAPTER 7 FAULT DIAGNOSIS AND ROOT CAUSE ANALYSIS FOR INTERCONNECTED SYSTEM

This chapter develops a two level fault diagnosis (FD) and root cause analysis (RCA) scheme for a class of interconnected invertible dynamic systems. By considering actuator as individual dynamic subsystem connected with process dynamic subsystem in cascade, an interconnected system is then constituted. Invertibility of the interconnected system in faulty model is studied. An interconnected observer introduced in chapter 5 is employed, aimed at monitoring performance of the interconnected system and providing information of actuator fault occurrence. A local fault filter algorithm is then triggered to identify the root causes of the detected actuator faults. According to real plant, outputs of the actuator subsystem are assumed inaccessible and are reconstructed by measurements of the global system, thus providing a means of monitoring and diagnosis of the plant at both local and global level.

7.1 Introduction

Many of the vital services of everyday life depend on highly complex and interconnected engineering systems which consist of large number of interconnected sensors, actuators and system components. From the system's perspective, the continuously increasing complexity contributes to the difficulties in monitoring complex processes in the modern industries. Thus, modern engineering systems comprise distributed control with highly connected control elements at local system levels and at higher levels. The safe and reliable operation of such systems through the early detection of an incipient fault before it becomes a serious failure is a crucial component of the overall system performance and sustainability. A fault can be considered as process degradation or degradation of the equipment performance caused by the change in the physical characteristic of the process, the input process or the external conditions, for example, bearings may jam, valves may leak or sensors may provide wrong readings. Advanced fault detection and diagnosis (FDD) can help accurate monitoring of process variables and interpreting their behaviors, thus providing better predictive maintenance aids. While the supervision, monitoring and diagnosis of these systems increase in complexity as the diagnosis of system operation and malfunction must be carried out at all process levels.

Actuators are fundamental components in the process industry and they are the most common final control elements in the control loop. For example, there can be thousands of manually operated valves and control valves in a process plant. Many important process variables, such as forces, flows and pressures, are controlled through actuators. In some cases, a fault that occurs in actuator may cause significant disturbances on the quality of the final product. In the last decades, there have been significant research activities in the design and analysis of fault diagnosis and accommodation schemes for systems that subject to actuator fault. One main category is system level based diagnosis approach where internal dynamics of actuator is ignored, aims at detecting and identifying actuator fault existence and location from the view point of global system. Fault symptoms can be detected without having the capability to pinpoint the root causes of the detected faults. Another common kind focuses on the field

component level which aims at analyzing internal dynamics of a specific actuator while dynamics of global system is neglected.

The most nature approach for diagnosing actuator fault that has appeared in the literature typically focus on system level where the major objective relates to performance supervision of the final product. In these methods, dynamics of actuator is normally ignored; instead, the control input is assumed to enter the system dynamics linearly, although this often does not hold in practice. A key approach is based on residual generation. Another approach different to residual generation is fault estimation or fault reconstruction which can determine the size, location and dynamics behavior of the fault. The relevant literature on this topic has its roots on system inversion theory.

With respect to the above mentioned approaches, researches efforts are mostly devoted in developing a comprehensive fault diagnosis methodology while the problem of root cause analysis (RCA) for the detected fault receive less attention. It is because these methods assume the control input to enter the system dynamics linearly, while varying failure signatures are denoted by the changes of elements of the input matrix/function. This assumption makes the results generally applicable in traditional systems, while increasing technological advancements have made actuators becoming increasingly integrated and complex. Each actuator may consist of more than one component connected in any configuration, therefore actuator itself is a dynamic system and exhibits complicate system dynamics. In some cases, it is important to determine the information provided by the failure actuator, in order to isolate the root causes that give origin to the anomalous operation of the process. For example, if a certain fault appears in an actuator, the root cause of that malfunction can have different causes: zero deviation, error of the range of measurement, deviations of the dead area, problems of linearity and hysteresis, etc. Each of these problems can be represented by root cause of the fault. Application of the above mentioned failure detection and identification (FDI) algorithms have essentially been limited to identification of a global fault in the system, and no further attempts have been made to locate subcomponent faults for root cause analysis. For instance, reference [184] shows that decrease of measured temperature in HEX reactor may be due to decrease of fluid flowrate, this implies an actuator fault. With the help of above FDD algorithms, we can detect and isolate the actuator fault, but fail to realize the root cause of the fault in that particular actuator. The involving candidate root causes of this fault could be valve clogging, stop of utility fluid pump or leakage.

In order to examine potential relationship from causes to effects of an actuator fault, efforts have been made to locate subcomponent faults for RCA from the view point of component level. The independent component analysis can be achieved either via a remote supervisory diagnostic system or autonomously using local intelligence, for instance employing intelligent self validation methods. Model based FDD approaches are proposed like in [3]. For example, reference [2] develops an interval observer based passive fault detection method for control valve. In [3], it presents a Kalman filter-based FDI method for identifying subcomponent faults in power regulating systems of nuclear reactors..

However, neither intelligent actuator nor component level FDI method could provide a means of monitoring and diagnosing of the overall plant at both local and global levels, as required for reliable operation of complex and highly interconnected process systems. A major difficulty to achieve this purpose via component level based diagnosis methodology is due to lack of dynamics information at global system. Moreover, another challenge when researching FDD methods locally is getting data from the subsystem being observed to develop and validate these methods. It is because direct access to actuators is often not possible or difficult via physical measurements due to distances or rough environment. Moreover, even if the output of the actuator is available for measurement, considering the noisy output of the actuator sensor, the numerical differentiation would be too noisy. The noisy control input made from these signals, not only could damage the actuator, but also would make less accuracy in tracking and then instability in the control scheme. A framework that utilizes information from both local and high level to diagnose different faults and identify their root causes has not yet been proposed in the literature, and is still open and challenging in the field of FDD. Therefore, there is the need to understand better the fault propagation, fault causes issues involved and the behavior of the system. What is in fact required is a combination of local intelligence with an advanced diagnostic capability to perform FDD functions on both plant process and individual subcomponents. That is to combine fault monitoring and diagnosis at both local and global levels. This requires the use of advanced diagnosis methods in which it is no longer sufficient to rely on the monitoring and diagnosis of individual system components (i.e. actuators or sensors) but rather on the combined monitoring of groups or sets of components (including process elements themselves).

Motivated by the above considerations, this chapter contributes towards these directions by proposing a fault diagnosis approach which is capable of addressing root cause analysis and fault propagation problems among interconnected subsystems. Specifically, the purpose is to investigate the problem of fault diagnosis (FD) and root cause analysis (RCA) in a class of interconnected invertible dynamic systems. The attempt is to explain how the behavior of global output can be interpreted to identify root cause of detected faults in actuator subsystem. We propose a left invertible interconnected nonlinear system structure with input reconstruction laws which is based on dynamic inversion, forming a new model based actuator FDD and RCA algorithm. Actuator is viewed as subsystem connected with the process subsystem in cascade manner, thus identifying reasons of actuator faults with advancing FDD algorithm in actuator subsystem. Outputs of the actuator subsystem are assumed unmeasured and reconstructed by measured global outputs. The left invertibility of individual subsystem is required for ensuring that faults occurring in actuator subsystem can be transmitted to the process subsystem uniquely, and for reconstructing inputs of process subsystem, also outputs of actuator subsystem, from measured global outputs. The developed fault diagnosis algorithm is an effort to combine the strength of system level and the component level model based fault diagnosis. Moreover, the fault detectability conditions are rigorously investigated, characterizing the class of detectable process faults in each subsystem.

This chapter is organized as follows. Section 7.2 describes the proposed strategy and formulates the problem. The main idea of the FD&RCA architecture is presented in section 7.3. In section 7.4, conditions regarding the implementation of the proposed approach are analyzed, involving fault diagnosability, invertibility of fault model for both subsystems and the interconnected system. An interconnected fault detection observer, together with local fault filters are then designed for system performance supervision and actuator fault RCA in section 7.5 and 7.6 respectively. Finally, conclusion is made in section 7.6.

7.2 Problem Formulation

Modern control system can be viewed as composed of dynamic subsystems connected in series and therefore it can be analyzed in a decentralized manner. In all situations, the global plant and/or each subsystem can be analyzed at different levels down to the component level in estimating the reliability of the whole plant. A typical control system, for example, has at least three cascade subsystems: sensor, process and actuator subsystems. The three parts function properly for the whole system to operate properly where the fault may occur in any level of the system. In this chapter, we focus on the internal dynamics of actuator and fault propagation among the interconnected system. Therefore, we assume the interconnected system consist of two dynamic nonlinear subsystems: the actuator and the process subsystems.

As shown in Fig.7.1, an interconnected system Σ is considered which consists of two subsystems: actuator Σ_a and process Σ_p . The basic idea is to identify the fault V at local level, while monitoring the whole plant at global level. The fault vector V indicates candidates of root causes of actuator faults.

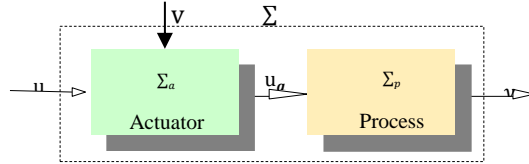


Fig. 7.1 Interconnected system structure

Assuming that the MIMO process subsystem is an input affine nonlinear system, and is described by (7.1):

$$\Sigma_p \begin{cases} \dot{x} = f(x) + g(x)u_a, & x(t_0) = x_0 \\ y = h(x, u_a) \end{cases} \quad (7.1)$$

where $x \in \mathfrak{R}^n$ is the state of the process subsystem, $y \in \mathfrak{R}^p$ is the output of the global system, which is also the output of the process subsystem. $u_a \in \mathfrak{R}^m$ is the input of process subsystem, which is also the output of the actuator subsystem. u_a is inaccessible and need to be reconstructed by measures of y . f and g are smooth vector field on \mathfrak{R}^n and h is smooth vector field on \mathfrak{R}^p .

Assuming that the actuator subsystem is a nonlinear system described by (7.2):

$$\Sigma_a \begin{cases} \dot{x}_a = f_a(x_a, u, \theta_a) \\ u_a = h_a(x_a, u, \theta_s) \end{cases} \quad (7.2)$$

where $x_a \in \mathcal{R}^n$ is the state, $u \in \mathcal{R}^l$ is the input, $u_a \in \mathcal{R}^m$ is the output of the actuator subsystem, which is also the input of the process subsystem, $\theta_a \in \mathcal{R}^k$ represents the parameters of the actuator subsystem, when no faults are present $\theta_a = \theta_{a0}$ (θ_{a0} is the nominal parameter vector). $\theta_s \in \mathcal{R}^k$ represents the parameters in the output equation (if a sensor fault occurs $\theta_s \neq \theta_{s0}$, where θ_{s0} represent the nominal parameters in the output equation).

Thus an interconnected cascade system Σ is then constructed by these two subsystems Σ_a and Σ_p depicted by (7.1) and (7.2) where the input is vector $u \in \mathcal{R}^l$ while output vector is $y \in \mathcal{R}^p$.

Considering fault vector $V = (v_1, \dots, v_k)$ as integration of either parameters faults in θ_a, θ_s or other disturbance signals, in general. Then a fault model of the actuator subsystem becomes:

$$\Sigma_a \begin{cases} \dot{x}_a = f_a(x_a, u) + g_a(x_a, u)V \\ u_a = h_a(x_a, u) + l_a(x_a, u)V \end{cases} \quad (7.3)$$

Where g, l are analytic functions of the system subject to multiple, possible simultaneously faults. The goal is to detect the occurrence of the components v_i of the fault signal independently of each other and identify which fault component specifically occurred. The detectability of one fault in nonlinear system (7.3) is defined as:

Definition 7.1: the fault v_i ($i = 1, \dots, k$) is said to be non-detectable if for $v_i \neq 0$ the relation

$$y(x_0, x; x_{a0}, x_a; u; 0) = y(x_0, x; x_{a0}, x_a; u; 0, \dots, v_i, \dots, 0)$$

is satisfied; if not, the fault v_i is detectable.

The initial motivation for this work came from the need to describe the cause and effect relationships between subsystem variables v_i and global system output y , thus providing advanced predictive maintenance techniques in an operating plant. The primary objective is to monitor system performance, as well as provide an early warning to the human operator regarding the failing health of control equipment, thereby avoiding major breakdown with its associated large plant downtime. Further, the attempt is also to identify faulty parameters in actuator subsystem, so as to carry out fault event sequencing and root cause analysis. A further step to this would be to develop RCA methods for identifying subcomponent faults in control equipment, resulting in improved fault localization and providing better predictive maintenance aids. That is to discover the locations and causes of the faulty actuator, and to identify the corresponding faulty parameters.

Considering interconnected systems depicted by Fig.7.1, firstly, it is desirable to monitor the performance of the interconnected system with respect to individual subsystems and the overall system. While the main objective is to identify the occurrence of the fault v_i in (7.3) independently from each other as required for reliable operation of complex and high interconnected process system. The property of distinguishability of two inputs or faults refers to their capacity to generate different output signals for a given input signal. Distinguishability is relatively important when studying the observability of interconnected systems. It characterizes in this context the ability to determine the root cause of an actuator fault from measured global output data. However, to the best of our knowledge, there is

currently no research on the determination of the class of fault parameter at local subsystem that generate given global output signals for dynamical interconnected systems, a problem we will attack here.

7.3 Fault Diagnosis and Root Cause Analysis Architecture

7.3.1 Performance Supervision and Fault Detection

In order to deal with the performance supervision task, as well as fault detection, one way to achieve this purpose is to have observers for each of the subsystems and the overall plant. However, the major difficulty lies on inaccessibility of the connection which is the output of the actuator subsystem, also the input of the process subsystem. It is because on-line measurements are either difficult to obtain due to physical reasons, or the measurement is uneconomical and unreliable. The reasons lie on that actuators are often far from the controller and their operation environment are often rough. Therefore the state observation in this work can only rely on the global system output, i.e. the process state at the terminal boundary.

Considering interconnected systems depicted by Fig.7.1, the particular aim in our design is to accurately estimate online the state vector x and x_a of each subsystem, as well as the unmeasured interconnection vector u_a . To achieve this purpose, as shown in Fig.7.2, a nominal interconnected nonlinear observer is designed to monitor performances of the overall system, as well as each subsystem, and guarantee that the state estimation error, for the nominal nonlinear system, converges to zero. While once there are faults occurred, the state estimation error will be no longer stay at zero which implies existence of the faults.

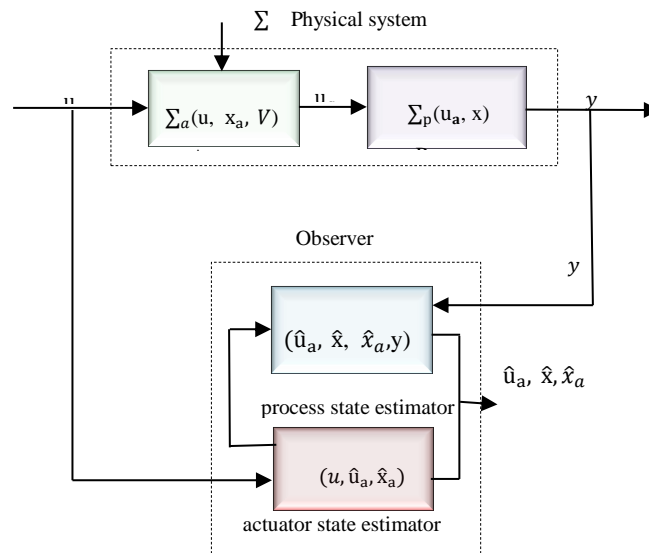


Fig. 7.2 Interconnected observer for performance supervision

As shown in Fig. 7.2, the main idea behind our design is as follows: suppose an nominal observer is already available for the nonlinear actuator subsystem Σ_a with output u_a , in which no fault is assumed, we implement that observer using an estimate of u_a , denoted by \hat{u}_a . In order to produce such an estimate, we extend the state space of the process subsystem Σ_p to include u_a as an additional state. By computing derivatives of u_a in actuator subsystem, we then obtain an expression for u_a which is a

function of u , derivatives of u and x_a . Then an observer is constructed for this extended process subsystem. State estimator of actuator subsystem, together with state estimator of process subsystem, a kind of nominal observer designed method is then proposed for the studied nominal interconnected nonlinear system.

7.3.2 Fault Detection

The above-mentioned nominal observer is designed to assume that there is no fault, so once the observer converges, the \hat{u}_a estimate is reliable, so that the estimate can be used as true signal u_a for the input reconstruction of the process subsystem to achieve the fault detection. For this purpose, an inverse system observer is constructed first. An important task of the observer is to eliminate the effects of initial conditions, drift and other factors, and to ensure the validity of the root cause analysis. As shown in Figure 7.3, the input of the observer of the inverse system is y , the observer estimates the output as \tilde{u}_a , where the reference output is \hat{u}_a . When the observer convergence, it satisfies $\tilde{u}_a = \hat{u}_a = u_a$, and the estimated error should be below the threshold; and it means that the failure of the generation the error is break the threshold. When the detection of a sudden failure occurs, the local filters are triggered to achieve root cause analysis.

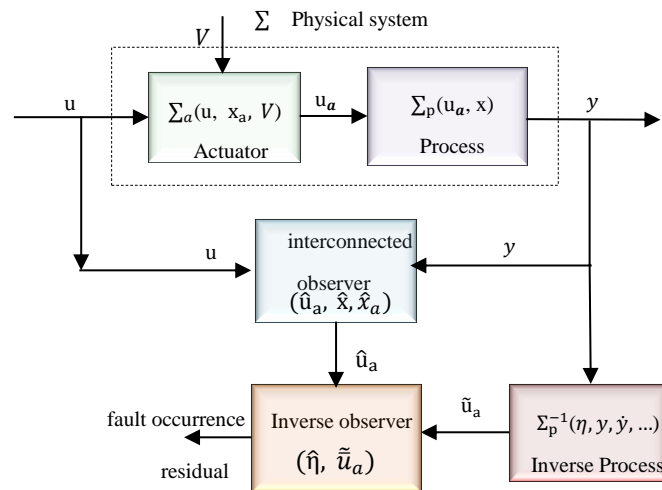


Fig.7.3 fault detection observer

7.3.3 Root Cause Analysis

After a fault is detected, next task is to identify the root cause of the fault. A RCA (root cause analysis) scheme is then proposed based on local fault filtering schemes with each one assigned to monitor one subsystem and provide a decision regarding its health. This procedure is denoted as root cause analysis (RCA). As shown in Fig.7.4, the main objective is to identify the occurrence of the fault v_i in (7.3) independently from each other whilst monitoring the whole plant at both local and global level, as required for reliable operation of complex and high interconnected process system. Fault v_i refers to fault resources of an actuator fault which is related with special physical meaning, e.g. v_i represents fault caused by leakage or valve clogging of an actuator. We propose a local filter based FDD strategy at local level of actuator subsystem, thus realizing these resources ($v_i, i = 1, \dots, k$) of actuator fault.

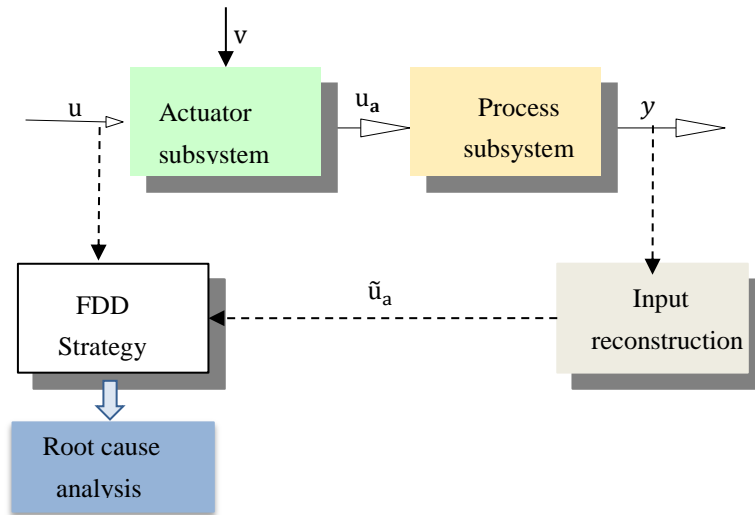


Fig.7.4 Main idea of the proposed RCA algorithm

Since advanced FDD strategy is performed in actuator subsystem, observers are then fed with input u and output u_a in actuator subsystem as shown in Fig.7.3. However, one major difficulty is that the only available measurements rely on the global system output y . That is because online diagnosis of actuator component is often achieved by a remote supervisory diagnostic system, therefore, it is impractical to measure u_a in realistic industrial condition. For that, u_a is supposed to be not accessible to measurements in this work. Besides, in order to monitor the plant at global level, information of global output should be included when FDD function is performed at local subsystem. As shown in Fig.7.3, if u_a can be reconstructed from the global measurement y uniquely, then the above two problems are solved. In that way, advanced FDD strategy performs validation of the nominal relationships of the system, using the input u , and the output \tilde{u}_a which is reconstructed from measured output y . Hence, a means of monitoring and diagnosis of the whole plant at both local and global level is provided, by which result in improved fault localization and provide better predictive maintenance aids.

In summary, to accomplish the aims, the key problem is to provide condition for validating cause and effect relationships between fault vector V and output vector Y . Besides, it is also critical for ensuring that reconstructed \tilde{u}_a and fault vector V has one to one relationship. In that case, advanced FDD strategy can be carried out in actuator subsystem to identify each component v_i , thus achieving root cause analysis (RCA) of the detected actuator fault. There are therefore mainly four tasks to follow:

- 1-) provide condition for guaranteeing that effects of the faults $V = (v_i, \dots)$ occurred in actuator subsystems are distinguishable by the global output y uniquely;
- 2-) reconstruct the unknown outputs u_a of actuator subsystem through measured outputs y of process subsystem, denoted by \tilde{u}_a ;
- 3-) provide condition for ensuring that reconstructed \tilde{u}_a and fault vector V has one to one relationship;
- 4-) propose a RCA algorithm for identifying fault $V(v_i, \dots)$ locally.

The rest of this chapter is to deal with these tasks.

7.4 On Condition of Fault Distinguishability Locally and Globally

7.4.1 Fault analysis and Faulty model

The important aspect of this approach is the development of individual subsystem models and fault model that describe the cause and effect relationships between the actuator subsystem internal variables and process subsystem outputs which is applicable of using state estimation or parameter estimation techniques. Different types of fault cause changes in either mode structure or model parameters or in the forcing functions of the differential equations constituting the nominal mode. These cause variations in the residues, state estimates, and covariance when a filter based algorithm is used for FD&RCA. That leads to an operation point shift for all the internal variables before the fault in the chain of the internal variables in the system. When these operation point changes are being detected, the faults can be detected and diagnosed. All nonlinearities of the system could be identified and estimated through selected parameters.

Fault analysis aims at obtaining the malfunction and behavioral knowledge about the actuator internal variables and the process. Specifically, its objective is to identify the sources of production losses and the most significant faults that are causing the losses in a process. These faults are then studied in accordance with the process decomposition to analyze their locations and effect on the process. Consequently, the development of fault detection methods is focused appropriately by concentrating on the key areas, i.e. the faults and subsystems, which have the most significant impact on plant performance. To this end, the faults shall be categorized into basic fault types and causes. Lastly, each fault is associated with the specific devices and components based on the maintenance data or root cause analysis.

An actuator is a kind of motor that controls or moves mechanisms or systems. It takes hydraulic fluid, electric current or other sources of power and converts the energy to facilitate the motion. Actuators are extremely useful devices and have a diverse range of uses in fields such as engineering, electronic engineering and can be found in many kinds of machinery such as printers, cars or disk drives. Most actuators produce either linear (straight line), rotary (circular) or oscillatory motion. There are four main types of actuators: Hydraulic, Pneumatic, Electric and Mechanical.

The modeling of an actuator and possible faults is based on understanding the physical process. Up to now, modelling of actuators has benefited to researches in automation, as shown in [42][185][186][187]. Reference [3] studies various model and fault mode encompasses actuators of control valve, pump and positioner in a reactor power regulating system. Paper [188] attempts to model system relate the dynamics of the control valve unit to the mechanics of the PAM actuator based on experimental identification from data of real physical behaviors. A sliding stem control valve model is presented by the work in [1]. There the same kind of fault simulator concept is used for fault detection and diagnosis research as in the study [45].

From the interesting references, despite different actuators and various considerations, the proposed dynamic models benefit from a parameter-affine characteristic described in (7.2) and (7.3). If viewed

unexpected variations in parameters as unknown inputs and denoted by vector $V = (v_1, v_2, \dots, v_k)$, then we get an input-affine dynamic faulty model as (7.4) form as:

$$\Sigma_a \begin{cases} \dot{\hat{x}}_a = f(x_a, u) + \sum_i^k g_{ai}(x_a, u)v_i \\ u_a = h_a(x_a, u) \end{cases} \quad (7.4)$$

7.4.2 On Condition of Fault Distinguishability

Fault distinguishability refers to the capacity of faults to generate different output signals for a given system. Two fault signals are strictly distinguishable if for any initial state vectors and control inputs of the systems (not both zero), their corresponding outputs are different. Studies of distinguishability deal with the determination of necessary and (or) sufficient conditions that allow to test whether or not two different faults are strictly distinguishable.

As mentioned above, a key feature, opportunity and technical challenge of the scheme is to obtain the condition by which the fault information $V = (v_1, v_2, \dots, v_k)$ in (7.4) provided by actuator subsystem has distinguishable effects on system output y in (7.1). If we view the overall interconnected system as a black box, this can be seen as problem of input observability where V is considered as the unknown input of the overall system and Y is the output. While input or fault observability are equivalent with left invertibility of system, as shown in reference [137], the input can be uniquely recovered from output and the initial state if dynamical system is left invertible. Also according to results that given in [148][159][139], if a fault affine dynamic system is left invertible, then the fault vector can be obtained by means of the output vector. Therefore, we can conclude that if the overall interconnected system is invertible, the fault vector V can be reconstructed from the system input u , system output y and possible their derivatives, as shown in Fig.7.4.

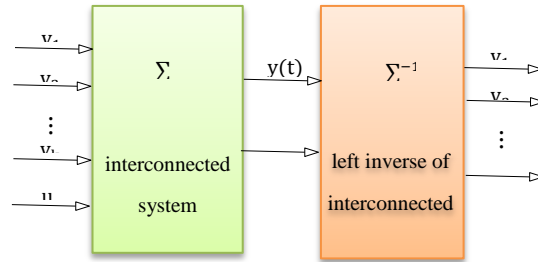


Fig. 7.5 detector for fault reconstruction

Fig.7.5 describes a detector capable of fault reconstruction. If we want to reconstruct the unmeasured fault signal at the output of the detector, the property of input observability is an important quality of the system which is equivalent to system invertibility. Therefore, input reconstruction addresses the problem of designing a filter or detector which, on the basis of the input and output measurements, returns the unknown input of the original system by utilizing its inverse representation. The detector in fact, is another dynamic system which is constructed with outputs $v_i(i = 1, \dots, k)$ and with inputs u , y and possibly their time derivatives or integrals which, in the most general form, can be thought of as:

$$\begin{cases} \dot{\xi}(t) = \varphi(\xi, y, \dot{y}, \dots, u, \dot{u}, \dots) \\ v(t) = \varpi(\xi, y, \dot{y}, \dots, u, \dot{u}, \dots) \end{cases} \quad (7.5)$$

with the state variable $\xi(t)$ assuming φ, ϖ are arbitrary analytic time functions. The filter reproduces the fault signal at its output that is zero in the normal system operation, while it differs from zero if a particular fault occurs. That is to say the fault is distinguishable at the final boundary.

Definition 7.2: (Algebraic observability condition). The fault $v_i (i = 1, \dots, k)$ is said to be diagnosable if it is algebraically observable depicted by (7.1) and (7.4).

Proposition 7.1: The fault $v_i (i = 1, \dots, k)$ is said to be diagnosable if it is possible to estimate the fault from the available measurements of the interconnected system depicted by (7.1) and (7.4).

Property 7.1: The fault $v_i (i = 1, \dots, k)$ can be obtained by the system output y if the interconnected system depicted by (7.1) and (7.4) is invertible.

Theorem 7.1: The fault $v_i (i = 1, \dots, k)$ is said to have distinguishable effects on the system output y if the interconnected system depicted by (7.1) and (7.4) is invertible.

7.4.3 On Condition of One to One Relationship between Estimated \tilde{u}_a and Fault Vector V

Moreover, an essential requirement of the combination of individual actuator with an advanced diagnostic capability is the availability and reliability of the output u_a of the actuator subsystem, which is also the input of the process system. This problem is considered as problem of input reconstruction, which is viewed as problem of system inversion. Some issues of inversion concepts for input reconstruction were discussed, e.g. [17,31]. In a sum, if the process subsystem is invertible, the input u_a can be recovered from the output y by means of a finite number of ordinary differential equations. With the kind of algebraic unknown input estimation method presented in chapter 5, we can obtain estimated \tilde{u}_a from output y .

Definition 7.3: If process subsystem (7.1) is left invertible, then the input vector u_a can be obtained by means of the output vector y , denoted by \tilde{u}_a .

Definition 7.4: If actuator subsystem in failure mode as in (7.4) is left invertible, then the fault vector $V (v_i, i = 1, \dots, k)$ can be obtained by means of the output vector u_a .

Theorem 7.2: If convergences of reconstructed \tilde{u}_a is guaranteed, then by substituting u_a as \tilde{u}_a , the fault vector $V (v_i, i = 1, \dots, k)$ can be obtained by means of the output vector \tilde{u}_a .

Proposition 7.2: If convergences of reconstructed \tilde{u}_a is guaranteed, then the fault vector $V (v_i, i = 1, \dots, k)$ has one to one relationship with the reconstructed output vector \tilde{u}_a .

As above mentioned, based on the condition that both interconnected system and individual subsystems are invertible, reconstructed \tilde{u}_a and fault vector V has one to one relationship. In that case, advanced FDD strategy can be carried out in actuator subsystem to identify each component v_i , thus achieving root cause analysis (RCA) of the actuator fault.

7.4.4 On Condition of Invertibility of Nonlinear Interconnected System in Faulty Model

With respect to the above analysis, the foundation of the proposed scheme is based on invertibility of the system. Therefore the key point is to provide condition for validating invertibility of the interconnected system and individual subsystems.

From chapter 4, non-invertibility of each subsystem results in non-invertibility of the interconnected system. Consider the interconnected system Σ which consists of the actuator Σ_a and process Σ_p subsystems, and an output set (U_a, Y) , as depicted by (7.1) and (7.2). The interconnected system is invertible at (x_0, x_{a0}) over (U_a, Y) , if and only if each subsystem actuator Σ_a and process Σ_p is invertible at x_{a0} over U_a , and x_0 over Y respectively. Moreover, it gives a sufficient and necessary condition on the subsystem dynamics which is based on differential output rank so that the interconnected system is invertible for set U, U_a and Y . After verifying the invertibility of individual subsystems, it is capable of constructing an interconnected invertible system that can recover the original input uniquely from the global measurement, by which implies that each original input affect the global output distinguishably.

The objective of this chapter is give the inversion algorithm for the diagnostic fault model with respect to the inputs $V (v_i, i = 1, \dots, k)$, and output Y depicted in (7.1) and (7.4). Therefore the invertibility of the interconnected system in failure mode should be refined in the following way.

Definition 7.5: Consider the interconnected diagnostic system Σ in failure mode which consists of two subsystems: actuator Σ_a subsystem in failure mode and process Σ_p subsystem, and an output set (U_a, Y) , as depicted by (7.1) and (7.4). The interconnected diagnostic system is invertible at (x_0, x_{a0}) over (U_a, Y) , if and only if each subsystem actuator Σ_a in failure mode and process Σ_p is invertible at x_{a0} over U_a , and x_0 over Y respectively.

With respect to the results that haven been obtained, we only need to check the invertibility of the diagnostic actuator subsystem in failure mode. This diagnostic system is considered affine in a sub-family of the failures which are considered as unknown inputs, and therefore the inversion can be achieved to this sub-family. In this article, the diagnosis problem is tackled as a left invertibility problem throughout the concept of differential output rank as introduced in chapter 4.

Definition 7.6: Faults are defined as transcendent elements over $\mathcal{K}\langle u \rangle$, therefore, a system with the presence of faults is a differential transcendental extension, denoted as $\mathcal{K}\langle u, f, y \rangle / \mathcal{K}\langle u \rangle$, where f is a vector that includes the faults and their time derivatives.

Definition 7.7: Let $\mathcal{G}, \mathcal{K}\langle u \rangle$ be differential fields. A fault dynamic consists of a finitely generated differential algebraic extension $\mathcal{G} / \mathcal{K}\langle u \rangle$, $\mathcal{G} = \mathcal{K}\langle u, f, \xi \rangle, \xi \in \mathcal{G}$. Any element of \mathcal{G} satisfies an algebraic differential equation with coefficients over \mathcal{K} in the components of u, f and their time derivatives.

Definition 7.8 (Algebraic observability condition): A fault $f \in \mathcal{G}$ is said to be diagnosable if it is algebraically observable over $\mathcal{K}(u, y)$. i.e. if it is possible to estimate the fault from the available measurements of the system.

It is also defined differential output rank as the maximum number of outputs that are related by a differential polynomial equation with coefficients over \mathcal{K} (independent of x and v). A simple way to compute differential output rank of system (7.4) is, therefore, defined by corollary 7.4.

Corollary 7.1: if there exists r possible differential polynomial equation of the form

$$P_r(u_{a1}, u_{a2}, \dots, u_{am}, \dot{u}_{a1}, \dot{u}_{a2}, \dots, \dot{u}_{am}, \ddot{u}_{a1}, \ddot{u}_{a2}, \dots, \ddot{u}_{am} \dots) = 0$$

then the differential output rank ρ is defined as $\rho = p - r$, which implies $p - r$ independent outputs.

Here, we view fault candidates as unknown input of local actuator system. That is, if the differential output rank is equal to the number of possible failures, the system is invertible. This implies that the number of outputs must be greater, or equal to the number of failures. In this communication, the outputs are mainly signals obtained from the sensors. Therefore their number is important to know whether a system is diagnosable or not.

Theorem 7.3: the actuator \sum_a subsystem in failure mode is left invertible if, and only if the differential output rank ρ is equal to the total number of faults, e.g. $\rho = v$ in (7.4).

Remark 7.1: If the actuator \sum_a subsystem in failure mode has more faults than outputs, it cannot be left invertible.

Proposition 7.2: From remark 7.1, the number of faults V ($v_i, i = 1, \dots, k$) that can be identified simultaneously is determined by the number of available outputs y .

7.5 Observer Design for Invertible Interconnected system

After checking invertibility of the interconnected diagnostic system, as well as individual subsystem, advanced FDD strategy can be proposed in order to monitor the performance of the interconnected system at both local level and global level. In addition, local filter is required to identify each component v_i in (7.4) in actuator subsystem once fault occurs, thus achieving root cause analysis (RCA) of the detected actuator fault.

7.5.1 Observer Design for Performance Supervision

As introduced in chapter 5, in order to estimate the state of the actuator subsystem, without any loss of generality, the nominal actuator subsystem in (7.2) can be transformed into the following form:

$$\begin{cases} \dot{\chi}_1 = A_1 \chi_1 + \Theta_1(\chi_1, u) \\ u_a = C_1 \chi_1 \end{cases} \quad (7.6)$$

$$\text{with } \chi_1^T = (\chi_{11} \quad \dots \quad \chi_{1n})^T, \quad A_1 = \begin{bmatrix} 0 & 1 & \dots & 0 \\ \vdots & \ddots & \ddots & \vdots \\ 0 & \dots & 0 & 1 \\ 0 & \dots & 0 & 0 \end{bmatrix}, \quad \Theta(\chi_1, u) = \begin{bmatrix} \Theta_1(\chi_{11}, u) \\ \vdots \\ \Theta_n(\chi_{11}, \dots, \chi_{1n}, u) \end{bmatrix}, \quad C_1 =$$

[1 0 ... 0],

this transformation with the structure ensures the existence of a high gain observer for system (7.4) introduced by [89], the observer is extended to the following form where output u_a is supposed to be inaccessible and replaced by its estimates \hat{u}_a :

$$\begin{cases} \dot{\hat{\chi}}_1 = A_1 \hat{\chi}_1 + \Theta(\hat{\chi}_1, u) - S_{\theta_1}^{-1} C_1^T (C_1 \hat{\chi}_1 - \hat{u}_a) \\ 0 = \theta_1 S_{\theta_1} + A_1^T S_{\theta_1} + S_{\theta_1} A_1 - C_1^T C_1 \end{cases} \quad (7.7)$$

Then to give an estimate for u_a , as well as monitor state of the process subsystem (7.1), we need to propose an observer, define $z = [z_1 \ z_2] = [x \ u_a]$, then system (7.1) can be extended as:

$$\begin{cases} \dot{z}_1 = f_1(z_1, u) + g_1(z_1, u)z_2 \\ \dot{z}_2 = \varepsilon(u, \dot{u}, x_a) \\ y = z_1 \end{cases} \quad (7.8)$$

System (7.8) can be expressed as in a condensed form:

$$\begin{cases} \dot{z} = l(z_1)G(z_1)z + F(z_1, u) + \bar{\varepsilon}(u, \dot{u}, x_a) \\ y = Cz \end{cases} \quad (7.9)$$

Where:

$$G(z_1) = \begin{pmatrix} 0 & g_1(z_1) \\ 0 & 0 \end{pmatrix}, F(x_1) = \begin{pmatrix} f_1(z_1) \\ 0 \end{pmatrix}, C(I_n \ 0), \bar{\varepsilon}(u, \dot{u}, x_a) = [0 \ \varepsilon(u, \dot{u}, x_a)]^T$$

, I_n is $n \times n$ identity matrix, $l(z_1)$ is a scalar real function with respect to their arguments and $\alpha_1 \leq |l(z_1)| \leq \beta_1$.

Supposed the assumptions related boundedness of the states, signals, functions defined in [171] are satisfied, then an extended high gain observer for the system (7.9) can be given in the following way:

$$\begin{cases} \dot{\hat{z}} = l(\hat{z}_1)G(\hat{z}_1)\hat{z} + F(\hat{z}_1, u) + \bar{\varepsilon}(u, \dot{u}, \hat{x}_a) + H(\hat{z}_1)(\hat{y} - y) \\ \hat{y} = C\hat{z} \end{cases} \quad (7.10)$$

Where: $H = [H_{z_1} \ H_{z_2}]^T = \Lambda^{-1}(\hat{z}_1)S_{\theta}^{-1}C^T$, $\Lambda(\hat{z}_1) = \begin{bmatrix} 1 & 0 \\ 0 & G_1(\hat{z}_1) \end{bmatrix}$, S_{θ} is the unique symmetric positive definite matrix satisfying the following algebraic Lyapunov equation:

$$\theta S_{\theta} + A^T S_{\theta} + S_{\theta} A - C^T C = 0 \quad (7.11)$$

Where $A = \begin{bmatrix} 0 & I \\ 0 & 0 \end{bmatrix}$, $\theta > 0$ is a parameter defined by (7.11) and the solution of eq. (7.11) is:

$$S_{\theta} = \begin{bmatrix} \frac{1}{\theta} I & -\frac{1}{\theta^2} I \\ -\frac{1}{\theta^2} I & \frac{2}{\theta^3} I \end{bmatrix}$$

Then, the gain of estimator can be given by:

$$H = \Lambda^{-1}(\hat{z}_1)S_{\theta}^{-1}C^T = \Lambda(\hat{z}_1) \begin{bmatrix} 2\theta I \\ \theta^2 G_1^{-1}(\hat{x}_1) \end{bmatrix}$$

System (7.7), together with (7.10), constitutes the observer for the studied interconnected system, as follows:

$$\begin{cases} \dot{\hat{\chi}}_1 = A_1 \hat{\chi}_1 + \theta(\hat{\chi}_1, u) - S_{\theta_1}^{-1} C_1^T (C_1 \hat{\chi}_1 - \hat{u}_a) \\ \dot{\hat{z}} = l(\hat{z}_1)G(\hat{z}_1)\hat{z} + F(\hat{z}_1) + \bar{\varepsilon}(u, \dot{u}, \hat{x}_a) + H(\hat{z}_1)(\hat{y} - y) \end{cases} \quad (7.12)$$

7.5.2 Observer Design for Inverse System and Fault Detection

(1) Inverse system modelling

According to previous chapters related with system inversion and input reconstruction, consider the invertible system (7.1), we could develop an dynamic inverse system as the following form:

$$\begin{cases} \dot{\eta} = \bar{f}(\xi, \eta) \\ u_a = A(\Phi^{-1}(\xi, \eta))^{-1} \left(\begin{bmatrix} \xi_1^{(r_1)} \\ \vdots \\ \xi_m^{(r_m)} \end{bmatrix} - \begin{bmatrix} L_f^{r_1} h_1(\Phi^{-1}(\xi, \eta)) \\ \vdots \\ L_f^{r_m} h_m(\Phi^{-1}(\xi, \eta)) \end{bmatrix} \right) \end{cases} \quad (7.13)$$

(b) Observer design for the inverse system

The input of the observer is the measurement y , and output is the estimated \tilde{u}_a , the reference output is \hat{u}_a provided by the previous interconnected observer, estimation of the observer is defined as $e_0(t) = \hat{u}_a - \tilde{u}_a$, once the observer converges, there have $\tilde{u}_a = \hat{u}_a = u_a$.

$$\begin{cases} \dot{\eta} = \bar{f}(\xi, \eta) - k_{ob}(\hat{u}_a - \tilde{u}_a) \\ \tilde{u}_a = A(\Phi^{-1}(\xi, \eta))^{-1} \left(\begin{bmatrix} \xi_1^{(r_1)} \\ \vdots \\ \xi_m^{(r_m)} \end{bmatrix} - \begin{bmatrix} L_f^{r_1} h_1(\Phi^{-1}(\xi, \eta)) \\ \vdots \\ L_f^{r_m} h_m(\Phi^{-1}(\xi, \eta)) \end{bmatrix} \right) \end{cases} \quad (7.14)$$

k_{ob} is the gain of the observer.

(c) Residual generation

The observer (7.14) error satisfies the equation:

$$\begin{cases} \dot{\tilde{e}}_a = \hat{x}_a - x_a \\ e(t) = \hat{z}(t) - z(t) \end{cases}$$

Define:

$$e_0(t) = \hat{y} - y = Ce(t) \quad (7.15)$$

Let $r_0(t)$ as residual for fault detection as:

$$r_0(t) = d\|\hat{y} - y\|/dt = d\|e_0(t)\|/dt \quad (7.16)$$

Then, we get :

$$\gamma_0 = \begin{cases} \|e_0(t)\| < \varepsilon; \text{ fault free} \\ \|e_0(t_f)\| \geq \varepsilon; \text{ exist fault} \end{cases} \quad (7.17)$$

where ε is a prespecified threshold.

7.6 Local Fault Filter for Root Cause Analysis

After a fault is detected, next task is to identify the causes of the fault. That is in fact to recognize the existence of the fault candidate v_i in (7.4) independently from each other. This task is assumed to be achieved at local level in actuator subsystem where measurement of the output is not permitted. Therefore the first issue is to reconstruct output of actuator system from output of the interconnected system y .

7.6.1 Input Estimation

According to the input estimation procedure introduced in chapter 6, if the process system (7.1) is differentially left invertible, the input can be recovered from the output by means of a finite number of ordinary differential equations. We need to follow the following steps:

Step 1: Obtain a differential algebraic polynomial of the input vector u_a by means of the output vector y through system inverse.

For invertible nonlinear system described by (7.1), the relative order r_i of the output y_i , is the smallest integer for which:

$$\begin{aligned} L_g L_f^{r_i-1} h_i(x) &= [L_{g_1} L_f^{r_i-1} h_i(x) L_{g_2} L_f^{r_i-1} h_i(x) \dots L_{g_m} L_f^{r_i-1} h_i(x)] \\ &\neq [0, 0, \dots, 0] \end{aligned}$$

Given finite relative order r_1, \dots, r_m for (7.1) with respect to the output y , calculating expressions for their derivatives, we get:

$$\begin{bmatrix} y_1^{(r_1)} \\ \vdots \\ y_m^{(r_m)} \end{bmatrix} = \begin{bmatrix} L_f^{r_1} h_1(x) \\ \vdots \\ L_f^{r_m} h_m(x) \end{bmatrix} + \begin{bmatrix} L_{g_1} L_f^{r_1-1} h_1(x) & \dots & L_{g_m} L_f^{r_1-1} h_1(x) \\ \dots & \dots & \dots \\ L_{g_1} L_f^{r_m-1} h_m(x) & \dots & L_{g_m} L_f^{r_m-1} h_m(x) \end{bmatrix} u_a \quad (7.18)$$

Let the matrix:

$$A(x) = \begin{bmatrix} L_{g_1} L_f^{r_1-1} h_1(x) & \dots & L_{g_m} L_f^{r_1-1} h_1(x) \\ \dots & \dots & \dots \\ L_{g_1} L_f^{r_m-1} h_m(x) & \dots & L_{g_m} L_f^{r_m-1} h_m(x) \end{bmatrix}$$

Define the following change of the coordinates:

$$\begin{aligned} \xi_i &= [\xi_i^1, \xi_i^2, \dots, \xi_i^{r_i}] = [\phi_i^1(x), \phi_i^2(x), \dots, \phi_i^{r_i}(x)] \\ &= [h_i(x), L_f h_i(x), \dots, L_f^{r_i-1} h_i(x)] \quad i = 1, \dots, m \\ \xi &= [\xi_1, \xi_2, \dots, \xi_m] = [\phi_1(x), \phi_2(x), \dots, \phi_m(x)] \\ \eta &= [\phi_{r+1}(x), \phi_{r+2}(x), \dots, \phi_n(x)] \\ y &= [\xi_1^1, \xi_2^1, \dots, \xi_m^1] \end{aligned}$$

By application new local coordinates transformation proposed in [122], it is always possible to find the function $\phi_{r+1}(x), \phi_{r+2}(x), \dots, \phi_n(x)$, thus

$$\Phi(x) = [\phi_1(x), \phi_2(x), \dots, \phi_m(x), \phi_{r+1}(x), \dots, \phi_n(x)]$$

$$x = \Phi^{-1}(\xi, \eta)$$

Then input vector u_a can be obtained by means of the output vector y and its derivatives.

$$u_a = A(\Phi^{-1}(\xi, \eta))^{-1} \left(\begin{bmatrix} \xi_1^{(r_1)} \\ \vdots \\ \xi_m^{(r_m)} \end{bmatrix} - \begin{bmatrix} L_f^{r_1} h_1(\Phi^{-1}(\xi, \eta)) \\ \vdots \\ L_f^{r_m} h_m(\Phi^{-1}(\xi, \eta)) \end{bmatrix} \right) \quad (7.19)$$

The inversion based algebraic polynomial (7.19), however, requires the computation of successive derivatives of outputs, which might be unrealistic in practical applications where measurements suffer noise and disturbances.

Step 2: estimate the derivatives of the output vectors

To avoid use any derivative information $\xi_i^j, 1 \leq i \leq m, 1 \leq j \leq r_i$ of measurement output directly, a high-gain second-order sliding mode observer is considered to exactly estimate them in a finite time.

By construction:

$$y_i = \xi_i^1$$

$$\dot{\xi}_i^j = \xi_i^{j+1}; 1 \leq j \leq r_i - 1$$

$$\xi_i^{r_i} = L_f^{r_i} h_i(\Phi^{-1}(\xi, \eta)) + \sum_{j=1}^m L_{g_j} L_f^{r_i-1} h_i(\Phi^{-1}(\xi, \eta)) u_{aj}; j = r_i$$

Following is structure of the observer:

$$\hat{y}_i = \hat{\xi}_i^1$$

$$\dot{\hat{\xi}}_i^j = \hat{\xi}_i^{j+1} + \lambda_i^j |\hat{y}_i - y_i|^{1/2} \text{sgn}(\hat{y}_i - y_i); 1 \leq j \leq r_i - 1$$

$$\dot{\hat{\xi}}_i^{r_i} = \lambda_i^{r_i} |\hat{y}_i - y_i|^{1/2} \text{sgn}(\hat{y}_i - y_i); j=r_i$$

Step 3: by using the estimates of output derivatives, a kind of algebraic unknown input reconstruction method is proposed.

$$\tilde{u}_a = A(\Phi^{-1}(\hat{\xi}, \hat{\eta}))^{-1} \left(\begin{bmatrix} \hat{\xi}_1^{(r_1)} \\ \vdots \\ \hat{\xi}_m^{(r_m)} \end{bmatrix} - \begin{bmatrix} L_f^{r_1} h_1(\Phi^{-1}(\hat{\xi}, \hat{\eta})) \\ \vdots \\ L_f^{r_m} h_m(\Phi^{-1}(\hat{\xi}, \hat{\eta})) \end{bmatrix} \right) \quad (7.20)$$

7.6.2 Local Fault Filter Design for RCA

Considering the actuator subsystem model (7.2) and fault model (7.4), by utilizing the reconstructed \tilde{u}_a , as well as analyzing the fault resources $v_i, i = 1, \dots, k$, we can recognize the root cause of the detected

fault. To achieve this purpose, through adaptive diagnostic techniques proposed in[20], m banks of k observers corresponding for all possible faulty models are constructed and extended as below:

$$1 \leq j \leq m, 1 \leq i \leq k, t \geq t_f$$

$$\begin{cases} \dot{\hat{x}}_a^{ij} = f_a^j(\hat{x}_a^{ij}, u_j) + \sum_{l \neq i} g_{al}^j(\hat{x}_a^{ij}, u_j) \theta_l^j + g_{ai}^j(\hat{x}_a^{ij}, u_j) \hat{v}_i^j + H_{ij}(\tilde{u}_a^j - \hat{u}_a^{ij}) \\ \hat{v}_i^j = 2\gamma_{ij}(\tilde{u}_a^j - \hat{u}_a^{ij})^T P_{ij} g_{ai}^j \\ \hat{u}_a^{ij} = h_a^j(\hat{x}_a^{ij}, u_j) \end{cases} \quad (7.21)$$

Where j denotes jth actuator, i is ith observer corresponding to the ith fault resource candidate v_i . $\hat{x}_a^{ij} \in \mathcal{R}^n$ is the estimated state vector of ith observer for jth actuator, \hat{v}_i^j is the fault estimation of v_i of jth actuator, and \hat{u}_a^{ij} is the estimated output vector of the ith observer for jth actuator. \tilde{u}_a^j is reconstructed output of jth actuator from y, u_j is the input of jth actuator. θ_l^j is the nominal value of parameters in jth actuator, subscript $l \neq i$. f_a^j, h_a^j, g_{ai}^j are analytic functions of jth actuator. H_{ij} is a Hurwitz matrix that can be chosen freely with a goal to increase as much as possible the dynamic of the observer, γ_{ij} is a design constant and P_{ij} is a positive definite matrix.

We can calculate the matrix P_{ij} with the help of (7.22); where Q_{ij} is a positive definite matrix that can be chosen freely.

$$H_{ij}^T P_{ij} + P_{ij} H_{ij} = -Q_{ij} \quad (7.22)$$

Denote $e_y^{ij}(t)$ as the tracking error of the ith observer for jth actuator as:

$$e_y^{ij}(t) = \tilde{u}_a^j - \hat{u}_a^{ij}$$

We define the RCA residual as:

$$s_{ij}(t) = \left\| e_y^{ij}(t) \right\|, \quad 1 \leq i \leq k, 1 \leq j \leq m \quad (7.23)$$

These residuals are designed to be “less” sensitive to a particular fault cause that comes from a specific actuator and sensitive to all the others actuator fault causes. For the jth actuator, if a fault is caused by the ith fault cause, then the ith RCA residual will leave its threshold and never comes back to zero again, but the other $(k - 1)$ residuals will stay below their thresholds. So every RCA filter is designed in such a way to identify a possible fault cause in a specific actuator.

The root cause analysis of detected faults is then achieved. The classes of faults considered are nonlinear process faults which directly affect the dynamics of actuator subsystem and include both abrupt and incipient faults. The method that is introduced is based on the observation that the internal

variable closest to the fault and reacts first to the final product when fault is occurred. That leads to an operation point shift for all the internal variables before the fault in the chain of the internal variables in the system. When these operation point changes are being detected, the faults can be detected and diagnosed. Along this article, we make the reasonable assumption that the number faults do not occur simultaneously more than the number of available measurement.

7.7 Summary

In this chapter, we investigate the problem of a fault diagnosis and root cause analysis scheme for a class of interconnected dynamic systems. The main contribution is the combination of local fault filtering capability with global system monitoring capability. It is accomplished by that output of the local subsystem that is used in root cause diagnoser is estimated by the output of global outputs and its derivatives. Also, the fault distinguishability and diagnosability conditions are rigorously investigated.

CHAPTER 8 APPLICATION OF FD AND RCA SCHEME TO HEX/REACTOR SYSTEM

This chapter confirms techniques proposed in Chapter 7 to the nonlinear model of the intensified Hex reactor system. It implements the optimal performances monitoring on internal dynamics of each components of the intensified Hex reactor system. And fault diagnosis (FD) and root cause analysis (RCA) of actuator are triggered once fault occur.

8.1 System Description

8.1.1 Introduction of Multifunctional Heat-Exchanger Reactor

Miniaturization of process equipment is one of the future development trends for chemical process and energy industry, since it significantly enhances transfer phenomenon, as shown in [189]. Process intensification is loosely described as a strategy that aims to achieve dramatic reductions in plant volume whilst maintaining production objectives in [190]. The intensified technologies offer new prospects for the development of hazardous chemical syntheses in safer conditions; the idea is to reduce the reaction volume by increasing the thermal performances and preferring the continuous mode to the batch one.

Advances in process engineering have led to numerous new findings and technologies that concentrate on minimizing the sizes of unit operations as well as improving the overall speed of production whilst maintaining the throughput of the processes. One of the routes to reach objectives of both process intensification and multifunctional devices is the use of mini multifunctional equipment. A compact device that combines reaction and heat transfer into a single equipment, i.e. using for instance a heat exchanger as a chemical reactor, the so-called multifunctional heat-exchanger/reactor, could be an appropriate example. In fact, a path way to realize process intensification is to develop multifunctional apparatuses where more than one unit operations are performed in a unique equipment. While multifunctional equipments are particularly interesting for various processes with the aim of process intensification. The multifunctional heat-exchanger/reactor design is particularly attractive for use process intensification applications as it is derived from existing well-known and proven compact heat exchanger technology and therefore presents less of a technological risk. This multifunctional system, an integration of heat exchanger with several system components, is not intended merely to heat exchange but involve other processes and functions. Thus, it may be interesting in that energy consumption might be reduced and the system performance may be raised, and reaction quality is another aspect that may benefit from integrated design.

Many benefits are expected by using the multifunctional heat-exchanger/reactor such as waste reduction, energy and raw materials savings, yield and selectivity increase, and cost reduction. For one side, unlike compact reactors, multifunctional heat-exchanger/reactor is above all heat exchangers in which reactions are carried out. It is a special heat exchanger that exchanges heat with the reactor hull.

This component can only be cooled by heat vents/exchangers that interact with adjacent heat cooling/exchanging components. As a consequence, their design is largely based on compact heat exchangers geometries. Compact heat exchangers and enhancement technologies allow reducing the heat exchanger volume, to increase its effectiveness and to reduce capital and operating costs. On the other side, unlike heat exchange processes, the implementation of chemical syntheses requires to control the residence time to complete the chemistry.

8.1.2 Characterization of Pilot HEX/reactor

The prototype of heat-exchanger/reactor discussed in this work is the open plate reactor. The open plate reactor, designed by Alfa Laval, is based on the concept of the plate heat exchanger. It is made of reaction plates, inside which reactants mix and reactions occur, and cooling plates which are inserted between the reaction plates. The general state-of-the-art has been studied by several prototypes in previous publications, such as in [193]. The main ideas are as follows: Firstly, each section is made up of a reaction plate where the reaction mixture flows, surrounded by two cooling plates containing the utility fluid. Besides, it is particularly well suited for process intensification, as it allows at the same time an increase of reactant concentration and a reduction of solvent consumption. The reduction in size also leads to increased safety with smaller amounts of hazardous chemicals being in use at each time which force the reactants to flowing changing directions. These inserts were specially designed to enhance heat transfer and micro-mixing.

A laboratory intensified heat-exchanger process is studied in this work. As illustrated in [160], the pilot is made of three process plates sandwiched between five utility plates, as shown in Fig. 8.1, which was designed and built for operation in LGC, Toulouse. The pilot has been manufactured in accordance with the results of the geometry optimization. The reactive plates as well as the utility plates have been engraved by laser machining to obtain 2 mm square cross-section channels. Both reactive and utility channels designs are presented in Fig. 1(a) and (b), after assembly the reactor has a 32 cm height, a 14 cm width, a 3.26 cm thickness, and a mass of 10.84 kg, which makes it a very compact HEX reactor, as shown in Fig.1(c). Its behavior can be assimilated to a counter-flow heat exchanger.

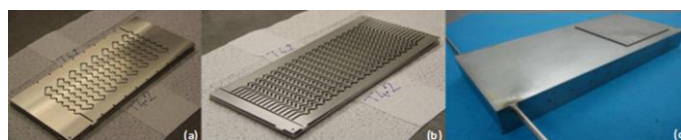


Fig. 8.1 (a) Reactive channel design; (b) utility channel design; (c) the heat exchanger/reactor after assembly.

The simulations and experiments carried out in this work are based on the size and properties of this prototype unit, however, all methods developed are generic for a reactor of any size.

8.1.3 Instrumentation Requirements

The HEX/Reactor system is a typical chemical process which consists of connected components and pipes through which utility streams and chemical reactants flow, together with controllers and

monitoring instruments. As a result that new concepts of reactor designed in compact multifunctional devices being less familiar than traditional ones, research work is necessary not only to assess their feasibility and potentialities but also to evaluate their efficiency and intrinsic characteristics.

Minimizing the physical sizes of process units whilst maintaining the same throughput inevitably means that these units will have shorter residence times than conventional sized units. In fact, adopting the process intensification design philosophy could lead to an order of magnitude change in equipment capacity, and would probably bring the response times of intensified systems down to milliseconds rather than the more usual tens of minutes encountered in conventional units. It implies that the dynamics of the systems will be much faster than those encountered in conventional scale units.

Under such circumstances, traditional instrumentation may be too slow for intensified processes to be controlled by conventional strategies. Firstly, measurement delays that may be tolerable in conventional units may be too large and unacceptable for intensified systems, making the control problem more difficult. Hence, fast responding process sensors are needed in order to achieve automatic control purpose. Secondly, as the philosophy of process intensification is to reduce equipment sizes without compromising on throughputs, actuators of the same size as those employed in conventional units will continue to be utilized. As a result, actuator dynamics could present problems, as they could be orders of magnitude slower than those of the manufacturing unit. Furthermore, interactions between process states and process units are also aspects that could lead to further difficulties.

There are therefore many factors that are needed to be considered in realizing automatic supervision and control of intensified systems. For instance, components that make up the control loop must be dynamically compatible with the controlled process for acceptable performance. This issue has been largely neglected when designing controllers for conventional process systems, since the time constants of such processes are significantly larger than those of associated actuators and instrumentation. Therefore, to realize the perceived benefits of process intensification technology, it is essential that intensified units are coupled with process monitoring and control systems that can cope with the very fast response times so that regulation of environmental variables, product quality, and operational safety can be ensured. Nonetheless, given a particular strategy, a deep appreciation of the influences of each component of an intensified system control loop is crucial so that desirable performances can be assured. Such an issue is particularly relevant as we are interested in this work.

8.2 Problem Formulation

8.2.1 Preliminary

As mentioned above, given the extremely complex dynamics and the increasing safety demands imposed to the operation requirements of current intensified industrial processes, they are still the subject of many studies. Specifically, the challenges in commercializing Hex reactors may be classified as those pertaining to material science, reaction kinetics, control and operation. A widespread implementation can be limited mainly due to intrinsic difficulties in achieving an efficient operation,

such as: (1) highly nonlinear dynamical behavior; (2) very complicated kinetics; (3) uncertain load disturbances due to fluctuations in the feeding composition; and (4) the lack of reliable estimations from on line measurements of the key process variables for monitoring and controlling. We are interested in the last consideration.

Even if the materials and kinetics related issues (1)-(3) are sorted out, there are several technological challenges relating to control and supervision that must be addressed before successful commercialization. One of the important issues in Hex reactors is the non-uniform spatial temperature distribution in the cell, which places serious limitations on its performance. The non uniformity of the temperature in the cell will lead to hot spots and thermal stresses that in turn increases the probability of failure and degradation of the cell. These issues are especially predominant during the transient operation of the Hex reactors. The thermal gradients are especially high in the case of Hex reactors with internal reforming. Thermal gradients would also be significant in Hex reactors systems intended for load following and frequent on/off applications. This thermal management problem has an important bearing on the efficiency, life and reliability of the cell. Therefore, thermal management is essential not only to prevent the damage to the cell and thereby maximize the cell life, but also to improve its efficiency and performance.

For effective thermal management, information about the temperature distributions inside the cell is required. Since this is generally not measurable, dynamic estimation is one option for obtaining this information. However, current works related to advancing process intensification technologies seem to focus mainly on proving the feasibility of concepts and ideas, as well as attempting to establish key design parameters of various process units. In [184] in the parallel to the development of the OPR, a specific computer simulation program has been written. In this program, a complex dynamic model, integrating modelling of hydrodynamic, thermal and reaction aspects, allows one to reproduce and predict the reactor behavior during normal operation. Also, work [193] has been carried out to perfect a process control system. In [195], a dynamic model of a three-phase catalytic slurry intensified continuous reactor is proposed.

For the purpose of preventing thermal run away required by safety operation, there are the limited amounts of research in the open literature related to performance monitoring and control design in chemical process. They are mainly divided into model-based [3][4] and data-based approaches [5] [198]. Model-based method uses deviations between the measured value and the reference value as an indicator to alarm faults and take action on timely fault diagnosis and correction. The process under consideration in this work has already been studied and modelled several times by the scientific communities. Most studies mainly focus on detailed mathematical models of the physics, aim at developing reliable and accurate models to predict both the thermal performance and conversion of the process, like nonlinear models derived in [191]. Other studies contribute from perspective of engineering control. In [193], a control system is developed and an extended Kalman filter is designed to estimate the unmeasured parameters. An optimization and control approach is presented in [201].

To authors' knowledge, few theoretical frameworks can be found in regards to reliable schemes for advising Hex/reactor diagnostic modelling problem. Existing results do not offer a suitable dynamic model of the typical faults which can be encountered and concerned with the application of FDD for HEX/Reactor. Moreover, little investigations have been carried out to study the supervision and control of individual process units. With the help of FD&RCA strategies proposed in Chapter 7, these two problems can be properly settled.

8.2.2 Main Contribution

In this work, the intensified heat-exchanger/reactor is introduced from a perspective of monitoring and supervising. The HEX/Reactor system can be modelled and diagnosed at several different levels of complexities, depending on the intended application of the model. For example, from the view point of concentration or fouling detector, it is often modelled from a system level; while from the view point of sensor or actuator supervision, the dynamics of control loop elements such as valves and measurement devices may no longer be negligible, then it should be modelled as a cascade system.

A deep consideration of the influences of composed components of the intensified Hex/reactor system is expected in this work. We mainly focus on the dynamics of actuator valves since it is significantly responsible for not only the process performances, but also the safety operation. Actuator faults are very common in intensified industrial systems, a faulty actuator may cause process performance degradation (e.g. lower product quality) or even fatal accidents (e.g. temperature run-away). Potential hazards of runaway scenarios are studied in work [189]. Three of them are highlighted as the most dangerous: no utility flow, no reactant flows, both stop at the same time. Clearly, all of the three cases are related with malfunction of fluid actuator. If not properly handled, they can lead to consequences ranging from failures to meet product quality specifications to plant shut downs, incurring substantial economic losses, safety hazards to facilities and personnel, and damages to the environment.

This chapter presents the results of an investigation into how the dynamics of control valves influence the performances of intensified Hex/reactor [190]. We consider therefore the intensified HEX/reactor system consists of two subsystems: control valve and Hex/reactor subsystems. As shown in Fig.8.2.

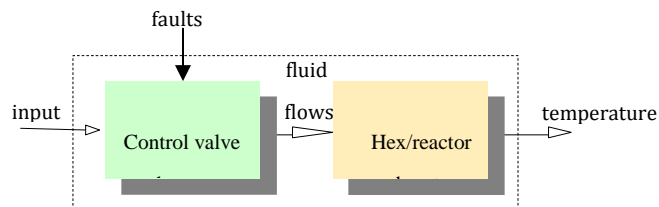


Fig. 8.2 cascade Hex reactor system structure

The work reported here investigates the effects of internal dynamics of control valve on final Hex reactor performances. One of the objectives is to monitor the performance of the hex reactor and provide estimation of the temperature distributions inside the hex reactor. Another attempt is to reconstruct utility and process fluid flow rates of both control valves from final measured temperature of utility and process fluid. If this can be achieved, then guidelines for the recognition of cause and

effect relationship between unexpected temperature behavior and faulty control valves could be extracted. Knowledge of internal faulty variables of faulty control valves can also be determined with the help of fault diagnosis and root cause analysis strategy developed in chapter 7.

The paper is structured as follows. First, suitable diagnostic modelling of both subsystems is presented in section 8.3 and 8.4. Then, detailed procedures for fault diagnosis and root cause analysis strategy are listed in section 8.5. Next in section 8.6, numerical simulations are considered to confirm the effectiveness of the proposed strategy. Finally, a conclusion is made in section 8.7.

8.3 Process Subsystem Modelling

8.3.1 Background

Model based diagnosis methods would be more efficiently and relatively applied, if a dynamic model of the system is available to evaluate the consequences of deviations and the efficiency of the proposed safety barriers. If no reactions take place, from the view point of heat exchange, HEX/Reactors can be seen as heat exchangers, so a dynamic model can be derived from first principles, with equations for heat transfer, mass, and energy balances. Development of dynamic models for HEX and continuous reactor has received considerable attention. They are two general approaches: lumped model and distributed model. The former one, also called cell-based model in the literature, is very often used, by which each cell is modelled by means of the energy and mass balances. This cell-based procedure has been used by different authors, such as [203][204][205].

Among these models, a series of assumptions have been considered to describe the heat transfer phenomena. Under normal operations the heat transfer coefficient will either be constant or slowly decreasing. Many authors working in the field of process control and controllability prefer the constant parameter because of the computational simplicity, and a simplified dynamic model containing only one cell is often the case on application of fault detection and isolation. Like sensor and/or actuator fault detection and isolation methods proposed in [208][209]. It is widely accepted that fouling influence the dynamics of overall heat transfer coefficient, thus constant value leads to some mismatch between the model and physical process, and this mismatch is usually handled as unstructured model uncertainties. Adaptive estimation techniques are used to explicitly account for this modeling uncertainty. In order to better minimize the mismatch, fouling influence was developed by considering heat transfer coefficient is slowly decreasing. To compute fouling, online updating rules based on observers are widely investigated, like extended Kalman filter (EKF) in [212], adaptive-high gain observer in [213] and recursive least-squares method in [17]. Another popular method is to calculate the parameter offline, as proposed in [208]. Several fault diagnosis (FD) approaches have been proposed with parameter regularly updated, to this purpose, H_∞ approach in [214], adaptive observer in [215], polynomial fuzzy observer in [217], EKF in [218] are mostly used.

These assumptions work well during normal conditions. However, effect of decreasing in overall heat transfer coefficient should be limited into a normal range with respect to specific engineering process. If the system difference greatly exceeds this normal range, a fault is considered. For instance, on

occasion that valve clogging causes sudden stop of mass flow rate or higher fouling results in insulating the heat transfer surface due to big pieces of settled material, both situations will cause damage and are considered as most dangerous situation in [189]. When these happen, positive jumps will emerge in the heat transfer coefficient whose effect may definitely exceed the normal rang. Few works formulate a model capable of identifying these two faults simultaneously.

8.3.2 Cell-based Intensified HEX/Reactor model

The primary objective of this work is to propose a dynamic model suitable for diagnostic requirements on the studied HEX/Reactor, and this model is capable of guaranteeing the model validity by accounting the influence of the mass flow rate and fouling on overall heat transfer coefficient. One of the key issues in modelling for fault detection and isolation is how to accommodate the level of detail of the model description to suit the diagnostic requirements. From view point of heat exchange performance, behavior of intensified HEX/reactor can be assimilated to a compact heat exchanger to derive a dynamic model. We follow the work of [204] to derive the cell-based dynamic model. The heat exchanger is modeled as N ideally mixed interconnected tanks in cell-based models, as shown in Fig. 8.3.

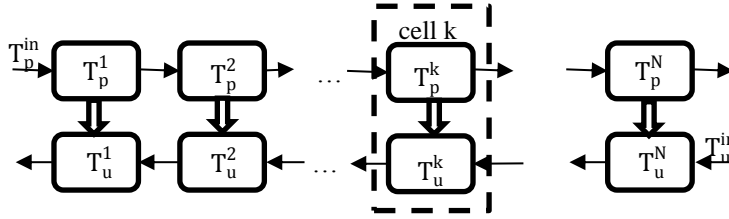


Fig.8.3 N cell models

8.3.3 Mathematical model

The modelling of a cell is based on the mass and energy balances which describe the evolution of the characteristic values: temperature, mass, composition, etc. Several assumptions should be fulfilled, more details are given in [32]. It is assumed that the liquid volume in each tank is constant. Each cell is perfectly homogenous, and that no back mixing occurred. Both fluids are liquid with constant densities, heat transfer to the surrounding is negligible, and there is no energy accumulation in the wall.

A cell based parameter model depicted in (8.1) is used to capture the thermal distribution in the cell. More detail about the modelling problem and determination of the number of cell are illustrated in Appendix 8.1 A. The model is capable of accurately describing the dynamics of the heat exchanger for a wide range of working conditions.

$$k = 1 \left\{ \begin{array}{l} \dot{T}_p^k = \frac{1}{\rho_p c_{pp}} \alpha \gamma (T_u^k - T_p^k) + \frac{1}{V_p} (T_p^{\text{in}} - T_p^k) F_p \\ \dot{T}_u^k = \frac{1}{\rho_u c_{pu}} \beta \gamma (T_p^k - T_u^k) + \frac{1}{V_u} (T_u^{k+1} - T_u^k) F_u \end{array} \right. \quad (8.1a)$$

$$1 < k < 3 \begin{cases} \dot{T}_p^k = \frac{1}{\rho_p c_{pp}} \alpha \gamma (T_u^k - T_p^k) + \frac{1}{V_p} (T_p^{k-1} - T_p^k) F_p \\ \dot{T}_u^k = \frac{1}{\rho_u c_{pu}} \beta \gamma (T_p^k - T_u^k) + \frac{1}{V_u} (T_u^{k+1} - T_u^k) F_u \end{cases} \quad (8.1b)$$

$$k = 3 \begin{cases} \dot{T}_p^k = \frac{1}{\rho_p c_{pp}} \alpha \gamma (T_u^k - T_p^k) + \frac{1}{V_p} (T_p^{k-1} - T_p^k) F_p \\ \dot{T}_u^k = \frac{1}{\rho_u c_{pu}} \beta \gamma (T_p^k - T_u^k) + \frac{1}{V_u} (T_u^{\text{in}} - T_u^k) F_u \end{cases} \quad (8.1c)$$

The cell model is constructed using 3 lumps for which the mass and the thermal balances are written. Increasing the number of cells may result in more accurate prediction of the temperature distribution, but more cells enhance computation burden also. Meanwhile, simulation results show that the dynamics do not differ much from 3 cells. An improvement in the model used in this work is that the overall heat transfer coefficient is considered as a function of both fluid flow rates and fouling. This makes the observer design more complicated but will improve the accuracy of the model.

8.3.3 Cell based diagnostic dynamic model

Define state vector as $x = [x_1, x_2, x_3, x_4, x_5, x_6]^T = [T_p^1, T_u^1, T_p^2, T_u^2, T_p^3, T_u^3]^T$, the input vector is $u = [u_1, u_2]^T = [F_p, F_u]^T$, related parameters $\theta = [\alpha, \beta]$, and finally $y = [y_1, y_2]^T = [T_p^3, T_u^1]^T$ is the vector of the outlet temperature. Using these notations, the model can be rewritten in a space-state representations.

$$\begin{cases} \dot{x} = f(x, \theta) + g(x)u \\ y = Cx \end{cases} \quad (8.2)$$

$$\text{Where } f(x, \theta) = \begin{pmatrix} f_1(x, \theta) \\ f_2(x, \theta) \\ \vdots \\ f_6(x, \theta) \end{pmatrix} = \begin{pmatrix} \frac{1}{\rho_p c_{pp}} \alpha \gamma (x_2 - x_1) \\ \frac{1}{\rho_u c_{pu}} \beta \gamma (x_1 - x_2) \\ \frac{1}{\rho_p c_{pp}} \alpha \gamma (x_4 - x_3) \\ \frac{1}{\rho_u c_{pu}} \beta \gamma (x_3 - x_4) \\ \frac{1}{\rho_p c_{pp}} \alpha \gamma (x_6 - x_5) \\ \frac{1}{\rho_u c_{pu}} \beta \gamma (x_5 - x_6) \end{pmatrix}, \quad g(x) = (g_1(x), g_2(x)) = \begin{pmatrix} \frac{(T_p^{\text{in}} - x_1)}{V_p} & 0 \\ 0 & \frac{(x_4 - x_2)}{V_u} \\ \frac{(x_1 - x_3)}{V_p} & 0 \\ 0 & \frac{(x_6 - x_4)}{V_u} \\ \frac{(x_3 - x_5)}{V_p} & 0 \\ 0 & \frac{(T_u^{\text{in}} - x_6)}{V_u} \end{pmatrix},$$

and the output matrix C is given by $C = [0, 1, 0, 0, 1, 0]$

8.4 Actuator Subsystem Modelling

8.4.1 Background

Many of today's nonlinear control methods assume the control input to enter the system dynamics linearly, this does not hold in intensified processes, since the composed units may have response times orders of magnitude faster than conventional units. Thus, the dynamics of control valves may no longer be negligible and a suitable diagnostic model is expected.

The modeling of an actuator and possible faults is based on understanding the physical process. The actuator encompasses pneumatic valve in this work. The important aspect of these approaches is the development of a model that describes the cause and effect relationships between the system variables using state estimation or parameter estimation techniques. Up to now, modelling of pneumatic actuators has benefited to researches in automation, like in [1]. Reference [3] provides an overview of various models of the fault mode of control valve. In [220], it introduced the first pneumatic actuator and the spool valve model as part of a complete pneumatic servo system model. The models that were derived have been verified with measurements and the modelling error is found to be acceptable for the fault simulations. Some typical control valve faults have been simulated and impacts on the internal variables of the flow control loop and control performance analyzed in [48]. The fault simulator presented in [45] can be used for fault detection and diagnosis, as well as robust control research.

8.4.2 Mathematical Model

In this work, we need actuators to control flowrate of both process fluid and utility fluid. Pneumatic control valve is employed to act as actuator in this system. The main function of this pneumatic valve is to regulate the flow rate in a pipe line.

By application of Bernoulli's continuous flow law of incompressible fluids, we have:

$$F = C_v f(X) \sqrt{\frac{\Delta P}{sg}}$$

where F is flow rate (m^3s^{-1}), ΔP is the fluid pressure drop across the valve (Pa), sg is specific gravity of fluid and equals 1 for pure water, X is the valve opening or valve "lift" ($X=1$ for max flow), C_v is valve coefficient (given by manufacturer), $f(X)$ is flow characteristic which is defined as the relationship between valve capacity and fluid travel through the valve. There are three flow characteristics to choose from: linear valve control; quick opening valve control; equal percentage valve control. For linear valve, $f(X) = X$, the valve opening is related to stem displacement. In [1],[3], a pneumatic control valve has a dynamic model of the type:

$$p_c A_a = m \frac{d^2 X}{dt} + \mu \frac{dX}{dt} + kX$$

where A_a is the diaphragm area on which the pneumatic pressure acts, p_c is the pneumatic pressure, m is the mass of the control valve stem, μ is the friction of the valve stem, k is the spring compliance, and X is the stem displacement or percentage opening of the valve.

In order to evaluate the proposed strategy, the dynamic model should have the affine form. Define subscript 1 to denote the actuator of process fluid, then parameters $X_1, p_{c1}, \Delta P_1, k_1, \mu_1, F_1$ represent the opening percentage of the valve, the pneumatic pressure, and the fluid pressure drop across the valve, the spring compliance process fluid, the friction of the valve stem and flowrate of the process fluid. And denote subscript 2 for the utility fluid, then one gets parameters $X_2, p_{c2}, \Delta P_2, k_2, \mu_2, F_2$ which represent

the same physical meaning for actuator of utility fluid. Since the control valves utilized in this work are linear, so $f(X_1) = X_1, f(X_2) = X_2$. So the vector state x_a , input u , and output u_a are defined as:

$$x_a^T = [x_{a1} \quad x_{a2} \quad x_{a3} \quad x_{a4}] = \left[X_1 \quad \frac{dX_1}{dt} \quad X_2 \quad \frac{dX_2}{dt} \right], \quad u^T = [u_1 \quad u_2] = [p_{c1} \quad p_{c2}], \quad u_a^T = [F_1 \quad F_2] = \left[C_v \sqrt{\frac{\Delta P_1}{sg}} X_1 \quad C_v \sqrt{\frac{\Delta P_2}{sg}} X_2 \right], \quad C = [c_1 \quad c_2 \quad c_3 \quad c_4] = \left[C_v \sqrt{\frac{\Delta P_1}{sg}} \quad 0 \quad C_v \sqrt{\frac{\Delta P_2}{sg}} \quad 0 \right].$$

the actuator subsystem is then described by four states, two inputs and two outputs, as:

$$\begin{cases} \dot{x}_a = \begin{bmatrix} 0 & 1 & 0 & 0 \\ -\frac{k_1}{m} & -\frac{\mu_1}{m} & 0 & 0 \\ 0 & 0 & 0 & 1 \\ 0 & 0 & -\frac{k_2}{m} & -\frac{\mu_2}{m} \end{bmatrix} x_a + \begin{bmatrix} \frac{A_a}{m} & 0 \\ 0 & 0 \\ 0 & \frac{A_a}{m} \\ 0 & 0 \end{bmatrix} u \\ u_a = \begin{bmatrix} C_v \sqrt{\frac{\Delta P_1}{sg}} & 0 & C_v \sqrt{\frac{\Delta P_2}{sg}} & 0 \end{bmatrix} x_a \end{cases} \quad (8.3)$$

8.4.3 Fault Analysis and Modelling

Fault analysis aims at identifying the sources of abnormal behavioral of fluid flow rates and the most significant malfunction of the internal variables that are causing the unexpected change in the control valve. This chapter provides an overview of various fault models in actuators of the studied system. The modeling of these faults is based on the understanding of the physical process. Totally, there are 19 kinds of faults that may occur as shown in [1], the causes of each fault are given in [45].

Four kinds of fault influencing dynamics of the valve are considered in this work:

- 1-) fault f1: valve clogging, occurs when the servomotor stem is blocked by an external event of a mechanical nature. It results in limitation of the piston movement in both direction, and therefore the flow cannot drop below a certain value.
- 2-) fault f2: change of pressure drop across valve, results in $\Delta P + \Delta P'$.
- 3-) fault f3: bellow-seal leakage due to leak, resulting in $p_c A_a + P$ changed; Valve internal leakage is a common malfunction with industrial control valves. The causes of such leakage are numerous, including damaged plug or seat, insufficient seat load or reduced spring rate.
- 4-) fault f4: control valve diaphragm perforation due to pinhole cracks in the periphery, resulting in k changed.

As above description shown, actuator fault may be caused by parameters $\mu, k, u, \Delta p$, then there are eight related parameters in two actuators: $[k_1 \quad \mu_1 \quad k_2 \quad \mu_2 \quad p_{c1} \quad p_{c2} \quad \Delta P_1 \quad \Delta P_2]$. The process of RCA is to identify abnormal variations of these eight parameters.

For the sake of RCA purpose, we should rewrite the above dynamic model into fault model as in failure affine format. Therefore, we extend the state, input and output vector as follows:

$$x_a^T = [x_{a1} \ x_{a2} \ x_{a3} \ x_{a4} \ x_{a5} \ x_{a6}] = \left[X_1 \ \frac{dx_1}{dt} \ X_2 \ \frac{dx_2}{dt} \ C_v \sqrt{\frac{\Delta P_1}{sg}} X_1 \ C_v \sqrt{\frac{\Delta P_2}{sg}} X_2 \right]$$

$$V = [v_1 \ v_2 \ v_3 \ v_4 \ v_5 \ v_6 \ v_7 \ v_8]^T = [k_1 \ \mu_1 \ k_2 \ \mu_2 \ p_{c1} \ p_{c2} \ \Delta P_1 \ \Delta P_2]^T$$

$$u_a^T = [u_{a1} \ u_{a2}] = [F_1 \ F_2] = [x_{a5} \ x_{a6}] = \left[C_v \sqrt{\frac{\Delta P_1}{sg}} X_1 \ C_v \sqrt{\frac{\Delta P_2}{sg}} X_2 \right]$$

$$\tilde{C} = [0 \ 0 \ 0 \ 0 \ 1 \ 1]$$

Then, the actuator subsystem is with six states, eight unknown inputs and two outputs. These two outputs are unmeasured which need to be constructed by the global measured outputs. The augmented actuator subsystem is:

$$\begin{cases} \dot{x}_a = f_a(x_a) + \sum_i^8 g_{ai}(x_a)v_i \\ u_a = \tilde{C}x_a \end{cases} \quad (8.4)$$

$$\text{Where } f_a(x_a) = \begin{bmatrix} 0 & 1 & 0 & 0 & 0 & 0 \\ 0 & 0 & 0 & 0 & 0 & 0 \\ 0 & 0 & 0 & 1 & 0 & 0 \\ 0 & 0 & 0 & 0 & 0 & 0 \\ 0 & 0 & 0 & 0 & 0 & 0 \\ 0 & 0 & 0 & 0 & 0 & 0 \end{bmatrix},$$

$$g_a(x_a) = \begin{bmatrix} 0 & 0 & 0 & 0 & 0 & 0 & 0 & 0 \\ -\frac{x_{a1}}{m} & -\frac{x_{a2}}{m} & 0 & 0 & \frac{A_a}{m} & 0 & 0 & 0 \\ 0 & 0 & 0 & 0 & 0 & 0 & 0 & 0 \\ 0 & 0 & -\frac{x_{a3}}{m} & -\frac{x_{a4}}{m} & 0 & \frac{A_a}{m} & 0 & 0 \\ 0 & 0 & 0 & 0 & 0 & 0 & C_v \frac{1}{sg} x_{a1} & 0 \\ 0 & 0 & 0 & 0 & 0 & 0 & 0 & C_v \frac{1}{sg} x_{a2} \end{bmatrix}$$

From (8.4), there are two outputs. According to invertibility condition developed in chapter 7, in order to guarantee invertibility of (8.4), there should be two inputs maximum. However, more than two parameters are in (8.4), therefore, we can only recognize two possible parameters faults simultaneously. According to [1], for most parts, single actuator faults are observed in industrial practice whilst multiple faults rarely occur. This characteristic is suited to the situation considered by the scheme proposed in this paper.

8.5 Fault Diagnosis & Root Cause Analysis Architecture

8.5.1 Structure of the FD&RCA Method

This work deals with the problem of FD&RCA for a Hex reactor systems. A major contribution is the development of a framework in which faulty variables affecting actuators can be recognized from the influenced final temperature. As shown in Fig. 8.4, the objective of this work is to identify V once fault occurs.

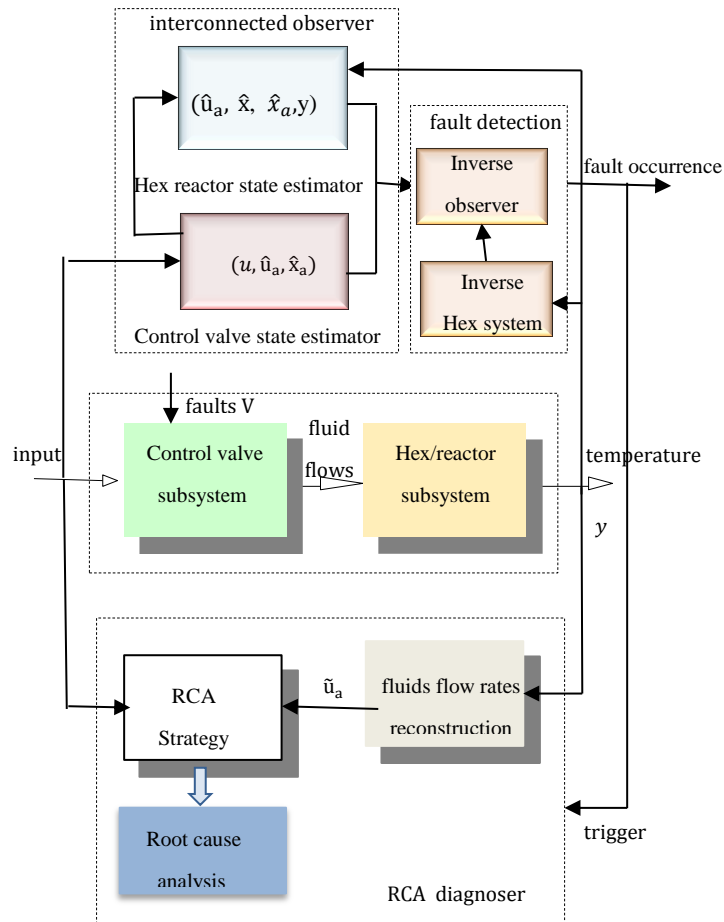


Fig. 8.4 architecture of the proposed FD&RCA approaches

As shown in Fig.8.4, the primary objective of this work is to propose an interconnected observer for performance monitoring requirements on the studied HEX/Reactor with two aims. The first one is to act as a software sensor to provide an adequate estimation of temperature distribution in the Hex reactor, as well as the unmeasured fluid flow rates of the control valves. Besides, the second purpose is to generate robust residuals for recognizing faulty control valves when faults occur by accounting the influence of the mass flow rates on temperature of both fluids.

Moreover, a major contribution of this work lies on that we propose an integrated RCA approach that aims at detecting, isolating and identifying internal faulty variables of the control valves that affected the fluid flow rates of both control valves. Once a fault occurs, it is detected immediately and then the RCA procedure is triggered. We first reconstruct the unmeasured fluid flow rates, and this reconstruction strategy is based on both system inversion and sliding mode observer. In order to achieve RCA of actuator faults, reconstructed fluid flow rates are tackled with several banks of local filters to generate several banks of residuals, each bank of residuals aim at identifying fault in one particular internal variables of control valve via adaptive updating rules. Physical meanings related to these variables are leakage, stiction, unexpected pressure drop, etc.

8.5.2 Observer Design for Performance Supervision

This section addresses the problem of accurately estimating the temperature distribution of the Hex reactor cell, as well as the fluid flow rates using only the outlet temperature measurements. A bank of residuals is generated, aims at identifying existences of control valve faults.

1-) System augmentation

For simplicity, we consider one cell model. Define the state vector as $x^T = [x_1, x_2]^T = [T_p, T_u]^T$, the control input $u_a^T = [u_{a1}, u_{a2}]^T = [F_p, F_u]^T$, the output vector of measurable variables $y^T = [y_1, y_2]^T = [T_p, T_u]^T$, then above two the equations can be rewritten in the following state-space form:

$$\begin{cases} \dot{x} = f(x) + \sum_{i=1}^2 g_i(x)u_a \\ y = h(x, u_a) \end{cases} \quad (8.5)$$

$$\text{where } f(x) = \begin{pmatrix} f_1(x) \\ f_2(x) \end{pmatrix} = \begin{pmatrix} \frac{h_p A}{\rho_p C_{p_p} V_p} (T_p - T_u) \\ \frac{h_u A}{\rho_u C_{p_u} V_u} (T_u - T_p) \end{pmatrix}, \quad \text{and } g(x) = (g_1, g_2) = \begin{pmatrix} \frac{(T_{pi} - T_p)}{V_p} & 0 \\ 0 & \frac{(T_{ui} - T_u)}{V_u} \end{pmatrix},$$

$y_1 = x_1, y_2 = x_2$, T_{pi}, T_{ui} are the outputs of the previous cell, for the first cell, they are the inlet temperature of process fluid and utility fluid, besides, they are measured and are constant. It is worth noting that the exclusive consideration of such measurements is the usual case in an industrial environment.

By using techniques introduced in chapter 5, we can obtain a function for the derivatives for u_a :

$$\begin{aligned} \dot{u}_a = \varepsilon(u, \dot{u}, x_a) &= \frac{\partial h_a}{\partial u}(u, x_a)\dot{u} + \frac{\partial h_a}{\partial x_a}(u, x_a)f_a(u, x_a) \\ &= \begin{pmatrix} C_v \sqrt{\frac{\Delta P_1}{sg}} & 0 & C_v \sqrt{\frac{\Delta P_2}{sg}} & 0 \end{pmatrix} x_a + \begin{pmatrix} \frac{A_a}{m} C_v \sqrt{\frac{\Delta P_1}{sg}} & \frac{A_a}{m} C_v \sqrt{\frac{\Delta P_2}{sg}} \end{pmatrix} u \end{aligned} \quad (8.6)$$

Define the state vector as $x_1^T = [x_{11}, x_{12}]^T = [T_p, T_u]^T$, unmeasured state $x_2^T = [x_{21}, x_{22}]^T = [u_{a1}, u_{a2}]^T = [F_p, F_u]^T$, the output vector of measurable variables $y^T = [y_1, y_2]^T = [T_p, T_u]^T$, then the equation (8.5) and (8.6) can be rewritten in the following state-space form:

$$\begin{cases} \dot{x}_1 = G_1(x_1)x_2 + g_1(x_1, u) \\ \dot{x}_2 = \varepsilon(u, \dot{u}, x_a) \\ y = x_1 \end{cases} \quad (8.7)$$

$$\text{Where, } G_1(x_1) = \begin{pmatrix} \frac{(T_{pi} - x_{11})}{V_p} & 0 \\ 0 & \frac{(T_{ui} - x_{12})}{V_u} \end{pmatrix}, \quad \text{and } f_1(x) = \begin{pmatrix} \frac{h_p A}{\rho_p C_{p_p} V_p} (x_{11} - x_{12}) \\ \frac{h_u A}{\rho_u C_{p_u} V_u} (x_{12} - x_{11}) \end{pmatrix}.$$

In this case, the full state of the studied system is given as:

$$\begin{cases} \dot{x} = G(x_1)x + F(x_1, u) + \bar{\varepsilon}(t) \\ y = Cx \end{cases} \quad (8.8)$$

Where $x = \begin{bmatrix} x_1 \\ x_2 \end{bmatrix}$, $G(x_1) = \begin{pmatrix} 0 & G_1(x_1) \\ 0 & 0 \end{pmatrix}$, $F(x_1, u) = \begin{pmatrix} f_1(x, u) \\ 0 \end{pmatrix}$, $C = (I \ 0)$, $\bar{\varepsilon}(t) = \begin{pmatrix} 0 \\ \varepsilon(t) \end{pmatrix}$

2-) Observer 1 designed for actuator subsystem

With the help of the method proposed in chapter 5, we first design an observer for the control valve subsystem. Outputs of the fluid flow rates are considered as unmeasured, and are substituted by the estimations proposed in observer 2. Then, an extended high gain observer for system (8.4) is given by:

$$\left\{ \begin{array}{l} \dot{\hat{x}}_a = \begin{bmatrix} 0 & 1 & 0 & 0 & 0 & 0 \\ 0 & 0 & 0 & 0 & 0 & 0 \\ 0 & 0 & 0 & 1 & 0 & 0 \\ 0 & 0 & 0 & 0 & 0 & 0 \\ 0 & 0 & 0 & 0 & 0 & 0 \\ 0 & 0 & 0 & 0 & 0 & 0 \end{bmatrix} \hat{x}_a + \begin{bmatrix} 0 & 0 & 0 & 0 & 0 & 0 & 0 & 0 \\ -\frac{x_{a1}}{m} & -\frac{x_{a2}}{m} & 0 & 0 & \frac{A_a}{m} & 0 & 0 & 0 \\ 0 & 0 & 0 & 0 & 0 & 0 & 0 & 0 \\ 0 & 0 & -\frac{x_{a3}}{m} & -\frac{x_{a4}}{m} & 0 & \frac{A_a}{m} & 0 & 0 \\ 0 & 0 & 0 & 0 & 0 & 0 & C_v \frac{1}{sg} x_{a1} & 0 \\ 0 & 0 & 0 & 0 & 0 & 0 & 0 & C_v \frac{1}{sg} x_{a2} \end{bmatrix} u - \begin{bmatrix} k_1 \\ k_2 \\ k_3 \\ k_4 \\ k_5 \\ k_6 \\ k_7 \\ k_8 \end{bmatrix} [\tilde{C}\hat{x}_a - \hat{x}_2] \\ \hat{u}_a = \tilde{C}\hat{x}_a \end{array} \right. \quad (8.9)$$

Where $k_{i(i=1,\dots,8)}$ are the gain of the observer.

3-) Observer 2 for process subsystem

We now consider an observer for the Hex reactor subsystem. The original system (8.7) has been augmented with the differential equation $\dot{u}_a = \varepsilon(u, \dot{u}, x_a)$, that is to say the unknown inputs are treated like an unmeasured state. Then, it is possible to design a high gain observer for the system by (8.7) as follows:

$$\left\{ \begin{array}{l} \dot{\hat{x}}_1 = \begin{pmatrix} \frac{(T_{pi} - \hat{x}_{11})}{V_p} & 0 \\ 0 & \frac{(T_{ui} - \hat{x}_{12})}{V_u} \end{pmatrix} \hat{x}_2 + \begin{pmatrix} \frac{h_p A}{\rho_p C_{p_p} V_p} (\hat{x}_{11} - \hat{x}_{12}) \\ \frac{h_u A}{\rho_u C_{p_u} V_u} (\hat{x}_{12} - \hat{x}_{11}) \end{pmatrix} - \begin{pmatrix} 2\theta \\ 2\theta \end{pmatrix} (\hat{y} - y) \\ \dot{\hat{x}}_2 = \begin{pmatrix} C_v \sqrt{\frac{\Delta P_1}{sg}} & 0 & C_v \sqrt{\frac{\Delta P_2}{sg}} & 0 \end{pmatrix} \hat{x}_a + \begin{pmatrix} \frac{A_a}{m} C_v \sqrt{\frac{\Delta P_1}{sg}} & \frac{A_a}{m} C_v \sqrt{\frac{\Delta P_2}{sg}} \end{pmatrix} u - \begin{pmatrix} \theta^2 \frac{h_p A}{\rho_p C_{p_p} V_p} (\hat{x}_{11} - \hat{x}_{12}) \\ \theta^2 \frac{h_u A}{\rho_u C_{p_u} V_u} (\hat{x}_{12} - \hat{x}_{11}) \end{pmatrix} (\hat{y} - y) \\ \hat{y} = \hat{x}_1 \end{array} \right. \quad (8.10)$$

It should be remarked that although F_p , F_u undergo different initial trajectories in each observer; they will converge to their “true values” as time tends to infinity.

4-) Fault detection residual generation

Define:

$$e_i(t) = \hat{y}_i - y_i$$

Let $r_i(t)$ as residual for fault detection as:

$$r_i(t) = d\|\hat{y}_i - y_i\|/dt = d\|e_i(t)\|/dt \quad (8.11)$$

Then, we get :

$$Y_i: \begin{cases} < \varepsilon; \text{ fault free} \\ \geq \varepsilon; \text{ exist fault} \end{cases} \quad (8.12)$$

where ε is a prespecified threshold.

Therefore (8.9), together with (8.10), constitutes the interconnected observer that could monitor the performance of the hex reactor system, as well as provide faulty information by (8.11) and (8.12) once fault occurs.

8.5 Local Filter Design for Root Cause Analysis of Control Valve Fault

8.5.1 Input Estimator

In order to achieve adequate and robust input reconstruction, according to the procedure proposed in chapter 6, there are four steps to follow.

Step 1: Invertibility Checking:

1-) differential all two outputs:

$$\begin{cases} \dot{y}_1 = a(y_2 - y_1) + \frac{u_{a1}}{V_p}(T_{pi} - y_1) \\ \dot{y}_2 = b(y_1 - y_2) + \frac{u_{a2}}{V_u}(T_{ui} - y_2) \end{cases}$$

2-) find all independent possible relations between outputs and inputs, states and possibly their derivatives

There exists no any differential equation that output is independent of x and u_a , therefore, both outputs are differential dependent, $r=0$

3-) there are 2 outputs, therefore:

$$\rho = p - r = 2$$

Output differential rank is equal to the total number of inputs, then the system is invertible.

Step 2: Represents the input of the process subsystem as a function of the output and its derivatives:

Thanks to the invertibility of the system, we can reconstruct the inputs as a function of the output and its derivatives. From the above equation, an expression for the two inputs can be derived as $\tilde{u}_a = [\tilde{u}_{a1} \quad \tilde{u}_{a2}]$:

$$\begin{cases} \tilde{u}_{a1} = \frac{V_p}{T_{pi-y_1}}(\dot{y}_1 - ay_2 + ay_1) \\ \tilde{u}_{a2} = \frac{V_u}{T_{ui-y_2}}(\dot{y}_2 - by_1 + by_2) \end{cases} \quad (8.13)$$

Step 3: estimating of output derivatives by sliding mode observer

In order to avoid compute the derivatives, a high-gain second-order sliding mode observer is considered to exactly estimate them in a finite time.

By construction:

$$y_1 = T_p = \xi_1^1$$

$$y_2 = T_u = \xi_2^1$$

$$\xi_i^j = \xi_i^{j+1}; 1 \leq j \leq r_i - 1$$

$$\xi_i^{r_i} = L_f^{r_i} h_i(\Phi^{-1}(\xi, \eta)) + \sum_{j=1}^{r_i} L_{g_i} L_f^{r_i-1} h_i(\Phi^{-1}(\xi, \eta)) u_{aj}; j = r_i$$

Following is structure of the observer:

$$\hat{y}_i = \xi_i^1$$

$$\dot{\xi}_i^j = \xi_i^{j+1} + \lambda_i^j |\hat{y}_i - y_i|^{1/2} \text{sgn}(\hat{y}_i - y_i); 1 \leq j \leq r_i - 1$$

$$\dot{\xi}_i^{r_i} = \lambda_i^{r_i} |\hat{y}_i - y_i|^{1/2} \text{sgn}(\hat{y}_i - y_i); j=r_i$$

Step 4: by substituting successive derivatives in (8.13) with their estimation made by the above sliding observer, a kind of algebraic unknown input reconstruction method is proposed.

$$\begin{cases} \hat{u}_{a1} = \frac{V_p}{T_{pi-y_1}}(\hat{\xi}_1^{j+1} - ay_2 + ay_1) \\ \hat{u}_{a2} = \frac{V_u}{T_{ui-y_2}}(\hat{\xi}_2^{j+1} - by_1 + by_2) \end{cases} \quad (8.14)$$

8.5.2 RCA filter design

As mentioned before, faults influence $\mu, k, \Delta P, P_c$ related to four possible faults resources f1, f2, f3, and f4. Now, let us construct two banks of four observers for recognizing those four possible faults in each control valve.

$$1 \leq j \leq 2, 1 \leq i \leq 4$$

$$\begin{cases} \hat{x}_{a_i}^j = f_a(\hat{x}_a) + \sum_{l \neq i} g_{a_l}(\hat{x}_a) \theta_l^i + g_{a_i}(\hat{x}_a) \hat{v}_i^j + H_i(\hat{u}_a^j - \hat{u}_{a_i}^j) \\ \hat{v}_i^j = 2\gamma(\hat{u}_a^j - \hat{u}_{a_i}^j)^T P_i g_{a_i}(\hat{x}_a) \\ \hat{u}_{a_i}^j = \tilde{C} \hat{x}_{a_i}^j \end{cases} \quad (8.15)$$

where $\hat{x}_{a_i}^j$ is the estimated state vector, \hat{v}_i^j is the estimation of root causes and $\hat{u}_{a_i}^j$ is the estimated output.

Denote $e_y^{ij}(t)$ as the tracking error of the i th filter for j th actuator that:

$$e_y^{ij}(t) = \tilde{u}_a^j - \hat{u}_a^j$$

We define the root cause analysis (RCA) residuals as:

$$s_{ij}(t) = \left\| e_y^{ij}(t) \right\|, \quad 1 \leq j \leq 2, 1 \leq i \leq 4 \quad (8.16)$$

The above RCA observers aim at generating two banks of four residuals for those above mentioned fault causes. One bank of residuals are $s_{11}, s_{12}, s_{13}, s_{14}$, aimed at identifying fault causes f_1, f_2, f_3 , and f_4 in actuator of process fluid, the other bank are $s_{21}, s_{22}, s_{23}, s_{24}$, aimed at identifying fault causes f_1, f_2, f_3 , and f_4 in actuator of utility fluid respectively. These residuals are constructed under rules (8.16), if any of these residuals exceeds its threshold, the fault is caused by the corresponding fault causes.

8.6 Numerical Simulation Results

The simulation results validate the proposed strategy. We first give the operating conditions of the simulation. The input of the inlet flow rate of the utility fluid F_u is $4.22e^{-5}m^3s^{-1}$, and inlet flow rate of the process fluid F_p is $4.17e^{-6}m^3s^{-1}$. Initial condition for observers supposed to be 0. Parameters in actuator subsystem are: $m = 2kg$, $A_a = 0.029m^2$, $\mu = 1500Nsm^{-1}$ and $k = 6089 Nm^{-1}$, P_c for utility fluid is $1MP_a$, $1.2Mpa$ for process fluid, pressure drop ΔP in utility fluid is $0.6MP_a$ and $60KP_a$ in process fluid.

As above mentioned, for most part in practical situation, single fault is observed while multiple faults rarely occur on each actuator. So we consider each actuator is subject to only one fault, then two faults may occur simultaneously in the actuator subsystem. Two cases are considered to illustrate: noise free and noise corrupted.

1-) Noise free case, fault f_3 exists in actuator of process fluid and fault f_4 exists in actuator of utility fluid

In this part, two faults are considered. For actuator of process fluid, fault f_3 is supposed to occur at 80s due to unexpected pressure drop across the valve, and for actuator of utility fluid, fault f_4 is supposed to occur at 60s. We supposed that an expected $50KP_a$ pressure drop adds to the nominal pressure drop across the valve at time 80s. While because of erosion, the gland packing of the valve may loosen, which leads to stem vibration, a failure value of $1000 Nm^{-1}$ is added to the spring compliance k . Simulation results are listed in Fig.8.5-Fig.8.8.

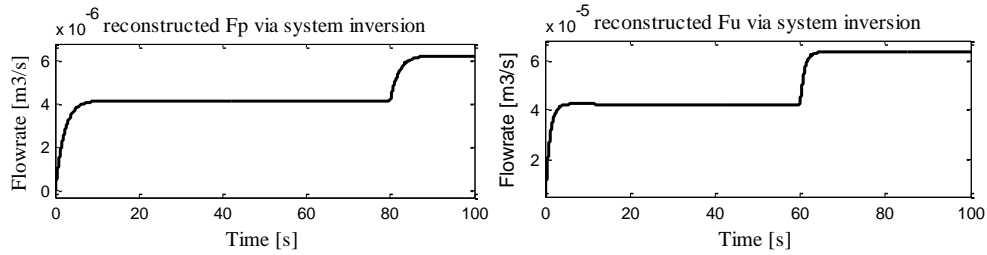


Fig.8.5 Reconstructed input \tilde{F}_u, \tilde{F}_p from output T_p, T_u in CASE (a)

From Fig.8.5, after a short transient time, reconstructed inputs $\tilde{u}_{a1} = \tilde{F}_p, \tilde{u}_{a2} = \tilde{F}_u$ give an accurate estimation value to the real inputs $u_{a1} = F_p, u_{a2} = F_u$. At 80s, the reconstructed \tilde{F}_p unexpectedly increases, and finally it stabilizes at a new level. This increase implies fault occurs and no further variations illustrate no additional fault occurs. The similar result is obtained in the reconstructed \tilde{F}_u of utility fluid. The simulation curve indicates that the input reconstruction proposed in this paper is proper for recovering unknown inputs.

As shown in Fig.8.6, at 80s and 60s, the detection residuals (r_1, r_2) break through their thresholds respectively. It implies that at time 80s, a fault occurs at actuator of process fluid, it takes 0.1s to detect the fault. While for actuator of utility fluid, at time 60s, the detection residual r_2 no longer remains zero which indicates a fault occurs, fault detection time is 0.2s.

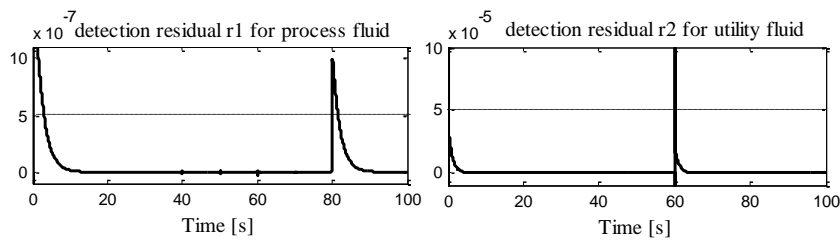
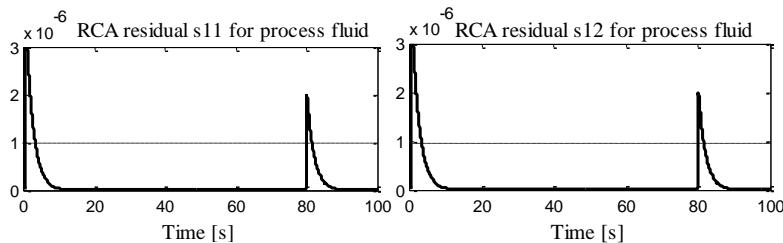


Fig.8.6 Detection residual in case (a)

Then, we recognize that, for each actuator, one fault exists. The main contribution of this paper is that we can not only detect and locate the fault, but also can analyze its root cause. Next, we focus on identifying the causes of these two faults.



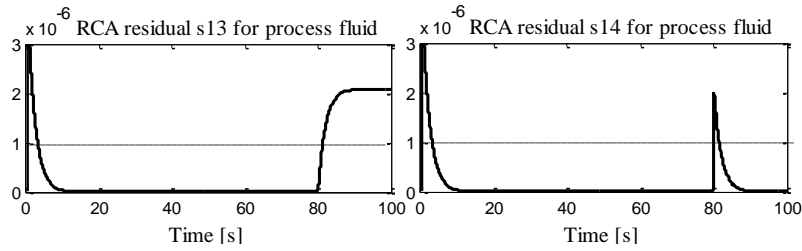


Fig 8.7 Residuals for identifying fault cause in process fluid in case (a)

Fig.8.7 aims at recognizing root cause of the fault at actuator of process fluid. RCA residuals $s_{11}, s_{12}, s_{13}, s_{14}$ are designed to recognize four possible candidates: $f_1, f_2, f_3,$ and f_4 . Detection residual r_1 has already implied fault occurred at 80s. It is obvious in Fig.8.7 that, only s_{13} breaks through and remains above the threshold, which means that fault in actuator of process fluid is caused by fault f_3 . Isolation time is 0.5s which is ideally.

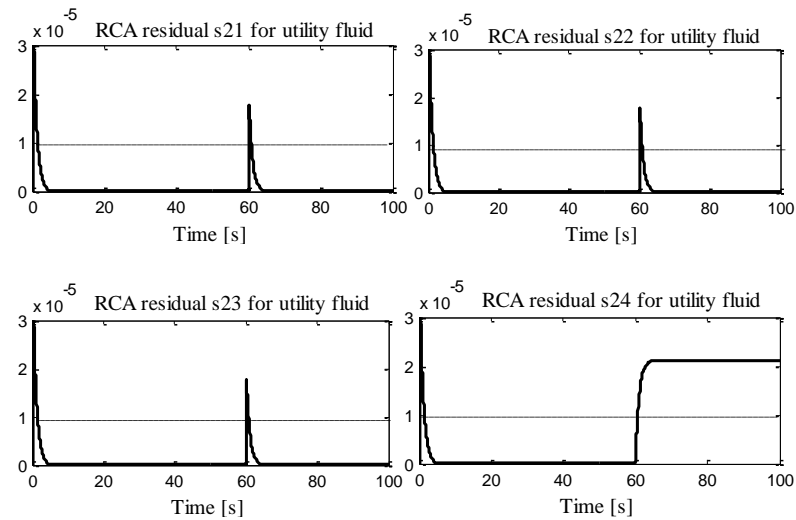


Fig.8.8 Residuals for identifying fault cause in utility fluid in case (a)

In Fig.8.8, RCA residuals $s_{21}, s_{22}, s_{23}, s_{24}$ are designed to recognize fault $f_1, f_2, f_3,$ and f_4 in actuator of utility fluid. Detection residual r_2 in Fig.8.6 has already implied fault occurred at 60s. It is obviously in Fig.8.8 that only s_{24} breaks the threshold and never comes back, which means that fault in actuator of utility fluid is caused by fault f_4 . In this case, isolation time is about 0.2s. The differences in isolation time are due to magnitude of fault and the effect it has impacted the system.

2-) Noise corrupted case, fault f_2 exists in actuator of process fluid and fault f_3 exists in actuator of utility fluid

To illustrate the robustness of the proposed scheme, external disturbance or measurement noise are considered in this case. Suppose the output measurement y is corrupted by a colored noise. The colored noise is generated with a second order AR filter excited by a Gaussian white noise with zero mean and unitary variance. The standard deviation of the colored noise is about 3.5.

The same situation as case (a), one fault is considered on each actuator separately. For actuator of process fluid, fault f_2 is supposed to be leakage, and reasons that can lead to the leakage are: valve tightness, leaky bushing, and terminals. Fault f_3 is supposed in actuator of utility fluid, fault f_3 is caused by valve clogging, and it is a commonly encountered fault. If not properly repaired, this kind of fault may cause severe impacts on system performance. Simulation results are demonstrated in Fig.8.9-Fig.10.

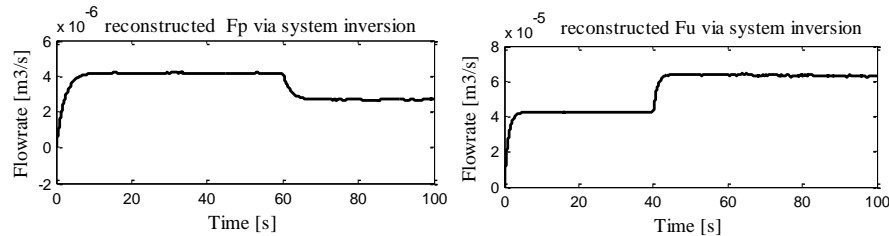


Fig. 8.9 Reconstructed input \tilde{F}_u, \tilde{F}_p from output T_p, T_u in CASE (b)

It can be seen from Fig.8.9 that although noise exists, the developed input reconstruction techniques can provide reconstructed inputs with a good accuracy. At actuator of process fluid, sudden decrease occurs at 60s which indicates occurrence of a fault, and it takes 4s to steady at new value. For actuator of utility fluid, the reconstructed value increases from 40s, and is stable after about 3s. A fault is detected due to the unexpected increase.

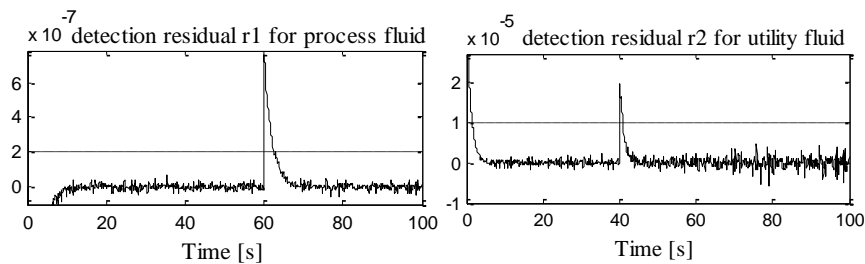


Fig.8.10 Detection residual in case (b)

As illustrated in Fig.8.10, detection residual r_1 indicates a fault in actuator of process fluid at 60s, it takes 1.2s to determine the occurrence of the fault. Detection residual r_2 refers to a fault in actuator of utility fluid at time 40s, and it takes 1.5s to detect it. We can shorten the detection time and detect smaller fault by employing larger gain for the detection observers or adopt a smaller threshold. However, larger gain or larger threshold may fail to detect the fault correctly, since observer with larger gain is too sensitive to noise and smaller threshold may lead to be undistinguished from noise. Therefore a trade between detectability and sensitivity should be made in order to detect the fault correctly. In summary, a small magnitude fault may not be detected within the existence of the noise. Again, after detection of the faults, we have to identify their root causes.

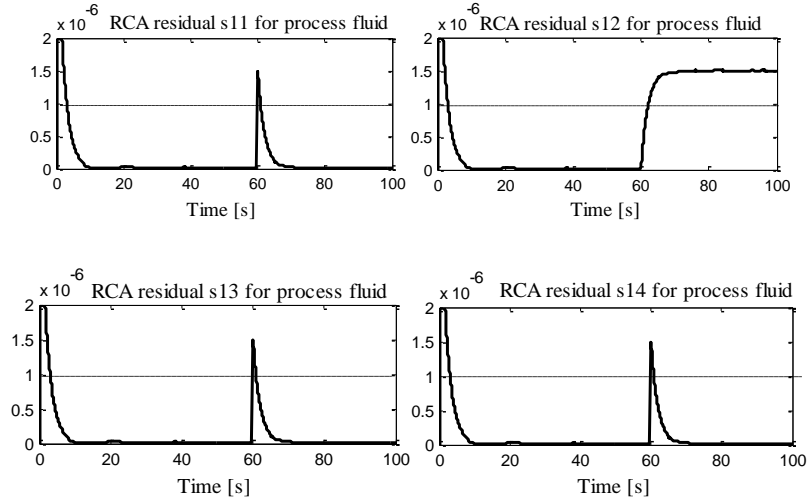


Fig. 8.11 Residuals for identifying fault cause in process fluid in case (b)

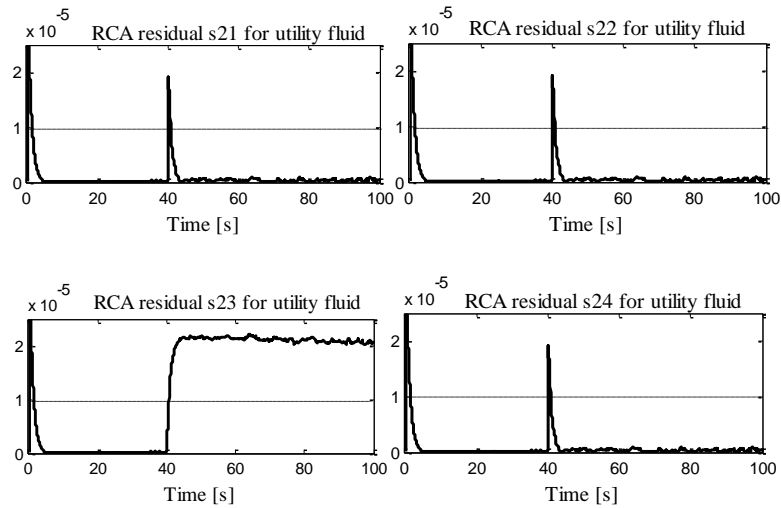


Fig. 8.12 Residuals for identifying fault cause in utility fluid in case (b)

We can see from Fig.8.11 that only RCA residual s_{12} breaks through its threshold and remains beyond it, the rest three RCA residuals are below their thresholds, then the fault resource f_2 of actuator of process fluid is identified. When come to RCA residuals for actuator of utility fluid in Fig.8.12, only s_{23} is beyond its threshold which verifies the occurrence of fault cause f_3 .

From the above simulation results, we can see that the proposed strategy is available to detect and locate a fault correctly, and root cause analysis for each detected fault is achieved with a good accuracy. Encouraging simulation results are obtained thanks to the robustness performance of the proposed scheme.

8.5 Summary

The main contribution of this chapter lies on the integration of both system level and component level based FDI approaches to facilitate FD and RCA of subcomponents actuators. The studied intensified Hex reactor system exhibits extremely complex dynamics because the small volumes and large

throughputs of such systems lead inescapably to smaller residence times. In some cases, their response times are of the same order of magnitude as those of actuators and measurement transmitters, perhaps even faster. Therefore deep considerations of individual constituted units are expected. The results presented provide further insights into how the internal dynamics of control valve influence overall performance, with particular reference to intensified Hex reactor systems. Simulated results are included to demonstrate the applicability and robustness of the proposed method and encouraging results are obtained.

Appendix 8.1A

1-) system modelling

The application of the energy balance rule considering a single cell per fluid (covering the whole length) to a counter flow HEX/Reactor gives rise to the following dynamical models, each cell consists of two perfect stirred tanks with inflows and outflows, as shown in Fig.8.2:

$$k = 1 \begin{cases} \dot{T}_p^k = \frac{UA}{\rho_p c_{pp} V_p} (T_u^k - T_p^k) + \frac{1}{V_p} (T_p^{in} - T_p^k) F_p \\ \dot{T}_u^k = \frac{UA}{\rho_u c_{pu} V_u} (T_p^k - T_u^k) + \frac{1}{V_u} (T_u^{k+1} - T_u^k) F_u \end{cases} \quad (1a)$$

$$1 < k < N \begin{cases} \dot{T}_p^k = \frac{UA}{\rho_p c_{pp} V_p} (T_u^k - T_p^k) + \frac{1}{V_p} (T_p^{k-1} - T_p^k) F_p \\ \dot{T}_u^k = \frac{UA}{\rho_u c_{pu} V_u} (T_p^k - T_u^k) + \frac{1}{V_u} (T_u^{k+1} - T_u^k) F_u \end{cases} \quad (1b)$$

$$k = N \begin{cases} \dot{T}_p^k = \frac{UA}{\rho_p c_{pp} V_p} (T_u^k - T_p^k) + \frac{1}{V_p} (T_p^{k-1} - T_p^k) F_p \\ \dot{T}_u^k = \frac{UA}{\rho_u c_{pu} V_u} (T_p^k - T_u^k) + \frac{1}{V_u} (T_u^{in} - T_u^k) F_u \end{cases} \quad (1c)$$

where ρ_p, ρ_u are density of the process fluid and utility fluid (in $\text{kg} \cdot \text{m}^{-3}$), V_p, V_u are volume of the process fluid and utility fluid (in m^3), c_{pp}, c_{pu} are specific heat of the process fluid and utility fluid (in $\text{J} \cdot \text{kg}^{-1} \cdot \text{K}^{-1}$), U is the overall heat transfer coefficient (in $\text{J} \cdot \text{m}^{-2} \cdot \text{K}^{-1} \cdot \text{s}^{-1}$). A is the heat transfer area (in m^2). F_p, F_u are mass flowrates of process fluid and utility fluid (in $\text{kg} \cdot \text{s}^{-1}$). T_p^{k-1} is the process fluid temperature of previous cell. For the cell 1, it is the inlet temperature of process fluid T_p^{in} . T_u^{k+1} is the utility fluid temperature of previous cell. For the cell N , it is the inlet temperature of utility fluid T_u^{in} .

In order to suit the diagnostic requirements better, there are two problems which need to be taken into consideration. The first one is with respect to the dynamics of the heat transfer coefficient. Another problem is the determination of the cell number N . It is accepted that large number of cell could keep dynamics better, but may lead to high computational loads.

2-) Parameterization of overall heat transfer coefficient

A drawback of the studied technologies is that the apparatus cannot open for cleaning and therefore fouling, which can cause gradual decline in the performance of HEX/Reactors, will limit its application

[221]. Therefore it is necessary to monitor dynamics of fouling and alarm a fault caused by higher fouling on timely. This is solved by expanding overall heat transfer coefficient U to introduce the fouling parameter in this work. Moreover, U is also mass flow and temperature dependent. However, the fluid characteristics have been considered constant, so this temperature dependency of U will not be taken into account here. In summary, we consider the influence of both mass flowrate and fouling dynamics on the heat transfer coefficient as in work [22].

The heat transfer coefficient (U) is calculated by the convective heat transfer coefficient of the process fluid side and utility fluid side, and is generally defined by: $\frac{1}{U} = \frac{1}{h_p} + \frac{1}{h_u} + R_f$. Where h_p, h_u denote the convection heat transfer coefficients for the process and utility fluid, and R_f denotes the thermal resistance or fouling parameter. For both sides of the heat exchanger used here, assuming that the heat transfer coefficient is a function of mass flow, the convection coefficient are: $h_p(t) = K_p F_p^y, h_u(t) = K_u F_u^y$, Where K_p, K_u are constants. Neglecting the thermal resistance (e.g. for a clean exchanger), this leads to:

$$U(t) = \frac{h_p(t)h_u(t)}{h_p(t)+h_u(t)} = \frac{K_p K_u (F_p(t)F_u(t))^y}{(K_p F_p^y(t) + K_u F_u^y(t))} = K_U \frac{(F_p F_u)^y}{(F_p)^y + e(F_u)^y} \quad (2)$$

Where e and y are constants. As the overall heat transfer coefficient decrease with fouling, we can assume that fouling can be characterized by the parameter K_U . Then the overall heat transfer coefficient at the reference mass flowrate F_p^*, F_u^* can be expressed as: $U^*(t) = K_U \frac{(F_p^* F_u^*)^y}{(F_p^*)^y + e(F_u^*)^y}$.

To account for variations in the mass flowrate, define α, β as fouling parameters, and γ as a function of mass flow rates, then we get:

$$\alpha = \frac{U^* A}{V_p}, \quad \beta = \frac{U^* A}{V_u}, \quad \gamma = \frac{U}{U^*} = \frac{(F_p F_u)^y ((F_p^*)^y + e(F_u^*)^y)}{(F_p^* F_u^*)^y ((F_p)^y + e(F_u)^y)}, \quad \text{then} \quad \frac{U_p A}{\rho_p c_p V_p} = \frac{1}{\rho_p c_p} \alpha \gamma, \quad \frac{U_u A}{\rho_u c_u V_u} = \frac{1}{\rho_u c_u} \beta \gamma$$

Thus, by letting the overall heat transfer coefficient be functions of mass flow and fouling, a process model is then obtained which is capable of accurately describing the dynamics of the heat exchanger for a wide range of working conditions.

$$k = 1 \begin{cases} \dot{T}_p^k = \frac{1}{\rho_p c_{pp}} \alpha \gamma (T_u^k - T_p^k) + \frac{1}{V_p} (T_p^{\text{in}} - T_p^k) F_p \\ \dot{T}_u^k = \frac{1}{\rho_u c_{pu}} \beta \gamma (T_p^k - T_u^k) + \frac{1}{V_u} (T_u^{k+1} - T_u^k) F_u \end{cases} \quad (3a)$$

$$1 < k < N \begin{cases} \dot{T}_p^k = \frac{1}{\rho_p c_{pp}} \alpha \gamma (T_u^k - T_p^k) + \frac{1}{V_p} (T_p^{k-1} - T_p^k) F_p \\ \dot{T}_u^k = \frac{1}{\rho_u c_{pu}} \beta \gamma (T_p^k - T_u^k) + \frac{1}{V_u} (T_u^{k+1} - T_u^k) F_u \end{cases} \quad (3b)$$

$$k = N \begin{cases} \dot{T}_p^k = \frac{1}{\rho_p c_{pp}} \alpha \gamma (T_u^k - T_p^k) + \frac{1}{V_p} (T_p^{k-1} - T_p^k) F_p \\ \dot{T}_u^k = \frac{1}{\rho_u c_{pu}} \beta \gamma (T_p^k - T_u^k) + \frac{1}{V_u} (T_u^{\text{in}} - T_u^k) F_u \end{cases} \quad (3c)$$

To summarize, detection of fouling will be linked to variations of parameters α, β in real time. Whilst, determination of jumps in flow rate is associated with γ .

3-) Determination of cells number N

As mentioned above, in this paper, we mainly focus on the heat exchange performance. A trade-off between accuracy and computation load is necessary to determine the minimum number of cells. For HEXs with counter flow geometry, experiments performed at Chalmers, see [222], have shown that perfect mixing conditions are achieved already after a few cells. Authors in [207] validated that models with three sections are sufficient for the majority of industrial heat exchanger. In [212],[217] it was shown two sections were enough to accurately estimate fouling with the counter flow type. It was also shown in [206] that the simulation results show that the model behaves like a real system just considering a limited number of cells. Moreover, analytical proofs are developed by works [205],[204], the thermodynamically possible minimum number of modelling cells are given conceptually by number of heat transfer units.

The FDD procedure requires the process to operate in steady state, several simulations are made to determine the minimal number of cells in steady state by considering the hex/reactor divided into a variable number of cells; in particular, the results refer to different cells:1, 3, 5, 10 and 20 cells respectively. The test conditions are: $T_{pi} = 76^\circ\text{C}$, $T_{ui} = 15.6^\circ\text{C}$, $F_u = 152\text{kg/h}$, $F_p = 15\text{kg/h}$. More detailed information can be found in [29].

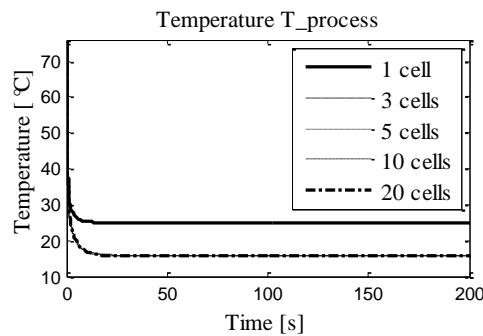


Fig. A.1 Temperature variation for the HEXs/reactor divided into different cells

As shown in Fig. A.1, the temperature of process fluid varies obviously between 1 cell case and multi cells case. While there seem no big differences among multi cells, simulation results seem to be quite insensitive to the increase of the number of cells. It derives that the dynamics do not differ much from 3 cells, the temperature varies less and less with the increase in the number of cells. Comparison between simulation results and experimental data corroborated the validity of the developed model. It is shown experimentally that decomposition into three cells is sufficient.

CHAPTER 9 SUMMARY, CONCLUSION AND SUGGESTION OR FUTURE

WORK

This chapter summarizes the results obtained in this thesis, and presents the concluding remarks. Some directions for further developments of the proposed approaches are also suggested.

9.1 Conclusions

In this thesis, the problem of system supervision, as well as fault diagnosis & root cause analysis (FD & RCA) of interconnected nonlinear system, is investigated. The interconnected nonlinear system is considered as composed of two nonlinear subsystems connected in cascade manners: the actuator and the process subsystems. The reason for the decomposition of this system structure is due to the increasing complexity and technological advances of subcomponents which result in the fact that their internal dynamics cannot be ignored as assumed by system level based FDD approaches. Fortunately, this decomposition allows to performance monitoring and diagnosing of internal variables of individual subcomponents, as well as the performance supervising of the global system simultaneously.

While as is well known, it is very difficult to address the problem of analyzing cascade interconnected system using a centralized architecture, thus in this work, an interconnected observer is developed for monitoring performance of sub-states in individual subsystems, and a distributed fault diagnosis architecture is triggered in the presence of fault. In addition, in the presented monitoring and FDD architecture, output of the final subsystem is assumed to be the only available measurement. The output of the actuator subsystem, which is the interconnection between the two subsystems and also the input of the process subsystem, is assumed to be inaccessible. It is due to that, according to real engineering situation, for the actuator, it can be uneconomic or unrealistic to measure its output. We then consider the problem that arises when the output from the actuator subsystem is not available directly, but instead available via the second subsystem, the process subsystem. That is, the output from the actuator subsystem acts as the input to the process subsystem, from which measurement of the final product is in turn available.

In solving the problem of system supervision and diagnosis of interconnected system, one should consider the problem of the input and (or) fault effect propagation which means the input and (or) fault effect in lower subsystems can be distinguished in higher subsystems. It refers to the capacity of two different variables at local level to generate identifiable output signals at global level for a given interconnected system. This consideration can be viewed as invertibility problem of the interconnected system since a motivation of invertibility is to prove the distinguishability of the input and (or) unknown input. In solving the problem of the invertibility problem, we give a necessary and sufficient condition for an interconnected system to be invertible which says that the individual subsystems should be invertible.

After solving problem of the input and (or) fault distinguishability, the next task focuses on interconnected observer design for achieving system supervision. The aim is to design an interconnected observer that provides accurately estimates of states of each subsystem, as well as the interconnection. It is a two level interconnected observer system which consists of two state estimators: the actuator and the process state estimators. Firstly, an existing converging observer is extended to estimate the states of the actuator subsystem, in particular, the information of outputs of actuator system are replaced by their estimation through the observer proposed in process subsystem. Second, an extended high gain observer is considered to exactly estimate the states of the process subsystem subject to unknown inputs which is also the outputs of the actuator subsystem. The unknown inputs are treated as new states of the process subsystem. While through computing the derivatives of the output vectors in actuator subsystem, the unknown input can be expressed as a function of the inputs, derivatives of the inputs and the states of the actuator subsystem. Then, by using the estimates information of two estimators, a kind of interconnected observer designed method is proposed for the studied invertible interconnected dynamic system.

The purpose of root cause analysis (RCA) is achieved by a distributed FDD architecture. Any unexpected variations of the variables of the component subsystem denote root cause of a detected fault. In the presented distributed FDD architecture, a local fault filter is designed for the actuator subsystem by utilizing local measurements and estimated information of output from neighboring interconnected process subsystem, thus achieving root cause analysis of detected actuator fault. Each local fault filter consists of two modules: a fault detection and isolation module is used to identify an occurrence of any fault variable in the actuator subsystem where banks of fault isolation estimators are employed to determine the particular faulty variables that have occurred in the subsystem; an input estimation module is used to determine the unknown interconnection of the interconnected system or determine the output of the actuator subsystem by global measurements. In addition, the important properties of robustness and fault sensitivity (fault detectability, isolability and distinguishability) of the local adaptive fault isolation estimators designed for each subsystem are also established.

The major contribution of the thesis lies on that it provides a means of monitoring and diagnosing of the interconnected plant at both local and global level which result in improved fault localization and provide better predictive maintenance aids. The presented FD&RCA algorithm is in fact a combination of local intelligence with a more advanced diagnostic capability (combining fault monitoring and diagnosis at both local and global levels) to perform FDD functions on different levels of the plant.

9.2 Future Work

The preceding section summarized the results obtained in this thesis. The proposed techniques and their application to improve the performance of FD&RCA system of nonlinear interconnected processes were briefly described. Besides the admired features of the proposed methods, there is a room for further improvements. In the following, some possible research directions for further extension of the proposed FD&RCA schemes are outlined.

For future work, one interesting problem is to develop loosing conditions for checking invertibility of the interconnected system which are more constructive as the purpose of invertibility in this work is to verify input (or fault) distinguishability; it is in general not needed to compute the inverse of the interconnected system. The analysis of systems having more inputs than outputs, of systems in which normal forms cannot be defined, and of systems in which the zero dynamics are unstable could be the substantially unexplored and open area of research. Moreover, in this work, modelling uncertainties, as well as measurement noise is difficult to avoid due to the complexity of the integrated modern sensors, as well as the overall systems. Thus, the case of invertibility of an interconnected model with modeling uncertainties and measurement noise could be another interesting research direction in order to extend the applicability of the method proposed. From the stability analysis we have to justify scaling the required modeling information without destabilizing the input reconstruction algorithm.

For the problem of fault diagnosis discussed in this thesis, the application of interconnected system presented involves only actuator and process subsystems. With the help of the presented supervision scheme, internal dynamics of actuator could be monitored and diagnosed. However, sensor equipment diagnostics is also very important in the fault diagnosis system to improve the operational safety and economics of modern engineering systems. We do not provide motivation for whether the developed technique can be successfully extended to a more general interconnected nonlinear system, by which internal dynamics of actuator, process and sensor are considered in an integrated interconnected system.

Moreover, the issue of multi fault isolability condition where fault may exit in any subsystems still needs further investigation. The fault isolability condition is a critical property in characterizing the class of faults that are isolable by the proposed FD&RCA method. Therefore an integrated FDD scheme is a further requirement for recognizing the faulty subsystem. Additionally, after a faulty subsystem is successfully isolated by using the proposed FDD scheme, we can extend the presented FD&RCA method to construct a hierarchical method which allows the isolation of the faulty subsystem and the particular faulty causes as well.

Finally, although the proof-of-principle was demonstrated for the developed algorithms using the Hex/reactor system, these algorithms was only implemented on a laboratory system and tested using laboratory data, focusing on control valve actuator only. It is sometimes impracticable to attempt performance assessments in realistic industrial conditions as the process safety and economy cannot easily be compromised by such tests. Therefore the proposed approach still needs to be tested by real plant data with more kinds of actuators before they can be integrated into a realistic process engineering problem.

BIBLIOGRAPHY

- [1] M. Bartyś, R. Patton, M. Syfert, S. de las Heras, and J. Quevedo, "Introduction to the DAMADICS actuator FDI benchmark study," *Control Eng. Pract.*, vol. 14, pp. 577–596, 2006.
- [2] V. Puig, a. Stancu, T. Escobet, F. Nejjari, J. Quevedo, and R. J. Patton, "Passive robust fault detection using interval observers: Application to the DAMADICS benchmark problem," *Control Eng. Pract.*, vol. 14, pp. 621–633, 2006.
- [3] K. Roy, R. N. Banavar, and S. Thangasamy, "Application of fault detection and identification (FDI) techniques in power regulating systems of nuclear reactors," *IEEE Trans. Nucl. Sci.*, vol. 45, no. 6, pp. 3184–3201, 1998.
- [4] M. Bask, "Dynamic Threshold Generators for Robust Fault Detection," Lulea University of Technology, Lulea, Sweden, 2005.
- [5] I. Izadi, S. L. Shah, D. S. Shook, and T. Chen, "An introduction to alarm analysis and design," *2009 SAFEPROCESS*, 2009, vol. 42, no. 8, pp. 645–650.
- [6] R. E. U. Andrei V. Gribok, Ibrahim Attieh, J. Wesley Hines, "Regularization of Feedwater Flowrate Evaluation for Venturi Meter Fouling Problem in Nuclear Power Plants," *J. Chem. Inf. Model.*, vol. 53, pp. 1689–1699, 2013.
- [7] M. Abid, "Fault detection in nonlinear systems: An observer-based approach," University Duisburg-Essen, 2010.
- [8] K. Zhang, "Fault Detection and Diagnosis for A Multi-Actuator Pneumatic System," Stony Brook University, 2011.
- [9] K. Zhao, "An Integrated Approach to Performance Monitoring and Fault Diagnosis of Nuclear Power Systems," University of Tennessee, Knoxville, 2005.
- [10] G. B. A Marcos, S Ganguli, "new strategies for fault tolerant control and fault diagnostic," *Proc. 5th Symp. Fault Detect. Superv. Saf. Tech. Process. (SAFEPROCESS'2003). Washing. D.C., USA*, pp. 277–282, 2003.
- [11] J. Ma, "Methods and Systems for Fault Disgnosis in Nuclear Power Plants," Western Ontario University, 2015.
- [12] S. Hansen, "Fault Diagnosis and Fault Handling for Autonomous Aircraft," Technical University of Denmark, 2012.
- [13] R. J. Patton and H. Hu, "Fault-Tolerant Control Systems : the 1997 Situation," *Proc. IFAC Symp. Fault Detect. Superv. Saf. Tech. Process. Kingst. Upon Hull, UK.*, pp. 1033–1054, 1997.
- [14] W. Chen, "Fault detection and isolation in nonlinear systems: observer and energy-balance based approaches," University of Duisburg-Essen, 2012.
- [15] Proefschrift, "Model Predictive Control on Open Water Systems," University Delft, 2006.
- [16] V. Venkatasubramanian, R. Rengaswamy, and K. Yin, "A review of process fault detection and diagnosis Part I : Quantitative model-based methods," vol. 27, pp. 293–311, 2003.
- [17] V. Venkatasubramanian, R. Rengaswamy, and S. N. Ka, "A review of process fault detection and diagnosis Part II : Qualitative models and search strategies," vol. 27, pp. 313–326, 2003.
- [18] V. Venkatasubramanian, R. Rengaswamy, and S. N. Ka, "A review of process fault detection and diagnosis Part III : Process history based methods," vol. 27, 2003.
- [19] Q. Zhang, "Fault detection and isolation based on adaptive observers for nonlinear dynamic systems," Rennes, Frances, 1999.
- [20] D. Fragkoulis, G. Roux, and B. Dahhou, "Detection, isolation and identification of multiple

- actuator and sensor faults in nonlinear dynamic systems: Application to a waste water treatment process,” *Appl. Math. Model.*, vol. 35, no. 1, pp. 522–543, 2011.
- [21] H. Noura and A. Chamseddine, “Sensor Gain Fault Diagnosis for a Class of Nonlinear Systems,” *Eur. J. Control*, vol. 12, no. 5, pp. 536–544, 2006.
- [22] G. Besancon and Q. Zhang, “Further developments on adaptive observers for nonlinear systems with application in fault detection,” *IFAC World Congress*, 2002, no. 1, pp. 732–732.
- [23] B. Jiang and F. N. Chowdhury, “Parameter fault detection and estimation of a class of nonlinear systems using observers,” *J. Franklin Inst.*, vol. 342, pp. 725–736, 2005.
- [24] X. Zhang, M. M. Polycarpou, and T. Parisini, “Fault diagnosis of a class of nonlinear uncertain systems with Lipschitz nonlinearities using adaptive estimation,” *Automatica*, vol. 46, no. 2, pp. 290–299, 2010.
- [25] A. Xu and Q. Zhang, “Nonlinear system fault diagnosis based on adaptive estimation,” *Automatica*, vol. 40, pp. 1181–1193, 2004.
- [26] X.-G. Yan and C. Edwards, “Nonlinear robust fault reconstruction and estimation using a sliding mode observer,” *Automatica*, vol. 43, pp. 1605–1614, 2007.
- [27] P. Vijay, M. O. Tade, K. Ahmed, R. Utikar, and V. Pareek, “Simultaneous estimation of states and inputs in a planar solid oxide fuel cell using nonlinear adaptive observer design,” *J. Power Sources*, vol. 248, pp. 1218–1233, 2014.
- [28] A. Martínez-Sibaja, C. M. Astorga-Zaragoza, A. Alvarado-Lassman, R. Posada-Gómez, G. Aguila-Rodríguez, J. P. Rodríguez-Jarquín, and M. Adam-Medina, “Simplified interval observer scheme: A new approach for fault diagnosis in instruments,” *Sensors*, vol. 11, pp. 612–622, 2011.
- [29] Y. Zhou, J. Liu, and A. L. Dexter, “Estimation of an incipient fault using an adaptive neurofuzzy sliding-mode observer,” *Energy Build.*, vol. 77, pp. 256–269, 2014.
- [30] H. Mekki, O. Benzineb, D. Boukhetala, M. Tadjine, and M. Benbouzid, “Sliding mode based fault detection, reconstruction and fault tolerant control scheme for motor systems,” *ISA Trans.*, pp. 1–12, 2015.
- [31] J. Bokor and Z. Szabó, “Fault detection and isolation in nonlinear systems,” *Annu. Rev. Control*, vol. 33, pp. 113–123, 2009.
- [32] J. Blesa, D. Rotondo, V. Puig, and F. Nejjari, “FDI and FTC of wind turbines using the interval observer approach and virtual actuators/sensors,” *Control Eng. Pract.*, vol. 24, pp. 138–155, 2014.
- [33] D. Theilliol, H. Noura, and J.-C. Ponsart, “Fault diagnosis and accommodation of a three-tank system based on analytical redundancy,” *ISA Trans.*, vol. 41, pp. 365–382, 2002.
- [34] U. Schubert, U. Kruger, G. Wozny, and H. Arellano-Garcia, “Input reconstruction for statistical-based fault detection and isolation,” *AIChE J.*, vol. 58, pp. 1513–1523, 2012.
- [35] F. Szigeti, J. Bokor, and A. Edelmayer, “Input Reconstruction by Means Of System Inversion: Application to Fault Detection and Isolation,” *15th Trienn. World Congr.*, 2002.
- [36] S. Chaib, D. Boutat, A. Banali, and F. Kratz, “Invertibility of switched nonlinear systems. application to missile faults reconstruction,” *Proc. IEEE Conf. Decis. Control*, pp. 3239–3244, 2007.
- [37] C. Edwards, S. K. Spurgeon, and R. J. Patton, “Sliding mode observers for fault detection and isolation,” *Automatica*, vol. 36, pp. 541–553, 2000.
- [38] K. C. Veluvolu, M. Defoort, and Y. C. Soh, “High-gain observer with sliding mode for

- nonlinear state estimation and fault reconstruction,” *J. Franklin Inst.*, vol. 351, no. 4, pp. 1995–2014, 2014.
- [39] N. Di Miceli Raimondi, N. Olivier-Maget, N. Gabas, M. Cabassud, and C. Gourdon, “Safety enhancement by transposition of the nitration of toluene from semi-batch reactor to continuous intensified heat exchanger reactor,” *Chem. Eng. Res. Des.*, vol. 94, pp. 182–193, 2015.
- [40] J. C. Yang and D. W. Clarke, “The self-validating actuator,” *Control Eng. Pract.*, vol. 7, pp. 249–260, 1999.
- [41] M. F. Rahmat, N. H. Sunar, S. N. S. Salim, M. S. Z. Abidin, a. a. M. Fauzi, and Z. H. Ismail, “Review on Modeling and Controller Design,” *Int. J. Smart Sens. Intell. Syst.*, vol. 4, no. 4, pp. 630–661, 2011.
- [42] J. Sarosi, I. Biro, J. Nemeth, and L. Cveticanin, “Dynamic modeling of a pneumatic muscle actuator with two-direction motion,” *Mech. Mach. Theory*, vol. 85, pp. 25–34, 2015.
- [43] J. Jin and J. Shi, “Automatic feature extraction of waveform signals for in-process diagnostic performance improvement,” *J. Intell. Manuf.*, vol. 12, pp. 257–268, 2001.
- [44] Q. Sun, “Singularity analysis Using Continuous Wavelet Transform for Bearing Fault Diagnosis,” *Mech. Syst. Signal Process.*, vol. 16, pp. 1025–1041, 2002.
- [45] T. Manninen, “Fault Simulator and Detection for a Process Control Valve,” Aalto University, 2012.
- [46] E. Richer and Y. Hurmuzulu, “A High Performance Pneumatic Force Actuator System Part 1 - Nonlinear Mathematical Model,” *ASME J. Dyn. Syst. Meas. Control*, vol. 122, no. 3, pp. 416–425, 2001.
- [47] A. Kayihan, “Friction compensation for a process control valve,” *Control Eng. Pract.*, vol. 8, 2000.
- [48] K. Prabakaran, T. U. Mageswari, D. Prakash, and a Suguna, “Fault Diagnosis in Process Control Valve Using Artificial Neural Network,” *Int. J. Innov. Appl. Stud.*, vol. 3, no. 1, pp. 138–144, 2013.
- [49] P. Subbaraj and B. Kannapiran, “Fault detection and diagnosis of pneumatic valve using Adaptive Neuro-Fuzzy Inference System approach,” *Appl. Soft Comput. J.*, vol. 19, pp. 362–371, 2014.
- [50] J. McGhee, I. a. Henderson, and A. Baird, “Neural networks applied for the identification and fault diagnosis of process valves and actuators,” *Measurement*, vol. 20, no. 4, pp. 267–275, 1997.
- [51] A. Tanwani and D. Liberzon, “Invertibility of switched nonlinear systems,” *Automatica*, vol. 46, no. 12, pp. 1962–1973, 2010.
- [52] L. Tang, L. Fang, J. Wang, and Q. Shang, “A new semi-physical model for pneumatic control valves with stiction nonlinearity,” *Nonlinear Dyn.*, no. April, p. inpress, 2016.
- [53] R. Isermann, “Model-based fault-detection and diagnosis – status and applications,” *Annu. Rev. Control*, vol. 29, pp. 71–85, 2005.
- [54] R. Isermann and P. Ballé, “Trends in the application of model based fault detection and diagnosis of technical processes,” *Control Eng. Pract.*, vol. 5, no. 5, pp. 709–719, 1997.
- [55] R. Isermann, *Fault-diagnosis systems: An introduction from fault detection to fault tolerance*. Berlin Heidelberg: Springer, 2006.
- [56] R. Milne, “Strategies for Diagnosis,” *IEEE Trans. Syst. Man. Cybern.*, vol. 17, pp. 333–339, 1987.

- [57] R. Isermann, "Supervision, fault-detection and fault-diagnosis methods - An introduction," *Control Eng. Pract.*, vol. 5, no. 5, pp. 639–652, 1997.
- [58] P. Goupil and A. Marcos, "The European ADDSAFE project: Industrial and academic efforts towards advanced fault diagnosis," *Control Eng. Pract.*, vol. 31, no. July 2009, pp. 1–17, 2014.
- [59] Steven X. Ding, *model-based fault diagnosis techniques*. Berlin Heidelberg: Springer, 2008.
- [60] P. M. Frank, "Analytical and Qualitative Model-based Fault Diagnosis – A Survey and Some New Results," *European Journal of Control*, vol. 2, pp. 6–28, 1996.
- [61] A. S. Willsky, "A survey of design methods for failure detection in dynamic systems," *Automatica*, vol. 12, pp. 601–611, 1976.
- [62] Spyros G. Tzafestas, Ed., *Knowledge-based System Diagnosis, Supervision, and Control*. Athens, Greece: Springer, 1989.
- [63] R. Isermann, *Fault-Diagnosis Applications: Model-Based Condition Monitoring: Actuators, Drives, Machinery, Plants, Sensors, and Fault-tolerant Systems*. Berlin Heidelberg: Springer, 2011.
- [64] F. Kimmich, A. Schwarte, and R. Isermann, "Fault detection for modern Diesel engines using signal- and process model-based methods," vol. 13, pp. 189–203, 2005.
- [65] T. F. Lootsma, "Observer-based Fault Detection and Isolation for Nonlinear Systems," Aalborg University, 2001.
- [66] E. A. García and P. M. Frank, "Deterministic nonlinear observer-based approaches to fault diagnosis: A survey," *Control Eng. Pract.*, vol. 5, no. 5, pp. 663–670, 1997.
- [67] J. Gerfler, "Fault detection and isolation using parity relations," vol. 5, no. 5, pp. 653–661, 1997.
- [68] J. Gertler and D. Singer, "A new structural framework for parity equation-based failure detection and isolation," *Automatica*, vol. 26, no. 2, pp. 381–388, 1990.
- [69] S. Simani, C. Fantuzzi, and J. R. Patton, *Model-based fault diagnosis in dynamic systems using identification techniques*. New York: Springer, 2002.
- [70] P. Weber and S. Gentil, "A Parameter Estimation Method for the Diagnosis of Sensor or Actuator Abrupt Faults," *Control Conference (ECC), European*, 1999, vol. 1, no. 1, pp. 3387–3392.
- [71] R. J. Chen, J., & Patton, *Robust Model-based Fault Diagnosis for Dynamic Systems*. New York: Springer Science+Business Media LLC, 1999.
- [72] K. R. Uren, G. van Schoor, C. P. du Rand, and A. Botha, "An integrated approach to sensor FDI and signal reconstruction in HTGRs – Part II: Case studies," *Ann. Nucl. Energy*, 2015.
- [73] A. Zakharov and V. Tikkala, "Fault detection and diagnosis approach based on nonlinear parity equations and its application to leakages and blockages in the drying section of a board machine," *J. Process Control*, vol. 23, no. 9, pp. 1380–1393, 2013.
- [74] V. Krishnaswami, G. Luh, and G. Rizzoni, "Nonlinear parity equation based residual generation for diagnosis of automotive engine faults," *Control Eng. Pract.*, vol. 3, no. 10, pp. 1385–1392, 1995.
- [75] L. B. Freidovich and H. K. Khalil, "Lyapunov-based switching control of nonlinear systems using high-gain observers," *Automatica*, vol. 43, pp. 150–157, 2007.
- [76] H. Alwi and C. Edwards, "An adaptive sliding mode differentiator for actuator oscillatory failure case reconstruction," *Automatica*, vol. 49, no. 2, pp. 642–651, 2013.
- [77] P. R. Mangsuli and N. J. Rao, "Nonlinear Luenberger-Like Observers for Nonlinear MIMO

- Systems,” *Asian Journal of Control*, vol. 10, no. 4, pp. 495–506, 2008.
- [78] M. Pourgholi and V. J. Majd, “Robust Adaptive Observer Design for Lipschitz Class of Nonlinear Systems,” *System*, pp. 29–33, 2012.
- [79] J. Zarei and E. Shokri, “Robust sensor fault detection based on nonlinear unknown input observer,” *Measurement*, vol. 48, pp. 355–367, 2014.
- [80] J. P. Gauthier, H. Hammouri, and S. Othman, “A simple observer for nonlinear systems applications to bioreactor,” *IEEE Trans. Automat. Contr.*, vol. 37, no. 6, pp. 875–879, 1992.
- [81] Q. Zhang, “A new residual generation and evaluation method for detection and isolation of faults in non-linear systems,” *Int. J. Adapt. Control Signal Process.*, vol. 14, pp. 759–773, 2000.
- [82] P. M. Frank and X. Ding, “Survey of robust residual generation and evaluation methods in observer-based fault detection systems,” *J. Process Control*, vol. 7, no. 6, pp. 403–424, 1997.
- [83] J. P. Gauthier, H. Hammouri, and S. Othman, “A simple observer for nonlinear systems applications to bioreactor,” *IEEE Transactions on Automatic Control*, vol. 37. pp. 875–879, 1992.
- [84] S. S. Stankovi, D. M. Stipanovi, and D. D. Iljak, “Decentralized dynamic output feedback for robust stabilization of a class of nonlinear interconnected systems,” *Automatica*, vol. 43, pp. 861–867, 2007.
- [85] J. Mohd Ali, N. Ha Hoang, M. a. Hussain, and D. Dochain, “Review and classification of recent observers applied in chemical process systems,” *Comput. Chem. Eng.*, vol. 76, pp. 27–41, 2015.
- [86] M. Zeitz, “The extended Luenberger observer for nonlinear systems,” *Syst. Control Lett.*, vol. 9, pp. 149–156, 1987.
- [87] T. S. a J. K. K. J. Burnham, “Nonlinear Unknown Input Observer Design for Nonlinear Systems : A New Method,” *Int. Fed. Auto. Con.*, 2011, pp. 11067–11072.
- [88] R. Seliger and P. M. Frank, “Fault-diagnosis by disturbance decoupled nonlinear observers,” *Proc. 30th IEEE CDC*, 1991, pp. 2248–2253.
- [89] N. Boizot, E. Busvelle, and J. P. Gauthier, “An adaptive high-gain observer for nonlinear systems,” *Automatica*, vol. 46, pp. 1483–1488, 2010.
- [90] P. M. Frank, S. X. Ding, and T. Marcu, “Model-based fault diagnosis in technical processes,” *Trans. Inst. Meas. Control*, vol. 22, no. 2000, pp. 57–101, 2000.
- [91] R. Marino and P. Tomei, “adaptive observers with arbitrary exponential rate of convergence for nonlinear system,” *IEEE Trans. Automatic Control*, vol. 40, no. 7, pp. 1–5, 1995.
- [92] G. Besançon, “Remarks on nonlinear adaptive observer design,” *Syst. Control Lett.*, vol. 41, pp. 271–280, 2000.
- [93] S. K. Spurgeon, “Sliding mode observers: a survey,” *Int. J. Syst. Sci.*, vol. 39, no. May, pp. 751–764, 2008.
- [94] P. M. Frank, “Fault diagnosis in dynamic systems using analytical knowledge-based redundancy – A survey and some new results,” *Automatica*, vol. 26, no. 3, pp. 459–474, 1990.
- [95] R. N. Clark, “Instrument Fault Detection,” *IEEE Trans. Aerosp. Electron. Syst.*, vol. AES-14, no. 3, pp. 456–465, 1978.
- [96] H. Ferdowsi, “Model based fault diagnosis and prognosis of nonlinear systems,” Missouri University of Science and Technology, 2013.
- [97] Q. Zhang, “Distributed Fault Diagnosis of Interconnected Nonlinear Uncertain Systems,”

- Wright State University, 2013.
- [98] A. Swarnakar and H. J. Marquez, "A New Scheme on Robust Observer-Based Control Design for Interconnected Systems With Application to an Industrial Utility Boiler," *IEEE Trans. Control Syst. Technol.*, vol. 16, no. 3, pp. 539–547, 2008.
- [99] R. Yan, Z. Dong, T. K. Saha, and R. Majumder, "A power system nonlinear adaptive decentralized controller design," *Automatica*, vol. 46, no. 2, pp. 330–336, 2010.
- [100] X.-G. Yan, C. Edwards, and S. K. Spurgeon, "Decentralised robust sliding mode control for a class of nonlinear interconnected systems by static output feedback," *Automatica*, vol. 40, pp. 613–620, 2004.
- [101] H. S. Ali, M. Alma, and M. Darouach, "Controllers design for two interconnected systems via unbiased observers," *Int. Fed. Auto. Con.*, 2014, vol. 19, pp. 10808–10813.
- [102] P. Ioannou, "Decentralized adaptive control of interconnected systems," *IEEE Trans. Automat. Contr.*, vol. 31, pp. 291–298, 1986.
- [103] H. Fan, L. Han, C. Wen, and L. Xu, "Decentralized adaptive output-feedback controller design for stochastic nonlinear interconnected systems," *Automatica*, vol. 48, pp. 2866–2873, 2012.
- [104] A. S. Tlili and N. B. Braiek, "Decentralized Observer based Guaranteed Cost Control for Nonlinear Interconnected Systems," *International Journal of Control & Automation*, vol. 2, no. 2, pp. 29–46, 2009.
- [105] X. G. Yan and L. Xie, "Reduced-order control for a class of nonlinear similar interconnected systems with mismatched uncertainty," *Automatica*, vol. 39, pp. 91–99, 2003.
- [106] R. Patton, C. Kambhampati, a Casavola, P. Zhang, S. Ding, and D. Sauter, "A Generic Strategy for Fault-Tolerance in Control Systems Distributed Over a Network," *Eur. J. Control*, vol. 13, no. 2–3, pp. 280–296, 2007.
- [107] S. Indra, L. Trav éMassuyès, and E. Chanthery, "A decentralized fault detection and isolation scheme for spacecraft: bridging the gap between model-based fault detection and isolation research and practice," *Prog. Flight Dyn. Guid. Navig. Control. Fault Detect. Avion.*, vol. 6, pp. 281–298, 2013.
- [108] C. Keliris, M. M. Polycarpou, and T. Parisini, "Distributed fault diagnosis for process and sensor faults in a class of interconnected input-output nonlinear discrete-time systems," *Int. J. Control*, vol. 88, no. September, pp. 1472–1489, 2015.
- [109] R. Ferrari, "Distributed fault detection and isolation of large-scale nonlinear systems: an adaptive approximation approach," *Openstarts.Units.It*, 2008.
- [110] N. Meskin and K. Khorasani, "Actuator Fault Detection and Isolation for a Network of Unmanned Vehicles," *IEEE Trans. Automat. Contr.*, vol. 54, no. 4, pp. 835–840, 2009.
- [111] R. M. G. Ferrari, T. Parisini, and M. M. Polycarpou, "Distributed Fault Detection and Isolation of Large-Scale Discrete-Time Nonlinear Systems: An Adaptive Approximation Approach," *IEEE Trans. Automat. Contr.*, vol. 57, pp. 275–290, 2012.
- [112] I. Shames, A. M. H. Teixeira, H. Sandberg, and K. H. Johansson, "Distributed fault detection for interconnected second-order systems," *Automatica*, vol. 47, no. 12, pp. 2757–2764, 2011.
- [113] X.-G. Yan and C. Edwards, "robust decentralized actuator fault detection and estimation for large-scale system using a sliding mode observer," *Int. J. Control*, vol. 81, no. May, pp. 591–606, 2008.
- [114] J. L. Speyer and R. H. Chen, "A Decentralized Fault Detection Filter 1," *J. Dyn. Syst. Meas. Control*, vol. 123, no. June 2001, pp. 237–247, 2001.

- [115] K. Smarsly and K. H. Law, "Decentralized fault detection and isolation in wireless structural health monitoring systems using analytical redundancy," *Adv. Eng. Softw.*, vol. 73, pp. 1–10, 2014.
- [116] F. Boem, Y. Xu, C. Fischione, and T. Parisini, "Distributed Fault Detection using Sensor Networks and Pareto Estimation," *2013 European Control Conference*, 2013, pp. 0–5.
- [117] C. Keliris, M. M. Polycarpou, and T. Parisini, "A robust nonlinear observer-based approach for distributed fault detection of input-output interconnected systems," *Automatica*, vol. 53, pp. 408–415, 2015.
- [118] F. Arrichiello, A. Marino, and F. Pierri, "Observer-Based Decentralized Fault Detection and Isolation Strategy for Networked Multirobot Systems," *IEEE Transactions on Control Systems Technology*, vol. 23, no. 4, pp. 1465–1476, 2015.
- [119] R. Hirschorn, "Invertibility of multivariable nonlinear control systems," *IEEE Trans. Automat. Contr.*, vol. 24, no. 2, pp. 289–297, 1979.
- [120] M. Bonilla Estrada, M. Figueroa Garcia, M. Malabre, and J. C. Martínez García, "Left invertibility and duality for linear systems," *Linear Algebra Appl.*, vol. 425, pp. 345–373, 2007.
- [121] H. Nijmeijer, "Invertibility of affine nonlinear control systems: a geometric approach," *Syst. Control Lett.*, vol. 2, no. 3, pp. 163–168, 1982.
- [122] A. Isidori, "Nonlinear Control Systems (Third Edition)." Berlin: Springer, 1995.
- [123] G. Marro, D. Prattichizzo, and E. Zattoni, "Convolution profiles for right inversion of multivariable non-minimum phase discrete-time systems," *Automatica*, vol. 38, pp. 1695–1703, 2002.
- [124] M. Hou and R. J. Patton, "Input Observability and Input Reconstruction," *Automatica*, vol. 34, no. 6, pp. 789–794, 1998.
- [125] M. Fliess, "A note on the invertibility of nonlinear input-output differential systems," *Syst. Control Lett.*, vol. 8, pp. 147–151, 1986.
- [126] L. Vu and D. Liberzon, "Invertibility of switched linear systems," *Automatica*, vol. 44, pp. 949–958, 2008.
- [127] R. Hirschorn, "Invertibility of multivariable nonlinear control systems," *IEEE Trans. Automat. Contr.*, vol. 24, no. 6, pp. 855–865, 1979.
- [128] A. Isidori, "Nonlinear Control Systems." Springer, 1985.
- [129] J. Descusse and C. . Moog, "Dynamic decoupling for right-invertible nonlinear systems," *Syst. Control Lett.*, vol. 8, pp. 345–349, 1987.
- [130] D. Boutat, J. Barbot, and M. Darouach, "A New Algorithm to Compute Inverse Dynamic of a Class of Nonlinear Systems," *Decision & Control*, vol.7, pp. 7–12, 2013.
- [131] Z. Yufan, "Minimal inversion and its algorithms of discrete time nonlinear systems," *J. Syst. Sci. Complex.*, vol. 18, no. 3, pp. 383–395, 2005.
- [132] F. Szigeti, C. E. Vera, J. Bokor, and a. Edelmayer, "Inversion based fault detection and isolation," *Proc. 40th IEEE Conf. Decis. Control (Cat. No.01CH37228)*, vol. 2, no. December, pp. 1005–1010, 2001.
- [133] A. Edelmayer, J. Bokor, Z. Szabo, and F. Szigeti, "Input reconstruction by means of system inversion: A geometric approach to fault detection and isolation in nonlinear systems," *Int. J. Appl. Math. Comput. Sci.*, vol. Vol. 14, n, no. 2, pp. 189–199, 2004.
- [134] M. Fliess, *on the inversion of nonlinear multivariable systems. Springer Berlin Heidelberg*, 58 :323-330 1986.

- [135] O. Markusson, "Model and System Inversion with Applications in Nonlinear System Identification and Control," *Stockholm: Signaler, sensorer och system*, 2002.
- [136] A. Isidori, "The zero dynamics of a nonlinear system: From the origin to the latest progresses of a long successful story," *Eur. J. Control*, vol. 19, no. 5, pp. 369–378, 2013.
- [137] P. Daoutidis and C. Kravaris, "Inversion and Zero Dynamics in Nonlinear Multivariable Control," *AIChE J.*, vol. 37, no. 4, pp. 527–538, 1991.
- [138] H. Nijmeijer, "Right-invertibility for a class of nonlinear control systems: A geometric approach," *Syst. Control Lett.*, vol. 7, no. April, pp. 125–132, 1986.
- [139] A. Edelmayer, "Fault Detection in Dynamic Systems: From State Estimation to Direct Input Reconstruction Methods," Hungarian Academy of Science, 2005.
- [140] H. K. Khalil, *Nonlinear Systems*, Second. Prentice-Hall, 1996.
- [141] G. Marro and E. Zattoni, "Unknown-state, unknown-input reconstruction in discrete-time nonminimum-phase systems: Geometric methods," *Automatica*, vol. 46, no. 5, pp. 815–822, 2010.
- [142] V. Maksimov and L. Pandolfi, "Dynamical reconstruction of unknown inputs in nonlinear differential equations," *Appl. Math. Lett.*, vol. 14, pp. 725–730, 2001.
- [143] T. Floquet and J. P. Barbot, "Super twisting algorithm-based step-by-step sliding mode observers for nonlinear systems with unknown inputs," *Int. J. Syst. Sci.*, vol. 0, pp. 803–815, 2007.
- [144] Q. P. Ha and H. Trinh, "State and input simultaneous estimation for a class of nonlinear systems," *Automatica*, vol. 40, no. 10, pp. 1779–1785, 2004.
- [145] G. Pillonetto and M. P. Saccomani, "Input estimation in nonlinear dynamical systems using differential algebra techniques," *Automatica*, vol. 42, pp. 2117–2129, 2006.
- [146] S. Kirtikar, H. Palanhandalam-madapusi, E. Zattoni, and D. S. Bernstein, "l-Delay Input Reconstruction for Discrete-Time Linear Systems," *Aerospace*, pp. 1848–1853, 2009.
- [147] T. W. Congress, "On FDI Filters and System Invertibility," *15th Triennial World Congress*, 2002.
- [148] F. Szigeti, "System Inversion and Fault Detection : the Failure Affine Nonlinear Case," *Automatica*, 2002.
- [149] a. Varga, "Inversion-based synthesis algorithm of periodic fault detection and isolation filters," *Proc. IEEE Conf. Decis. Control*, pp. 4367–4372, 2013.
- [150] H. Souley Ali, M. Darouach, C. Delattre, and Y. Becis-Aubry, "Functional observers design for two interconnected linear systems via LMI," *IFAC Proc. Vol.*, vol. 18, no. PART 1, pp. 14348–14352, 2011.
- [151] W. S. Gray, "A unified approach to generating series for nonlinear cascade systems," *Int. J. Control*, vol. 85, no. 15, pp. 1737–1754, 2012.
- [152] T. A. J. Håvard Fjær Grip , Ali Saberi, "Observers for interconnected nonlinear and linear systems," *Automatica*, vol. 48, no. 7, pp. 1339–1346, 2012.
- [153] G. Antonio Susto and M. Krstic, "Control of PDE-ODE cascades with Neumann interconnections," *J. Franklin Inst.*, vol. 347, no. 1, pp. 284–314, 2010.
- [154] W. S. Gray, L. a. Duffaut Espinosa, and M. Thitsa, "Left inversion of analytic nonlinear SISO systems via formal power series methods," *Automatica*, vol. 50, no. 9, pp. 2381–2388, 2014.
- [155] W. S. Gray, H. Herencia-Zapana, L. A. Duffaut Espinosa, and O. R. González, "Bilinear system interconnections and generating series of weighted Petri nets," *Syst. Control Lett.*, vol.

- 58, no. 12, pp. 841–848, 2009.
- [156] A. Tanwani, A. D. Dominguez-Garcia, and D. Liberzon, “An Inversion-Based Approach to Fault Detection and Isolation in Switching Electrical Networks,” *IEEE Trans. Control Syst. Technol.*, vol. 19, no. 5, pp. 1059–1074, 2011.
- [157] F. M. Callier, W. S. Chan, and C. A. Desoer, “Input-Output Stability of Interconnected Systems Using Decompositions: An Improved Formulation,” *IEEE Trans. Automat. Contr.*, vol. 23, no. 2, pp. 150–163, 1978.
- [158] S. Singh, “A modified algorithm for invertibility in nonlinear systems,” *IEEE Trans. Automat. Contr.*, vol. 26, no. 2, pp. 595–598, 1981.
- [159] R. Martínez-Guerra, J. L. Mata-Machuca, and J. J. Rincón-Pasaye, “Fault diagnosis viewed as a left invertibility problem,” *ISA Trans.*, vol. 52, no. 5, pp. 652–661, 2013.
- [160] F. Théron, Z. Anxionnaz-Minvielle, M. Cabassud, C. Gourdon, and P. Tochon, “Characterization of the performances of an innovative heat-exchanger/reactor,” *Chem. Eng. Process. Process Intensif.*, vol. 82, pp. 30–41, 2014.
- [161] J. Yang, F. Zhu, K. Yu, and X. Bu, “Observer-based state estimation and unknown input reconstruction for nonlinear complex dynamical systems,” *Commun. Nonlinear Sci. Numer. Simul.*, vol. 20, no. 3, pp. 927–939, 2015.
- [162] A. S. Tlili and N. Benhadj Braiek, “ H_∞ optimization-based decentralized control of linear interconnected systems with nonlinear interconnections,” *J. Franklin Inst.*, vol. 351, no. 6, pp. 3286–3304, 2014.
- [163] A. El Fadili, F. Giri, A. El Magri, R. Lajouad, and F. Z. Chaoui, “Adaptive control strategy with flux reference optimization for sensorless induction motors,” *Control Eng. Pract.*, vol. 26, pp. 91–106, 2014.
- [164] G. Besançon and H. Hammouri, “On observer design for interconnected systems,” *J. Math. Syst. Estim. Control*, vol. 8, no. 3, pp. 1–26, 1998.
- [165] M. Farza, M. M’Saad, T. Menard, M. L. Fall, O. Gehan, and E. Pigeon, “Simple Cascade Observer for a Class of Nonlinear Systems With Long Output Delays,” *IEEE Trans. Automat. Contr.*, vol. 60, pp. 3338–3343, 2015.
- [166] S. Dashkovskiy and L. Naujok, “Quasi-ISS/ISDS observers for interconnected systems and applications,” *Syst. Control Lett.*, vol. 77, pp. 11–21, 2015.
- [167] C. P. Tan and C. Edwards, “Sliding mode observers for detection and reconstruction of sensor faults,” *Automatica*, vol. 38, pp. 1815–1821, 2002.
- [168] Q. Zhang, “Adaptive Observer for Multiple-Input–Multiple-Output (MIMO) Linear Time-Varying Systems,” *IEEE Trans. Automat. Contr.*, vol. 47, no. 3, pp. 525–529, 2002.
- [169] F. J. Bejarano, T. Floquet, W. Perruquetti, and G. Zheng, “Observability and detectability of singular linear systems with unknown inputs,” *Automatica*, vol. 49, no. 3, pp. 793–800, 2013.
- [170] A. Chakrabarty, S. Sundaram, M. J. Corless, G. T. Buzzard, A. E. Rundell, and S. H. Zak, “Distributed Unknown Input Observers For Interconnected Nonlinear Systems,” *American Control Conference*, 2016, pp. 101–106.
- [171] M. Farza, K. Busawon, and H. Hammouri, “Simple nonlinear observers for on-line estimation of kinetic rates in bioreactors,” *Automatica*, vol. 34, no. 3, pp. 301–318, 1998.
- [172] F. Zhu and F. Cen, “Full-order observer-based actuator fault detection and reduced-order observer-based fault reconstruction for a class of uncertain nonlinear systems,” *J. Process Control*, vol. 20, no. 10, pp. 1141–1149, 2010.

- [173] A. Chakrabarty, G. T. Buzzard, S. H. Zak, F. Zhu, and A. E. Rundell, "Simultaneous state and exogenous input estimation for nonlinear systems using boundary-layer sliding mode observer," *Int. J. Robust Nonlinear Control*, vol. 18, pp. 1–29, 2016.
- [174] M. Saif, "Sliding mode observer for nonlinear uncertain systems," *IEEE Trans. Automat. Contr.*, vol. 46, no. 12, pp. 2012–2017, 2001.
- [175] C. De Persis and a. Isidori, "A geometric approach to nonlinear fault detection and isolation," *IEEE Trans. Automat. Contr.*, vol. 46, pp. 1–22, 2001.
- [176] S. Kirtikar, H. Palanhandalam-Madapusi, E. Zattoni, and D. S. Bernstein, "L-delay input and initial-state reconstruction for discrete-time linear systems," *Circuits, Syst. Signal Process.*, vol. 30, pp. 233–262, 2011.
- [177] H. Fu, S. Kirtikar, E. Zattoni, H. Palanhandalam-madapusi, and D. S. Bernstein, "Approximate Input Reconstruction for Diagnosing Aircraft Control Surfaces," *Aerosp. Eng.*, no. August, 2009.
- [178] J. Marzat, H. Piet-Lahanier, F. Damongeot, and E. Walter, "Nonlinear FDI based on state derivatives, as provided by inertial measurement units," *IFAC Proc. Vol.*, pp. 951–956, 2010.
- [179] H. Fang, R. a. De Callafon, and J. Cortés, "Simultaneous input and state estimation for nonlinear systems with applications to flow field estimation," *Automatica*, vol. 49, no. 9, pp. 2805–2812, 2013.
- [180] H. Wang, J. Zhao, Z. Xu, and Z. Shao, "Input and state estimation for linear systems with a rank-deficient direct feedthrough matrix," *ISA Trans.*, pp. 1–6, 2015.
- [181] S. Pan, D. Xiao, S. Xing, S. S. Law, P. Du, and Y. Li, "A general extended Kalman filter for simultaneous estimation of system and unknown inputs," *Eng. Struct.*, vol. 109, pp. 85–98, 2016.
- [182] L. ; Fridman, S. Yuri, E. Christopher, and X.-G. Yan, "Higher-order sliding-mode observer for state estimation and input reconstruction in nonlinear systems," *Int. J. Robust Nonlinear Control*, vol. 18, pp. 557–569, 2008.
- [183] A. Levant, "Robust exact differentiation via sliding mode technique," *Automatica*, vol. 34, pp. 379–384, 1998.
- [184] W. Benaïssa, N. Gabas, M. Cabassud, D. Carson, S. Elgue, and M. Demissy, "Evaluation of an intensified continuous heat-exchanger reactor for inherently safer characteristics," *J. Loss Prev. Process Ind.*, vol. 21, pp. 528–536, 2008.
- [185] P. Harris, S. Nolan, and G. E. O'Donnell, "Energy optimisation of pneumatic actuator systems in manufacturing," *J. Clean. Prod.*, vol. 72, pp. 35–45, 2014.
- [186] a. Mehmood, S. Laghrouche, and M. El Bagdouri, "Modeling identification and simulation of pneumatic actuator for VGT system," *Sensors Actuators, A Phys.*, vol. 165, no. 2, pp. 367–378, 2011.
- [187] S. M. Barakati, A. Mohammadi, and M. J. Fotuhi, "Modelling and Controller Design of Electro-Pneumatic Actuator Based on PWM," *Int. J. Robo. Auto.*, vol. 1, no. 3, pp. 125–136, 2012.
- [188] K. C. Wickramatunge and T. Leephakpreeda, "Empirical modeling of dynamic behaviors of pneumatic artificial muscle actuators," *ISA Trans.*, vol. 52, no. 6, pp. 825–834, 2013.
- [189] N. Di Miceli Raimondi, N. Olivier-Maget, N. Gabas, M. Cabassud, and C. Gourdon, "Safety enhancement by transposition of the nitration of toluene from semi-batch reactor to continuous intensified heat exchanger reactor," *Chem. Eng. Res. Des.*, vol. 94, no. August, pp. 182–193,

- 2015.
- [190] S. R. a. Shukor and M. T. Tham, "Performance envelopes of process intensified systems," in *Proc. of International Symposium on Advanced Control of Chemical Processes*, 2004.
- [191] D. Wassila Benaissa, Sebastien Elgue, Nadine Gabas, Michel Cabassud and M. D. Carson, "Dynamic Behaviour of a Continuous Heat Exchanger/Reactor after Flow Failure," *Int. J. Chem. React. Eng.*, vol. 6, pp. 1–21, 2008.
- [192] X. Guo, Y. Fan, and L. Luo, "Multi-channel heat exchanger-reactor using arborescent distributors: A characterization study of fluid distribution, heat exchange performance and exothermic reaction," *Energy*, vol. 69, pp. 728–741, 2014.
- [193] S. Haugwitz, "Modeling, Control and Optimization of a Plate Reactor," lund university, 2007.
- [194] S. Haugwitz and P. Hagander, "Dynamic Optimization of a Plate Reactor Start-Up Supported By Modelica-Based," *Symp. A Q. J. Mod. Foreign Lit.*, vol. 1, pp. 99–104, 2007.
- [195] S. Li, S. Bahroun, C. Valentin, C. Jallut, and F. De Panthou, "Dynamic model based safety analysis of a three-phase catalytic slurry intensified continuous reactor," *J. Loss Prev. Process Ind.*, vol. 23, no. 3, pp. 437–445, 2010.
- [196] Z. Li and B. Dahhou, "A new fault isolation and identification method for nonlinear dynamic systems: Application to a fermentation process," *Appl. Math. Model.*, vol. 32, pp. 2806–2830, 2008.
- [197] M. Kettunen, P. Zhang, and S. L. Jämsä-Jounela, "An embedded fault detection, isolation and accommodation system in a model predictive controller for an industrial benchmark process," *Comput. Chem. Eng.*, vol. 32, pp. 2966–2985, 2008.
- [198] D. Ruiz, J. Cantón, J. M. Nogués, A. Espuña, and L. Puigjaner, "On-line fault diagnosis system support for reactive scheduling in multipurpose batch chemical plants," *Comput. Chem. Eng.*, vol. 4–6, pp. 829–837, 2001.
- [199] P. Van den Kerkhof, G. Gins, J. Vanlaer, and J. F. M. Van Impe, "Dynamic model-based fault diagnosis for (bio)chemical batch processes," *Comput. Chem. Eng.*, vol. 40, pp. 12–21, 2012.
- [200] N. Niedbalski, D. Johnson, S. S. Patnaik, and D. Banerjee, "Study of a multi-phase hybrid heat exchanger-reactor (HEX reactor): Part II – Numerical prediction of thermal performance," *Int. J. Heat Mass Transf.*, vol. 70, pp. 1086–1094, 2014.
- [201] S. Li, S. Bahroun, C. Valentin, C. Jallut, and F. De Panthou, "Control and optimization of a three-phase catalytic slurry intensified continuous chemical reactor," *J. Process Control*, vol. 220, no. 5, pp. 664–675, 2010.
- [202] F. Ebrahimi, T. Virkki-Hatakka, and I. Turunen, "Safety analysis of intensified processes," *Chem. Eng. Process. Process Intensif.*, vol. 52, pp. 28–33, 2012.
- [203] A. Zavala-Ró and R. Santiesteban-Cos, "Reliable compartmental models for double-pipe heat exchangers: An analytical study," *Appl. Math. Model.*, vol. 31, pp. 1739–1752, 2007.
- [204] K. W. Mathisen, M. Morari, and S. Skogestad, "Dynamic models for heat exchangers and heat exchanger networks," *Comput. Chem. Eng.*, vol. 18, pp. S459–S463, 1994.
- [205] P. S. Varbanov, J. J. Klemeš, and F. Friedler, "Cell-based dynamic heat exchanger models-Direct determination of the cell number and size," *Comput. Chem. Eng.*, vol. 35, pp. 943–948, 2011.
- [206] S. Bracco, I. Faccioli, and M. Troilo, "A Numerical Discretization Method for the Dynamic Simulation of a Double-Pipe Heat Exchanger," *Int. J. ENERGY*, vol. 1, no. 3, pp. 47–58, 2007.
- [207] E. Weyer, G. Szederkényi, and K. Hangos, "Grey box fault detection of heat exchangers,"

- Control Eng. Pract.*, vol. 8, pp. 121–131, 2000.
- [208] R. F. Escobar, C. M. Astorga-Zaragoza, a. C. Tllez-Anguiano, D. Jurez-Romero, J. a. Hernandez, and G. V. Guerrero-Ramrez, “Sensor fault detection and isolation via high-gain observers: Application to a double-pipe heat exchanger,” *ISA Trans.*, vol. 50, no. 3, pp. 480–486, 2011.
- [209] F. Caccavale and F. Pierri, “An integrated approach to fault diagnosis for a class of chemical batch processes,” *J. Process Control*, vol. 19, no. 5, pp. 827–841, 2009.
- [210] S. Persin and B. Tovornik, “Real-time implementation of fault diagnosis to a heat exchanger,” *Control Eng. Pract.*, vol. 13, pp. 1061–1069, 2005.
- [211] O. a Z. Sotomayor and D. Odloak, “Observer-based fault diagnosis in chemical plants,” *Chem. Eng. J.*, vol. 112, pp. 93–108, 2005.
- [212] G. R. Jonsson, S. Lalot, O. P. Palsson, and B. Desmet, “Use of extended Kalman filtering in detecting fouling in heat exchangers,” *Int. J. Heat Mass Transf.*, vol. 50, pp. 2643–2655, 2007.
- [213] C. M. Astorga-Zaragoza, a. Zavala-R ó, V. M. Alvarado, R. M. Méndez, and J. Reyes-Reyes, “Performance monitoring of heat exchangers via adaptive observers,” *Meas. J. Int. Meas. Confed.*, vol. 40, pp. 392–405, 2007.
- [214] F. Pierri, G. Paviglianiti, F. Caccavale, and M. Mattei, “Observer-based sensor fault detection and isolation for chemical batch reactors,” *Eng. Appl. Artif. Intell.*, vol. 21, pp. 1204–1216, 2008.
- [215] S. Delrot, T. M. Guerra, M. Dambrine, and F. Delmotte, “Fouling detection in a heat exchanger by observer of Takagi-Sugeno type for systems with unknown polynomial inputs,” *Eng. Appl. Artif. Intell.*, vol. 25, pp. 1558–1566, 2012.
- [216] C. M. Astorga-Zaragoza, V. M. Alvarado-Mart ínez, A. Zavala-R ó, R. M. Méndez-Oca ña, and G. V. Guerrero-Ramírez, “Observer-based monitoring of heat exchangers,” *ISA Trans.*, vol. 47, pp. 15–24, 2008.
- [217] F. Delmotte, M. Dambrine, S. Delrot, and S. Lalot, “Fouling detection in a heat exchanger: A polynomial fuzzy observer approach,” *Control Eng. Pract.*, vol. 21, no. 10, pp. 1386–1395, 2013.
- [218] M. Benkouider, R. Kessas, a. Yahiaoui, J. C. Buvat, and S. Guella, “A hybrid approach to faults detection and diagnosis in batch and semi-batch reactors by using EKF and neural network classifier,” *J. Loss Prev. Process Ind.*, vol. 25, no. 4, pp. 694–702, 2012.
- [219] Y. Wang, T. Megli, M. Haghgoie, K. S. Peterson, and A. G. Stefanopoulou, “Modeling and Control of Electromechanical Valve Actuator,” *World Congr. Exhib.*, 2002.
- [220] F. L. F. Radtke, “Fault detection of a control vavle using structured parity equations.”
- [221] Z. Anxionnaz, M. Cabassud, C. Gourdon, and P. Tochon, “Heat exchanger/reactors (HEX reactors): Concepts, technologies: State-of-the-art,” *Chem. Eng. Process. Process Intensif.*, vol. 47, pp. 2029–2050, 2008.
- [222] R. Andersson, B. Andersson, F. Chopard, T. Norén, and T. Noren, “Development of a multi-scale simulation method for design of novel multiphase reactors,” *Chem. Eng. Sci.*, vol. 59, pp. 4911–4917, 2004.